UNIVERSIDADE D
COIMBRA

Maria Helena Henriques Antunes

BIOACTIVE NANOVESICLES FROM UMBILICAL CORD BLOOD TO TREAT DIABETIC CHRONIC WOUNDS

Tese no âmbito do Programa Doutoral em Ciências da Saúde, Ramo Ciências Biomédicas, orientada pelo Professor Doutor Lino da Silva Ferreira e pelo Professor Doutor João Oliveira Malva e apresentada à Faculdade de Medicina da Universidade de Coimbra

Dezembro de 2021

UNIVERSIDADE D
COIMBRA

Maria Helena Henriques Antunes

Bioactive nanovesicles from umbilical cord blood to treat diabetic chronic wounds

Tese no âmbito do Programa Doutoral em Ciências da Saúde, Ramo Ciências Biomédicas, orientada pelo Professor Doutor Lino da Silva Ferreira e pelo Professor Doutor João Oliveira Malva e apresentada à Faculdade de Medicina da Universidade de Coimbra

Dezembro 2021

'Miracles happen every day.'

'Acontecem milagres todos os dias.'

Deepak Chopra

A meus pais.

Agradecimentos

Terminando este projeto, quero apresentar os meus mais sentidos agradecimentos a todos os que me acompanharam e apoiaram científica, profissional e pessoalmente, tendo de uma forma ou de outra permitido a concretização deste meu sonho, nascido numa aula de secundário quando pela primeira vez ouvi falar em Bioquímica, na pessoa de Oparin.

Ao meu orientador, Lino Ferreira, pela valiosa orientação, perseverança e inspiração. O seu espírito crítico foi essencial para me desafiar a avançar neste percurso investigativo, acompanhando-o sempre com rigor científico, comentários construtivos e inestimável amizade. Agradeço-lhe toda a paciência e apoio ao longo destes anos que me ajudaram a chegar aqui.

Ao João Oliveira Malva pela sua orientação, permitindo a submissão deste trabalho à Faculdade de Medicina da Universidade de Coimbra.

À Joana Simões Correia que desempenhou um papel precioso na orientação inicial do desenvolvimento do trabalho, sendo uma importante fonte de inspiração, apoio e amizade.

Ao André Gomes e à Crioestaminal – Stemlab, S.A. por me proporcionarem a oportunidade de desenvolver este trabalho em contexto empresarial, disponibilizando condições necessárias para o desenvolvimento deste projeto. O meu agradecimento pelo suporte e estima.

À Carla Cardoso por me ajudar a manter o rumo através do seu auxílio e orientação no contexto empresarial. O meu apreço pelo seu apoio e amizade.

Ao Renato Cardoso pelo seu companheirismo, amizade e por manter um espírito de equipa construtivo, que derivaram numa valiosa contribuição para este processo investigativo.

Ao Hugo Fernandes que se disponibilizou para realizar a revisão desta tese numa fase essencial, revelando-se um grande auxílio.

Aos meus colegas e amigos que integram o grupo de Biomateriais e Terapias Baseadas em Células Estaminais, pelo seu espírito de equipa e entreajuda incríveis, apresentando uma enorme capacidade científica. Àqueles que diretamente participaram no desenvolvimento deste projeto - Adrián Jiménez-Balsa, Miguel Lino, Alessandra Zonari, Ana Barradas -, ou que indiretamente permitiram o seu desenvolvimento, disponibilizando o seu tempo e conhecimento técnico e científico - Patricia Pitrez, Catarina Praça, Susana Rosa, Susana Simões, Vitor Francisco, Ana Francisca, Sandra Pinto, Luís Estronca, Josephine Blersch, Michela Commune, António Santinha, José Paiva; Vanessa Pinto, Catarina Rebelo, Sónia Pinho, Ricardo Abreu, Andreia Vilaça, Tânia Barata, Malwina Kotowicz, Carolina Santos e muitos mais. Agradeço-lhes por todo o apoio a amizade.

Agradeço também a todos os meus e amigos e bom colegas que tive a honra de conhecer e preservar durante o meu percurso na Crioestaminal (Marylin, Isabel, Olímpia, Ana Canha, …) e no meu percurso académico (Susana, Sofia, Bete, Joana, Teresa, Mónica, …).

Aos muitos amigos da vida, que me apoiaram pela sua amizade e presença durante este percurso: à Alexandra, Joana, Delfina e Rita pela motivação contínua e pelas escapadinhas que me ajudaram a desanuviar e me deram a paz que precisava para continuar no caminho certo; à Ana Lúcia, Sandra, Dora, Lígia e Ana Cláudia pelas gargalhadas que me ajudaram a manter o ânimo durante este percurso; à Cláudia, Sérgio, Nelson, Rui e Jô pela presença constante que têm na minha vida desde cedo; à Susana Pereira pelo apoio, sorriso e integridade científica. A todos os que menciono e tantos mais que marcaram também o meu percurso ao longo destes anos, o meu muito obrigada.

Por fim, e em especial, agradeço à minha família, pelo carinho e alento que sempre concederam:

Ao Bruno, pelo apoio inicial na altura certa, fundamental para que pudesse iniciar este percurso. Aos meus cunhados, Paulo e Beta, e sobrinhos, Pedro e Luís, simplesmente por serem, pelo apoio, amizade e carinho.

A ternura e suporte incondicional dos meus irmãos, Inês, Aida, Duarte e Célia, que sempre me apoiaram em todas as decisões que tomei, reconfortando-me nos momentos piores e acompanhando-me nas ocasiões melhores. Os irmãos são o melhor presente.

Aos meus filhos, que são a minha maior concretização e orgulho, e que me deram a força e amor necessário para concluir este estudo apesar dos obstáculos. À Joana, *a minha sorte grande*, ao Afonso, *o meu menino de oiro,* e à Leonor, *a flor que nos completa.* E ao meu sobrinho e afilhado Tiago, *um raio de luz constante*.

Finalmente aos meus pais. À minha mãe por ter sido sempre o farol que me orienta na vida, uma força que e nos motiva a sermos mais e melhor. Ao meu pai pela sua presença, o seu sorriso, força de viver e amabilidade para com todos. Sei que estaria orgulhoso de me ver submeter este trabalho àquela que é a sua faculdade. Não há palavras suficientes que possam descrever o apreço que lhes tenho por me ajudarem e ampararem sempre que precisei, em todas as etapas da minha vida. Obrigada.

Support and financial acknowledgments

This work was supported by FCT (SFRH/BDE/103512/2014; MITP-TB/ECE/0013/2013; EXCL/DTP-PIC/0069/2012; UID/NEU/04539/2013); QREN-COMPETE funding (FCOMP-01-0202-FEDER-038631; Project "ExoCord" promoted by Stemlab, SA and Biocant); Portugal 2020-COMPETE funding (Project "Stem cell based platforms for Regenerative and Therapeutic Medicine", Centro-07-ST24-FEDER-002008; Project "StrokeTherapy" co-promoted by Stemlab, Rovisco Pais and Universidade de Coimbra) and ERA Chair project ERA@UC (Ref: 669088).

This project has received funding from the European Union's Horizon 2020 research and innovation programme under grant agreement No 669088

Publications and Communications

Patent

Lino Da Silva Ferreira, Joana Rita Simões Correia, Renato Manuel Soares Cardoso, Maria Helena Henriques Antunes. **Use of umbilical cord blood derived exosomes for tissue repair.** PCT/IB2017/000412. Pub. No. WO/2017/163132, 28.09.2017.

Publications

Henriques-Antunes H[#], Cardoso RMS[#], Zonari A, Correia J, Leal EC, Jiménez-Balsa A, Lino MM, Barradas A, Kostic I, Gomes C, Karp JM, Carvalho E Ferreira L. **The Kinetics of Small Extracellular Vesicle Delivery Impacts Skin Tissue Regeneration.** ACS Nano. 2019 Aug 27; 13 (8):8694-8707. doi: 10.1021/acsnano.9b00376. Epub 2019 Aug 16**.**

Josephine Blersch, Vitor Francisco, Catarina Rebelo, Adrian Jiménez-Balsa, Helena Antunes, Sandra Pinto, Susana Simões, Akhilesh Rai and Lino Ferreira. **A light-triggerable formulation to control the stability of pro-angiogenic transcription factor hypoxia inducible factor-1A (HIF-1A).** Nanoscale. 2020 May 14; 12(18): 9935-9942. doi: 10.1039/C9NR10503D.

Blersch J, Francisco V, Rebelo C, Jiménez-Balsa A, Antunes H, Gonzato C, Pinto S, Simões S, Liedl K, Haupt K, Ferreira L. **A Light-Triggerable Nanoparticle Library for the Controlled Release of Non-Coding RNAs.** Angew Chem Int Ed Engl. 2020 Jan 27; 59 (5): 1985-1991. doi: 10.1002/anie.201911398.

Blersch J, Francisco V, Rebelo C, Jiménez-Balsa A, Antunes H, Gonzato C, Pinto S, Simões S, Liedl K, Haupt K, Ferreira L. **A Light-Triggerable Nanoparticle Library for the Controlled Release of Non-Coding RNAs.** Angewandte Chemie. 2020 Jan 27; 132 (5): 2001-2007. doi: 10.1002/ange.201911398.

Lino MM, Simões S, Vilaça A, Antunes H, Zonari A, Ferreira L. **Modulation of Angiogenic Activity by Light-Activatable miRNA-Loaded Nanocarriers.** ACS Nano. 2018 Jun 26; 12 (6): 5207-5220. doi: 10.1021/acsnano.7b07538.

Oral communications

Vitor Francisco1,2, Josephine Blersch1, Catarina Rebelo1,2, Adrian Jimenez1, Helena Antunes1,2, Carlo Gonzato3, Sandra Pinto1, Susana Simões1, Klaus Liedl4, Karsten Haupt2, Lino Ferreira1,2. **Efficient non-coding RNA delivery in wound healing by photo-triggerable nanoparticles.** 53rd Annual Scientific Meeting of the European Society for Clinical Investigation "The Clocks of Metabolism and Disease", 2019. 22nd – 24th May, Coimbra, Portugal.

Josephine Blersch, A. Jiménez-Balsa A., C. Rebelo, H. Henriques-Antunes, V. Francisco , S. Pinto, A. Rai, K. Haupt, K. Liedl, L. S. Ferreira. **HT-Screening identifies light triggerable NP formulation for efficient *in vivo* non-coding RNA delivery in wound healing.** XII Spanish-Portuguese Conference on Controlled Drug Delivery - Tailoring drug delivery systems to the patients' needs, 2018. 14 – 16 January, Coimbra, Portugal.

Blersch, Josephine, Jiménez-Balsa A., Rebelo C., Henriques-Antunes H., Francisco V., Pinto S., Rai A., Haupt K., Liedl K., Ferreira L.S **Light-triggerable nanoparticles for efficient *in vivo* non-coding RNA delivery in wound healing.** The 10th International Meeting of the Portuguese Society for Stem Cells and Cell Therapies, 2017. 12-14 October, Covilhã, Portugal.

Helena Henriques-Antunes, Renato Cardoso, Joana Correia, Ermelindo Leal, Alessandra Zonari, Ana Barradas, Eugénia Carvalho, Lino Ferreira. **Exosomes to enhance diabetic wound healing.** European Cells and Materials Vol. 33 Suppl. 2, 2017 (CL 1). TERMIS European Chapter Meeting, 2017. 26 - 30 June, 2017, Davos, Switzerland.

Helena Henriques-Antunes, Renato Cardoso, Joana Correia, Ermelindo Leal, Alessandra Zonari, Ana Barradas, Eugénia Carvalho, Lino Ferreira. **EXOCORD - Bioactive nanovesicles from umbilical cord blood to treat diabetic chronic wounds.** Invited speaker: PhD in Experimental Biology and Biomedicine. Advanced Therapies Module, 2016. 13--17 June, Cantanhede, Portugal.

Poster communications

Helena Henriques-Antunes[#], Renato Cardoso[#], Alessandra Zonari, Joana Correia, Ermelindo Leal, Ivana Kostic, Adrián Jiménez-Balsa, Ana Barradas, Vanessa Pinto, Eugénia Carvalho, Lino Ferreira. **Bioactive nanovesicles from umbilical cord blood controlled delivery system for chronic wounds.** TERMIS World Congress 2018. 4 – 7 September, Kyoto, Japan.

Helena Henriques-Antunes, Margarida Vieira, Carla Cardoso, Sofia Couceiro, Francisco Santos, Mónica Brito, André Gomes.**From 15 years of cell banking to the development of cell-therapies - CRIOESTAMINAL experience** TISSUE ENGINEERING & REGENERATIVE MEDECINE Exposition 2018 (TERMEX2018) – TERMIS World Congress 2018. 4 – 7 September, Kyoto, Japan.

Helena Henriques-Antunes[#], Renato Cardoso[#], Alessandra Zonari, Joana Correia, Ermelindo Leal, Ivana Kostic, Adrián Jiménez-Balsa, Ana Barradas, Vanessa Pinto, Eugénia Carvalho, Lino Ferreira. **Desenvolvimento de um hidrogel para libertação controlada de exossomas - uma nova esperança para tratamento de ulceras diabéticas.** 14º Congresso de Diabetes, 2018. 9-11 março, Vilamoura, Algarve, Portugal.

Helena Henriques-Antunes[#], Renato Cardoso[#], Alessandra Zonari, Joana Correia, Ermelindo Leal, Ivana Kostic, Adrián Jiménez-Balsa, Ana Barradas, Vanessa Pinto, Eugénia Carvalho, Lino Ferreira. **Controlled delivery of exosomes for chronic wound healing.** XII Spanish-Portuguese Conference on Controlled Drug Delivery- Tailoring drug delivery systems to the patients' needs, 2018. 14 – 16 January, Coimbra, Portugal.

Miguel M. Lino, Susana Simões, Andreia Vilaça, Helena Antunes, Alessandra Zonari, and Lino Ferreira. **Near infrared triggered release of miRNAs for modulation of cell activity.** XII Spanish-Portuguese Conference on Controlled Drug Delivery- Tailoring drug delivery systems to the patients' needs, 2018. 14 – 16 January, Coimbra, Portugal.

Helena Henriques-Antunes, Renato Cardoso, Joana Correia, Ivana Kostic, Ermelindo Leal, Alessandra Zonari, Ana Barradas, Eugénia Carvalho, Lino Ferreira. **Umbilical cord blood exosomes for diabetic wound healing.** The 10th International Meeting of the Portuguese Society for Stem Cells and Cell Therapies, 2017. 12-14 October, Covilhã, Portugal.

Lino, Miguel, Simões S., Vilaça A., Antunes H., Zonari A., Ferreira L. **Spatio-temporal controlled delivery of miRNAs for modulation of angiogenic activity**. The 10th International Meeting of the Portuguese Society for Stem Cells and Cell Therapies, 2017. 12-14 October, Covilhã, Portugal.

Table of Contents

List of Figures

List of Tables

Abstract

Worldwide, there are 382 million patients with diabetes and is estimated that this number will rise up to 592 million by 2035. Approximately 15% of these individuals have or will develop diabetic foot ulcer. The increase in the incidence and prevalence of chronic wounds demands the development of more efficient therapies. Advanced therapies including growth factor and cell based therapies have been tested with limited success. Recently, small extracellular vesicles (SEVs), also known as exosomes, carrying functional proteins and RNA have been evaluated as a potential therapeutic platform for chronic wounds. However, some issues need to be addressed before any clinical translation including (i) the selection of an ideal source of extracellular vesicles for chronic wounds and (ii) the development of deliver systems for the efficient release of SEVs.

In the present work, we have evaluated the skin healing potential of SEVs isolated from umbilical cord blood mononuclear cells (hUCBMNCs) and we have further developed an advanced delivery system to enhance SEV therapeutic effect. Our results show that diabetic chronic wounds treated with the advanced delivery system containing SEVs healed faster, presenting, at day 10, a reduction of wound size to approximately 10% versus the reduction to approximately 40% observed for non-treated wounds.

SEVs were collected from the conditioned media hUCBMNCs and isolated by sequential ultra-centrifugation and characterized for their morphology, surface marker expression, miRNA composition (by RNA deep sequencing and miRNAs validated by qRT-PCR) and *in vitro* and *in vivo* bioactivity tests.

The SEVs presented a round morphology, size of 100-130 nm and zeta potential of -30mV. They show the presence of the following proteins at the surface CD9, CD81, CD63, TSG101 and CD45. SEVs were internalized by skin cells, keratinocytes, fibroblasts and endothelial cells in a concentration and time dependent manner, reaching a plateau between 16h to 24h. At 4h, approximately 50% of keratinocytes and fibroblasts and 20% of endothelial cells presented detectable levels of internalized SEVs (3 μg/mL). Our *in vitro* results demonstrated that SEVs increased cell proliferation (up to 50% in all three types of skin cells), enhanced cell survival under ischemic conditions (up to 50% in endothelial cells and 15% in fibroblasts and keratinocytes), promoted cell migration in a wound healing assay (up to 20% more in scratches inflicted in keratinocytes and fibroblasts monolayers) and induced endothelial cells to form tubes and a more complex network (from 20% to 30%). Our in vivo results show that SEVs are very effective in the treatment of diabetic and non-diabetic wounds. The bi-daily administration of low amounts of SEVs (0.02 μg) in wounds of diabetic mice lead to enhanced wound healing kinetics of approximately 20%, at day 10, as compared to the control group. Additionally, the healing was significantly enhanced by this treatment versus an advanced therapy approved by FDA and EMA (PDGFBB).

In a subsequent stage of the work, we have developed an advanced drug delivery system for SEVs based on a light-triggerable hyaluronic acid hydrogel. The motivation here was to allow the remote delivery of SEVs according to specific needs. In this case, we have chemically immobilized SEVs to hyaluronic acid polymer chains by a photo-cleavable linker (PCL). This PCL was cleaved after exposure to UV/blue light releasing the SEVs. Our results show that the controlled release of SEVs into the wound site enhanced the wound healing kinetics, as evaluated by wound size measurements, histological and gene analyses. Our results further identified a very complex miRNA composition and miR-150-5p as the most prevalent in hUCBMNCs-SEVs and as partially responsible of the bioactivity of these exosomes by targeting

the transcription factor c-Myb. Additionally, the system developed to control and sustain the delivery of SEVs to the wound is able to modulate the expression of miRNAs in the skin surrounding the wound, normalizing some miRNA levels, e.g. miR-150-5p, which can be responsible for better wound resolution.

In summary, a new platform to delivery therapeutic SEVs was successfully developed and represents a promising tool for the treatment of chronic wounds.

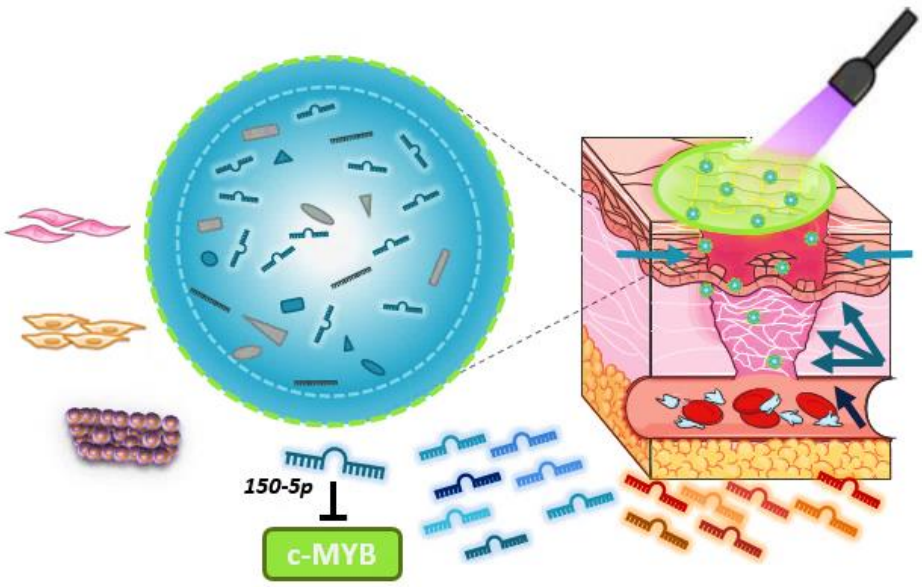

Resumo

No mundo existem cerca de 382 milhões de doentes diabéticos (2013), um número que se estima que chegue aos 592 milhões em 2035. Aproximadamente 15% destes doentes desenvolverão ulceras diabéticas, mais conhecidas como pé diabético. O desenvolvimento de terapias mais eficientes é necessário para fazer face ao contíno aumento da incidência e prevalência de feridas crónicas. Terapias baseadas em fatores de crescimento e cdllulares têm vindo a ser desenvolvidas e testadas, embora com sucesso limitado. Recentemente, o potencial terapeutico de pequenas vesiculas extracellulares (em inglês: Small Extracellular Vesicles – SEVs), comummente conhecidas como exosomas, que transportam biomoleculas funcionais (proteinas e RNAs), têm vindo a ser estudado pela comunidade cientifica como uma nova plataforma terapêutica para feridas crónicas. Contudo, alguns pontos relevantes têm ainda de ser avaliados da translação para o contexto clínico, incluindo (i) a selecção da fonte de células ideal para obtenção de vesiculas extracellulares para tratamento destas feridas e (ii) o desenvolvimento de um sistema que permita uma entrega eficiente destas vesiculas extracellulares na ferida.

No presente trabalho, avaliamos o potencial regenerativo de SEVs secretadas por células mononucleares do sangue do cordão umbilical (em inglês: human Umbilical Cord Blood MonoNuclear Cells – hUCBMNCs) e desenvolvemos um sistema avançado para a entrega eficiente destas vesiculas na ferida, aumentando o seu potencial terapêutico. Os nossos resultados demontraram que feridas crónicas diabeticas tratadas com este sistema avançado contendo SEVs cicatrizam mais rapidamente, apresentando, 10 dias após o tratamento, uma redução significativa do tamanho da ferida para aproximadamente 10% da área da ferida original, versus uma redução até aproximadamente 40% nas feridas não tratadas.

As SEVs foram obtidas do meio condicionado de hUCBMNCs por ultra-centrifugação sequencial e caracterizadas quanto à sua morfologia, expressão de marcadores membranares, composição de microRNAs (por RNA deep sequencing seguido de validação por RT-PCR) e bioactividade *in vitro* e *in vivo*.

Estas SEVs apresentam uma morfologia esférica com cerca de 100-130 nm de diametro e possuem um potencial zeta que ronda os -30mV. Na sua superfície membranar possuem os marcadores proteicos típicos de exosomas, CD9, CD81, CD63 e TSG1101 e o marcador típico das células secretoras, o CD45. Estas SEVs foram internalizadas por diferentes tipos de células da pela, queratinócitos, fibroblastos e células endoteliais, apresentado uma internalização dependente da sua concentração e do tempo de incubação, atingindo um plateau entre as 16h e 24h. Após 4h de incubação, aproximadamente 50% dos queratinócitos e fibroblastos e 20% deas células endoteliais apresentavam valores detectáveis de SEVs (3μg/mL) internalizados. Os nossos resultados *in vitro* demontraram que estas SEVs potenciavam a proliferação celular (com aumento de até 50% nos três tipos celulares estudados), aumentavam a sobrevivência das células a condições isquémicas (até 15% para queratinócitos e fibroblastos e até 50% para as células endoteliais), promoviam migração celular (até cerca de 20% mais, em rasgos (scratches) inflingidos numa monocamada de queratinócitos e fibroblastos em cultura) e induziam a formação de tubos nas células endoteliais, que apresentavam uma rede mais complexa (entre 20% a 30%). Os nossos resultados *in vivo* demonstraram, por sua vez, que estas SEVs são muito eficientes no tratamento de feridas diabéticas e não-diabéticas. A Administração bi-diária de baixas quantidades de SEVs (0.02 μg) em feridas infligidas a ratinhos diabéticos traduziu-se num aumento da cinética de cicatrização da ferida de aproximadamente 20% mais, quando comparado com o grupo controlo, ao dia 10 após início de tratamento.

Adicionalmente, esta estratégia de tratamento mostrou cicatrização significativamente melhor do que a terapia avançada actualmente aprovada pela FDA e EMA (PDGFBB).

Numa fase subsequente do trabalho, nós desenvolvemos um sistema avançado, que consistia num hidrogel de ácido hialurónico para administração de SEVs por acção da luz. O objectivo, era desenvolver um Sistema que permitisse controlar a libertação de SEVs de acordo com as necessidades específicas da sua aplicação. Neste caso, nós immobilizamos quimicamente as SEVs a candeias poliméricas de ácido hialurónico através moléculas fotossensíveis (em inglês: photo-cleavable linker - PCL). Este PCL era clivado por exposição à luz UV/azul libertando assim as SEVs. Os nossos resultados demontraram que a libertação controlada de SEVs na ferida melhorava ainda mais a cinética de cicatrização da mesma, de acordo com analyses de medida de área da ferida e análises histológicas e genéticas. Adicionalmente, analisámos a composição em microRNAs (miRs) dos exosomal, que se revelou bastante complexa e rica em diferentes miRs, e indentificámos o miR-150-5p como o mais prevalente nas SEVs de hUCBMNCs e como parcialmente responsável pela bioactividade destas vesiculas, através da modulação da expressão do factor de transcrição c-Myb. Adicionalmente, verificámos que o sistema desenvolvido para controlar e manter de forma sustentada a administração de SEVs na ferida tinha a capacidade de modular a expressão de miRs na pele circundante à ferida, levando à normalização dos níveis de alguns miRs, nomeadamente, o miR-150-5p, reforçando a sus importância para uma melhor resolução das feridas.

Resumindo, uma nova plataforma de administração de SEVs foi desenvolvida com sucesso, apresentando-se como uma ferramenta de elevado potencial para o tratamento de feridas crónicas.

Aims and outline of the thesis

The present work presents umbilical cord blood mononuclear cells (hUCBMNCs) as source of bioactive small extracellular vesicles (SEVs) with wound healing potential and the development of a new platform for an efficient controlled delivery of SEVs, which potentiates their therapeutic effect while minimizing the need for manipulation, thus presenting itself as a promising new tool to address the chronic wounds global problem.

This thesis is divided in 4 major sections: an introduction to the work; the communication of the results obtained; a general discussion and conclusion; and future work.

The first section consists of 4 Chapters were the problematic of chronic wounds is explored (I), the exosomes are introduced (II), presented as major communication vehicles (III) and as potential therapeutic tool for chronic wounds (IV).

In the second section the results of our work are presented in the form of a scientific communication (Abstract, Introduction, Results, Discussion, Materials and methods, and Supplemental information).

In the third section a general discussion of the results obtained is exposed and concludes regarding the major outcomes of this work

In the fourth section, it is presented 3 distinct areas of study that would be scientifically interesting to further study in order to address some of the questions that aroused from this work and remain unanswered.

I. Chronic wounds

1. Definition and social impact of chronic wounds

Wound is a rupture in skin's continuity exposing the inner body structure. It can be superficial, affecting only the epidermis (also called erosion or abrasion) or more profound, penetrating the dermis, constituting an ulcer or a fissure, this last consisting of a sharp incision comparing to the previous, in which a boarder skin area is affected. A superficial wound usually heals easily without scaring, when the dermis is affected the progress of healing can be affected and inconsistent, we may be in the presence of a chronic or non-healing wound [1, 2]. Chronic wounds are, by definition, wounds that do not heal within a reasonable interval of time, 6 weeks / 3 months, and enter a pathological state of inflammation, failing to evolve in the healing process [2, 3]. Chronic wounds have different etiologies: venous ulcers, pressure ulcers, diabetic ulcers, neuropathic ulcers, traumatic ulcers and arterial insufficiency ulcers, among others. The wound classification is related with several factors, including the (i) cause and (ii) underlying predisposition factors for origin and healing impairment, such as a disease or other conditions. A major issue in chronic wound development and care is the occurrence of infection [1, 2, 4-6].

Chronic wounds have a high impact in public health, economy and society [7, 8]. In 1999, approximately 6.5 million patients had chronic wounds of different etiologies in the USA alone [4]. Nowadays, approximately 15% of aged individuals in the USA suffer from chronic wounds with increasing incidence of 2 to 3 million a year [4, 9, 10]. In developed countries it is estimated that 1% to 2% of the population will experience a non-healing wound during their lifetime [4]. A representative part of the diabetic population develops chronic wounds. Globally, in 2013 there were around 382 million diabetic patients according to the International Diabetes Federation, 36 million more than the reported by the world health organization (WHO) in 2012 (Figure - 1), and the number is estimated to rise to 592 million by 2035 [9, 10]. Approximately 15% - 25% of this patients present or will develop diabetic foot ulcer, which represented an estimated cost of $10.9 billion in US and £252 million in UK, in 2001 [3-5, 10-12]. Additionally, it is estimated that 12% of patients with foot ulcers will need amputation [4]. Due to loss of sensation, diabetic patients have 15% higher risk of being amputated in consequence of non-healing ulcers than the general population [9, 11].

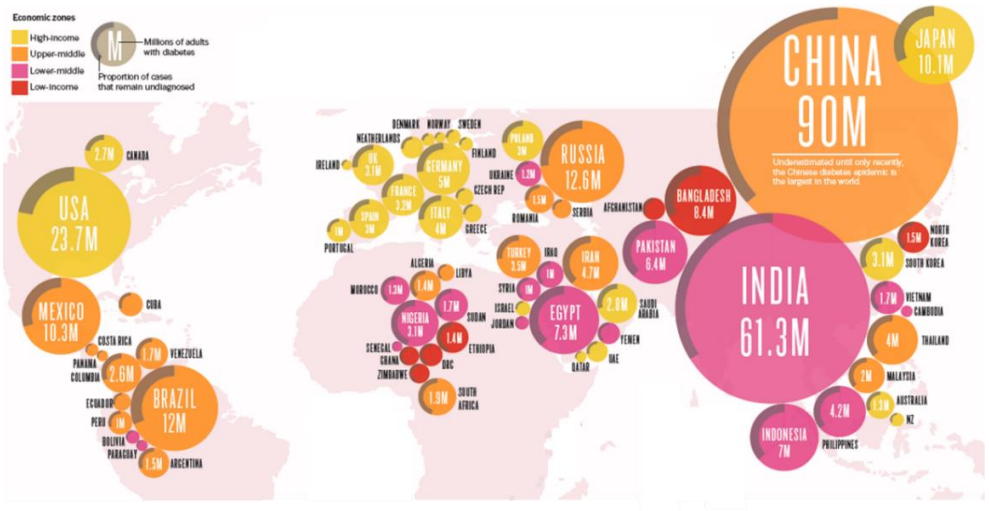

Figure - 1. Worldwide incidence of diabetes in 2012.
According to WHO diabetes affected 346 million people all over the world in 2012, a rising condition in, both, developed and developing countries [13].

2. Wound healing molecular mechanisms and impairment

Wound healing comprises a dynamic and intricate network of process and events, involving soluble mediators, blood cells, extracellular matrix and parenchymal cells. There are 3 stages of wound healing that can overlap in time: **I.** Hemostasis and inflammation, **II.** New tissue formation / proliferation and **III.** Tissue remodeling [9, 10, 14-21].

I. Hemostasis and inflammation.

This phase should last until about 48 hours after injury. Bacteria, neutrophils and platelets are abundant in the wound [10, 15]. Platelets adhere to the damage blood vessels leading to clot formation, preventing bleeding, restoring hemostasis and providing protection for the wounded area. Additionally, they secrete soluble factors giving rise to a blood-clotting cascade. For example, the secreted platelet-derived growth factor (PDGF) attract and activate macrophages and fibroblasts. Transforming growth factors (TGFs) attract inflammatory cells, such as leukocytes, neutrophils, and macrophages, initiating the inflammatory phase. Neutrophils clean the wounded area of foreign particles and bacteria and are then extruded with the crust or phagocytosed by macrophages. In response to specific chemoattractants, such as fragments of extracellular-matrix protein and transforming growth factor β (TGF-β), monocytes also infiltrate the wound site and become activated macrophages. Additionally monocytes and macrophages express several factors including colony - stimulating factor 1 (CSFR1), a cytokine necessary for survival of monocytes and macrophages, tumor necrosis factor-α (TNF-α), a potent inflammatory cytokine, PDGF, a potent chemoattractant and mitogen for fibroblasts, transforming growth factor-α (TGF-α), interleukin-1 (IL-1) and insulin like growth factor I (IGF-I) [9, 14, 16].

II. New tissue formation / proliferation.

This stage occurs about 2–10 days after injury. A crust has formed on the surface of the wound and migration of epithelial cells occurs. Most cells from the previous stage of repair have migrated from the wound, and new blood vessels now populate the area [15]. As the inflammatory phase ends, the proliferative phase begins. Local release of growth factors like epidermal growth factor (EGF), TGF-α and keratinocyte growth factor (KGF), produced by remaining inflammatory cells and migrating epidermal and dermal cells stimulate and maintain cellular proliferation while initiating cellular migration. At this stage it's very important that a robust and sustained angiogenic response occurs to support the formation of granulation tissue and epithelialization [14, 16]. A new tissue with granular appearance is formed, it's rich in new capillaries necessary to sustain the newly formed tissue. The macrophages provide a continuing source of growth factors (e.g. PDGF, TGF-β and Vascular endothelial growth factor - VEGF) necessary to stimulate fibroplasia and angiogenesis. The fibroblasts produce the new extracellular matrix (ECM), including hyaluronan (hyaluronic acid), fibronectin, proteoglycans and type 1 and type 3 pro-collagen, necessary to support cell ingrowth. The blood vessels carry oxygen and nutrients necessary to sustain cell metabolism. Endothelial progenitor cells (EPCs) are recruited into the circulation in response to injury and constitute a major intervenient in neo-angiogenesis. EPCs mobilization is mediated by nitric oxide (NO), VEGF, and matrix metalloproteinases (MMP), particularly MMP-9. In the wound, EPCs engraft into the remodeling microvasculature, the engraftment and possibly differentiation occur in response to stromal cell–derived factor 1 (SDF1) and IGF. Angiogenesis is also stimulated by fibroblast release of basic fibroblast growth factor (FGF-β) [10, 14, 16].

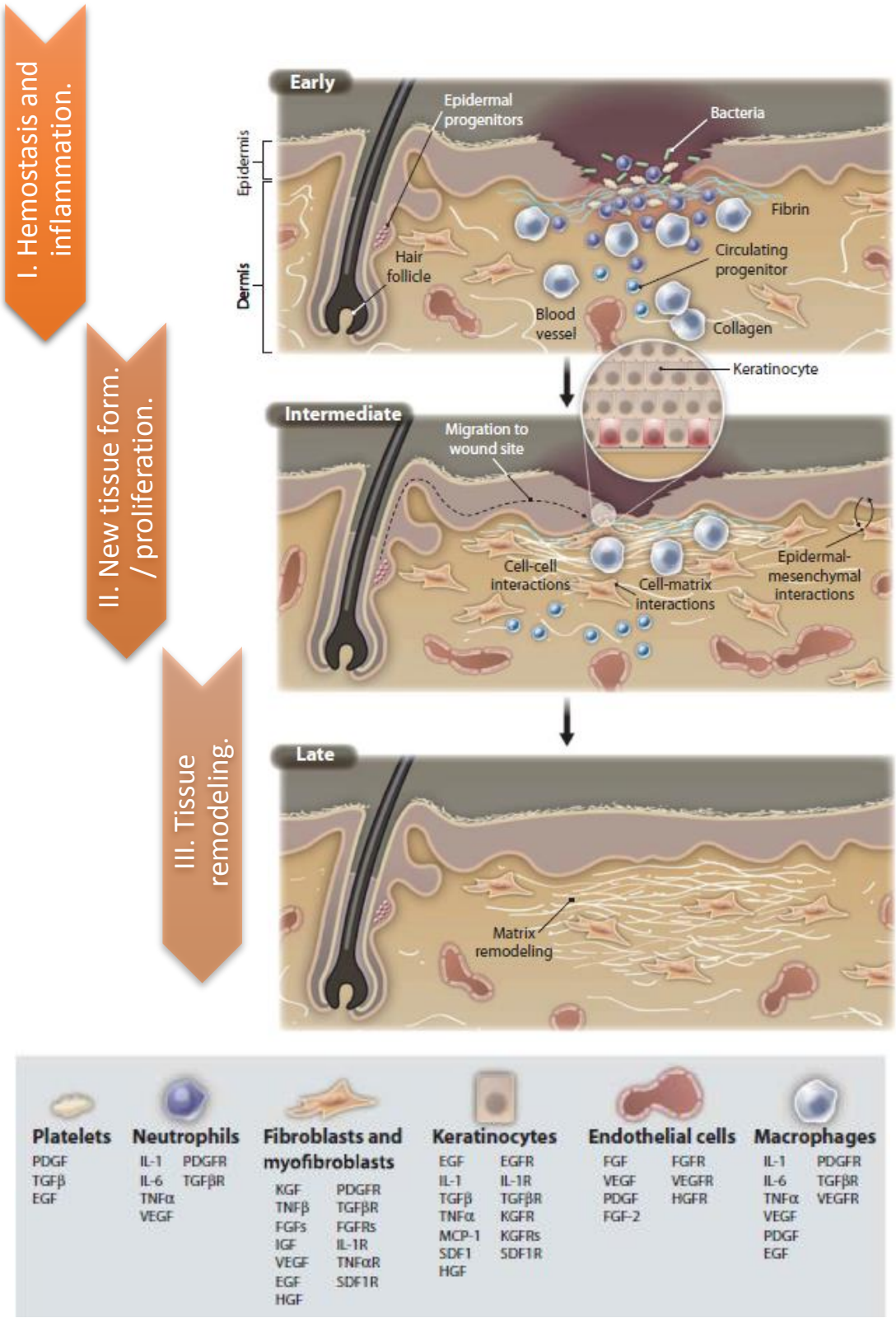

Figure - 2. Wound healing phases, molecular and cellular mechanisms.

Wound healing includes hemostasis and activation of inflammatory cells (I.), followed by proliferation and migration of keratinocytes and fibroblasts, matrix deposition, and angiogenesis (II.), and remodeling of ECM, resulting in scar formation and restoration of skin barrier (III.). This process is tightly controlled by multiple cell types that secrete numerous growth factors, cytokines, and chemokines (listed below). Adapted from [17].

III. Tissue remodeling.

The final phase of wound healing is the tissue remodeling. It begins 4-5 days after injury and lasts for 2 weeks or more, depending on the wound healing environment. Reestablishment of a normal blood supply offers the necessary microenvironment for epidermal and dermal cell migration and proliferation, promoting epithelization and the restoration of epidermis integrity. Fibroblasts proliferate within the wound and synthesize ECM forming granulation tissue perfused with newly formed blood vessels. Wound contraction involves a complex and orchestrated interaction of cells, ECM and cytokines. Matrix-remodeling enzymes, such as MMPs, play important roles in remodeling the local matrix microenvironment in support of several healing responses, including cellular migration, proliferation, and angiogenesis. Contraction is also achieved by differentiated fibroblasts or myofibroblasts that, in response to TGF-α, tissue tension, and the presence of certain matrix proteins, acquire smooth muscle actin–containing stress fibers. Finally, apoptosis of fibroblastic cells occurs, probably triggered by TGF-α, TNF, and FGF-2, leading to the formation of a relatively acellular scar tissue whose tensile strength is comparable with unwounded skin [9, 14, 16].

The complexity of the wound-healing process, which involves many cell types and factors, is still not completely understood as so are the molecular mechanisms that lead to impairment of wound healing, which give rise to two major conditions that require clinical attention: excessive scaring and chronic non-healing wounds [9, 14-18, 20, 21]. Excessive scar is related with the impairment of phase III of wound healing, tissue remodeling, and leads to hypertrophic scar and keloid formation. It is characterized by excess of collagen deposition and has been linked with the inability of dermal cells, particularly myofibroblasts, to undergo timely apoptosis. This excessive scar formation leads to tissue dysfunction and is the major problem associated with acute wound healing, but also occurs upon chronic wounds resolution [9, 14, 15, 17]. On the other end, a skin lesion has the potential to become chronic by impairment of any of the phases of wound healing, and hence, chronic wounds are classified on the basis of their underlying cause. The major causes and categories of non-healing skin wounds are diabetes mellitus, vascular insufficiency and local-pressure effects. Additionally, factors like infection, compromised nutritional or immunological status, advanced age, chronic mechanical stress, and other comorbidities can contribute to delayed healing or even inhibit the complete healing of the wound [1, 2, 4-6, 16, 17, 20, 21]. The majority of chronic wounds are characterized by a prolonged or excessive inflammatory phase, persistent infections, and the inability of dermal or epidermal cells to respond to reparative stimuli [1, 2, 4-6, 16, 17, 20].

Diabetic ulcers are a consequence of physiologic and biochemical defects associated with a metabolic disease. Diabetic patients are unable to sense and relieve cutaneous pressure because of neuropathy. These patients present vascular disease that leads to ischemia in the wound and develop wound infections due to their immune-compromised status. Other abnormalities associated with diabetic ulcers include prolonged inflammation, decreased synthesis of collagen, increased levels of proteinases, and defective macrophage function [9, 14, 16-18]. In this thesis, we will pay special attention to diabetic chronic wounds, despite not being the most common type of ulcers, they have high impact in patients quality of live and are more prone to require limb amputation [8, 9, 11].

3. Chronic wounds management and treatment

The efficacy of chronic wound management and treatment is closely related with their etiology and comprehension of mechanisms responsible for healing impairment. In order to address this societal problem the Wound Healing Society (WHS) issued guidelines to the medical community and multistep approach was established, known by the acronym TIME [5, 22, 23].

Table I. TIME approach to wound management

Tissue- assessment and debridement of nonviable or foreign material (including host necrotic tissue, adherent dressing material, multiple organism-related biofilm, or slough, exudate, and debris) on the surface of the wound.
Infection/inflammation- assessment of the etiology of each wound, need for topical antiseptic and/or systemic antibiotic use to control infection, and management of inappropriate inflammation unrelated to infection.
Moisture imbalance- assessment of the etiology and management of wound exudate. Edge of wound: assessment of non-advancing or undermined wound edges (and state of the surrounding skin).

The debridement of the wound consists in the removing of necrotic or devitalized tissue and is essential for wound care. Methods of debridement used in clinical practice include surgical, autolytic, biological, and enzymatic approach. Surgical, also known as sharp debridement, is performed by excising necrotic tissue with surgical tools. Autolytic debridement involves either careful removal of spontaneously separated necrotic tissues or the use of moisture-retaining dressings to induce crust softening prior to its removal. Biological debridement uses larvae of the green blowfly species (maggot therapy). During enzymatic debridement, naturally occurring matrix-degrading enzymes are used [5, 16].

The available therapies can be classified in two major groups: (i) topical wound therapies / dressings and (ii) advanced therapies.

Topical wound therapies / dressings

A topical wound dressing should be suitable for the wound, for that an assessment of wound type and phase of healing is required [24]. In summary the wound dressing should: (i) have the capacity to provide thermal insulation, gaseous exchange, and to help drainage and debris removal thus promoting tissue reconstruction processes; (ii) should be biocompatible and not provoke any allergic or immune response reaction; (iii) should protect the wound from secondary infections; and (iv) should be easily removed without causing trauma [24, 25].

Initially, wound dressings were first considered to play only a passive and protective role in the healing process. However, in recent decades, wound treatment has been revolutionized by the discovery that moist dressings can help wounds heal faster. Moist is an important factor to induce the proliferation and migration of fibroblasts and keratinocytes as well as to enhance collagen synthesis, leading to reduced scar formation [24]. Cotton gauze dressing has been considered the standard of care for many years. Nevertheless, many other are commercially available, like foams, films, acrylics, alginates, hydrofibers, hydrocolloids, hydrogels, silver and honey alginates, among others, that are highly absorbent and moisture retaining, Table II [5, 23-27].

Table II. Common wound dressings and additives.

Dressing type	Description
Foam	Inert material which is hydrophilic and non-adherent, modified polyurethane foam
Transparent film	Polyurethane and polyethylene membrane film coated with a layer of acrylic hypoallergenic adhesive. Moisture vapor transmission rates (MVTR) vary
Hydrocolloid	Gelatin, pectin, carboxymethylcellulose in a polyisobutylene adhesive base with polyurethane or film backing. Hydrophilic colloid particles bound to polyurethane foam
Hydrogel	Water or glycerin-based, non-adherent, cross-linked polymer. May or may not be supported by a fabric net, high water content, and varying amounts of gel-forming material (glycerin, co-polymer, water, propylene glycol, and humectant)
Calcium alginate	Calcium sodium salts of alginic acid (naturally occurring polymer in seaweed). Nonwoven composite of fibers from a cellulose-like polysaccharide which acts via an ion exchange mechanism, absorbing serous fluid or exudate and forming a hydrophilic gel which conforms to the shape of the wound
Silver	Topical silver has broad spectrum antimicrobial activity that has been shown to be effective against many antibiotic-resistant wound pathogens and can be added to a variety of composite dressings
Honey	Use of or addition of certain honeys as a part of a variety of composite dressings. Honey provides a hypertonic environment thought to assist with microbial control

Different synthetic and natural polymer-based biocompatible materials, as well as their mixtures or combinations and different processing methodologies, have been proposed and assayed both *in vitro* and *in vivo* for wound dressing (and, in particular, DFUs) applications. Some of these materials are already commercially available and in clinical use (Table III) [24].

Furthermore, in order to enhance the general wound dressing activity the incorporation of bioactive compounds (e.g. growth factors, peptides, synthetic drugs and/or naturally based compounds / extracts) and stem cells has been tested. For example, Regranex®, a therapy that consists in recombinant human platelet-derived growth factor administrated in a gel (rhPDGF-BB incorporated in gel solution of aqueous sodium carboxymethylcellulose), is a bioactive product that has been designed to enhance skin regeneration (Table III) [24, 28].

Table III. Commercial dressings for DFU treatment.

Commercial dressing	Fabricant	Composition
Bionect®	Dara BioScience	0.2% of sodium salt of hyaluronic acid
Unite® Biomatrix	Synovis Orthopedic and WoundCare, Inc.	Non-reconstituted collagen
BGC Matrix®	Mölnlycke Health Care US, LLC	Collagen and the advanced carbohydrate beta-glucan
Promogran Prisma® Matrix	Systagenix	Collagen, ORC and silver-ORC matrix
Dermacol/Ag™ Collagen Matrix Dressing with Silver	DermaRite Industries	Collagen, sodium alginate, carboxyl methyl-cellulose, ethylenediaminetetraacetic acid (EDTA) and silver chloride
Fibracol® Plus Collagen Wound Dressing with Alginate	Systagenix	Collagen and calcium alginate fibers wound
Aquacel Hydrofiber® Wound Dressing	ConvaTec	Antimicrobial hydrofiber containing carboxymethyl cellulose with ionic silver

Table III. Commercial dressings for DFU treatment (cont.).

MediHoney® Adhesive Honeycolloid Dressing	Derma Sciences, Inc.	80% active Leptospermum honey with colloidal alginate
MediHoney® Calcium Alginate Dressing	Derma Sciences, Inc.	Contains 95% active Leptospermum honey with calcium alginate
Algisite* Calcium Alginate Dressing	Smith & Nephew, Inc.	Calcium-alginate
Sorbalgon®	Hartman USA, Inc.	Calcium alginate
Kaltostat® Dressing	ConvaTec	Sodium and calcium salts of alginic acid
Tegaderm™ High Gelling Alginate Dressing	3 M Health Care	Polyurethane dressing containing alginate
GranuDerm™ Sentry™	Acute Care Solutions, LLC	Alginate hydrocolloid with polyurethane
Biatain® Heel Foam Dressing	Coloplast Corp.	3-D non-adhesive foam of polyurethane
Biatain Ibu Foam Dressing Nonadhesive	Coloplast Corp.	Combination of polyurethane-foam, polyurethane film, polyethylene and ibuprofen
MANUKAhd®	ManukaMed USA, Inc.	Polyurethane foam and film in backing and an absorbent dressing pad of polyacrylate polymers impregnated with ManukaMed® honey
DuoDERM® CGF®	ConvaTec	Polyurethane foam
SOLOSITE® Conformable Wound Gel Dressing	Smith & Nephew, Inc	Polyurethane and polyethylene hydrogel
Silverlon® Island Wound Dressing	Argentum Medical, LLC	Polyurethane film containing silver
Allevyn	Smith & Nephew, Inc.	Polyurethane films combined with polyurethane foam containing 5% silver sulphadiazine.
Meliplex Ag	Molnlycke Heath Care	Polyurethane foam containing a silver compound (silver sulphate)
Ligasano	Ligasano	Honeycomb-polyurethane foam
Regranex® Gel	Healthpoint Biotherapeutics	rh PDGF-BB incorporated in aqueous sodium carboxymethylcellulose

Advanced therapies

Advanced therapies have been described to heal chronic wounds when conventional approach fails. These therapies include negative pressure based treatments, oxygen therapy, application of biophysical stimuli, the use of topic growth factors (e.g. PDGF, VEGF, FGF), skin substitutes, engineered skin, cell-based therapies (stem cells and vascular progenitor cells) and the use of hydrogels, such as hyaluronic acid [4, 16, 17, 23, 26, 29].

Wound care protocols advocate the use of standard measures for an initial period of 4 weeks, after which an assessment of wound area reduction should be made. Wounds failing to achieve a 50% area reduction at this time point need to be reassessed and subsequently considered for advanced therapies in the absence of underlying disease or nonadherence to prescribed basic treatment. Once it is determined that the patient might benefit from an advanced therapeutic agent, there are a number of options currently available, summarized in Table IV [23]. Advanced wound therapies can be categorized according to the underlying technology [23, 29].

1-Negative pressure wound therapy (NPWT). Since its introduction in the mid-1990s, negative pressure therapy has assumed a major role in management of traumatic, acute, and chronic wounds, as well as for stabilizing skin grafts, flaps, and surgical incisions [30-32]. As an adjunct to standard chronic wound care, NPWT very efficiently manages wound drainage and can provide expedited granulation tissue development, wound area contraction/reduction, preparation for delayed closure or grafting, or primary healing [33, 34].

2- Hyperbaric oxygen therapy (HBOT). HBOT has been advocated as being beneficial for a wide variety of chronic wounds for over two decades [35-38]. Nevertheless a review of HBOT in a large observational cohort study by Margolis, in 2013, found that the use of HBOT neither improved the likelihood that a wound would heal nor prevented amputation in patients with adequate lower limb arterial perfusion [39, 40].

3- Biophysical modalities. *Electrical stimulation* has been the most studied biophysical device for healing chronic wounds to date, primarily utilized by physical therapists and physiatrists [41-43]. Several studies advocate the beneficial healing effect of electrical stimulation at various modes and frequencies for a variety of chronic wounds [44-46]. Other non-thermal forms of electromagnetic energy have also been used for wound healing, including *pulsed radiofrequency energy* (PRFE), pulsed shortwave diathermy, and pulsed electromagnetic fields [47, 48]. In general, by interacting with endogenous bioelectric currents, electromagnetic fields indirectly upregulate the production of nitric oxide and multiple growth factors, resulting in cellular mobilization, angiogenesis enhancing wound repair [46]. *Ultrasound*, most frequently used for diagnostic and musculoskeletal therapy purposes, has also assumed a role in wound management. Several lower frequency devices are currently available for debridement that use the delivery of sound waves to generate cavitation at the wound bed [49, 50]. Wounds with thick fibrinous slough and necrosis can thereby be very aggressively debrided with low-frequency ultrasound (LFU) [49-52]. *Extracorporeal shock wave therapy* (ESWT) has been used for a number of years for a variety of musculoskeletal conditions and has recently been adapted for the treatment of cutaneous wounds. ESWT is defined as a series of high-energy acoustic pulses delivered to tissues by electrohydraulic, electromagnetic, and piezoelectric sources [53]. The pressure pulses generated promote a cascade of cytokine and growth factor upregulation leading to enhanced neovascularization, anti-inflammatory response and tissue regeneration [54, 55].

4- Biological and bioengineered therapies. Biological therapies refer to tissue-based treatments (acellular and cellular), autologous platelet-rich plasma (PRP), as well as recombinant human growth factor therapies. Despite the enormous amount of preclinical research on cytokine and growth factor-mediated wound-repair, currently only a few are available to clinicians: human PDGF, FGF and EGF. Numerous other growth factors have been investigated, such as VEGF, KGF-2, TGF-β and granulocyte-macrophage colony-stimulating factor (GM-CSF), but these currently are not approved for use in wound care [56, 57].

Platelet-rich plasma (PRP) and growth factors. Autologus PRP application makes use of a cascade of growth factors released from activated platelets during the centrifugation of whole blood, which the topical application enhances healing of chronic lower extremity wounds [58-61]. Based on the potential benefit of topically applied PDGF to chronic wounds, becaplermin gel (rhPDGF) was studied in the setting of chronic neuropathic DFUs and became the first commercially available advanced therapy for the management of chronic wounds (it is the only growth factor approved for use in the US and EU – European Union) [28, 62]. The rhEGF growth factor is one of the best studied for cutaneous ulcers and wounds. The use of rhEGF in

a clinical setting is available only in Cuba. EGF has been found to enhance the healing of a variety of types of cutaneous wounds when applied as a topical cream, or more commonly, by intralesional injections [63-66]. FGF has been studied primarily in Asia for a variety of chronic wounds and is approved in Japan for this use [67]. FGF, considered a potent angiogenic growth factor, also has an isoform (FGF-10) commonly known as KGF-2 or repifermin [57, 68, 69]. The topical application of this factor has been evaluated in the US for chronic venous leg ulcers (VLUs). The results showed an acceleration in the wound healing [68].

Acellular therapies. These therapies are based in the application of decellularized matrixes including dermal, amniotic or collagen. Often referred as acellular and/or ECMs, these biological products serve as substrates into which cells can migrate and initiate angiogenesis, thereby promoting granulation tissue development and tissue regeneration [70]. ECMs are now known to play an active part in tissue regeneration through a dynamic interaction with growth factors and host cells [71, 72]. ECMs contain structural collagen, glycosaminoglycans, proteoglycans, and glycoproteins—all essential components to replace the defective ECM of injured tissues [73]. Human dermal allografts have become increasingly popular in recent years for augmenting tissue regeneration in chronic lower extremity wounds, like DFUs and VLUs. The allografts are harvested from screened donors, and each is prepared with proprietary processes to decellularize and cryopreserve the dermis while maintaining the natural structure of the ECM [74-77]. Amniotic membranes (AMs) and umbilical cord tissues (UCT) are the earliest reported biomaterials used for wound repair. Likely due to the wide availability of placental tissues after cesarean deliveries. Due to their rich cellular content in the native state, AMs contain a number of cytokines and growth factors bound to the ECM after decellularization and preparation that remain available to augment angiogenesis and tissue repair when implanted into chronic wounds [78, 79].

Bioengineered cellular therapies. Two allogeneic bioengineered skin replacement therapies based in neonatal expanded cells are approved in the US for chronic wound treatment. Apligraf® is a bilayered construct consisting of a bovine collagen matrix seeded with living human neonatal fibroblasts and a neonatal keratinocyte neoepidermis [80-82]. Dermagraft®, a human fibroblast-derived dermal substitute, is a cryopreserved, absorbable, three-dimensional polyglactin mesh substrate seeded with living neonatal dermal fibroblasts [83, 84]. Similar to the bilayered skin replacement, these cells secrete a host of growth factors, cytokines, matrix proteins, and glycosaminoglycans that induce tissue regeneration through the development of granulation tissue and ingrowth of host fibroblasts and keratinocytes [84, 85].

Stem cell therapies. Mesenchymal stem / stromal cells (MSCs) have been tested for wound healing applications. MSCs are multipotent progenitor cells that can directly differentiate into mesenchymal tissues, such as bone, tendon, and cartilage. It is believed that MSC ability to improve cutaneous repair is by an indirect paracrine function. MSCs synthesize and secrete essential growth factors and cytokines that affect cell migration, proliferation, and metabolic activity of host cells and tissues [86, 87]. In this manner, MSCs play an active role in the inflammatory, proliferative, and remodelling phases of wound repair. Of special interest are the placental tissues—including the umbilical cord, the amnion, and the chorion— as a rich source of MSCs that are readily available without the ethical concerns of embryonic stem cells [88, 89]. Furthermore, the MSCs in these tissues do not suffer from the age-related effects nor decreased cell counts as found in MSCs harvested from adult patients with comorbid diseases [23, 87, 90].

Table IV. Advanced wound care technologies *[23].*

- Negative pressure wound therapy
  - Standard electrically powered—VAC®
  - Mechanically powered—SNaP®
- Hyperbaric oxygen therapy
  - Topical oxygen therapy
- Biophysical
  - Electrical stimulation, diathermy, pulsed electromagnetic fields
  - Pulsed radiofrequency energy
  - Low-frequency noncontact ultrasound—MIST®
  - Extracorporeal shock wave therapy–DermaPACE®
- Growth factors
  - Becaplermin—platelet-derived growth factor—Regranex®
  - Fibroblast growth factor (Japan)
  - Epidermal growth factor (Cuba)
  - Platelet-rich plasma
- Acellular matrix tissues
  - Xenograft dermis
    - Primatrix®–bovine neonatal dermis
    - Integra®–bovine collagen
    - Matriderm®–bovine dermis
  - Xenograft acellular matrices
    - Oasis®–small intestine submucosa
    - Matristem®– porcine urinary bladder matrix
    - Ovine forestomach—Endoform®
    - Equine pericardium
  - Human dermis
    - Graftjacket®
    - D-cell®
    - DermACELL®
    - Theraskin®
  - Human pericardium
  - Placental tissues
    - Amniotic tissues/amniotic fluid
    - Umbilical cord
    - Dehydrated human amnion/chorion membrane (dHACM)—Epifix®
- Bioengineered allogeneic cellular therapies
  - Bilayered skin equivalent—Apligraf®
  - Dermal replacement therapy—Dermagraft®
- Stem cell therapies
  - Autogenous—bone marrow-derived stem cells
  - Allogeneic—amniotic matrix with mesenchymal stem/stromal cells—Grafix®
- Miscellaneous
  - Hyalomatrix(R) (Hyaluronan)

Despite all the efforts made to better understand the pathophysiology of chronic wounds and the advances in wound care therapies, some wounds remain nonresponsive to current therapies and no new therapy has received FDA efficacy approval for the treatment of chronic wounds since 1997, despite the large number of treatments receiving FDA approval for safety [21, 23, 27, 91]. The development of a new therapy is costly and time consuming, the clinical trials aim to demonstrate more efficacy than the standard of care in a challenging environment of complex wound biology (size, duration, position, infection, etc.) and patient co-morbidities (such as diabetes, cardiovascular disease, age, etc.), being the full wound clousure the primary output accepted by the regulatory agencies, versus functional recovery, which means a reduced social and economic impact for healthcare systems and societies [7, 8, 21, 91, 92].

Development and implementation of wound management strategies, better designed studies and clinical trials, and clear guidelines for therapy efficacy evaluation, considering the benefits for the patients, is required for the implementation of more efficacious therapies and improvement of wound care status [8, 23, 91-93]. Becaplermin gel was a significant advance in diabetic foot ulcers whith very promising results. Nevertheless, its usage in a rotine is still not established due mainly to the high cost and the need for continued administration [93]. In fact, topically applied growth factors are easily degraded in the hostile environment of diabetic wounds and therefore have transient effects [93, 94].

The use of stem cells for therapeutic purposes is limited by many risk factors such as tumor formation, thrombosis, and unwanted immune responses [95-97]. Additionally, one of the major draw-backs is that transplanted cells present low survival and engraftment rates in the injuried area. To overcome these limitations cells can be incorporated in a biomaterial that can offer protection from the inhospitable environment of the wound, increasing cell viability and availability, enhancing their therapeutic effect and significativelly improving wound healing [26, 98-102].

The field of biomaterials for wound healing applications presents exciting opportunities. Nevertheless, the development of biomaterial-based therapies for chronic wounds, for application as a standalone therapy or as a complex therapy where the biomaterial acts as a scaffold for encapsulating pro-healing factors, faces limitations such as, the limited supply (particularly in the case of natural biomaterials), the manufacturability (associated with the increasing level of complexity), the toxicity and biocompatibility of the materials with the host tissue [103, 104].

4. Development of new therapies for chronic wounds

An advanced therapy for chronic wounds should be more efficacious as the standard of care. With this objective, scientists from different research areas, from pharmaceutics to biomaterials, nanotechnology, bioengineering and stem cells, have been studying new approaches for chronic wound healing, either by developing new more effective dressings, ppliying more effective therapeutical agents, or by improvement of the administration route and bioavailability of the therapeutic agents (nanoparticles, antimicrobial agents, cell derivatives, stem cell / cell progenitors, etc…), either as a standalone therapy or as a conjugated therapy based on two or more of these technologies combining therapeutic agents [24, 26, 101]. For example, advanced wound therapies on different biomaterials have been used as an approach for treatment of chronic wounds as dressings and scaffolds for native

cells, improving skin tissue regeneration, but also, as drug delivery systems, matrixes to encapsulate bioactive components, such as proteins (e.g. Growth-factors) and cells, and /or nanoparticles with wound healing properties [24-26, 98, 101, 103, 105-107].

Biomaterial-based therapies

The biomaterials can be of three sources: metallic, ceramic and polymeric [26]. Hydrogels are hydrophilic polymer-based biomaterials that have been used very often in the context of wound healing. The mechanical properties of hydrogels, stiffness, viscoelastic behavior, and initial state recovery (self-healing) are tunable by copolymerization, nanoparticle incorporation, and changing the polymer(s) concentrations and ratios. Various hydrogels based on alginate, collagen, agarose, hyaluronic acid (HA), and chitosan, among others materials, have been synthesized by using physical crosslinking approaches for engineering different tissues [26, 103, 105, 108, 109]. Hydrogel 3D structure offer stability to the incorporated bioactive components, such as growth factors, vesicles and nanoparticles, increasing their bioavailability in the wound. For example, hydrogels provide an appropriate scaffold for cell migration and encapsulation due to their 3D matrix, high levels of water content, physical characteristics that resemble the native extracellular matrix and their biodegradability properties. Additionally, hydrogels biomimetic structures that mimick the natural microenvironment of cellular tissues, enable cell–cell interactions and interactions with the surrounding tissue [26, 103, 105, 108, 109].

Hydrogels have been widely used as a standalone therapy or in combination with other therapeutic agents. For example, a dextran-based hydrogel consisting of UV-cross-linked dextran-allylisocyanate-ethylamine and polyethylene glycol diacrylate polymers was demonstrated to be able to promote skin regeneration in a third-degree burn wound mouse model [110]. Glycosaminoglycan-based hydrogels have the ability to capture inflammatory chemokines in the wound, thus controlling inflammation and enhancing healing [111]. A hydrogel based on carrageenan-coated starch / cellulose nanofibers promote blood clotting, thus promoting hemostasis and hemorrhage control [112]. A hypoxia-inducible (HI) hydrogel composed of gelatin and ferulic acid was able to guide vascular morphogenesis in vitro via hypoxia-inducible factors activation of matrix metalloproteinases (MMPs) and promote rapid neovascularization in the host tissue improving subcutaneous wound healing [113]. Hydrogels with variable lengths of polypeptides linked to polyethylene glycol (PEG) have been shown to have both antibacterial and cell adhesive properties [114]. The incorporation of an antibiotic in a PEG hydrogel was able to maintain a sustained antimicrobial activity by light – controlled release of the antibiotic in the wound [115]. The encapsulation of growth factors [116-119], nucleic acids [120], cells [121, 122] and extracellular vesicles (EVs) [123-126] in different types of hydrogels has shown improved wound healing and skin regeneration versus the single application of the biomaterial or bioactive component.

Another class of biomaterials with high expression in terms of wound healing are nanomaterials including nanocapsules, nanoparticles, nanofibers and nanosheets [24, 26, 101]. This was due to their high surface area, ability to penetrate the skin, capacity to increase drug solubility, targeted drug delivery, among others. Nanocapsules have a core-shell structure with the inner core cavity acting as a reservoir of the drug or biomolecule and the shell composed of a polymeric or lipid support material. Polymeric nanocapsules, lipid core nanocapsules and

liposomes are generally classified as nanocapsules. Polymers such as polylactic acid, polylactic-co-glycolic acid (PLGA), poly (D, L-glycolide), poly-L-lactide (PLA), polycaprolactone (PCL), chitosan, gelatin and alginate have been used for nanocapsule preparation. Polymeric nanocapsules are inert and do not pose much compatibility issues. Sustained release, improved drug bioavailability and decreased drug toxicity are few of the advantages of this system. However the drug loading in these polymeric nanocapsules is low, as the percentage of the polymer is much higher than its drug counterpart [24, 26, 101]. Nanoparticles can be engineered into various shapes like spherical, cubical, hollow or core shell from inorganic or polymeric materials. Nanofibers are synthesized from natural (collagen, gelatin, elastin, chitosan, fibrinogen, laminin, hyaluronic acid) or synthetic polymers (polylactide-co-glycolide (PLGA), poly acrylic acid-poly pyrene methanol (PAAPM) and poly(caprolactone) (PCL). The method of fabrication of these nanomaterials include electrospinning, self-assembling and phase separation [24, 101].

Nanomaterials may play different roles during wound healing, including the control of infection, immune response, regeneration, among others. For example, some nanomaterials, such as silver, copper and zinc exhibit antibacterial properties in their bulk form, other metals like iron oxide, titanium dioxide are antibacterial in nanoparticulate form [26, 101]. For example, thrombin plays a major role in the process of coagulation, and its bioavailability can be enhanced by conjugating it with iron oxide nanoparticles [119, 127]. Other nanomaterials containing biomolecules such as peptides [128], proteins [26, 101] or gases (e.g. nitric oxide) [129-131] are very effective in enhancing wound healing. Nitric oxide (NO) is a small radical synthesized during the early phase of wound healing by inflammatory cells, acting as a antimicrobial agent and promoting wound healing by modulating collagen formation, cell proliferation, angiogenesis and wound contraction [129-131]. Nanomaterials have been engineered to facilitate the storage and delivery of this gas to wounds. For example, a silane based hydrogel/glass composite allowed NO to be maintained within the dry nanoporous matrix until exposure to moisture, that open the water channels inside the particles, facilitating the release of NO for an extended period of time [129, 131]. Nanomaterials can also modulate the immune response by the delivery of anti-inflammatory drugs or molecules suppressing immune response [101]. Nanofiber/sponges mimicking the ECM containing nanoparticles loaded with anti-inflammatory drugs enhanced wound healing by the sustained release of anti-inflammatory cytokines [132]. Finally, nanomaterials such as nanofibers may be used for the delivery of proteolytic enzymes to enhance wound debridement [133]. Some examples of biomaterials application in chronic wounds as standalone therapies or conjugated with bioactive molecules are presented in Table V.

Table V. Biomaterials based therapies for wound healing.

Type of material	Molecule	Mechanism of action	Outcomes	Model	Ref.
Dextran-based hydrogel	_	Increased cell infiltration into the wound	↗ skin regeneration in 3rd degree burn wound	Wistar rats wound model	[110]
Glycosaminoglycan-based hydrogels	_	Capture inflammatory chemokine	↘ inflammation ↗ wound healing	Db/db mice wound model	[111]
Gelatin and ferulic acid hypoxia-inducible (HI) hydrogel	_	Controllable and stable hypoxic environment	↗ neovascularization	Sprague dawley rats and C57/6 mice	[113]

Table V. Biomaterials based therapies for wound healing. (Cont.)

Microporous gel scaffold	_	Increased cell migration and infiltration into the wound	↗ tissue structure and regeneration ↗ wound healing	BALB/c mice wound model	[107]
Silane based hydrogel	Nitric Oxide (NO)	Increased and sustained NO bioavailability	↘ wound infection and inflammation ↗ wound healing	BALB/c mouse wound / skin infection model	[129] [131]
Gold nanoparticles	Antimicrobial peptide (LL37)	Antibacterial action Keratinocyte migration	↘ wound infection ↗ wound healing	RjHan:NMRI mice wound model	[128]
Iron oxide nanoparticles	Thrombin	Increase thrombin bioavailability - promotion blood clotting	↗ hemostasis	Wistar rats wound model	[127]
Collagen latice	PDGF-B and PDGF-A plasmids	Increased PDGF-B and PDGF-A bioavailability	↗ wound healing (granulation tissue formation and epithelialization)	Dermal ulcer wound rabbit model	[134]
Cationic liposomes	FGF plasmid	Increased FGF expression and bioavailability, upon cell transfection.	↗ wound healing (re-epithelialization and regeneration of connective tissue)	Db/db mice wound model	[135]
Photocrosslinkabe chitosan hydrogel	FGF-2	Sustained delivery of FGF-2	↗ wound healing (contraction, epithelialization, and tissue filling)	Db/db and db/+ mice wound model	[116]
Dextran hydrogel	EGF, IGF-I, PDGF-A, bFGF, QCN + O_2	Sustained delivery of growth-factors, quercetin and oxygen	↗ wound healing (re-epithelialization and regeneration of connective tissue)	Db/db mice wound model	[117]
Dextran hydrogel with chitosan spherical microparticles	VEGF and EGF	Sustained delivery of growth-factors	↗ wound healing (production of new extracellular matrix and angiogenesis)	Wistar rats burn wound model	[118]
Hyaluronic-based porous hydrogels	VEGF plasmid	Increased cell infiltration and angiogenesis	↗ wound healing	Db/db mice wound model	[119]
Hyaluronic Acid – MMP porous hydrogel	VEGF plasmid	Increased VEGF expression and bioavailability, upon cell transfection.	↗ wound healing ↗ granulation tissue formation	Db/db mice wound model	[120]
β-cyclodextrin and poly(amidoamine) cationic star-shaped polymer	MMP-9 siRNA	Reduced MMP-9 expression in skin fibroblast cells, upon cell transfection.	↗ wound clousure	Sprague Dawley rats diabetic (STZ) wound model	[136]
Photolabile cage	Anti-miR-92a	downregulate miR-92a and derepresses its targets Itga5 and Sirt1, upon cell transfection.	↗ wound healing (cell proliferation and angiogenesis)	Db/db mice wound model	[137]

QCN – quercetin (naturally occurring flavonoid found in vegetables, tea, and berries. It has anti-ulcer, -inflammatory, and -infective activities due to its ability to scavenge oxygen free-radicals and inhibit lipid peroxidation.) **O_2** – oxygen molecules.

Cytokine and growth factor-based therapies

Cytokines and growth factors govern the progression of the healing process through the modulation of the cellular and molecular components involved in proliferation and skin restoration [138, 139]. Chronic wounds show decreased levels of several growth factors, like EGF, FGF-2, TGF-β, PDGF and VEGF, and cytokines, IL-1, IL-6 and TNF-α, known to regulate several skin cells activity. The down regulation in the expression of growth factors and cytokines impair wound healing process at different stages, from inflammation to granulation tissue formation, reepithelization and remodeling [139]. Based on these findings several growth factors were tested as topical treatments to enhance wound healing (Table VI –

adapted from [56] and [23]). For example, a topical spray with KGF-2 (or FGF-10), a potent angiogenic growth factor, has been studied in the United States [23, 68]. However, these growth factor therapies have shown limited success in clinical trials (Table II), reviewed in [23].

Table VI. Growth factor therapies for chronic ulcers.

Growth factor	Mechanism of action	Outcomes	Phase	Ref.
EGF	Mitogenic effect on keratinocytes, fibroblasts.	↗ healing of human acute wounds and ulcers.	Clinical use in Cuba	[63-65, 138, 140]
FGF	Cellular proliferation, migration, angiogenesis and morphogenesis.	↗ healing in rats; ↗ healing human pressure ulcers.	Clinical use in Japan.	[67, 138, 141, 142]
KGF – 2 ***Topical spray***	Selective action on epithelial cells, fibroblasts recruiting.	↗ granulation tissue; ↗ healing human ulcers.	Clinical trial.	[57, 68, 69]
PDGF	Proliferation of fibroblasts and smooth muscle cells.	↗ granulation tissue; ↗ healing human ulcers.	Clinical use in USA + EU.	[28, 62, 143]
GM-CSF	Neutrophils proliferation and enhanced activity.	↗ healing human venous ulcers.	Clinical trial.	[57, 144, 145]
TGF-β	Stimulates fibroblasts and endothelial cells.	↗ healing in animal models.	Pre-clinical.	[57, 138]
FGF-2 ***Chitosan hydrogel***	Cellular proliferation, migration, angiogenesis and morphogenesis	↗ healing in animal models	Pre-clinical	[116]
EGF, IGF-I, PDGF-A, bFGF + QCN + O_2 ***Dextran hydrogel***	Enhanced scratch clousure rate (*in vitro*) Stimulation of reepithelialization and regeneration of connective tissue (*in vivo*).	↗ healing in animal models	Pre-clinical	[117]
VEGF, EGF	Stimulates production of new extracellular matrix and promote angiogenesis	↗ healing in animal models	Pre-clinical	[118]

QCN – quercetin (naturally occurring flavonoid found in vegetables, tea, and berries. It has anti-ulcer, -inflammatory, and -infective activities due to its ability to scavenge oxygen free-radicals and inhibit lipid peroxidation.) **O_2** – oxygen molecules

The immobilization of growth factors on biomaterials may increase their life-time and controlled release in the wound [93, 106, 146]. PDGF-BB daily treatment for chronic pressure ulcers was first described in 1992, in a phase I/II, double-blind, placebo controlled study, where patients treated with 100 µg/mL presented significantly better healing than the placebo group [147, 148]. More recently, rhPDGF administration in a gel wound dressing presentation (becaplermin gel) has been shown to increase significantly the effect of this growth factor in chronic neuropathic ulcers, becoming the first FDA approved advanced therapy for chronic wound management [23, 28, 56, 93]. Nevertheless, this approach still requires daily application [56]. Sustained delivery of growth factors may reduce the need for frequent application by incorporation in hydrogels, for example, a photocrosslinkabe chitosan hydrogel containing FGF-2 improve wound closure in diabetic mice [116]. The combination of several growth-factors and other molecules as also been tested with promising results, reducing the interval of application from 2 to 7 days [117]. The combination of different biomaterials can also be a strategy to improve growth factor delivery and effect in chronic wounds. For example, a dextran hydrogel loaded with chitosan spherical microparticles containing VEGF and EGF, demonstrated significant improvement of wound healing versus the administration of free VEGF and EGF every two days [106, 118].

DNA and RNA-based therapies

Gene expression profile studies during the cutaneous wound healing has motivated the development of gene delivery strategies to facilitate wound healing [149]. DNA-based therapeutics may restore the expression of growth factors or inhibit the expression of upregulated genes (e.g. MMP-9); however, the delivery of these therapies is still a major issue. They may be deliver by viral vectors including recombinant retrovirus, adenovirus and herpes simplex virus-1, and non-viral techniques, such as direct application, injection (followed or not by electroporation), plasmid DNA and nanoparticles [150]. For example, an adenoviral mediated gene transfer of PDGF-B was found to enhance wound healing in type I and type II diabetic animal model [151]. Electroporation of the wound after direct injection of KGF-1 DNA plasmid was also able to accelerate wound closure [152]. Biomaterial-based delivery systems may enhance the uptake of DNA-based therapies by reducing degradation and improving control of the treatment dose [26, 101]. For example, collagen matrixes encapsulating DNA encoding the PDGF-BB gene were effective in accelerating wound healing in ischemic dermal ulcers in New Zealand white rabbits [134]. In addition, hyaluronic acid-based porous hydrogels containing a MMP-degradable linker to VEGF plasmid DNA resulted in enhanced wound healing in mice, due to cell infiltration of the hydrogel upon matrix degradation [120]. Moreover, a plasmid encoding FGF encapsulated in cationic liposomes improved wound healing in db/+ and db/db mice [135]. Gene modulation may also be obtained by manipulating the patient cells *in vitro* with a vector containing the therapeutic DNA of interest, selecting the transfected cells and then administrating the transgenic cells into the patient, which can be done by incorporation in biodegradable matrix (biological, synthetic) that is applied in the patient wound. This approach conjugates gene and cell therapy techniques [150].

RNA-based therapeutics, including siRNA, lncRNA, piRNA, miRNA or shRNA, are under intense scrutiny of the scientific community for wound healing applications. Small interfering RNA (siRNA) can provide gene-specific silencing and present a safe and effective way for knockdown of inflammatory or other target proteins in chronic skin wounds. The silence of MMP-9 by siRNA complexed on cationic star-shaped polymers improved wound healing on diabetic mice [136]. Micro RNAs (miRNAs/miRs) constitue a very appealing therapy because they target multiple genes at the same time regulating multiple biological events. Imbalance on miRNAs levels have been observed in chronic / diabetic wounds versus acute wounds, such as miRNAs from the let-7 family, miR-16, miR-21 and many others [153-156]. Nevertheless, despite the progresses, the research in this area is still in an embryonic status and still little is known about miRNAs delivery, stabilization in the wound and full impact of its administration [156, 157]. MiRNAs display many common features with small interfering RNA (siRNA), sharing several molecular machineries and similar mechanisms of action. Thus, technological solutions adopted for therapeutic protocols using siRNA may find use for miRNAs as well [157]. Two studies report induction of miRNA overexpression, both related with miR-21 effect in acute wound models. In the first work miR-21 was administrated in phosphate buffered saline solution (PBS) directly in the rat skin, previously (2 days) to wound infliction, this treatment inhibited epithelization and granulation tissue formation [158]. In the second reported an injection of miR-21 expressing plasmid in the wound edge, after wound creation, enhanced wound contraction and granulation tissue formation [159]. These contradictory findings may be explained by several reasons including the time of administration (skin conditioning can occur by the administration previously to wounding) to the effective quantity of miRNA

delivered to the cells and intrinsic differences of the animal model used. In fact, the knockdown of endogenous miR-21 by a specific antagomir delayed wound reepithelization in mice [160]. On the other end, the inhibition of miR-21 in a hypertrophic scar model reduced collagen deposition [161]. Inhibition of miRNA expression by different approaches have been reported by different groups to enhance wound healing, namely, miR-26a, which the down-regulation was achieved by LNA-anti-miR injection prior to wounding, and miR-92a, inhibited by topically application of a specific anti-miR entrapped in a photolabile protecting cage followed by skin irradiation ten minutes after [137, 162].

Cell-based therapies

Stem cells might be a promising therapy for several skin pathologies. Stem cells therapies can be categorized based on their source of procurement into allogenic (donor and recipient are different persons) and autologous (donor and recipient are the same person). Stem cells for allogenic applications include placental or amnion-derived mesenchymal stem/stromal cells (A-MSCs), pluripotent stem cells (PSCs), endothelial progenitor cells (EPCs), bone-marrow (BM), umbilical cord blood (UCB) and umbilical cord (UC, wharton jelly) mesenchymal stem/stromal cells (MSCs), BM and UCB hematopoietic stem cells (HSCs), mesenchymal stem/stromal cells derived from adipose tissue (ASCs) and skin and hair follicles stem cells. Stem cells from various sources have been used to modulate the healing response of acute and chronic wounds [86, 88, 89, 98-100, 163-176]. MSCs and ASCs are able to regulate and control the inflammatory state of the wound [88, 89, 98, 165, 169], recruit endogenous stem cells, progenitor cells and somatic cells to the wound site [86, 88, 98, 165-169] and engraft in the wounded tissue [86, 98, 99, 165, 166, 168], where they can differentiate into several different cell types helping to restore the skin tissue. HSCs exert a pro-angiogenic effect and once engrafted can differentiate into endothelial cells [99, 170]. Mononuclear cells (MNCs), which include HSCs, or BM lysates are also used for wound healing applications [171]. EPCs promote wound healing by releasing pro-angiogenic factors and/or by the differentiation into endothelial cells (ECs) [98, 99, 163, 174, 175]. Table VI displays examples of cell-based therapies for wound healing.

Table VII. Cell-based therapies for chronic wounds.

Cells	Biomaterial	Condition	Model	Outcomes	Ref
UCB-MNCs	**Fibrin platelet glue**	Chronic wounds	Human patients	↗ wound healing	[172]
BM-MSCs	**_**	Chronic wounds	NOD/SCID mice	↗ wound closure and epithelization	[165]
UC-MSCs	**_**	Diabetic wounds	Db/db mice	↗ wound closure and angiogenesis	[167]
BM-MSCs	**_**	Diabetic and acute wounds	BALB/c; db/db mice + normal littermates	↗ wound closure and epithelization	[166]
BM-MSCs	**Fibrin polymer spray**	Diabetic and acute wounds	human and C57BL/6 and db/db mice	↗ wound closure; ↘ chronic wound size	[177]
BM-MSCs	**Polyethylene glycol diacrylate (PEGDA) hybrid hydrogel**	Diabetic wounds	C57BKS Cg-m+ /+ $Lepr^{db}$	↗ wound closure, granulation tissue and ECM formation, angiogenesis, and reepithelialization	[121]

Table VII. Cell-based therapies for chronic wounds. (Cont.)

PB-MNCs	**_**	Diabetic wounds	Diabetes I nude mice (STZ)	↗ wound closure and vascularization	[170]
UCB-MNCs	**_**	Diabetic wounds	Diabetes I rat model (STZ)	↗ wound closure and epithelization	[171]
PB-HSCs	**_**	Diabetic wounds	Diabetes I nude mice (STZ)	↗ wound closure and vascularization	[170]
UCB-HSCs	**_**	Diabetic wounds	Diabetes I rat model (STZ)	↗ wound maturation	[173]
UCB-HSCs UCB-HSCs +dECs	**Fibrin gel**	Diabetic wounds	Diabetes I mice (STZ)	↗ wound healing	[174]
Mature B cells	**_**	Diabetic and acute wounds	C57BL/6 & B6.BKS(D) – *Lepr^{db}* /J mice	↗ wound closure	[178]
BM-MSCs	**Composite silk nanofiber hydrogel + microgels**	Acute wounds	Sprague-Dawley (SD) rat	↗ wound healing, angiogenesis ↘ inflammation	[122]
UC-MSCs, UCB-MSCs	**_**	Acute wounds	Nude mice	Less scar of the wound, ECM remodeling	[89]
ASCs	**Cytocare ® 532 (HA solution)**	Acute wounds	Nude mice	↗ wound closure and maturation	[169]
ASCs	**Collagen gel**	Acute wounds	BALB/c nude mice	↗ wound closure and scar thickness	[179]
Expanded UCB-HSCs	**Nanofiber mesh**	Acute wounds	NOD/SCID mice	↗ wound healing ↘ inflammation	[180]
PB-EPCs	**_**	Acute wounds	Athymic nude mice	↗ wound maturation and vascularization	[175]
Dermal fibroblasts	**Collagen gel**	Acute wounds	BALB/c nude mice	↗ wound closure and scar thickness	[179]
BM-MSCs	**Collagen-chitosan sponge scaffold**	Hindlimb ischemia	Diabetes I rat model (STZ)	↗ wound closure and angiogenesis	[181]
ASCs	**_**	Radiation ulcers	Sprague-Dawley (SD) rat	↗ wound closure and vascularization	[168]

BM - Bone marrow; **UC** - Umbilical cord (Wharton jelly); **UCB** - Umbilical cord blood; **PB** - Peripheral blood; **MNCs –** mononuclear cells; **MSCs** - Mesenchymal stem/stromal cells; **ASCs** - Adipose tissue stem cells; **HSCs** - Hematopoietic stem cells; **dECs –** UCB-HSCs derived endothelial cells; **EPCs** - Endothelial progenitor cells.

The major limitation of cell-based therapies is low cell survival and cell engraftment. To overcome this, biomaterials have been used for encapsulating cells [26, 98-101]. For example, autologous BM-MSCs delivered in a fibrin spray accelerate healing in murine and human cutaneous wounds [177]. Expanded human UCB-derived $CD34^+$ (HSCs) cells administrated on a nanofiber mesh to the wounds inflicted in immunocompromised murine model (NOD/SCID) increased wound healing by attenuating the pro-inflammatory factors [180]. A biocompatible multifunctional crosslinker based temperature sensitive hydrogel developed to deliver BM-MSCs promoted granulation tissue formation, angiogenesis, extracellular matrix secretion, wound contraction, and re-epithelialization [121]. A composite of silk nanofiber hydrogels and MSC-laden microgels increased wound healing and form scarless tissues with hair follicles, by protecting and stabilizing MSCs in the wound, promoting angiogenesis and M1-M2 phenotype switching of macrophages [122]. Furthermore, hypoxia pretreatment of a skin substitute composed of BM-MSCs seeded in collagen-chitosan sponge scaffolds accelerated wound closure via reduction of inflammation and promotion of angiogenesis in diabetic rats with hindlimb ischemia [181]. More examples can be found on Table VI.

Several registries of cell therapies clinical trials for wound healing, all over the world. A total of 33 studies were found when searching for 'cell therapy' + 'chronic Ulcer' in clinicaltrials.gov, Figure - 3 [182]. Of the 33 clinical trials found, 31 were interventional and 2 were observational studies. In the majority of the interventions (9), bone marrow or peripheral blood cells were administrated, which include one trial in Phase III (Treatment of Chronic Critical Limb Ischemia with G-CSF-mobilized Autologous Peripheral Blood Mononuclear Cells – NCT01853384). Adipose derived stem cells (2) and mesenchymal stem/stromal cells (1) were administrated in 3 trials. The search also included 3 studies in which platelet rich plasma (PRP – 2 trials) or platelet gel (1 trial in phase III, NCT00273234) was applied. Skin grafts have been evaluated in 3 different trials, one in phase III (NCT00368693). Several studies for commercial labelled therapies were found (7), 3 in phase III (NCT01421966; NCT02130310; NCT01853384) and one already in phase IV (NCT01596920).

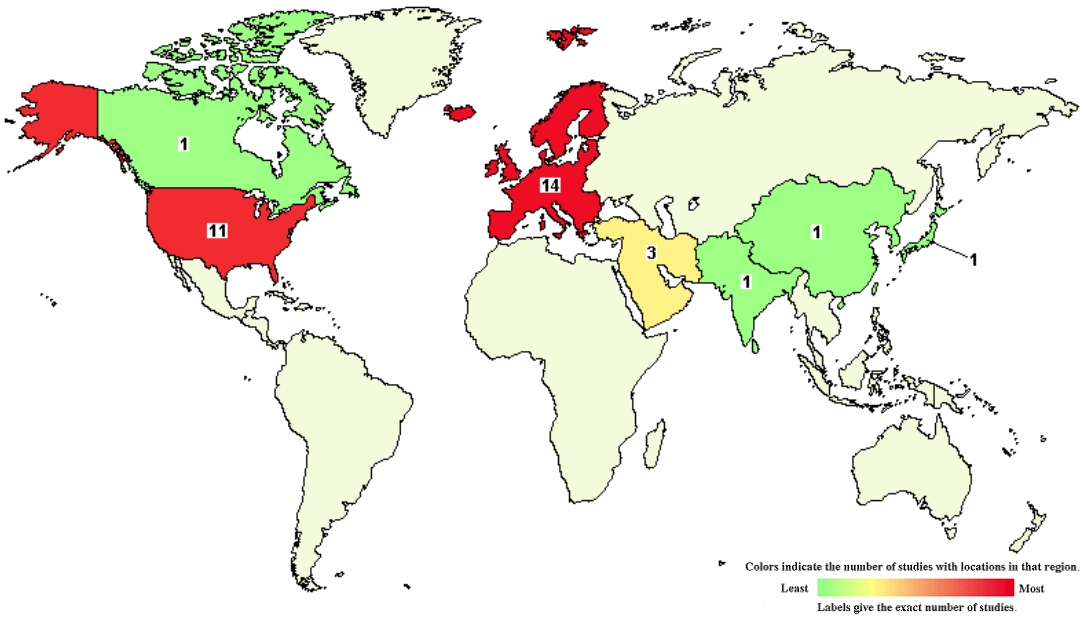

Figure - 3. Registered clinical trials of cell therapies for Chronic Ulcers.
The map presents the locations of 33 Studies found for the following research terms: 'cell therapy' + 'chronic Ulcer'. Data from clinicaltrials.gov accessed in 2018 Jan 26. Studies with no locations are not included in the counts or on the map. Studies with multiple locations are included in each region containing locations [183].

The regenerative effect of cell-based therapies seems to be related to their paracrine effect than cell engraftment effect [98, 163, 184]. For example, the application of BM-MSCs or BM-MSC-conditioned media was found to enhance wound reepithelization and increase endothelial cell tube formation [165, 166]. In addition, UCB-MSC- conditioned media was able to induce accelerated wound closure and angiogenesis in db/db mice wounds [167]. Moreover, UCB-HSCs ($CD34^+$ cells) administration on rat diabetic wounds improved wound healing by increasing FGF1, IL-1, TGF-β and VEGF expression [173]. Interestingly, the wound healing after topical administration of UCB hemodialysate on streptozotocin (STZ) induced diabetic rat wounds was higher than the injection of UCB-MNCs in the wound. Indicating the present of micro- or nano-soluble components with pro-healing bioactivity [171]. Peripheral blood (PB) MNCs secretome (APOSEC^{TM}) has been also studied for chronic wound healing purposes. APOSEC^{TM} enhanced skin regeneration and vascularization in a mice wound-healing model and porcine skin third degree burn model and a Phase I clinical trial have recently demonstrated the safety and tolerability of this product in healthy volunteers with artificial dermal wounds, although it did not affect wound closure [185-187].

Extracellular-vesicle-based therapies

The application of cell paracrine factors seems to be a good alternative to the transplantation of cells because they do not present constrains related to low cell retention and poor survival [184, 188, 189], they offer no risk of aneuploidy, and they are relatively easy to process and have a competitive cost [188-190]. Extracellular vesicles (EVs) are membrane-enclosed vesicles that are released into the extracellular environment by various cell types, which can be classified as apoptotic bodies, microvesicles and exosomes [191-197]. Apoptotic bodies are the largest vesicle population, with a diameter ranging from 1 to 5 µm and have a heterogeneous morphology. Apoptotic bodies are released when cells undergo apoptosis and therefore they contain various components from their parental cells often including organelles and DNA fragments [198]. Microvesicles, also known as "ectosomes", are the second largest vesicle type between 100 and 1000 nm in diameter, which are formed by the outward budding and fission of the plasma membrane [199]. Exosomes are the smallest class of EVs with diameters between 40 and 100 nm and a cup shape morphology according to previous studies using electron microscopy [200, 201]. Cancer cells also generate several types of vesicles, including, a particular type particular type of EVs are produced by cancer cells, oncosomes and large oncosomes (LOs), with sizes ranging from 100 to 500 nm and 1 e 10 mm, respectively. Like MVs, oncosomes and LOs are produced by budding of the plasma membrane [194].

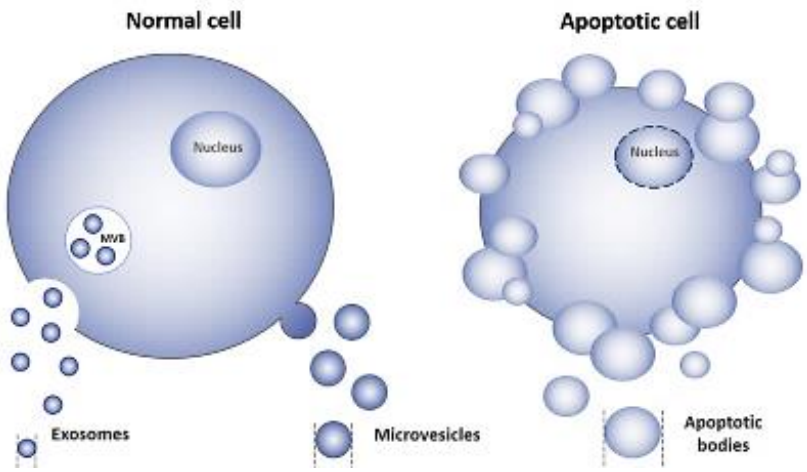

Figure - 4. Types of extracellular vesicles (EVs).
Exosomes are formed in multivesicular bodies (MVBs), which fuse with the plasma membrane and release the exosomes. Microvesicles (MVs) are formed by budding of the plasma. Apoptotic bodies are produced by dying cells, and they have a wide range of sizes. Adapted from [194]

EVs contain proteins, lipids, RNA, characteristics of their secreting cells, and are thought to play an important role in cellular communication, between neighbouring cells or distant cells [10, 191-193, 197, 202-205]. In the context of wound healing, EVs from different sources have shown promising regenerative results, both in *in vitro* and *in vivo* experiments [10, 191, 206-215]. In addition, the combination of biomaterials with EVs is a promising area that is expected to increase in terms of visibility and impact in the upcoming years. So far, only a few studies reported the use of biomaterials for the delivery of EVs [123-126, 216-221]. A summary of studies of EVs for wound healing may be found in Table VIII.

Table VIII. EVs studies on wound healing.

Source	*In Vitro* [(a)]	*In Vivo* [(b)]	**Outcomes** (*in vitro* [(a)] *& in vivo* [(b)])	Ref.
hPRP *	Endothelial cells Fibroblasts	Diabetic (STZ) wound rat model	[(a)] ↗ cell proliferation, migration and angiogenesis [(b)] ↗ wound closure, reepithelization and angiogenesis, collagen remodeling	[125]
hUCB – EPCs	Endothelial cells	Diabetic (STZ) wound rat model	[(a)] ↗ cell proliferation, migration and angiogenesis; [(b)] ↗ wound closure, reepithelization, collagen maturity and angiogenesis, ↘ scar	[207]
hUCB – EPCs	Endothelial cells	Diabetic (STZ) wound rat model	[(a)] ↗ cell proliferation, migration and angiogenesis [(b)] ↗ wound closure	[222]
hUC – MSCs (LPS condit.)	Macrophages	Diabetic (STZ) wound rat model	[(a)] ↗ M2 differentiation [(b)] ↗ wound closure and angiogenesis, ↘ inflammatory cell infiltration	[223]
mouse ASCs *	Endothelial cells	Diabetic (STZ) wound mouse model	[(a)] ↗ cell proliferation, migration and angiogenesis [(b)] ↗ wound closure, reepithelization, collagen deposition and angiogenesis	[123, 224]
human SMSCs * *(+ miR-126-3p)*	Endothelial cells Fibroblasts	Diabetic (STZ) wound rat model	[(a)] ↗ cell proliferation [(b)] ↗ wound closure, reepithelization, collagen maturity and angiogenesis	[217]
human GMSCs *	_	Diabetic (STZ) wound rat model	[(b)] ↗ wound closure, reepithelization, collagen maturity; angiogenesis and neuronal ingrowth	[124]
mouse M2 *§ *(+ miR-223)*	Endothelial cells Fibroblasts	Diabetic (STZ) wound mouse model	[(a)] ↗ cell survival, proliferation, migration and angiogenesis [(b)] ↗ wound closure, reepithelization, granulation tissue formation and angiogenesis; ↘ infection and ROS damage	[218]
human fibrocyte	Endothelial cells Fibroblasts Diabetic keratinocytes	Diabetic (db/db) wound mouse model	[(a)] ↗ cell proliferation, migration and angiogenesis [(b)] ↗ wound closure	[225]
hUCB – MNCs (CD34-) *	Endothelial cells Keratinocytes Fibroblasts	Diabetic (STZ and db/db) and acute wound mouse model	[(a)] ↗ cell survival, cell proliferation, migration and angiogenesis [(b)] ↗ wound closure, reepithelization, remodeling and angiogenesis	[126]
hUC – MSCs *	Endothelial cells	Diabetic (STZ) and acute wound rat model	[(a)] ↗ proliferation, migration and angiogenesis [(b)] ↗ wound closure, reepithelization, remodeling, maturation and angiogenesis	[219]
hUCB plasma	Endothelial cells Fibroblasts	Acute wound mouse model	[(a)] ↗ cell proliferation, migration and angiogenesis [(b)] ↗ wound closure, reepithelization and angiogenesis, ↘ scar	[226]
hUC – MSCs *	Fibroblasts	Acute wound (nude) mouse model	[(a)] ↗ proliferation and migration; ↘ myofibroblast differentiation [(b)] ↗ wound closure, ↘ scar	[216]
cBM – MSCs	_	Acute wound dog model	[(b)] ↗ wound closure, reepithelization, collagen maturity and angiogenesis	[227]
human ASCs *	Keratinocytes Fibroblasts	Acute wound rat model	[(a)] ↗ cell proliferation and migration [(b)] ↗ wound closure	[228]
human ASCs	Fibroblasts	Acute wound mouse model	[(a)] ↗ cell proliferation, migration and collagen synthesis [(b)] ↗ wound closure and maturation, ↘ scar	[229]
human ASCs	Fibroblasts	Acute wound mouse model	[(a)] ↘ differentiation fibroblast→ myofibroblast [(b)] ↘ scar; ↗ collagen and extracellular matrix maturation	[230]
rat ASC *	Endothelial cells	Acute wound mouse model	[(a)] ↗ cell proliferation, migration and angiogenesis [(b)] ↗ wound closure and angiogenesis	[220]
hiPSC – MSCs	Endothelial cells Fibroblasts	Acute wound rat model	[(a)] ↗ cell proliferation, migration and angiogenesis [(b)] ↗ wound closure, reepithelization, collagen maturity and angiogenesis	[231]
human AECs	Fibroblasts	Acute wound rat model	[(a)] ↗ cell proliferation and migration [(b)] ↗ wound closure and collagen-fibers organization; ↘ scar	[232]
mouse fibroblasts *	Endothelial cells Fibroblasts	Acute wound mouse model	[(a)] ↗ cell proliferation, migration, and angiogenesis [(b)] ↗ wound closure, reepithelization, collagen maturity and angiogenesis	[221]
hBM – MSCs	Endothelial cells Keratinocytes Fibroblasts	Acute wound mouse model	[(a)] ↗ cell proliferation, migration, and angiogenesis [(b)] ↗ wound collagen maturity and angiogenesis	[215]

Table VIII. EVs studies on wound healing. (Cont.)

hPB – EPCs	_	Ischemic hind limb (SCID) mouse model	(b) ↗ limb perfusion, vascularity, ↘ limb amputation	[233]
hPB – HSCs (CD34+)	Endothelial cells	Ischemic hind limb mouse model	(a) ↗ angiogenesis (b) ↗ limb perfusion, vascularity, motor function; ↘ limb amputation	[206]
hUC – MSCs	Keratinocytes Fibroblasts	Skin burn rat model	(a) ↗ cell survival; ↘ apoptosis (b) ↗ burn repair, reepithelization and collagen maturity	[234]
hUC – MSCs	Endothelial cells	Skin burn rat model	(a) ↗ cell proliferation, migration and angiogenesis (b) ↗ burn repair, angiogenesis	[235]
hUC – MSCs	Macrophages	Skin burn rat model	(a) (b) ↘ inflammation	[236]
hBM – MSCs	Endothelial cells Patient's skin fibroblasts	_	(a) ↗ normal and diabetic cell proliferation and migration ↗ angiogenesis	[237]

hPRP – human platelet-rich plasma; **hUCB** – human umbilical cord blood; **hUC** – human umbilical cord (wharton jelly); **hPB** – human peripheral blood; h**BM** – human bone marrow; c**BM** – canine bone marrow; **EPCs** – endothelial progenitor cells; **MNCs** – mononuclear cells; **HSCs** – hematopoietic stem cells (CD34+); **MSCs** – mesenchymal stem/stromal cells; **ASCs** – adipose tissue stem cells; **SMSCs** – synovial mesenchymal stem/stromal cells; **GMSCs** – gingival mesenchymal stem/stromal cells; h**iPSCs** – human induced pluripotent stem cells; **AECs** – amniotic epithelial cells; **M2**- M2 phenotype macrophages; **LPS** condit.- lipopolysaccharide conditioning; **STZ** – streptozotocin; **ROS** – reactive oxygen species - oxidative stress. ***** Studies where biomaterials were used as scaffold and allowed delayed and sustained release of EVs in the wound. **§ FGF-2** was administered with EVs to the wound.

The majority of the studies regarding the use of EVs on wound healing are at pre-clinical stage. Nevertheless, Kumamoto University is leading a phase 1 clinical trial. In this study autologous plasma-derived exosomes are applied in chronic ulcers with the aim of inducing faster wound closure and relief of patient's pain [238].

II. Biogenesis, composition and isolation of exosomes

1. Biogenesis and secretion

Cells secrete different types of vesicles to the extracellular environment. These vesicles may be originated on multivesicular bodies (MVBs) (exosomes) or by the budding of the plasma membrane (microvesicles, MVs) [191-196, 239]. Exosome biogenesis involves 4 main stages: 1) inward budding of the cell membrane creating endocytic vesicles; 2) early endosome formation and early endosome membrane budding forming intra-lumminal vesicles (ILVs); 3) evolution to multivesicular bodies (MVBs, or multivesicular endosomes – MVEs); and 4) fusion of MVBs with the plasma membrane and subsequent exosome release to the extracellular milieu. Not all MVBs fuse with the plasma membrane, some are targeted for the lysosome, and once in the lysosomal pathway, MVBs are prone to fuse with lysosomes for degradation of their contents (Figure - 5) [239].

The formation of endocytic vesicles can be both clathrin- or non-clathrin-mediated endocytosis at the plasma membrane. These vesicles are then transported to early endosomes that develop to late endosomes develop by acidification, changes in their protein content and their tendency to fuse with vesicles or other membranes [240]. These different vesicles can be distinguished by their physical shape and cellular location. In particular, early endosomes display a tubular appearance and are located at the outer margin of the cell, whereas late endosomes are spherical in shape and are located close to the nucleus. The key step in the formation of MVBs from late endosomes is reversed budding. During this process, the limiting membrane of late endosomes buds into their lumen, which results in a continuous enrichment

ILVs. MVBs can then degraded by fusing with the lysosome or fuse with the plasma membrane secreting exosomes (Figure - 5) [239, 241-244].

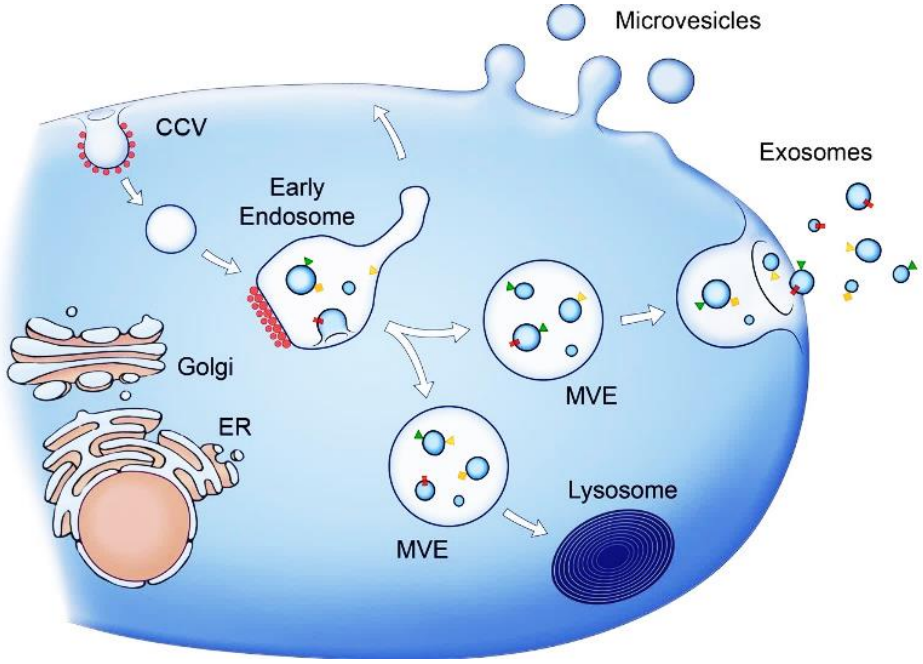

Figure - 5. Exosome biogenesis and secretion.
Clathrin-coated vesicles (CCVs) bud from the plasma membrane, and exosomes (smaller vesicles of different sizes) are formed by budding into early endosomes and MVEs that posteriorly fuse with the plasma membrane. Other MVEs fuse with lysosomes. Red spots symbolize clathrin associated with vesicles at the plasma membrane or bilayered clathrin coats at endosomes. Membrane-associated and transmembrane proteins on vesicles are represented as triangles and rectangles, respectively. Arrows represent proposed directions of exosome biogenesis and secretion and lysosome degradation pathways [239].

Exosome designation was initially applied to name a broad range of vesicles (40 nm – 1 µm) released by cultured cells [245]. Later, the term exosome, was limited to the designation of vesicles of endosomal origin (40–100-nm), released by MVBs fusion with the plasma membrane during reticulocyte differentiation [246-248]. In the late 1990 secretion of similar vesicles (exosomes) by fusion of MVBs with the plasma membrane was also described for B lymphocytes and dendritic cells [249, 250].

There are distinct populations of MVBs coexisting in the cell, although morphologically identical, one is enriched in cholesterol and another have low amounts of cholesterol. The cholesterol-rich population is related with exosome secretion and the other, poor in cholesterol, is targeted for lysosomal fusing and degradation [251, 252]. On the other end, lysobisphosphatidic acid seem to target MVBs for lysosomal degradation, since it's absent of exosomes, but present in MVBs containing EGF destined for lysosome degradation [253, 254].

The molecular machineries related to MVBs biogenesis and degradation and/or fusion with the plasma membrane involves evolutionarily conserved proteins, namely four multiprotein complexes: endosomal sorting complex responsible for transport (ESCRT) -0, -I, -II, and –III; and accessory proteins (e.g., TSG101, Alix and VPS4). ESCRT-0 is responsible for cargo clustering in an ubiquitin-dependent manner, ESCRT-I and ESCRT-II induce bud formation, ESCRT-III drives vesicle scission, some accessory proteins allow for the dissociation and recycling of the ESCRT machinery [243, 255-259]. One example where ESCRT components have been implicated in EV formation involves the transferrin receptor, which is fated for

exosome secretion in reticulocytes, this receptor interacts with the ESCRT accessory protein Alix during its sorting at MVBs [260]. This protein, Alix, was also shown to interact with syntenin and syndecans in exosome biogenesis and sorting [261]. In denditric cells, the ESCRT-0 component Hrs (Hepatocyte growth factor–associated tyrosine kinase) has been reported to be involved in exosome formation and secretion [262]. Also in dendritic cells, the ESCRT family was demonstrated to interact with TSG101 and Alix [263]. Additionally, p53 activity has been linked to the ESCRT-III component Chmp1A, indicating that p53 plays a role in MVB and exosome biogenesis [264]. The p53 and its transcriptional target TSAP6 was already been implicated in the regulation of exosome secretion [265]. Moreover, the depletion of TSG101, an ESCRT-I component, also leads to reduced exosome secretion in the tumor cells HeLa-CIITA and MCF-7, and in immortalized RPE1 epithelial cells [261, 266]

Actually, there are 2 types of exosome biogenesis, at least partially demonstrated, an ESCRT-dependent and a ESCRT-independent mechanism and different cells seem to prefer specific exosomal biogenesis pathways [239, 243, 258, 259, 267]. The existence of ESCRT-independent mechanisms for MVB formation is supported by the finding that cells concomitantly depleted of four subunits of the ESCRT complex are still able to generate CD63-positive MVBs [265]. CD63 have been demonstrated to function in ESCRT-independent sorting to ILVs of the melanosomal protein PMEL, a protein that is targeted to exosomes in melanoma cells [268, 269]. In oligodendroglial cell lines the biogenesis of exosome and secretion but are dependent on sphingomyelinase, an enzyme that produces ceramide, and do not require ESCRT involvement [270]. Moreover, tetraspanins, transmembrane proteins highly enriched in MVBs, seem also to be related to exosome biogenesis [271]. Tetraspanins are involved in with large protein complexes and appear associated with MHC class II molecules in exosomes [253, 272]. In fact, denditric cells recruit MHC II to exosomes, for storage and processing before presentation of the antigen loaded MHC II molecules in the cell membrane, in a way that is independent of the ESCRT machinery [242, 272]. In neuronal cells, plasma membrane depolarization increases the rapid secretion of exosomes [273, 274]. Increasing intracellular Ca^{2+} levels was also demonstrated to be related with the release of EVs in a human erythroleukemia cell line and mast cells [275, 276].

Some mechanistic elements are shared by MVBs and MVs. The processes related to MV release and MVB mobilization, docking and fusion with the cell membrane require the cytoskeleton (actin and microtubules), associated molecular motors (kinesins and myosins), molecular switches (small GTPases, Rabs), and the fusion machinery (SNAREs and tethering factors) [239, 243, 258, 259, 277, 278]. The SNARE complex involved in Ca^{2+} regulated exocytosis of lysosomes includes VAMP7 and Ca^{2+} binding synaptotagmin VII [279]. Similarly exosome secretion by maturing reticulocytes appeared to be dependent on VAMP7 function (Fader et al., 2009), whereas in MDCK (Madin-Darby canine kidney) cell lines the expression of the the Longin domain of VAMP7 impairs lysosomal secretion and seems to play a role in the endocytic system, without affecting exosome release [280, 281]. Other study, demonstrated that secretion of exosomes carrying the morphogen Wnt is dependent on the R-SNARE Ykt6 (Gross et al., 2012). The Rab GTPases relation to exosome secretion was shown on reticulocyte cell lines via Rab 11 involvement [275, 282]. Other Rab GTPase, Rab27, associated with secretory lysosome–related organelles, could be involved directly or indirectly in the transport and tethering at the cell periphery of the secretory MVBs [283]. In fact, Rab27a or Rab27b knockdown, or silencing of 2 known Rab27 effectors Slp4 (synaptotagmin-like 4, or SYTL4) and Slac2b (or exophilin 5 - EXPH5), was demonstrated to reduce significantly exosome secretion [284]. Additionally, the knockdown of the Rab GTPase-activating proteins TBC1D10A–C and/or interference with its effector, Rab35, also resulted in reduced exosome secretion [285]. In summary, Rab11, Rab27, and Rab35 appear to be involved in exosome release, but its selective

inactivation only partially impacted this pathway. The roles of these GTPases could be either complementary, cell type dependent, or only indirect by regulating pathways upstream of exosome secretion [239].

2. Exosome packaging and composition

The first time exosomes were described they were being secreted by reticulocytes cultured *in vitro* [246, 247]. But, exosomes, and EVs in general, are released from several different type of cells including stem cells, progenitor cells, somatic cells and cancer cells [10, 189, 200, 206-208, 249, 250, 271, 286]. Exosomes can be found present in all body fluids, like blood, saliva, urine, amniotic fluid, semen, breast milk, and cerebrospinal fluid, they carry several bioactive molecules, such as lipids, proteins and RNAs [239, 287-298].

As referred, exosomes are release by different cells types and in different ways, therefore it is expected that their composition will differ depending on the cell type and the environment and/or stimuli cells are exposed to. Exosomes are mainly composed of lipids, proteins (soluble and membrane linked) and nucleic acids (small RNAs), that present a particular profile related to the endosomal pathway and cell of origin [239, 259]. Nowadays, there are 3 comprehensive online databases were EV researchers register, annotate and review information regarding exosome and EVs composition, exosomal lipids, proteins and nucleic acids: Exocarta (www.exocarta.org), EVpedia (www.evpedia.info), and Vesiclepedia (www.microvesicles.org) [192, 193, 204, 205].

Exosomes present a particular profile related to the endosomal pathway and cell of origin, regarding their lipid, protein and RNA content [239, 259, 299]. For example, MSCs originated from bone marrow (BM-MSCs), adipose tissue (ASCs), and umbilical cord (UC-MSCs) present different growth factor composition, with VEGF-A, FGF-2, HGF and PDGF-BB present in exosomes from all the three sources and TGF-β only being present in exosomes from UC-MSCs, which exerted a greater effect in keratinocytes as opposed BM-MSCs exosomes that had a higher effect in fibroblasts [300]. Cell donor health status also impacts EVs composition. Diabetes have been found to impair progenitor cells regenerative potential and number, namely EPC cells were found to be present in less number in diabetic patients and to be dysfunctional, thus with less pro-angiogenic capability [163, 301]. Moreover, expression of certain exosomal cargo, such as miR-126 was significantly lower under high-glucose or diabetes conditions in human CD34+ exosomes, indicating that the exosomal cargo is dependent on the physiological condition of the cell of their origin [206]. Age also represent a major factor on EVs regenerative potential. Effectively old bone marrow was demonstrated to inhibit skin wound vascularization[302]. At a EV / exosome level, cardiac progenitor cell (CPC) derived exosomes isolated from neonatal patients were found to have higher regenerative potential for cardiac tissue repair compared to CPC exosomes from older children, demonstrating the high potential associated to young or perinatal cells [217, 218, 223, 303, 304]. Additionally, a significant reduction of circulating EVs numbers were found in older individuals [305]. When comparing MSCs EVs composition from different age stage groups, newborn, infant young, pre-pubertal, pubertal and adult individuals an overall decrease on EVs miRNAs levels that would transduce in altered bioactivity, namely in regulating inflammatory response [306].

Stimulation of exosome secretion as well as exosome content modulation has been reported by several groups upon application of different stimuli to their secreting cells, incubation with growth factors, calcium, LPS or specific miRs, or cells irradiation to induce apoptosis [215, 223, 225, 236, 307, 308]. Cells conditioning by culture under hypoxia and/or

ischemic conditions was found to increase their regenerative potential towards wound repair, enhancing wound healing and angiogenesis [181, 188]. With this purpose, hypoxia or ischemia can be applied to enhance cells bioactivity and also to stimulate EVs secretion and modulate their composition [181, 188, 309-311].

Lipid composition

Exosomes are double membrane vesicles, therefore, rich in lipids. The exosome membrane is similar to the plasma membrane, including integral and pheripheral proteins in a lipid bilayer composed of phospholipids (glycerophospholipids, like, phosphatidyl choline - PC, lysophosphatidyl choline, phosphatidyl serine – PS, phosphatidyl ethanolamine- PE, phosphatidyl inositol – PI, and phosphosphingolipids, namely, sphingomyelin – SM), glycolipids (sphingoglycolipids, cerebrosides and gangliosides) and steroids (cholesterol - CHOL). The lipid composition of exosomes presents unique features relatively to other small vesicles secreted by cells. For example, the phospholipid distribution is not asymmetric like in the plasma membrane, where PS and PE are exclusive to the intracellular leafet [278, 312-315]. In addition, exosomal membrane is rich in cholesterol (CHOL) [251, 315]. Similarly, SM and PS are present in high levels, nearly 15 times the amount present in the plasma membrane, at the expense of PC and PE [253, 314-317]. Additionally, exosomes contain ceramides in their membrane that are absent on other EVs [253, 314, 315, 318]. The fatty acids in exosomes are mostly saturated or monounsaturated.

Until now, few studies have investigated exosomal lipid composition and exosomal lipid biological function. Nevertheless, sphingolipids seem to present an important role in binding and endocytosis, probably related with CHOL-rich domain [319]. In addition, internal membranes of MVBs are enriched in lipids, such as lysobisphosphatidic acid (LBPA) that plays an important role in exosome biogenesis, by interacting with Alix it can induce internal budding of small vesicles from large liposomes when in a lipid mixture similar to MVB membrane composition [320-323].

Protein composition

Exosome composition in proteins is closely related to their endosomal origin, exosomes from different cell types contain endosome-associated proteins involved in membrane transport and fusion (e.g., Rab GTPase, SNAREs, Annexins, and flotillin), proteins involved in MVB biogenesis (e.g., Alix and Tsg101), protein families associated with lipid microdomains, such as integrins and tetraspanins, such as CD63, CD81, CD82, CD53, and CD37, a family of proteins that are composed of four transmembrane domains, and associated with lipid rafts, including glycosylphosphatidylinositol-anchored proteins and flotillin [243, 253, 278, 315, 321, 324-327]. Exosome protein content includes both conserved proteins, identified in almost all exosomes despite their origin, and cell-type-specific proteins [321, 328].

Cytosolic constituents are recruited into exosomes probably by the involvement of chaperones such as Hsc70, found in exosomes from most cell types [260, 263]. The development of quantitative mass spectrometry allowed the identification of many other cytosolic proteins by analysis of exosomal lysates, such as Hsp90, 14–3-3 epsilon, and PKM2, that, together with tetraspanins, coimmunoprecipitated with MHC II [329]. Moreover, other frequently found proteins are linked to cytoskeleton (β-actin, myosin, cofilin and tubulins) or to metabolism (e.g., glyceraldehyde 3-phosphate dehydrogenase (GADPH, ENO1). Of interest, exosomes contain also proteins involved in cell signaling pathways, like β-catenin, Wnt5B or

Notch ligand, Delta-like 4, mediators of intercellular cell signaling, like interleukins, TNF-α or TGF- β, cytokines, and growth factors depending on the cell source [278, 315, 321, 330].

RNA composition

A major breakthrough in EV field was the discovery that exosomes, or EVs, isolated from cell cultures and body fluids, contain nucleic acids, such as mRNA and miRNA , and that mRNAs could be translated into proteins by target cells [202, 331]. Many RNAs that were isolated within EVs were found to be enriched relative to the RNA profiles of the originating cells, indicating that RNA molecules are selectively incorporated into EVs [202, 258, 278, 315, 328, 331, 332]. Examples of miRNAs deteted in EVs from different sources are presented in Table IX.

Table IX. MicroRNAs composition of EVs according to their cell source.

EVs source	Expressed microRNAs	Ref
hPB plasma (patients)	Let-7a-5p; Let-7b-5p; miR-15b-5p; miR-23a-3p; miR-23b-3p; miR-26b-5p; miR-126-3p; miR-126-5p; miR-151a-3p; miR-374b-5p; miR-632; miR-1972	[333]
hPB – HSCs (CD34+)	miR-10a; miR-10b; miR-92b; miR-99a; miR-100; miR-125b; miR-126-3p; miR-130a; miR-335; miR-551b	[206]
hPB – MNCs (CD34-)	miR-21; miR-22; miR-132; miR-143; miR-150; miR-765; miR-3184; miR-4286	[206]
hUCB plasma	miR-21-3p; miR-19b; miR-27b; miR-125b; miR-126; miR-214	[226]
hUCB – MNCs (CD34-)	Let-7a-5p;Let-7f-5p; Let-7g-5p; miR-16-5p; miR-19b-3p; miR-20a-5p; miR-21-5p; miR-23a-5p; miR-26a-5p; miR-142-3p; miR-150-5p; miR-181a-5p; miR-223-3p; miR-342-3p; miR-451a	[126]
hUC – MSCs	miR-21; miR-23a; miR-125b; miR-145	[216]
hUC – MSCs (LPS cond.)	Let-7b, miR-133a; miR-183; miR-550b; miR-1180	[223]
human fibrocyte	miR-21; miR-124a; miR-125b; miR-126; miR-130; miR-132	[225]
human CDCs	miR-19a; miR-19b; miR-22; miR-24; miR-27a; miR-27b; miR-140-3p; miR-150; miR-210	i[334]
human melanoma cells	Let-7c; miR-23b; miR-25; miR-27a; miR-34a; miR-125b; miR-130a; miR-138; miR-146a; miR-149; miR-196a; miR-199-3p; miR-200b; miR-205; miR-146a	[335]
porcine ASCs	Let-7f; miR-148a; miR-378; miR-32-5p	[336]
rat CPCs	miR-15b; miR-17; miR-20a; miR-199a-5p; miR-210; miR-292-5p; miR-292-3p	[337]

hUCB – human umbilical cord blood; **hUC** – human umbilical cord; **hPB** – human peripheral blood; **EPCs** – endothelial progenitor cells; **MSCs** – mesenchymal stem/stromal cells; **ASCs** – adipose tissue stem cells; **CPCs** – cardiac progenitor cells; **CDCs** – cardiosphere-derived cells.

How RNA species are sorted into EVs is still unknown. Six potential modes for sorting of miRNAs into exosomes have been proposed, although the underlying mechanisms remain largely unclear: 1) neural sphingomyelinase 2 (nSMase2)-dependent; 2) miRNA motif and sumoylated heterogeneous nuclear ribonucleoproteins (hnRNPs)-dependent; 3) 3'-end miRNA sequence-dependent; 4) miRNA induced silencing complex (miRISC)-related; 5) IL-4 cellular activation dependent; and 6) KRAS-dependent (Figure - 6) [338-346].

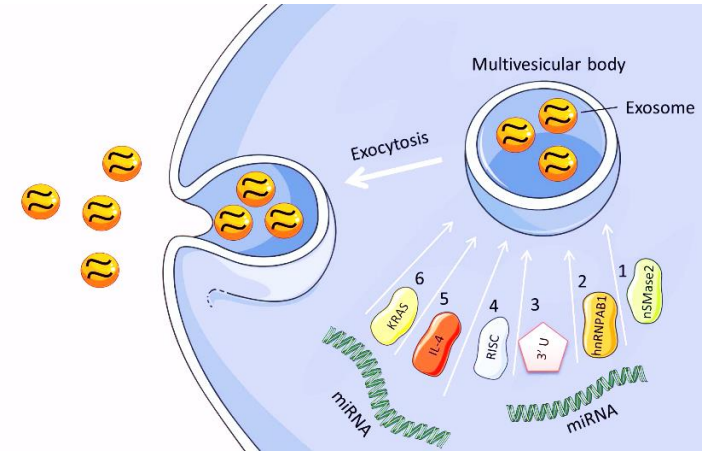

Figure - 6. Cellular mechanisms of miRNA sorting to exosomes.
Different cellular mechanisms have been proposed to regulate sorting of miRNA into exosomes: (1) nSMase2-dependent; (2) hnRNPA2B1-dependent; (3) miRNA 3' end base modifications; (4) miRISC-dependent; (5) IL-4 cellular activation dependent; and (6) KRAS-dependent. Reviewed in [340].

As referred, exosomes are enriched in cholesterol, sphingomyelin, glycosphingolipids and phosphatidylcholine with saturated fatty acids because ILVs are created during the spontaneous inward budding of the raft-like region of the MVB limiting membrane, a proposed mechanism for RNA loading into exosomes is that the first step occurs before this budding process, when an RNA molecule binds to this raft-like region, and this RNAs internalization will depend on: (1) the presence of a lipid-bilayer binding motif within the RNA sequence; (2) RNA hydrophobic modifications; (3) RNA concentration in cytoplasm; and (4) the presence of raft-like regions, enriched in specific lipids, in the MVB limiting membrane [347]. RNAs in EVs seem to share specific sequence motifs that may potentially function as elements for targeting to EVs [348]. ESCRT-II also acts as an RNA binding complex, therefore it may also function to select RNA [349]. Additionally, MVBs are sites of miRNA-loaded RISC (RNA-induced silencing complex) accumulation and exosome-like vesicles are considerably enriched in GW182 and AGO2 which can play a role in RNA sorting to exosomes [239, 321, 341]. An interesting finding is that, also endogenous RNAs play a role on miRNA sorting to exosomes, using a macrophages and endothelial cells (ECs) as a model of heterotypic cell communication, it was demonstrated that miRNA sorting to exosomes is modulated by cell activation-dependent changes of miRNA target levels in the producer cells [342]. This study further showed that the transferred miRNAs were active in receptor cells and modulated cellular miRNA expression [342]. Exosomes released by immune cells have been demonstrated to selectively incorporate miRNA that can be functionally transferred as a consequence of fusion with recipient cells [350, 351]. This transferred miRNAs were also suggested to be functional in target cells, as miRNAs from T-cell exosomes caused inhibition of target genes in dendritic cells (DCs), miRNAs of exosomes from Epstein-Barr virus infected B-cells affected the expression of target genes in monocytes, and apoptosis of pancreatic beta-cells has been demonstrated to be induced by exosomal miRNA transfer from neighboring cells [350, 352, 353].

Deep sequencing RNA analysis demonstrated that, in addition to mRNA and miRNA, exosomes and EVs also contain a large variety of other small noncoding RNA species, including RNA transcripts overlapping with protein coding regions, repeat sequences, structural RNAs, tRNA fragments, small interfering RNAs, among others [315, 336, 354-356]. An important fact is that extracellular RNAs also have been found to be available in biological fluid and cell culture media in RNA–protein complexes that can be co-isolated with EVs [357]. Also, different RNA isolation methods give extensive variation in exosomal RNA yield and patterns [358].

3. Isolation and characterization

One major challenge in the field of EVs is to improve and standardize methods for EV isolation and analysis. Currently, EVs are mostly isolated from the supernatants of cultured cells and body fluids by differential ultracentrifugation [359]. Nevertheless, circulating vesicles are likely composed of exosomes, microvesicles (MVs), and other small EVs (SEVs), which the currently available purification methods do not allow to fully discriminate [239, 258, 328]. Exosomes can be more efficiently separated from contaminating particles, such as protein aggregates, by using their relatively low buoyant density, applying a density gradient centrifugation [249, 253, 326]. Additionally, differences in floatation velocity can be used to separate differently sized classes of EVs [295]. Additional purification can be achieved by immunoadsorption using a protein of interest, which also selects for vesicles with an exoplasmic or outward orientation [253]. More recently, size exclusion chromatography has been proved to efficiently isolate exosomes from other vesicles and contaminants [360]. Several commercial kits are also available, claiming fast and simple exosome-purification procedures without ultracentrifugation [244]

In general, EVs are characterized by complementary techniques, such as immunoblotting, mass spectrometry, nanoparticle tracking analyses and imaging (e.g. transmission electron microscopy - TEM). Large EVs may be analyzed by conventional electron microscopy, but, small EVs can only be observed as “whole mount” samples when deposited without sectioning on electron microscopy grids [249]. In this case, EVs may collapse during drying, resulting in a cup-shaped morphology, which is often considered erroneously as a typical feature of exosomes [239, 249]. The size and charge of EVs can be characterized by dynamic light scattering (DLS) and zeta potential analyses, respectively. Nanoparticle tracking analysis (NTA) allows also the determination of the size distribution of isolated EVs based on the Brownian motion of vesicles in suspension [361]. Conventional flow cytometers cannot distinguish between vesicles that are <300 nm, but a novel high resolution flow cytometry–based method has been recently developed for quantitative high throughput analysis of individual (immunolabeled) nanosized vesicles [362, 363].

Table X. Extracellular vesicles characterization.

EVs	Size	Biogenesis	Isolation	Detection	Markers	Contents
Exos	40-100 nm	Exocytosis of MVBs	Ultracentrifugation (UC) and gradient UC (100.000-200.0000g)	DLS, NTA, TEM, WB, Flow cytometry, MS.	CD9, CD 63, CD81, TSG101, Alix, LAMP1, flotilin	Proteins and ncRNAs (e. g. mRNA, miRNA)
MVs	100-1000 nm	Budding from PM	Differential centrifugation (18.000 – 20.000g)	Flow cytometry, capture based assays	Integrins, selectins, CD40 ligand	Proteins and ncRNAs (e. g. mRNA, miRNA)
ABs	1- 5 µm	Blebs release - apoptotic cells	No stablished protocol	Flow cytometry	DNA content, Phosphatidyl-serine	Nuclear fractions, cell organelles

Exos – exosomes; **MVs** – microvesicles; **ABs** – apoptotic bodies; **MVB** – multivesicular bodies; **PM** – plasma membrane; **DLS** – dynamic light scattering; **MS** – mass spectrometry. Adapted from [196] and [197]

A major challenge in the EV field is the establishment of methods that allows one to discriminate exosomes from other small EVs (SEVs) and MVs [252, 364]. Differences in properties such as size, morphology, buoyant density, and protein composition seems insufficient for a clear distinction [239, 365]. To help in the standardization and coordination of

research in EVs area, the International Society for Extracellular Vesicles was launched in 2011. This is a global society of leading exosomes and microvesicle researchers focused guiding EV research and to advance the understanding of EV biology. In 2012, the Journal of Extracellular Vesicles (JEV) was launched with this purpose [366]. The society promotes annual meetings with top researchers in the field and regularly holds regional workshops. In addition, ISEV has developed a MOOC (Massive Open Online Course) through Coursera. More importantly, ISEV issued several guidelines and studies regarding EVs classification, analysis and overall characterization and of EVs components [339, 367-371]. And recently formed a consortium for transparent report and centralization of knowledge in EVs [372].

III. Exosome communication, stability and targeting

1. Exosomes in cell communication

Intercellular communication is an essential hallmark of multicellular organisms and can be mediated through direct cell–cell contact or transfer of secreted molecules. EVs represent an important mode of intercellular communication by serving as vehicles for transfer bioactive molecules (lipids, proteins and RNAs) between cells [239]. It is well established that exosomes induce physiological changes in recipient cells upon interaction [328]. Although lipids are expected to have a biological role, not much is known about this molecules contribution for intercellular communication, but have been shown to carry functional lipid-related enzymes [314]. Nevertheless, exosome-mediated transfer of lipids seems to be related with lipid metabolic diseases [373]. On the other end, several exosomal proteins and RNAs have already been described as playing important roles in neighboring and distant cells activity [242, 258, 259, 328, 339].

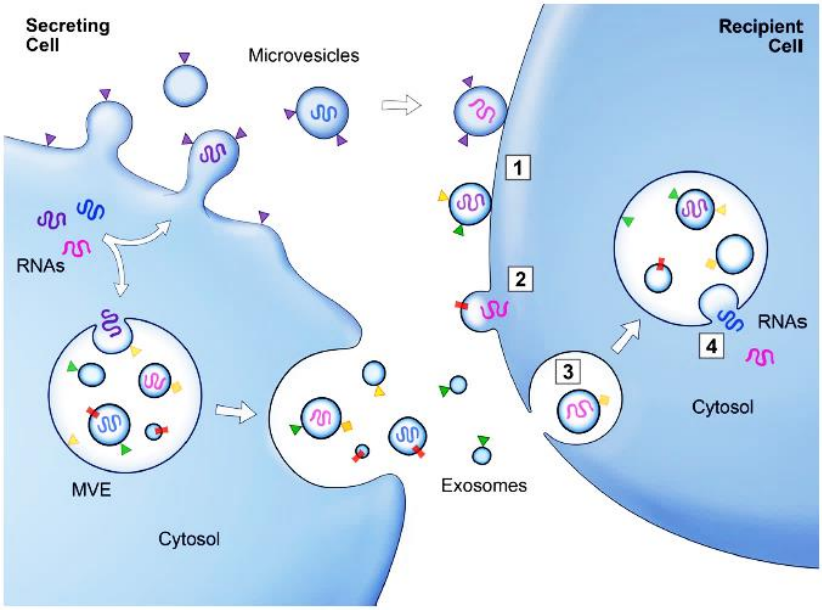

Figure - 7. Schematic representation of EV mediated protein and RNA transfer.
Membrane-associated (triangles) and transmembrane proteins (rectangles) and RNAs (curved symbols) are selectively incorporated into the ILV of MVEs or into MVs budding from the plasma membrane. MVEs fuse with the plasma membrane to release exosomes into the extracellular milieu. MVs and exosomes may dock at the plasma membrane of a target cell (1). Bound vesicles may either fuse directly with the plasma membrane (2) or be endocytosed (3). Endocytosed vesicles may then fuse with the delimiting membrane of an endocytic compartment (4). Both pathways result in the delivery of proteins and RNA into the membrane or cytosol of the target cell. Fusion and endocytosis are only represented for exosomal vesicles [239].

As referred, exosomes contain proteins involved in cell signaling pathways, like β-catenin, Wnt5B or the Notch ligand, Delta-like 4 [321]. Additionally, cell signaling mediators, like interleukin-1β, TNF-α or TGF- β, have also been found in exosomes [321, 330]. Exosomes also play a role in immunologic response, e.g. by transporting MHC II proteins, they can either stimulate or repress immunologic response, especially in the case of cancer cell-derived exosomes [249, 250, 374, 375]. During pregnancy, serum exosomes were related with suppression of T-cell signaling components, contributing to a state of immune privilege that correlates with term versus pre-term pregnancies [376]. A study demonstrated that MSCs secrete exosomes with TSG-6, an anti-inflammatory protein that seems to have a beneficial effect in myocardial infractions [377]. Exosome are also known to contribute to the communication in the central nervous system, either between neurons, or between different cells types, like microglia, oligodendroglia cells and neurons [378-380]. In neurodegenerative disorders exosomes were also found to transport disease specific deleterious peptides, like β-amyloid, α-synuclein, tau protein and prions [242, 297, 381, 382].

Since the first report showing that exosomes could transfer mRNAs and miRNAs, many research groups have been actively studying the impact of this transfer in different contexts [202, 339, 350, 351, 383]. For example, mast cell exosomes can transfer bioactive mRNA, leading to protein expression in the recipient cells [202]; miRNAs from T-cells can be transferred via $CD63^+$ exosomes to dendritic cells (DCs), modulating gene expression in DCs cells [350]; endothelial cells (ECs) secrete exosomes containing miR-214, which suppress senescence and stimulates an angiogenic program in target cells, both human and mouse ECs [384]; exosomes derived from K562 cells with enforced miR-92a expression were able to enhance ECs migration and tube formation [385]; exosomes secreted by keratinocytes enhance melanin synthesis by increasing both the expression and activity of melanosomal proteins in recipient cells [386]. All these findings demonstrate the broad range of action of exosomes as cellular communication vehicles.

2. Exosome stability and targeting

Exosomes, and EVs in general, are released from different types of cells and can be found in all body fluids, allowing for intercellular communication even at distant sites Exosomes, and EVs in general, are released from different types of cells and can be found in all body fluids, allowing for intercellular communication even at distant sites [239, 242, 258, 259, 287-298, 328, 339]. How far can these vesicles travel in the body? For how long are they stable? How do they target the recipient cells and modulate their fate? The answers to these questions remain scarce…

Exosomes / EVs pharmacokinetics and is closely related to intrinsic characteristics of these vesicles and it is determined by cell source, route of administration and targeting [387]. The pharmacokinetics of exosomes and EVs is one of the most important aspects when developing therapeutic systems since their bioavailability at the target site is paramount to elicit the desired biological effect [388, 389]. To study sEVs pharmacokinetics, several labelling methods are commonly used such as fluorescent dyes capable of labelling the outer and/or inner leaflet, luciferase labelling and radiolabeling, being the latter capable of providing both qualitative and quantitative information regarding sEVs pharmacokinetics (Table XI) [388, 389].

Table XI. sEV labelling methods for pharmacokinetic Study. *Adapted from [389].*

sEV labelling methods	Example	Advantages	Disadvantages	Reported application
Qualitative analysis				
Fluorescent dye	PKH dye, DiI	Easy to use	Low sensitivity Labelling of contaminants	Cellular uptake
Near-IR dye	DiR, DiD	Easy to use Low absorption of biological molecules	Low sensitivity Labelling of contaminants	Tissue distribution (*in vivo* and *ex vivo)*
Quantitative analysis				
Reporter proteins	Luciferase	High sensitivity High quantitation	High cost	Tissue distribution (*in vivo*) Blood clearance
Radio Isotopes (RI)	^{125}I, ^{111}In, ^{99m}Tc	High sensitivity High quantitation	High cost Dedicated facilities	Tissue distribution (*in vivo* and *ex vivo*) Blood clearance
Magnetic nanoparticles	SPION5	Spatial resolution Clinical translation	Low sensitivity High half-life	Tissue distribution (*in vivo* and *ex vivo*) Blood clearance

IR – Infrared region; **RI** – Radio isotopes; **PKH** –PKH26 red dye / PKH67 green dye; **DiI** – 1,1'-Dioctadecyl-3,3,3',3'-Tetramethylindocarbocyanine Perchlorate; **DiR** – 1,10-dioctadecyltetramethyl indotricarbocyanine iodide; **DiD** – 1,10-dioctadecyl-3,3,30,30-tetramethylindodicarbocyanine perchlorate; **^{125}I** – iodine-125; **^{111}In** – indium-111; **^{99m}Tc** – technetium-99m; **SPION5** - 5-nm superparamagnetic iron oxide nanoparticles.

Fluorescent probes have been widely used in studies aimed at evaluating the cellular uptake of EVs. Lipophilic fluorescent dyes, such as PKH26, PKH67 and DiI, have been the most frequently used dyes to label EV membranes since the labelling can be accomplished upon a simple and quick mixing step followed by hydrophobic interaction between the dye and the membrane [389]. In addition to these dyes, near-infrared dyes (DiR, DiD) have also been frequently used. EVs labelled with PKH26 were found to be taken up by lung epithelial cells and liver macrophages (Kupffer cells) [390, 391]. EVs labelled with NIR dyes were tracked *in vivo* by whole-body imaging at organ level [392] and their biodistribution was evaluated as a function of time by *ex vivo* imaging of organs excised from mice after injection [387, 393]. However, results should be carefully considered given the labelling stability of lipophilic dye. The hydrophobic-based interaction between the sEV membrane and the lipophilic dye is a reversible reaction and therefore the lipophilic dye can be released from the sEV membrane and transferred to lipoprotein particles after systemic administration into mice [394].

Luciferase labelling presents high sensitivity which allows for sequential *in vivo* tracking of labelled EVs by genetic engineering the EVs secreting cells [389]. A fusion protein consisting of gLuc, a reporter protein that emits chemiluminescence, and lactadherin (LA), a protein located on the outer surface of sEVs, was developed and gLuc-LA-labeled sEVs were successfully obtained by collecting sEVs from B16-BL6 murine melanoma cells after transfection with a plasmid DNA encoding gLuc-LA. The *in vivo* distribution of the gLuc-LA-labeled B16-BL6 sEVs was visualized by detecting chemiluminescence emitted from gLuc-LA after intravenous injection [395-397]. Luciferase labeling is also possible at the inner side of sEV membranes using the Gag protein [398]. B16-BL6 melanoma cells through transfection with a plasmid encoding a fusion protein consisting of Gag protein and gLuc (Gag-gLuc) secrete labelled sEVs [389]. Gag localizes at the inside of the plasma membrane through interaction between the polybasic region of the Gag protein and phosphatidylinositol 4,5-bisphosphate in the plasma membrane [399, 400]

Radiolabeling can be used to study EVs pharmacokinetics in a more quantitative manner [393, 401-403]. Genetically engineered B16-BL6-derived sEVs were labelled with iodine-125 (^{125}I) using a streptavidin (SAV)-biotin system. A plasmid vector encoding the fusion protein SAV-LA was constructed and B16-BL6 cells were transfected with the plasmid to obtain SAV-LA labelled sEVs. SAV-LA-labeled sEVs were then incubated with (3-^{125}I-iodobenzoyl)

norbiotinamide (^{125}I-IBB) to obtain ^{125}I-labeled B16-BL6 sEVs. Single-photon emission computed tomography (SPECT)/CT imaging studies of the B16-BL6 sEVs were carried out in mice after intravenous injection to quantitatively analyze sEV biodistribution [401].

Magnetic resonance imaging (MRI) can also be used for EV tracking. For example, melanoma cells (B16-F10) exosomes were loaded by electroporation with 5-nm superparamagnetic iron oxide nanoparticles (SPION5) and administered to mice by footpad injection. Accumulation of SPION5-loaded B16-F10 exosomes in popliteal lymph nodes could be detected by magnetic resonance [404].

Radionuclide-based imaging (PET and SPECT) can be easily translated from animals to humans and, given its high sensitivity, this method can be used to perform whole-body imaging in a quantitative manner [403]. SPECT, PET and MRI-based methods provide good imaging depth but it is important to note that these labelling compounds have a half-life longer than the EVs and thus may generate a signal even after EVs are degraded [393, 401-403, 405].

Stability

The levels of exosomes and EVs in circulation should reflect the balance between their generation/secretion and clearance. Analysis of exosomes and EVs pharmacokinetic profiles, (half-life in circulation or time to elimination from the blood circulation, and biodistribution or bioaccumulation in the organs) has been limited due to lack of sensitivity and quantitative capacity of the available methodology [388, 389].

Studies indicate that the half-life of exogenous exosomes and EVs, artificially introduced into circulation (systemic administration), is very short. For instance, in one study, exosomes were labelled with gLuc-LA (Gaussia luciferase (gLuc) and lactadherin (LA)) and administrated by intravenous injection into mice. This gLuc-LA labelled sEVs quickly disappeared from the blood circulation, with a half-life of approximately 2 min, and *in vivo* imaging revealed that the exosomes mainly distributed to the lung, spleen, and liver [395]. In a separate study, exosomes from different murine cell sources (B16BL6 melanoma cells, C2C12 myoblast cells, NIH3T3 fibroblasts, MAEC aortic endothelial cells, and RAW264.7 macrophage-like cells) rapidly disappeared (half-life of approximately 2 to 4 min) from the blood circulation after intravenous injection into mice and mainly distributed to the liver [406]. PC3 EVs labelled with ^{111}In rapidly disappeared from blood circulation and were primarily distributed to the liver (12% injection dose/g at 24 h) after intravenous injection [393]. Similarly, radioactivity derived from B16-BL6 ^{125}I-labeled EVs disappeared from the blood rapidly and accumulated in the liver (40%/dose), lung (10%/dose) and spleen (3%/dose) [401]. Biotinylated EVs were shown to be cleared from rabbit circulation in approximately 10 min [407]. Other exosomes/EVs from splenocyte supernatants and derived from red blood cells showed a clearance of more than 90% after 30 min [408, 409]. Expi293F-derived EVs labelled with a nanoluciferase reporter (palmGRET) administered intravenously (IV) to a non-human primate model (*Macaca nemestrina*) had markedly longer circulation times in plasma than reported in mice and were detectable in Cerebrospinal fluid (CSF) after 30-60 minutes. EV uptake by PBMCs, most notably B-cells, was observed only after one minute of IV administration. Additionally, EVs were detected in the liver and spleen within one hour of IV administration [410]. However, human platelet concentrate-derived EVs, or platelet-derived microparticles (PMP), remained in the circulation with a half-life of 5.5 hours, evaluated in thrombocytopenic patients undergoing apheresis procedures [411]. Whereas, mouse plasma-derived sEVs (MP-sEVs) presented a half-life of

approximately 7 min in the blood [412]. These data suggest that EVs clearance from the blood can be accelerated in small animal models versus larger animals and humans.

These data suggest that EVs or exosomes clearance from circulation is most likely due to retention and uptake by specific cells that interact with certain components of EVs membrane regardless of the origin of the producing cells [388, 389, 406, 413]. It has been shown that macrophages are responsible for the hepatic and splenic uptake of B16-BL6 exosomes and endothelial cells are responsible for the uptake in the lungs [391]. Macrophages are well-known for their capacity to uptake negatively charged nanoparticles, such as chemically modified lipoproteins and anionic liposomes, by recognition by scavenger receptors [414]. Exosomes and EVs display a negative charge due to the presence of the negatively charged membrane phospholipid phosphatidylserine (PS) that is abundantly present at the surface regardless of the EV origin. Pre-injection of PS-containing liposomes significantly delayed elimination of gLuc-labeled B16BL6 EVs from blood circulation and decreased accumulation of ^{125}I labelled EVs in the liver after intravenous injection in mice [415]. Moreover, in macrophage-depleted mice, the clearance of EVs from the blood circulation was extremely delayed compared with that in untreated mice, highlighting the importance of macrophages in the pharmacokinetics of intravenously injected exosomes [391, 412]. Exosomes collected from C2C12 cells, NIH3T3 cells, MAEC cells and RAW264.7 cells were mainly taken up by macrophages in the liver after intravenous administration [406]. Polyethylene glycol (PEG) lipid modification improved retention of EVs in blood after systemic administration with no significant effect on the liver and spleen accumulation [416]. Additionally, protease treatment significantly decreased the accumulation of EVs into the lungs after intravenous injection without affecting the accumulation in the liver, suggesting that surface proteins play an important role in the uptake by the lung [391, 398]. These findings are in agreement with a report that pulmonary epithelial cells recognize tetraspanin proteins and integrins present on the EVs surface [390].

After local injection, nanoparticles, including EVs, are absorbed predominantly into lymphatic capillaries rather than into blood capillaries given the larger size of the former [417]. After subcutaneous injection in mice, EVs labelled with fluorescent dyes are rapidly transported (within minutes) from the periphery to the lymph node by lymphatics being macrophages and B cells key players in EV uptake [418].

EVs labelled with PKH67 were retained for 3 days in the wound after topical application to the wound [226]. Nevertheless, PKH67 is a lipophilic membrane dye that can diffuse to the cell membrane and emit fluorescence despite the integrity of the vesicles [394].

Biodistribution

The distribution of exosomes and their subsequent cellular uptake are the main steps governing their pharmacokinetics. Quantitative information regarding the EV elimination profile and their biodistribution is of utmost importance for the successful development of EV-based therapies [388, 389]. When evaluating exosomes/EVs biodistribution, most studies reveal that systemic administrated EVs accumulate mainly in the liver, spleen, lung, gastrointestinal tract, bone, skin, muscle and kidney, regardless of the EV type/origin [387, 395, 407, 419]. Macrophages commonly mediate the uptake in most tissues, while endothelial cells preferentially mediate the uptake in the lungs [390, 391, 406]. For example, PKH26-labeled B16- BL6 sEVs were taken up by macrophages in the liver while PKH26-labeled sEVs were taken up by endothelial cells in the lung [391]. Moreover, 4 h after intravenous injection of ^{125}I-labelled B16-BL6-derived EVs, the radioactivity was distributed among the liver

(28%/dose), spleen (1.6%/dose) and lung (7%/dose) and accumulated to 40%/dose in the liver, 10%/dose in the lung and 3%/dose in the spleen [401]. The PC3 EVs labelled with ^{111}In were detected in the liver in a percentage of 12% dose /g at 24 hours [393]. For example, tumor-derived EVs labelled with PKH26 were taken up by lung epithelial cells and liver macrophages (Kupffer cells) through specific recognition by integrins [390].

Intratumoral injection allows longer exosome detection in tumours [420]. After intratumoral injection of ^{125}I labelled sEVs, most of the radioactivity was detected within the tumour tissues of mice whilst some signal was also detected in the liver and the lungs. Detailed analysis of the cells present in the tumour tissue showed that PKH26-labeled sEVs were mainly taken up by B16-BL6 cells. Interestingly, tumour growth was significantly promoted after intratumoral injection of the sEVs suggesting that B16-BL6 cells secrete and take up their own sEVs to induce their proliferation and inhibit their apoptosis, thereby promoting tumour progression [421].

Oral administration of exosomes/EVs shows biodistribution to most organs, including liver, lung, kidney, pancreas, spleen, ovaries, colon and brain [388, 419, 422]. Intranasal administration favours delivery to the brain [423, 424] whereas local injections favour exosomes/EVs biodistribution in nearby lymph nodes [404, 418, 425, 426]. Accumulation of SPION5-loaded B16-F10 exosomes in popliteal lymph nodes closest to the injection site could be detected by magnetic resonance [404] whereas PKH26-labeled EVs were transported into lymph nodes after subcutaneous injection in mice [425]. Serum-derived sEVs (< 50 nm in size) and cell-derived sEVs (> 100 nm in size) were delivered to lymph nodes in a size-dependent manner, suggesting that smaller serum-derived sEVs might serve as efficient carrier systems of immune stimulators to lymph nodes for desired immune responses [426]. Interaction between glycans on sEVs and lectins on the recipient cells might play an important role in EVs pharmacokinetics after local administration [389].

Extracellular vesicle *in vivo* biodistribution is determined by cell source, route of administration and targeting [387]. A simple characteristic such as exosome/EVs size influences transport and biodistribution, as larger EVs preferentially accumulate in bones, lymph nodes and liver [392]. More detailed studies comparing different injection sites, donor cells and healthy or disease conditions are necessary to establish clearance and organ uptake of EVs and to better understand the mechanisms governing the cellular recognition of EVs [388, 413].

Targeting and delivery

Vesicles interact with recipient cells by binding at the cell surface via specific receptors followed by internalization by endocytosis or micropinocytosis, and/or fusion with the plasma membrane or membranes of internal compartments (Figure - 8) [197]. EV surface molecules, including phospholipids and proteins, are important factors in determining the in vivo behaviour of exosomes and specific targeting, reviewed in [239, 321, 388, 389, 406]. After binding to recipient cells, EVs may remain stably associated with the plasma membrane, directly fuse with the plasma membrane or be internalized through distinct endocytic pathways [239, 272, 278, 328, 351, 413, 427]. Exosomes are recruited as single vesicles to the cell body and guided by filopodia to endocytic hot spots at the filopodial base [428]. After internalization, exosomes shuttle within endocytic vesicles to scan the endoplasmic reticulum before being sorted into the lysosome as their final intracellular destination, a process that resembles the mechanisms used by the virus [428].

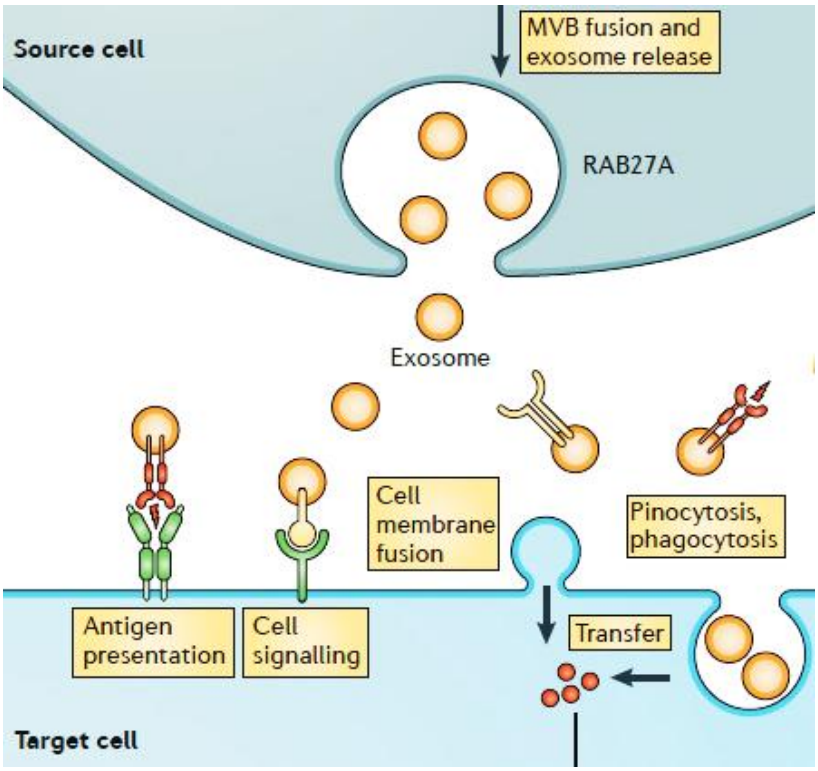

Figure - 8. Biogenesis of extracellular vesicles and their interactions with recipient cells.
Extracellular vesicles can be regarded as signalosomes for several biological processes. They can be involved in antigen presentation, transfer of both major histocompatibility complex (MHC) molecules and antigens, participating in immune regulation, can directly activate cell surface receptors via protein and bioactive lipid ligands, transfer cell surface receptors or deliver effectors. Additionally can fuse with the plasma membrane, delivering bioactive molecules directly to the cytoplasm, or be internalized by endocytosis or micropinocytosis. Adapted from [197].

Macrophages present scavenger receptor class A family (SR-A) receptors that recognize negatively charged molecules and thus partially explain the tropism of EVs to macrophages. Pulmonary epithelial cells recognize tetraspanin proteins and integrins present on exosomes surface [390, 391]. Interaction between glycans on sEVs and lectins on the recipient cells might also play an important role in EVs pharmacokinetics after local administration [389]. In lymph nodes, internalization of the EVs by antigen-presenting cells (APCs) is observed, particularly by those expressing CD11b positive for cell-surface-bound sialic acid-binding immunoglobulin-like lectins (siglecs), but not by APCs negative for siglecs, suggesting that cellular uptake of exosomes involved recognition of sialic acids by siglecs [409, 425]. Additionally, carbohydrate moieties on the exosomes contributed to the uptake of exosomes by cells, C-type lectin and mannose-rich CLR was determined to be involved in exosome uptake by dendritic cells (DV), As determined by a study were DC_{OVA}-derived EXO, harbouring MHC class I and II, CD11b, CD11c, CD54, CD80, CD86 chemokine receptor CCR7, mannose-rich C-type lectin receptor DEC205, TLR4 and TLR9, were internalized by DC, and stimulated the expression of immunologically important molecules such as MHC class II, CD40, CD54 and CD80 on DC [429].

These findings allow researchers to take advantage of exosomes biology to leverage their therapeutic use, since they are rich in bioactive molecules and, more importantly, their content and membrane composition can be modulated to improve their bioactivity and/or targeting potential [217, 236, 388]. Some examples of exosome/EVs surface modifications methods and applications are summarized in Table XII.

Table XII. Application Examples of Surface Modification. *In [430]*

Surface Modification Methods	Targeting Method	Drug Loading	Targeted Tissues and Applications	Ref.
Genetic Engineering	Dendritic cells (DCs) are genetically modified to express fusion proteins containing the membrane protein Lamp2b and RVG peptides, and engineered exosomes are harvested from the cells.	siRNA (Electroporation)	Targeting the central nervous system (neurons, microglia, oligodendrocytes) to treat Alzheimer's disease	[431]
Chemical reaction combined with post-insertion	c (RGDyK) is a tumor-targeting peptide. DSPE-PEG 2000-cRGDyK is prepared by chemical reaction. The ligand is spontaneously inserted into the exosomal lipid bilayer through hydrophobic interactions and combined to obtain the targeted exosomes.	PTX (Co-incubation)	It can penetrate the blood-brain barrier, target glioblastomas, and significantly reduce the activity of cancer cells.	[432]
Genetic Engineering	Donor cells are engineered to express the transmembrane domain of the platelet-derived growth factor receptor fused to the GE11 peptide to achieve targeting, thereby assimilating exosomes from this source.	let-7a miRNA (Transfection)	Targeting breast cancer tissues expressing EGFR to treat breast cancer	[433]
Genetic Engineering	Engineered mouse immature dendritic cells expressing Lamp2b fused to iRGD peptide to produce tumour-targeted exosomes.	DOX (Electroporation)	It targets tumour tissues, inhibits the growth of the tumour, and has good antitumor activity.	[434]
Chemical reaction	Extracellular vesicles containing azide lipids were firstly prepared and then conjugated to the targeted peptide using a copper-free catalytic click chemistry.	PTX, TPZ (Loaded on liposomes)	Targeting tumour cells	[435]
Electrostatic interaction	The complex formed by a cationic lipid and a pH-sensitive fusion peptide binds exosomes through electrostatic interaction to target the receptor cell membrane.	Dextran, Saponin (Electroporation)	Targeting the receptor's cell membrane to enhance cell uptake and cytoplasmic release of exosomes	[436]
Magnetic nanoparticle technology	The SPMN-Tf conjugates were co-incubated with pre- dialyzed serum to form SMNC-Exo through interaction with the Tf-Tf receptor. After drug loading, SMNC-Exos were concentrated in the tumour region in the presence of an external magnetic field.	DOX (Co-incubation)	Targeting mouse subcutaneous H22 cells to inhibit the growth of tumour	[437]

Increasing EVs stability and bioavailability would, in an indirect manner, increase EVs delivery to the target tissue/cells. Biomaterials can confer stabilization and prolong the bioavailability of these vesicles in the targeted site. For example, different strategies were applied to entrap exosomes and sustain their delivery, and ultimately their bioavailability, in the wound, and the results showed better wound healing kinetics, regardless of the delivery time during the wound healing process [124, 125, 216, 217, 228].

IV. Clinical potential of exosomes and EVs

1. EVs in the clinic – guidelines and requirements

EVs, such as exosomes and microvesicles, are released by different cell types and participate in physiological and pathophysiological processes by mediating intercellular communication. EVs of defined cell types may serve as novel tools for various therapeutic approaches, including (a) immune-modulatory therapy, (b) vaccination (anti-tumour or anti-pathogen), (c) regenerative therapies and (d) drug delivery [278, 369, 438, 439].

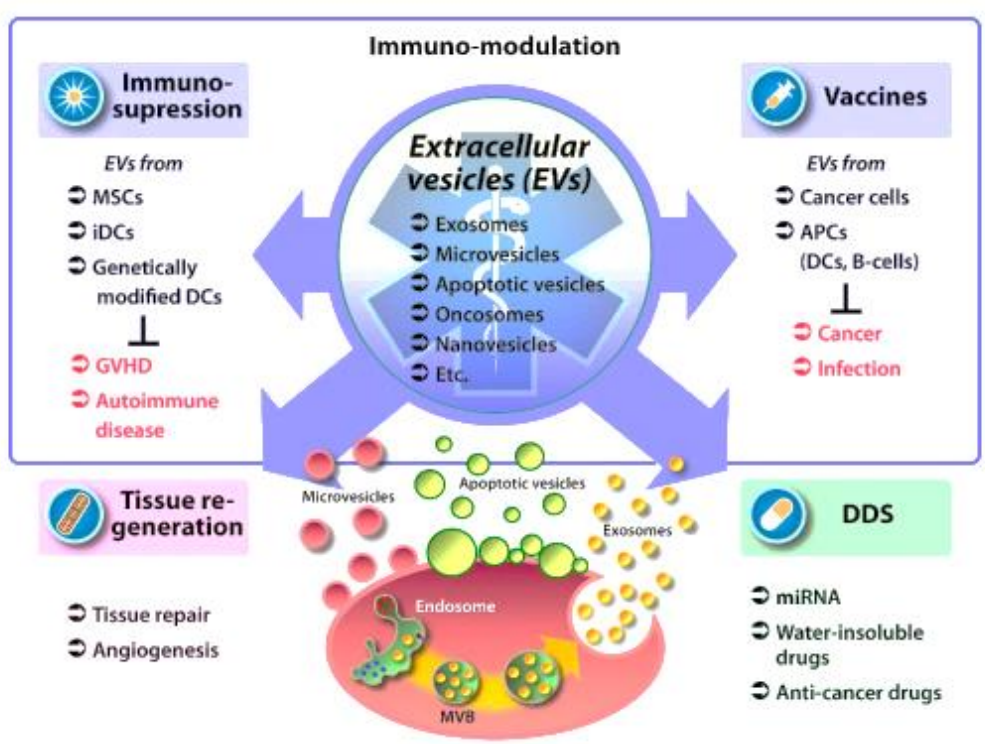

Figure - 9. Extracellular vesicles (EVs) potential for clinical applications.
Natural or modified EVs have high potential as new therapeutic tools: (a) immune-modulatory therapy, (b) vaccines, (c) regenerative agents and (d) drug delivery. **MSCs** – mesenchymal stem cells; **iDCs** – immature dendritic cells; **DCs** – dendritic cells; **GVHD** – graft-versus-host disease; **APC** – antigen presenting cells; B-cells – B lymphocytes **DDS** – drug delivery system; .Image from [438]

The translation of EVs into clinical therapies requires the categorization of EV-based therapeutics in compliance with existing regulatory frameworks, namely, requirements for manufacturing, quality control and clinical investigation, and definition if EVs will act as active drugs/therapy or will serve as drug/therapy delivery vehicles [369]. Since the EV-based therapeutics can be defined as biological medicine and belong to the pharmaceutical class of biologicals should be subjected to the regulatory frameworks concerning biological medicinal products, available in the EU, US, Australia and Japan. Regulatory aspects of manufacturing and application of new therapeutics have to be implemented and safety aspects must be taken into account (e.g. donor, recipient, product, manufacturing, clinical application, biovigilance). The medicinal product framework addresses the safety standards for inadvertent microbial and viral contamination and demands GxP standards (GxP: Good Manufacturing/ Good Laboratory/ Good Distribution/ Good Clinical/ Good Scientific Practice or GMP/ GLP/ GDP/ GCP/ GSP) for the production and quality control of corresponding therapeutics. Furthermore, it regulates the conduct of clinical trials [369].

For the development of EV-based therapeutics ATMP guidance may be relevant, since EVs are produced, in many cases, from human material by a manufacturing process comparable to ATMP production. According to the legislation for tissues and cells, and ATMPs, a panel of minimal criteria to characterize human cell-based medicinal products have to be considered before use in clinical trials. It has to be addressed if the product is (a) of autologous, allogeneic or xenogeneic origin; (b) extensively or minimally manipulated and (c) immunologically active or neutral. Additionally, have to be defined (d) the proliferative capacity of cells; (e) the cell or tissue-like organization as well as the dynamic interaction between cells and with structural components and (f) the intended use. It is anticipated that requirements (a-d) and (f) will be relevant for the characterization of sources of EVs used to generate EV-based therapeutics and this information should be provided by the producing manufacturers. Reviewed in [369].

Table XIII. Proposed ISEV requirements for EVs evaluation before clinical application. *In [369]*

- **Source of the starting material**
  - Donor inclusion/exclusion, donor release criteria
  - Autologous, allogeneic, xenogeneic, bacterial, pathogen or plant EVs
  - EV-source characterization (donors, donor cells/tissues/ fluids, culture reagents)
- **EV isolation and storage**
  - Isolation techniques and standardization
  - Purity and impurities
  - Scalability of technology
  - Storage conditions
  - Adequate quality of reagents and materials
  - In-process controls
- **Quality control**

  Molecular and physical characterization
  - Quantitative Analyses (counts and size)
  - Qualitative Analyses (presence of EV marker(s), purity)
  - Composition (surrogate marker)
  - Contamination (viral, microbiological, endotoxins, toxins, allergens)

  In vitro biological characterization
  - Complexity and heterogeneity
  - Mode of Action
  - Potency of EVs (in vitro bioassays)
  - Quality release criteria
- **In vivo analyses/EV application**
  - Selection of relevant animal models (disease specificity? / species specificity?)
  - Dose selection (single / multiple applications)
  - Route of application (local, systemic)
  - Pharmacokinetics/ADME: Absorption _ Distribution _Metabolism _ Excretion
  - Toxicity
  - Immunogenicity, Immunotoxicity
  - Tumourigenicity
  - Biodistribution
  - Potency of EVs (in vivo bioassays)
- **Before clinical trial**
  - Informed consent of donors and host
  - Study protocol
  - Investigational medicinal product dossier
  - Investigators brochure
  - Ethics committee approval
  - Register Entry (EMA, EudraCT or NIH, www.ClinicalTrials.gov)

2. EVs in clinical trials

There are several registries of exosome clinical trials all over the world. A total of 70 studies were found when searching for 'exosome' in clinicaltrials.gov (Figure - 10) [440]. When searching for 'extracellular vesicles' we found 11 studies (1 registered in Canada, 1 in the US; 2 in China and 6 in the EU), 6 of which represent different studies than the found in the previous research [441]. A more detailed analysis of the registered clinical trials revealed that 3 of them did not refer directly to the use of exosomes or EVs, neither as markers or therapeutic / regenerative tools. So, in total we can account for 73 clinical trials involving exosomes and/or EVs registered in the clinicaltrils.gov (US database) up to date.

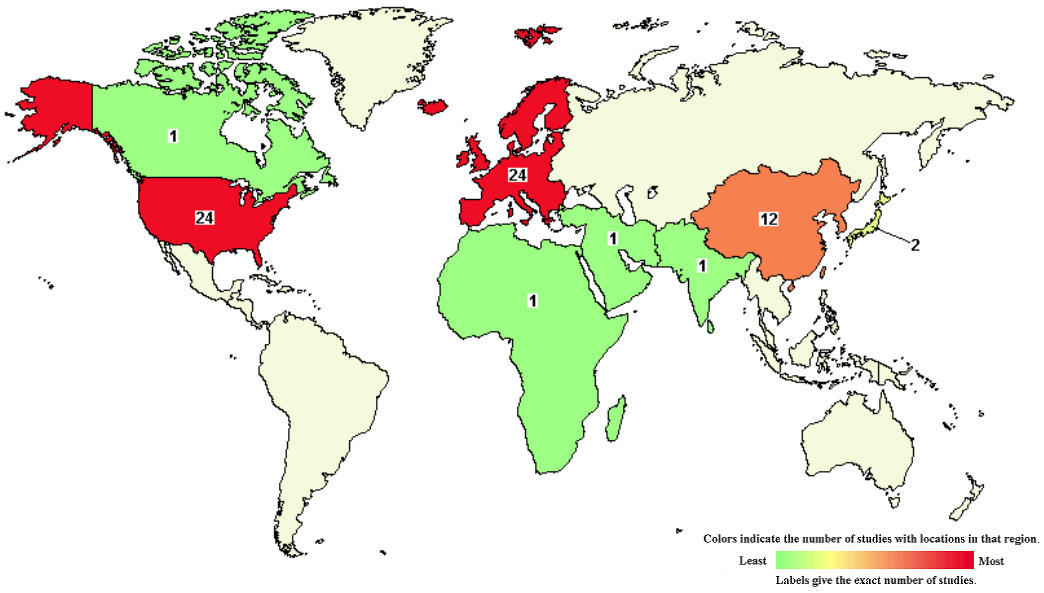

Figure - 10. Exosome registered clinical trials.
The map presents the locations of 70 studies found in clinicaltrials.gov with the research term: 'exosome' accessed in 2018 Feb. 5. Studies with no locations are not included in the counts or on the map. Studies with multiple locations are included in each region containing locations. Studies found for search of 'extracellular vesicles' are also not present in the map. In [442].

The majority of the clinical trials explore exosomes and/or EVs as 'markers' (63). Indeed, these EVs can be used as diagnostic and prognostic markers for patient/disease follow-up and for preventive medicine (they can be use as indicators of risk, allowing individuals and clinicians to adopt measures to prevent or delay a disease onset). Table XIV presents a list of the clinical trials involving exosomes and EVs as markers.

Table XIV. Clinical trials with exosomes and EVs for disease diagnosis and monitoring

Trial Code	Base	Source	Condition	Observations	Phase
NCT02702856	Exos	Plasma	Prostate Cancer		
NCT03236688	Exos	Plasma	Prostate Cancer	Metastatic Castrate Resistant	
NCT03031418	Exos	Urine	Prostate Cancer		
NCT03235687	Exos	Urine	Prostate Cancer		
NCT02935816	Exos	Blood	Prostate Cancer	Radiotherapy	
NCT00578240	Exos / DNA	Blood, BF	Prostate Cancer		
NCT02890849	Exos	Plasma, tissue	NSCLC		
NCT02869685	Exos	Plasma, tissue	NSCLC	Radiotherapy	
NCT02921854	Exos	Serum	NSCLC	Radiotherapy	
NCT03228277	Exos / EVs	BLF	NSCLC		2
NCT03236675	Exos	Plasma	NSCLC	Drug treatment	

Trial Code	Base	Source	Condition	Observations	Phase
NCT03317080	Exos/ CTCs	Blood	Lung Cancer		
NCT03109873	Exos / Ctk	_	Oropharyngeal Cancer	Radiotherapy / Drug treat.	Early 1
NCT02147418	Exos	Blood / saliva	Oropharyngeal Cancer	HPV	
NCT02464930	Exos	Serum, bile, EsoCs	Esophagus Adenocarcinoma	Other esophagus diseases	
NCT01779583	Exos	Plasma	Gastric Cancer		
NCT03102268	Exos / EVs	Plasma	Cholangiocarcinoma	Benign Biliary Stricture	
NCT02393703	Exos	Blood, tissue	Pancreatic Cancer	Benign Pancreatic Disease	
NCT03032913	Exos/ CTCs	Blood	Pancreatic cancer	Ductal Adenocarcinoma	
NCT03334708	Exos	Blood	Pancreatic Cancer	Other pancreatic diseases	
NCT03109847	Exos	Serum, saliva	Thyroid Cancer	Drug: metformin	2
NCT02862470	Exos	Urine	Thyroid Cancer	Drugs treatment (2)	
NCT01344109	Exos	Plasma	Cancer / chemotherapy	Breast Neoplasms	
NCT02063464	Exos	Monoc	Ovarian Cancer / Neoplasms		
NCT02977468	Exos	Serum	Breast Cancer	Triple neg. / Drug treatment	1
NCT03108677	Exos	Blood	Osteosarcoma	Lung Metastases	
NCT03217266	Exos	Blood (?)	Soft Tissue Sarcoma	Drug treatment	1
NCT02310451	Exos	Blood	Metastatic Melanoma		
NCT02071719	Exos	Serum, urine	Renal Cell Cancer	Drugs (5)	
NCT02662621	Exos / EVs	Blood, urine	Cancer	All kinds	
NCT03262311	EVs	Blood	Cancer	Several.	
NCT03264976	Exos	Serum	Diabetic Retinopathy		
NCT03392441	Exos	Blood	Diabetes I /	Insulin Deprivation	
NCT03106246	Exos /EVs	Blood	Diabetes I / II	Islet Cell Transplantation	
NCT02649465	Exos	Blood (?)	Diabetes II, FLD	Drugs treatment (2)	4
NCT03027726	Exos	Blood	Diabetes II Risk	Overweight Children	
NCT00285805	Exos	Urine	Insulin resistance	Drug	
NCT02957279	Exos	DCs	Sepsis	Antibiotic administration	
NCT03267160	Exos	Blood / urine	Sepsis		
NCT03222986	Exos	Blood / urine	Sepsis	MOD	
NCT03280576	Exos	Plasma	Sepsis		
NCT01860118	Exos	Blood / urine	Dementia (Parkinson's)	Drug treatment	
NCT03275363	Exos	Serum, plasma, BC	Dementias		
NCT01811381	Exos	Plasma	Dementia / MCI	Drug: curcumin	2
NCT03381482	EVs	Plasma, CSF	Dementia	Alzheimer disease	
NCT03419000	Exos	Blood	Epilepsy	Drug Resistant	
NCT02931045	EVs	Platelets	Myocardial Infarction	Antiplatelet therapy	4
NCT03372174	EVs	Blood (?)	Cardiopulmonary bypass	mechanical ventilation	
NCT02890147	Exos	Plasma, urine	Autoimmune Diseases	Healthy Subjects	
NCT02890134	Exos	Plasma, urine	SAD - Healthy		
NCT02890121	Exos	Plasma, urine	SAD		
NCT02226055	Exos	Blood, urine	CKD	Unknown etiology	
NCT03227055	Exos	Urine	CKD		
NCT02327403	EVs	Urine	Proteinuria	Drug treatment (Belatacept)	2
NCT03049202	Exos	Serum, plasma, urine	COPD	Other pulmonary disorders	
NCT02653339	Exos	Blood, urine	Rhinitis, Allergic, Perennial	Drugs treatment (2)	
NCT03203512	EVs	Blood	Cardiovascular diseases	Risk / Dietary supplement	
NCT03034265	Exos	Urine	Hypertension		
NCT02822131	Exos	Urine	Hypertension	Diet Suppl. vs Drugs (3)	
NCT02823613	Exos	Urine	Healthy	Salted diet	
NCT02748369	Exos	Blood	Healthy	Somastostatin / Glucagon	
NCT02737267	Exos	Blood, serum	Healthy	high protein diet	
NCT02797834	Exos / EVs	End.F	Healthy		
NCT02051101	Exos	Biopsy, blood	Nevus flammeus	Port-Wine Stain	1

Exos – exosomes; **EVs** – extracellular vesicles; **CTCs** – circulating tumor cells; **Ctk** – cytokines; **BF** – body fluids; **BLF** - bronchoalveolar lavage fluid; **EsoCs** - esophageal cells; **DCs** – dendritic cells; **BC** – buffy coat; **CSF** – cerebrospinal fluid; **End.F** – endometrial fluid; **NSCLC –** non small cell lung cancer; **FLD** - fatty liver disease (non-alcoholic); **MCI** - mild cognitive impairment; **SAD** - systemic autoimmune diseases; **CKD** – chronic kidney disease; **COPD** – chronic obstructive pulmonary disease; **HPV** – human papillomavirus; **MOD** - multiple organ dysfunction.

The samples used for these studies vary from body fluids, cells to biopsy tissues, but commonly is used blood, including plasma and serum, and urine. The majority of the studies are evaluating EVs/exosomes as biomarkers of cancer on patient diagnosis, prognosis and follow-up upon treatment (Figure - 11). There is also a set of studies that are evaluating EVs/exosomes as biomarkers of diseases such as diabetes, sepsis, heart/ brain/ lung/ kidney disorders, autoimmune diseases and evaluation of healthy individuals to diet, supplements or some drugs (Figure - 12). The majority of the clinical trials are without phases (for example, studies of devices or behavioral interventions). In 2 trials, exosomes and EVs are used to monitor patient follow-up on 2 conditions upon therapy administration, namely, non-alcoholic fatty liver disease (diabetes II related) and myocardial infarction. A study has registered the intent of using exosomes for prevention of diabetes II. Three studies are referred as exploratory: (i) a study to evaluate diet impact on healthy individuals, (ii) a study to evaluate endometrial fluids of healthy women for the establishment of potential markers and (iii) a study to evaluate the pathogenesis of nevus flammeus (port-wine stain).

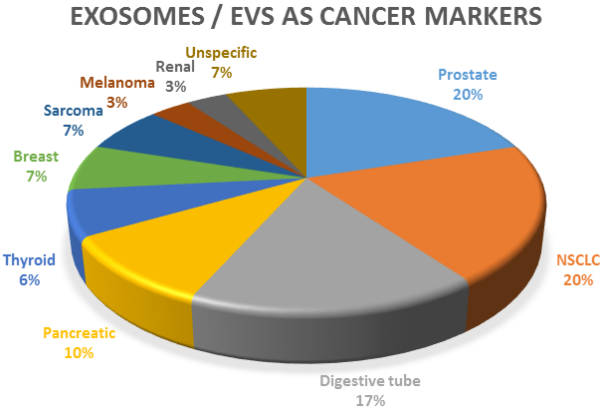

Figure - 11. Clinical trials studying exosomes and EVs as cancer markers.
Graphs present de percentage of studies for different cancers (Total = 30 clinical trials). NSCLC refers to non-small cell lung cancer, digestive tube cancers englobes lip, oral cavity, larynx, pharynx, esophagus, gastric and bile duct tumours. Sarcoma includes osteosarcoma (with lung metastases) and soft tissue sarcoma. Unspecific refers to 2 trials, 1 that englobes several types of cancers and other that do not refer the type of cancer.

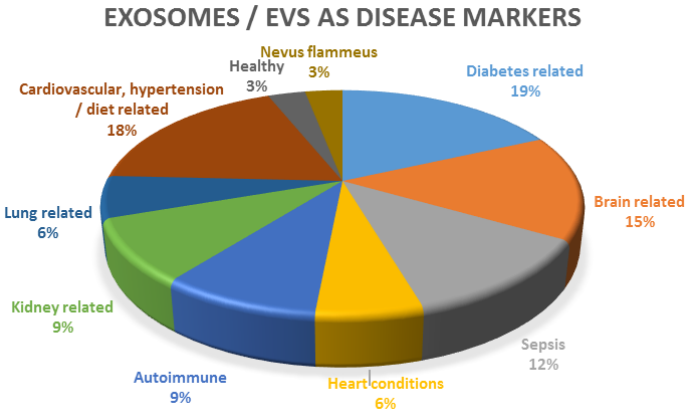

Figure - 12. Clinical trials studying exosomes and EVs as disease markers (except cancer).
Graphs present de percentage of studies for different diseases/conditions (Total = 33 clinical trials). Diabetes related diseases englobes diabetes I and II, diabetic retinopathy, fatty liver disease and insulin resistance studies. Brain related studies includes 4 studies of dementia (1 mild cognitive impairment) and 1 of epilepsy. Heart conditions its 1 myocardial infarction a 1 cardiopulmonary bypass study. Kidney related diseases are 2 chronic kidney diseases and 1 of proteinuria (commonly related with kidney failure). Lung related is 1 study of chronic obstructive pulmonary disease and 1 of allergic rhinitis. Cardiovascular, hypertension and diet related englobes several studies evaluating the effect of diet or specific drugs in the cardiovascular or global health state of the individuals enrolled.

From the 73 clinical trials with exosomes and/or EVs, 10 applied them for therapy or regenerative purposes. Interestingly, in 4 of the 10 studies, exosomes were used to encapsulate drugs (Table XI).

Table XV. Clinical trials with exosomes and EVs for therapy and regenerative purposes.

Trial Code	Base	Source	Manipulation	Application	Condition	Phase
NCT01550523	Exos	ATCs	Cells treated with IGF-1R/AS ODN	Autologous	Malignant Glioma of Brain	1
NCT02507583	Exos	ATCs	Cells treated with IGF-1R/AS ODN	Autologous	Malignant Glioma / Neoplasms	1
NCT01159288	Exos	DCs	Dex2 loaded	Autologous (?)	Non Small Cell Lung Cancer	2
NCT01294072	Exos	Plant	Curcumin loaded	Xenogenic	Colon Cancer	1
NCT01668849	Exos	Grape	_	Xenogenic	Head and Neck Cancer|Oral Mucositis	1
NCT02138331	Exos / MVs	UCB-MSCs	_	Allogenic	Diabetes Mellitus Type 1	2|3
NCT03384433	Exos	MSCs	_	Allogenic	Cerebrovascular Disorders	1|2
NCT02565264	Exos	Plasma	Exos enriched plasma	Autologous	Ulcer (Chronic Wounds)	Early 1
NCT02594345	Exos	RBCs	_	Autologous	Blood Coagulation / Platelet Function	

Exos – exosomes; **MVs** – microvesicles; **ATCs** – apoptotic tumor cells; **DCs** – dendritic cells; **Monoc** – monocytes; **UCB** – umbilical cord blood; **MSCs** – mesenchymal stem cells; **RBCs** – Red blood cells

In most studies, EVs/exosomes were isolated from autologous human cells (7, being 5 of autologous origin and 2 of allogenic origin). In 2 studies, EVs/exosomes were isolated from plants (xenogenic use). Most of the trials are still in phase 1 (4), one is in phase 1/2, another in phase 2, and other applying UCB-MSCs for diabetes mellitus I is already in phase 2/3. For ulcers plasma enriched in exosomes is being used as therapeutic and regenerative agent (Figure - 13B).

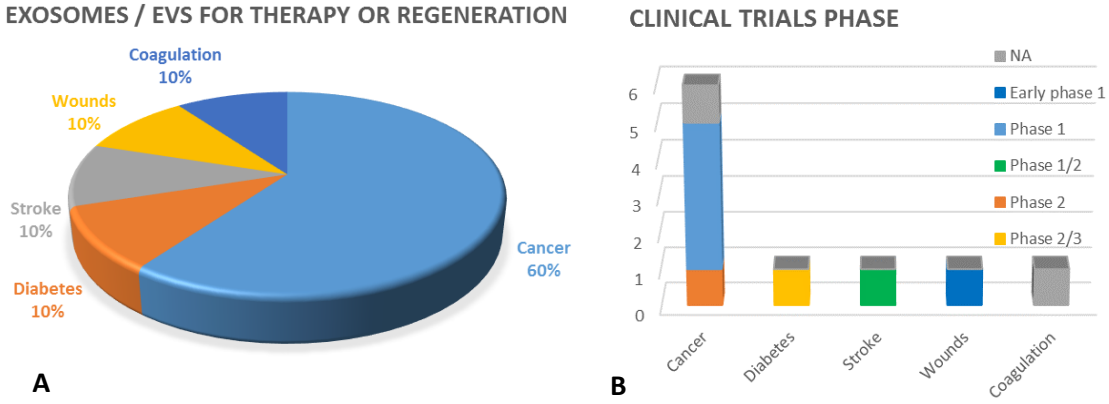

Figure - 13. Clinical trials with exosomes and EVs for therapy or tissue regeneration.
Graphs present de percentage of studies for different diseases/conditions. Cancer includes 5 different types of cancer (malignant glioma, non-small cell lung cancer, ovarian cancer, colon cancer, and head and neck cancer). Stroke refers to one study of cerebrovascular disorders. Coagulation refers to one study talking with coagulation and platelet dysfunction.

The application in a clinic setting of exosome and / or EVs derived products is still in its infancy, nevertheless, there are already several companies with the purpose of developing EV-based products (Table XII) [443].

Table XVI. Companies with EV- based services and products. *Adapted from [443]*

Company	Base	Source	Product	Therapeutic target	Web address
Anjarium Biosciences	EVs * Exos *	NA	Hybridosome™ - delivery of drugs	Broad range of severe diseases	anjarium.com
Aposcience AG	Secr	PBMNCs	APOSEC™ – Secr. of apototic PBMNCs	Stroke, spinal cord injury, skin lesions, acute and chronic myocardial infarction	aposcience.at
Capricor Therapeutics	Cells Exos	CDCs	CAP-1002 – cell product CAP-2003 – exos	Cardiovascular and non-cardiovascular diseases	capricor.com
Codiak Biosciences	Exos *	NA	Exos for targeted drug delivery and diagnostic	Pancreatic cancer	codiakbio.com
The Cell Factory (Esperite Group)	Cells EVs / Exos	MSCs	autologous stem cells; allogenic "off-the-shelf" EVs and exos	Various diseases: Crohn's disease, epilepsy, … Cerebral palsy, tissue eng., …	cell-factory.com esperite.com
Evox Therapeutics	Exos *	NA	Targeted delivery	Serious life-threatening diseases (inflammatory and neurological diseases)	evoxtherapeutics.com
ExoCyte Therapeutics	Exos *	DCs *	Cancer vaccines (*Autologous DCs electroporated with tumor -derived exosomes, co-adm. with checkpoint inhibitor*)	Cancer	exocytetherapeutics.com
Exogenus Therapeutics	Exos	NA	Exo-Wound	Skin lesions	exogenus-t.com
Exovita Biosciences	Exos *	NIC	Exos that are cytotoxic to cancer cell	Diverse Cancers	exovitabio.com
Kimera Labs	Exos fluids	MSCs AMNIO	XoGlo™ Amnio2x™	Orthopedic, cosmetic and regenerative medicine	kimeralabs.com
Paracrine Therapeutics	EVs	ESC-MSCs	*Embryonic stem cell-derived MCS-EVs*	Stroke, MI, osteochondral defect, GVHD	paracrinetherapeutics.com
ReCyte Therapeutics	Cells Secr EVs	Embryonic PCs	*Embryonic progenitor cells and their secreted factors, including EVs*	Vascular disorders	recyte.com
ReNeuron	Cells EVs	RPCs NPCs	*RPCs and NPCs, and secreted EVs*	Neurologic and ophthalmologic disorders	reneuron.com
Stemedica Cell Technologies, Inc.	Cells Secr	MSCs NSCs	Ischemia-tolerant MSCs and NSCs; stem cell factors from MSCs	Cardiovascular diseases, traumatic brain injury, cutaneous photoaging, Alzheimer's disease	stemedica.com
ZenBio	Exos	Pre-Adip; pMSCs; CB	Exos from pre-adip., pMSCs and CB serum	Skin lesions	zen-bio.com

Secr – secretome; **Exos –** exosomes; **EVs** – extracellular vesicles; **NA** – not available; **PBMNCs** – Peripheral blood mononuclear cells; **CDCs** – cardiosphere cells; **MSCs** – mesenchymal stem cells; **DCs** – dendritic cells; **NIC** – non-immune cell type whith anti-cancer properties; **AMNIO** – amniotic fluid; **ESC-MSCs** – embryonic stem cells derived mesenchymal stem cells; **PCs** – progenitor cells; **RPCs** – retinal progenitor cells; **NPCs** – neural progenitor cells; **NSCs** – neural stem cells; **Pre-Adip** – pre-adipocytes; **pMSCs** – placental mesenchymal stem cells; **CB** – cord blood; **MI** – myocardial infarction; **GVHD** – graft-versus-host disease. * Manipulated product. Adapted from [443]

The high number of companies pursuing this new field of research for clinical purposes, and the broad range of different diseases / conditions being targeted, reflects the recognized potential of the field. Interestingly, 3 companies are actually developing secretome / exosome-based products, from different cell sources (peripheral blood mononuclear cells, pre-adipocytes, placental mesenchymal stem cells and cord blood), for skin lesions, which would include chronic wounds, the focus of this work.

3. EVs in wound healing – underlying mechanisms

The wound healing process is a complex process, requiring the coordination of many cellular and extracellular processes, like cell migration and proliferation, angiogenesis, collagen synthesis and deposition, and skin tissue remodeling [9, 10, 14-20]. Any impairment in this

cascade leads to chronic non-healing wounds such as diabetic ulcers or pathological scarring such as keloid scars [1, 2, 4, 5, 9, 14-18]. As described earlier, different approaches have been studied to tackle with this urgent issue, including the administration of growth factors, DNA and RNA-based therapies, biomaterials, among others [16, 23, 56, 139, 150]. The wound is a harsh environment, rich in proteolytic enzymes, which can lead to the degradation of growth factors administered to the wound, or secreted by the skin cells, disrupting the subsequent signaling cascades and, thus contributing to an impaired wound healing [444, 445]. Because EVs are lipid bilayer vesicles, they offer protection from proteolytic degradation to the enclosed biomolecules, enhancing their availability and consequently increasing the targeting of skin cells [10, 191-193, 197, 202-205]. Additionally, these vesicles offer advantages relatively to cell-based therapies, since they offer no risk of aneuploidy and limited possibility of immunological response in an allogenic context, are easier to manipulate and maintain with low costs [188-190].

In the context of wound healing, it has been demonstrated that exosomes have the capacity to mediate several signaling pathways relevant for wound healing, like PI3K/Akt, MAPK/ERK, JAK/STAT, Hippo/YAP, Wnt/β-Catenin, TLR4/NF-κB, and TGF-β/SMAD2 pathways, which, in turn modulate gene expression and induce a specific response from the cell [19, 446-464]. Exosome-containing biomolecules important for wound healing as well as their target genes and pathways are presented on Table XVI. The identified pathways are known to play critical roles in wound healing at different stages, modulating crucial biological processes, such as cell proliferation, migration, and angiogenesis [125, 207, 216, 217, 223, 225, 226, 228, 230, 234-237]. Furthermore the modulation of these pathways was demonstrated to be, at least in part, mediated by biomolecules transported by exosomes, proteins, growth factors and different miRNAs [125, 216, 217, 223, 225, 226, 228, 234-237].

The majority of the studies that attempt to unravel the molecular mechanisms beyond exosome regenerative properties in wounds refer to exosomes secreted by mesenchymal stem / stromal cells (MSCs), from different tissue sources, namely, umbilical cord (UC), bone-marrow (BM), adipose tissue (also named as adipose-derived stem cells – ASCs), synovium or stratum synovial, and derived from induced pluripotent stem cells (iPSCs) [216, 217, 223, 225, 228-231, 234-237]. One study reported the use of exosomes derived from fibrocytes, a group of bone marrow-derived mesenchymal progenitor cells [225]. Two studies were based on exosomes from endothelial progenitor cells (EPCs), in one study EPCs were obtained from umbilical cord blood (UCB) and the respective exosomes were used in excessive scar, in the other exosomes derived of EPCs from peripheral blood (PB) were applied in ischemic hind limb animal model [207, 233]. Furthermore, platelet rich plasma (PRP), UCB plasma, hematopoietic stem cells (HSCs) from PB and amniotic epithelial cells (AECs) are also reported as sources of exosomes in studies regarding their molecular mechanism in the context of wound healing [125, 206, 226, 232].

From all wound healing studies involving exosomes, it is difficult to evaluate the importance of the exosome source in the final therapeutic effect and action mechanism because it is difficult to normalize the effect between different animal models, concentration of exosomes, and methodologies adopted to identify the action mechanism. In case of PRP, UCB plasma and EPC exosomes, their effect seems to target skin regeneration and tissue maturation (with less scaring), via the PI3K/Akt, MAPK/ERK, and Hippo/YAP pathways [125, 207, 226].

Table XVII. Underlying mechanisms of EVs in wound healing. *Adapted from [443]*.

Source	Outcome(s)	Molecule(s)	Proposed mechanism(s)	Ref
hPRP *	↗ ECs and fib. proliferation, migration and angiogenesis; ↗ STZ-rat wound closure, reepithelization, angiogenesis and collagen remodeling	PDGF-BB; TGF-β1; bFGF; VEGF.	YAP pathway: YAP dephosphorylation / activation trough Rho-ROCK axis → translocation to nucleus → reepithelization PI3K/Akt + ERK pathways: Akt and ERK activation / phosphorylation → angiogenesis	[125]
hUCB – EPCs	↗ ECs proliferation, migration and angiogenesis; ↗ STZ-rat wound closure, angiogenesis, reepithelization and collagen maturation; ↘ scar	_	ERK pathway: ERK phosporylation / activation→ cell proliferation, migration and angiogenesis	[207]
hUC – MSCs (LPS cond.)	↗ M2 differentiation; ↗ STZ rat wound closure and angiogenesis, ↘ inflammation	Let-7b (miR-133a; miR-183; miR-550b; miR-1180)	TLR4/NF-κB/STAT3/Akt pathway: ↘ TLR4; phosphorylation P65; STAT3 and Akt → M1 to M2 macrophage polarization	[223]
human SMSCs *	↗ ECs and fib. cell proliferation; ↗ STZ rat wound closure, angiogenesis, reepithelization, collagen maturation	+ miR-126-3p (…)	Akt/ERK pathway: phosphorylation Akt and ERK → cell proliferation and angiogenesis	[217]
Human fibrocyte	↗ ECs, fib., diabetic ker. proliferation, migration and angiogenesis; ↗ Diabetic mice wound closure	HSP-90α; STAT3; (miRs …)	↗ COL1; COL3 and α-SMA STAT3 pathway activation	[225]
hUCB plasma	↗ ECs and fib. cell proliferation, migration and angiogenesis; ↗ Mice acute wound closure, reepithelization and angiogenesis; ↘ scar	miR-21-3p (miR-19b; miR-27b; miR-125b; miR-126; miR-214)	Inhibition of PTEN and SPRY1 PI3K/Akt + ERK pathways: Akt and ERK phosphorylation / activation→ cell proliferation, migration and angiogenesis	[226]
hUC – MSCs *	↗ Fib. proliferation and migration; ↘ myofibroblast differentiation ;↗ Mice wound closure, ↘ scar	miR-21; miR-23a; miR-125b; miR-145	TGF-β/SMAD2 pathway: inhibition TGF-β2; TGF-βR2 and SMAD2. Inhibition excess α-SMA	[216]
human ASCs	↗ Fib. proliferation, migration and collagen synthesis; ↗ Mice wound closure and maturation, ↘ scar	_	↗ PCNA; cyclin-1; cyclin-D3, N-cadherin, elastin, collagen I and III	[229]
human ASCs	↘ Differentiation fib. → myofib.; ↗ diabetic mice wound closure, reepithelization, angiogenesis and collagen remodeling ↘ scar	_	ERK/MAPK pathway: phosphorylation ERK1/2 → ↗ MMP3; ↗ COL3A1, TGF-β3; ↘ α-SMA, COL1A1	[230]
human ASCs	↘ Differentiation fib. → myofib.; ↘ Mice wound scar; ↗ collagen maturation	_	ERK/MAPK pathway: phosphorylation ERK1/2 → ↗ MMP3; ↗ COL3A1, TGF-β3; ↘ α-SMA, COL1A1	[230]
human ASCs	↗Ker. and fib. proliferation and migration; ↗ Rat wound closure	miR-205	Akt pathway: Akt phosporylation → Bcl-2 → cell survival; proliferation, and migration MSC EVs modulated miR-205 expression	[228]
human AECs	↗ Fib. proliferation and migration; ↗ Rat wound closure and collagen-fibers organization; ↘ scar	_	↗ MMP-1; ↘ collagen I and III → ↘ scar	[232]
hiPSC – MSCs	↗ ECs and fib. proliferation, migration and angiogenesis; ↗ Rat wound closure, reepithelization, collagen maturation and angiogenesis	_	↗ elastin, collagen I and III	[231]
hPB – EPCs	↗ Mice ischemic hind limb perfusion, vascularity, ↘ limb amputation	(miR-126; miR-296)	_	[233]
hPB – HSCs (CD34+)	↗ ECs angiogenesis; ↗ Mice ischemic hind limb perfusion, vascularity, ↘ limb amputation	miR-126-3p (…)	Inhibition of SPRED-1	[206]
hUC – MSCs	↗ Ker. and Fib. survival, migration and proliferation; ↗ Rat skin burn repair, reepithelization and collagen maturation	Wnt4 PDGF-BB; G-CSF; VEGF; MCP-1; IL-6 and IL-8	Wnt/β-catenin pathway: β-catenin translocation to nucleus → ↗ PCNA; cyclin-D1; cyclin-D3 and N-cadherin Akt pathway: : Akt phosporylation → Bcl-2 → cell survival; proliferation, and migration	[234]
hUC – MSCs	↗ ECs proliferation, migration and angiogenesis; ↗ Rat skin burn repair, angiogenesis	Wnt4	Wnt/β-catenin pathway: β-catenin translocation to the nucleus → ↗ PCNA; cyclin-D3 → angiogenesis	[235]
hUC – MSCs	↘ Macrophage inflammation; ↗ Rat skin burn repair, ↘ inflammation	+ miR-181c (…)	TLR4/NF-κB pathway: ↘ TLR4; phosphorylation P65; ↘ TNF-α, IL-1β; ↗ IL-10	[236]
hBM – MSCs	↗ Normal and diabetic fib. proliferation and migration; ↗ ECs angiogenesis	STAT3 and p-STAT3	STAT3/Akt/ERK1/2 pathway: phosphorylation STAT3; Akt and ERK → ↗ c-myc; cyclin-A1; cyclin-D2; HGF; IGF1; NGF; SDF1; and IL-6.	[237]

hPRP – human platelet-rich plasma; **hUCB** – human umbilical cord blood; **hUC** – human umbilical cord (Wharton jelly); **hPB** – human peripheral blood; **hBM** – human bone marrow; **EPCs** – endothelial progenitor cells; **HSCs** – hematopoietic stem cells; **MSCs** – mesenchymal stem/stromal cells; **ASCs** – adipose tissue stem cells; **SMSCs** – synovial mesenchymal stem/stromal cells; **iPSCs** – induced pluripotent stem cells; **AECs** – amniotic epithelial cells; **STZ** – streptozotocin; **ECs** – endothelial cells; **Fib.** – fibroblasts; **Ker.** – keratinocytes; **PI3K** - phosphoinositide 3-kinase; **Akt** – protein kinase B; **MAPK** - mitogen-

activated protein kinases; **ERK** - extracellular signal-regulated kinases; **JAK** – janus kinase; **STAT** - signal transducer and activator of transcription; **Hippo** - protein kinase hippo; **YAP** – yes associated protein; **TLR4**- toll-like receptor 4, **NF-κB** - nuclear factor kappa B. ***** Studies where biomaterials were used as scaffold and allowed delayed and sustained release of EVs in the wound.

In case of MSC exosomes they seem to act at 3 different levels: (i) reduction of inflammation, (ii) improvement in skin regeneration, and (iii) induction of tissue maturation with low scaring, by acting in several pathways, namely PI3K/Akt, MAPK/ERK, JAK/STAT, Wnt/β-Catenin, TLR4/NF-κB, and TGF-β/SMAD2 pathways [216, 217, 223, 225, 228-230, 234-237]. It is important to note that Akt and ERK signaling pathways were the focus of the majority of the studies reported so far (Table XIII). The activation of these pathways leads to the phosphorylation of Akt and ERK, which then translocate to the nucleus and induce the expression of specific genes (e.g. PCNA, c-myc, cyclins, MMP3, etc.), leading to an increase in skin cells proliferation, migration and survival, and angiogenesis and ultimately enhancing wound healing [125, 207, 217, 223, 226, 228, 234, 237]. The Wnt/β-catenin and STAT3 pathways seem to have also an important role in the wound healing effect of exosomes. These pathways respond to exosomes from MSCs and fibrocyte (only STAT3) transporting signaling molecules (Wnt4 and STAT3) in the activated and inactivated form [223, 234, 235, 237]. The activation of these pathways leads to increased cell proliferation and angiogenesis [234, 235, 237].

The therapeutic effect of exosomes seems to be mediated by both miRNAs and proteins. Proteins such as Wnt4, PDGF-BB, G-CSF, VEGF, MCP-1/CCL2, IL-6 and IL-8 mediated the bioactive effect of UC-MSC exosomes, through the activation of Akt signaling pathway [234]. In addition, proteins such as bFGF, PDGF-BB, TGF-β and VEGF on PRP exosomes lead to an increase in skin reepithelization by the activation of YAP, Akt and ERK pathways [125]. Moreover, proteins such as STAT3 and heat shock protein HSP-90α mediated the wound healing effect of fibrocyte derived exosomes [225]. Yet, some miRNAs have been also described to mediate the healing effect of exosomes [216, 223, 226, 228, 236]. For example, miRNAs (e.g. miR-181c) on UC-MSC exosomes mediated the TLR4 pathway inhibition and reduction of inflammation [223, 236]; let-7b on UC-MSCs exosomes mediated their wound healing properties [223]; miR-21-3p on UCB plasma- derived exosomes induce *in vitro* proliferation and migration of fibroblasts and endothelial cells and *in vivo* cutaneous wound healing by the activation of Akt and ERK pathways [226]; miR-21 along with miR-23a, miR-125b and miR-145 on MSC exosome mediated TGF-β pathway inhibition and reduction of excessive scar during wound healing [216]; miR-126-3p on SMSC exosomes mediated skin cell proliferation and survival by the activation of Akt and ERK signalling pathways [217].

The modulation of exosome content it's a very interesting possibility, not only because exosomes are a biocompatible vehicle offering protection for the encapsulated biomolecules, but also by the possibility of enhancing their native bioactivity, and the targeting of specific pathways, genes and even cell types or tissues [217, 236]. One study, used exosomes secreted by MSCs treated with LPS, which correlated to presence of Let-7b an anti-inflammatory agent and M2 macrophage activator [223].

To the best of our knowledge, only 2 studies addressed the bioavailability of exosomes during wound healing [226, 229]. Hu, Y. *et al*, stained exosomes from UCB plasma with PKH67 and monitored the fluorescence by microscopy until 8 days after exosome injection in the wound, concluding that exosomes were retained in the skin cells of the wound for only 3 days [226]. On the other end, Hu, L. *et al*, were able to detect ASCs derived exosomes *in vivo* in the wound site by bioluminescence 7 days after tail vein injection [229]. Additionally, tail vein injection of exosomes induced faster healing than locally injected exosomes, a difference that

the authors attributed to wound disturbance by direct injection of the exosomes to the wound [229].

As exosomes and EVs offer protection to their cargo, different biomaterials compositions are being used to protect these vesicles of the harsh environment of the wound, and increase their bioavailability in the wound site. From the reported studies 3 involved the combination of biomaterials with exosomes, which should lead to a delayed and sustained delivery in the wound bed [125, 216, 217]. Guo *et al*, used a sodium alginate hydrogel (SAH) for exosome derived from PRP delivery to the wound, and compared the effect with PRP direct application, observing an increased healing kinetics [125]. A HydroMatrix, a commercially available composition, was also used as a scaffold for administration of MSCs derived exosomes to the wound [216]. The SMSCs derived exosomes were entrapped in a chitosan (CS) hydrogel before application in the wound [217]. Unfortunately, in all the studies reported, it was difficult to evaluate the advantages of the controlled release of exosomes by the biomaterial as compared to the application of exosomes alone (i.e. without the biomaterial) [125, 216, 217].

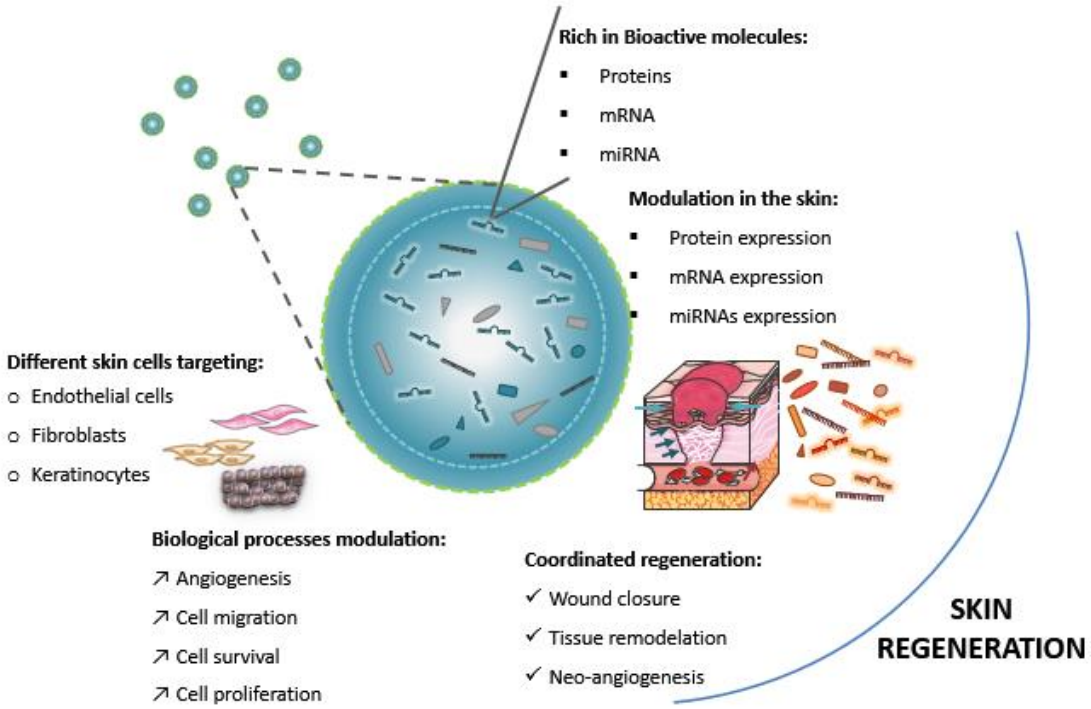

Figure - 14. Exosomes for wound regeneration.
Exosomes from several sources, plasma (including platelet rich plasma), endothelial progenitor cells (EPCs), hematopoietic stem cells (HSCs), mesenchymal stem / stromal cells and similar (MSCs, including adipose derived stem cells, ASCs, synovial mesenchymal stem / stromal cells, SMSCs, and fibrocytes), and amniotic epithelial cells (AECs), are able to enhance wound healing by delivery of growth factors, signalling proteins, messenger RNAs (mRNAs), and microRNAs (miRNAs), targeting and modulating skin cells proliferation, migration, survival and angiogenesis, which translate in improved wound closure, new tissue formation and higher maturation of the tissue, extracellular matrix and blood vessels.

The Kinetics of Small Extracellular Vesicle Delivery Impacts Skin Tissue Regeneration

H. Henriques-Antunes,[†,§,#,‡] R. M. S. Cardoso,[†,‖,‡] A. Zonari, [†,‖] J. Correia, [†,‖] E. C. Leal, [†,‖] A. Jimenez-Balsa, [†,‖] M. M. Lino,[†,‖] A. Barradas,[†,‖] I. Kostic,[†,‖] C. Gomes,[#] J.M. Karp,[▽] E. Carvalho,[†,‖,⊥,○] L. Ferreira[†,#,]*

[†] CNC-Center of Neurosciences and Cell Biology, University of Coimbra; 3004-517 Coimbra, Portugal.

[§] Crioestaminal – Stemlab, S.A. Biocant Park, Núcleo 04, Lt.2, 3060-197 Cantanhede, Portugal.

[#] Faculdade de Medicina da Universidade de Coimbra, R. Larga, 3000-354 Coimbra, Portugal.

[‖] Instituto de Investigação Interdisciplinar, University of Coimbra, Casa Costa Alemão - Pólo II, Rua Dom Francisco de Lemos, 3030-789, Coimbra, Portugal.

[▽] Harvard-MIT Division of Health Sciences and Technology, Cambridge, Massachusetts, USA.

[⊥] Department of Geriatrics, University of Arkansas for Medical Sciences, Arkansas, United States

[○] Arkansas Children's Research Institute, Little Rock, Arkansas, United States

ABSTRACT.

Small extracellular vesicles (SEVs) offer a promising strategy for tissue regeneration, yet their short lifetime at the injured tissue limits their efficacy. Here, we show that kinetics of SEV delivery impacts tissue regeneration at tissue, cellular and molecular levels. We show that multiple carefully timed applications of SEVs had superior regeneration than a single dose of the same total concentration of SEVs. Importantly, diabetic and non-diabetic wounds treated with a single time point dose of an injectable light-triggerable hydrogel containing SEVs demonstrated a robust increase in closure kinetics relative to wounds treated with a single or multiple doses of SEVs or platelet derived growth factor BB, an FDA-approved wound regenerative therapy. The pro-healing activity of released SEVs was mediated at tissue/cell level by an increase in skin neovascularization and re-epithelization and at molecular level by an alteration in the expression of 7 miRNAs at different times during wound healing. This includes an alteration of has-miR-150-5p, identified here to be important for skin regeneration.

KEYWORDS. small extracellular vesicles, exosomes, hydrogel, light-triggerable, skin

Table of Contents

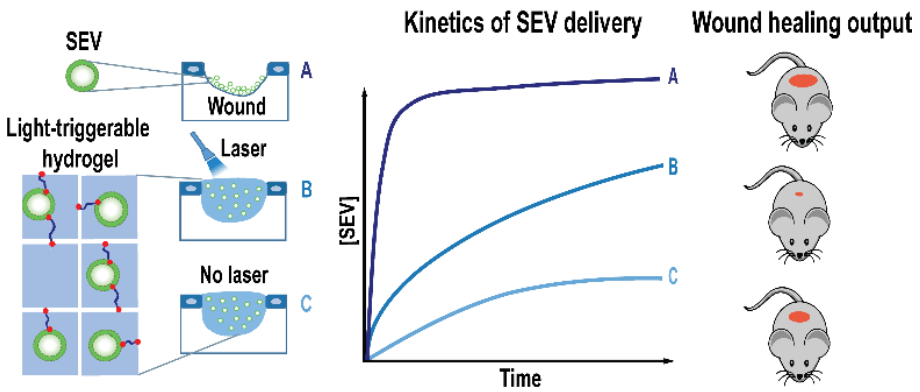

SEVs, commonly designated as exosomes, are cell-based vesicles with a diameter of 50-200 nm, containing a cocktail of miRNAs as well as other biomolecules (*e.g.* proteins, lipids, mRNA), with an important role in cell/tissue communication.[1,2] The transfer of SEV biomolecules modulates the biological functions of acceptor cells which in turn may have impact in tissue regeneration.[3-5] For example, the transfer of miRNAs [3, 6,7] as well as proteins [5] from SEVs collected from different sources (mesenchymal,[3] blood cells,[6] stem or progenitor cells [7,8]) to heart,[7,8] pancreas,[9] limb ischemia [6] or skin [3, 10] cells has been demonstrated to control neovascularization, cell proliferation and migration, among other biologic functions. The effect of SEVs largely depends in their source, isolation method, administration route, dose and target tissue. The systemic administration of SEVs leads to a predominant accumulation of SEVs in the spleen and liver, and most of SEVs are cleared from the animals by 6 h postinjection.[11] The local administration, at the injured tissue, increases SEV targeting efficacy; however, the vesicles not affected by proteases or changes in pH present a short lifespan because they are rapidly taken up by tissue cells, including immune and endothelial cells. [12, 13] These vesicles are uptake as single vesicles within minutes and they cluster into filopodia active regions.[13] Interestingly, a significant portion of SEVs (40-60%) seem to accumulate in lysosomes after several hours and thus their content is likely degraded.[13] The remaining portion of SEVs releases their content in cell cytoplasm. Because tissue regeneration requires the intervention of multiple biomolecules at different times,[14-16] a single administration of SEVs is not desirable to maximize their regenerative effect.

The hypothesis of the current work is that the regenerative impact of SEVs depends in their delivery kinetics to the injured tissue. We have tested this hypothesis in the context of chronic wounds (topical application). Wound healing is a complex process involving the intervention of multiple biomolecules at different times.[17] For example, miR-16, miR-21 and miR-29b have separate roles at the inflammatory, proliferation and maturation phases, respectively, which occur at different times during wound healing.[18] Conventional treatment of chronic wounds includes regular wound debridement (*i.e*. removal of necrotic tissue, foreign debris and infection) in order to stimulate the healing process and the protection of the wound by a specific dressing.[19] With the exception of Regranex (platelet derived growth factor BB, $PDGF_{BB}$, formulation) approved in 1997 to stimulate the healing in chronic lower extremity diabetic neuropathic ulcers,[17] there is a lack of formulations to accelerate the regeneration of chronic wounds. Recent pre-clinical studies have demonstrated that SEVs have the capacity to help regenerate chronic wounds by accelerating re-epithelization and neovascularization,[3-5, 20-22] yet the regeneration program is limited because of the short lifespan of SEVs. The short lifespan of SEVs necessitates multiple doses, which is not desirable because it would require medical staff assistance for each application and each administration could disrupt the wound healing process. Therefore, it would be desirable a single application of a formulation containing SEVs, such as a hydrogel, able to release SEVs overtime and provide a temporary extracellular matrix for cell infiltration and adhesion. During hydrogel degradation, cells would infiltrate the space occupied by the hydrogel and would be modulated by the released SEVs.

Engineered biomaterials with capacity to control the temporal release of SEVs may provide an opportunity to enhance the regenerative process. Towards this goal, it is important that the hydrogel releases SEVs over the duration of the healing process and the space occupied by the hydrogel should be replaced by cells that proliferate and migrate from the proximity (Figure 1A). The application of SEVs in scaffolds, including hydrogels, has been demonstrated in previous studies; however, (i) the controlled release of SEVs from pre-formed scaffolds was not compared to a single dose of SEVs and thus the advantage of controlled release was not demonstrated,[8, 22, 23] (ii) often the controlled release of SEVs have exhibited only modest regenerative effects (up to 20% improvement beyond the scaffold alone without

SEVs or SEVs alone),[22-25] (iii) the *in vivo* SEV release was not demonstrated [22, 23, 26] and (iv) the molecular mechanism of the released SEVs was not evaluated.[8, 22-24, 26] To the best of our knowledge, no study has demonstrated the impact of SEV delivery kinetics in tissue regeneration at tissue, cell and molecular levels.

In this work, we have studied the impact of SEV delivery kinetics in 2 different ways: (i) using single or multiple administrations of the same total concentration of SEVs or (ii) using a single administration of an injectable SEV-containing light-disassembly hydrogel, with or without activation. The hydrogel was prepared by the crosslinking of hyaluronic acid, a polymer used in the clinic on wound dressings,[27] by a photo-cleavable linker (PCL) that is either attached to SEVs by one moiety or alone. The wound healing properties of SEVs isolated from human umbilical cord blood mononuclear cells (hUCBMNCs) from different donors was evaluated in three full-thickness excision wound models (wild type, streptozotocin-induced type I diabetes, and diabetes type II using the *db/db* genetic model). To demonstrate the full potential of SEV-containing hydrogel, its wound healing activity was compared with a FDA-approved treatment based on $PDGF_{BB}$ (~8 µg of the growth factor per cm^2 of wound).[28] To monitor the *in vivo* distribution and stability of SEVs we have developed a Forster resonance energy transfer system based on lipid-conjugated dyes. In this case, the FRET efficiency decreased once SEVs were disrupted. Moreover, the pro-healing activity of SEVs was studied at tissue, cellular and molecular level. The expression of miRNAs released by SEVs in skin as well as a miRNA that has not been reported in the context of wound healing was evaluated. By combining injectability, ability to maintain the integrity and bioactivity of SEVs, ability to release SEVs with temporal control that might match the *in vivo* healing profile, we have designed a formulation for efficient tissue regeneration.

Results and discussion

SEV properties and skin cell internalization studies. We have used SEVs secreted from hUCBMNCs (approximately 60% of the cells were monocytes, see Figure S1A) because these cells are easily obtained from multiple banks. These cells have demonstrated regenerative potential in the setting of wound healing [29, 30] and SEVs isolated from neonatal cells have shown improved regenerative properties compared to the ones isolated from adult cells.[31] To isolate SEVs we have cultured cryopreserved hUCBMNCs in serum-free cell culture medium under hypoxia for 18 h, collected the conditioned media from the cells and isolated SEVs by sequential ultra-centrifugation.[32] Hypoxic conditions were selected because it has been shown that SEVs isolated under these conditions had enhanced regenerative properties.[7, 31] The isolated SEVs presented variable morphology (Figure 1B), an average diameter of 100-130 nm (by DLS and NTA measurements) (Figures 1C-1D) and a negative zeta potential (-30 mV) (Figure 1C). NTA analyses also showed that isolated SEVs did not have measurable protein aggregates as well as large extracellular vesicles. The vesicles expressed typical SEV surface markers such as CD9, TSG101, CD63 and CD81, and they showed lower levels of the hematopoietic marker CD45 as compared to the secreting cells (Figures 1E-F, Fig. S1B).

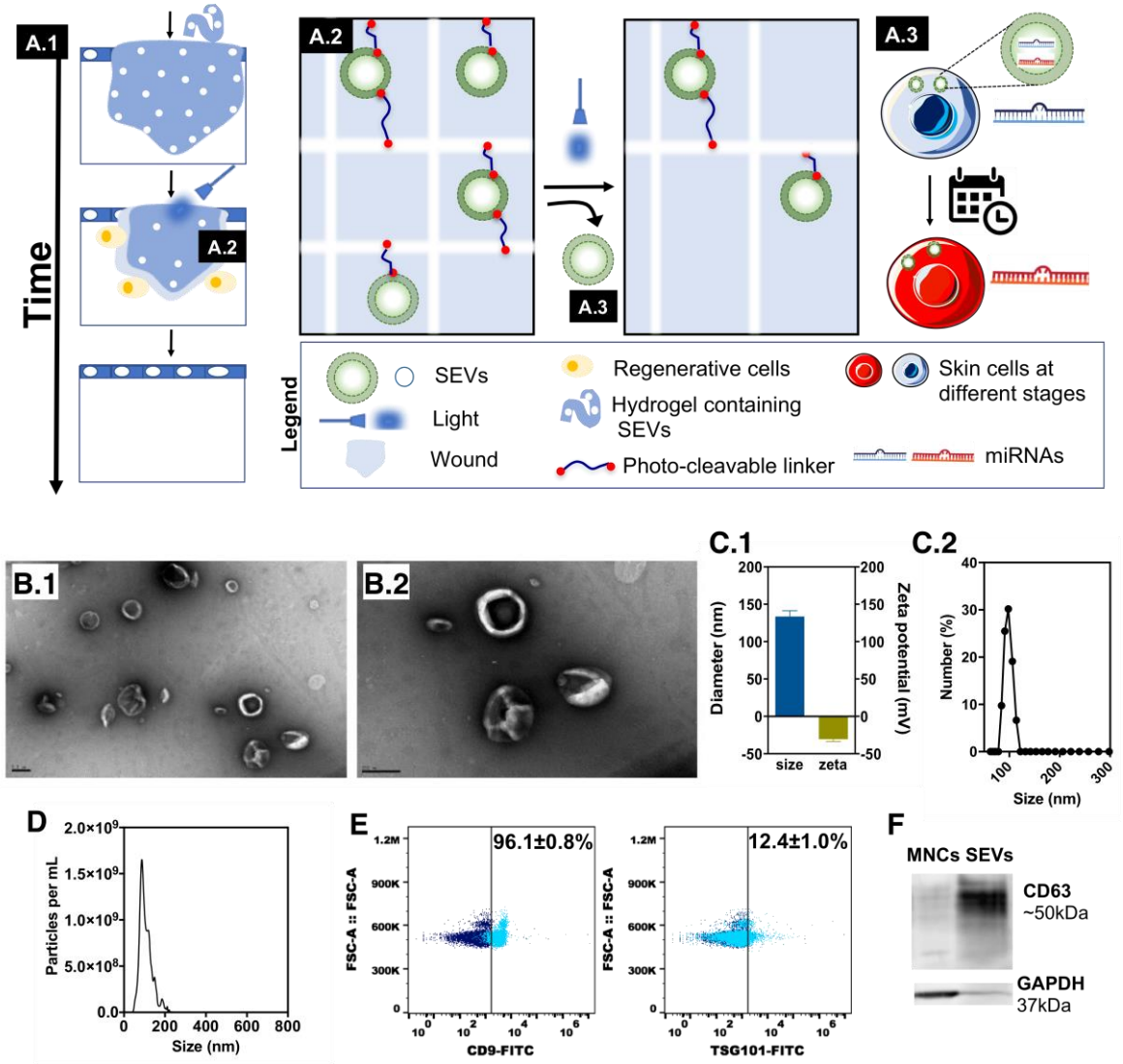

Figure 15. Concept and characterization of SEVs.
(A) Schematic representation of the proposed function of SEV-containing vesicles. SEV-containing hydrogels are applied topically in a single administration followed by their incorporation into the wound (A.1). Both the degradation of the hydrogel and the linker that immobilizes the SEVs (A.2) are controlled remotely by a light. During hydrogel degradation, cells infiltrate the space occupied by the hydrogel and are modulated by the released SEVs. This strategy contrasts with single or multiple applications of SEVs, where a scaffold does not exist to provide a temporary extracellular matrix for cell adhesion and where the stability of SEVs is low due to pH conditions, tissue remodeling enzymes and inflammatory cells. (B) Representative TEM images of SEVs. Bar corresponds to 100 nm. (C) Size and Zeta potential of SEVs fraction, as evaluated by DLS. Results are average ± SEM, n=4-17. (D) Size and particle concentration of SEVs, as evaluated by NTA analyses. (E) Expression of proteins in SEVs as evaluated by flow cytometry. Results are average ± SEM, n=4. (F) Representative western blot image of CD63 expression in total protein lysates of SEVs and secreting cells. SEVs present 2.14 ± 1.08 (n=4 donors) fold more CD63 than secreting cells.

To determine whether skin cells could internalize SEVs, endothelial cells, fibroblasts and keratinocytes were incubated for 24 h with fluorescently-labeled SEVs (under non-cytotoxic concentrations, Figure S2A) and monitored by high-content microscopy (Figure S2B) or flow cytometry (Figure S2F) to evaluate their internalization rate and they were imaged by confocal microscopy (Figures S2C-S2E) to confirm their intracellular location. High-content microscopy images show the internalization of SEVs in all three cell types. At 24 h, most of SEVs were located outside the lysosomal compartment as evaluated by co-localization of the

SEV label (PKH67) with lysotracker red (Figures S2C-S2E). Since SEVs accumulate in lysosomes but also in multivesicular bodies13, which are located in the same cellular region of the lysosomes but not stained with lysotracker, it is likely that part of SEVs outside the lysosomes are in multivesicular bodies. The uptake kinetics and magnitude were dependent on the cell type, with keratinocytes and fibroblasts the most efficient in the uptake of SEVs compared to endothelial cells. The differential uptake might be due to differences in the expression of caveolin-1 and clathrin in each cell type, that mediate caveolae-dependent and clathrin-dependent endocytosis of SEVs.33 The differential uptake was also confirmed by flow cytometry (Figure S2F). In the 3 cell types, SEVs accumulated in a time dependent manner in the overall cytoplasm of the cell, which peaked at approximately 16 h of incubation. Importantly, SEVs did not interfere with the biological signature of somatic cells such as endothelial cells. Endothelial cells transfected with SEVs for 48 h had similar levels of endothelial markers (CD31, VECAD and vWF), at gene (Figure S2G) and protein (Figure S2H) levels. Collectively, SEVs have typical size, zeta potential and surface markers and they are internalized by skin cells at variable magnitudes.

SEVs skin bioactivity. We then asked whether SEVs could enhance the biological properties of skin cells. SEVs increased up to 40-50% the survival of endothelial cells cultured under ischemic conditions (Figures S3A-S3B). SEVs obtained from hUCBMNCs with CD34+ cells had equivalent bioactivity compared to SEVs obtained from hUCBMNCs without CD34+ cells at the best effective concentration (2 μg/mL; approximately 1.2□108 particles/mL as measured by NTA) (Figures S3A-S3C). Therefore, the therapeutic value of SEVs was not entirely due to the CD34+ cell population. We decided to characterize more deeply SEVs obtained from CD34+-depleted hUCBMNCs. In this case, SEVs were able to increase fibroblasts and keratinocytes survival up to 10% (Figure S3C). The survival studies were then extended to cell proliferation, migration and angiogenesis. The SEVs induced skin cell proliferation (up to ≈50%) (Figure 2A), enhanced fibroblasts and keratinocytes migration (up to ≈15%) (Figure S3D) and increased endothelial cells network complexity (up to ≈25%) (Figure S3E). In most cases, the bioactivity was dependent on SEV concentration.

The in vivo wound healing effect of SEVs was initially evaluated on type I diabetic mice (Figure 2B). A single topical application of a low dose of SEVs (0.4 μg) immediately after wound induction had no significant impact on wound healing kinetics (Figure 2C). However, a single topical application of a high dose of SEVs (2 μg) improved wound-healing kinetics, particularly from day 7 onwards. Interestingly, wounds treated with a very small dose (0.02 μg) every day (2 applications per day) for 10 days (0.4 μg of SEVs in total) showed the highest acceleration on wound healing. This effect was even superior to the FDA-approved growth factor therapy based in the administration of a daily dose of PDGFBB 34 (Figure 2D). At day 10, wounds treated with a bi-daily administration of SEVs had completed re-epithelization and showed higher tissue remodeling as compared to the control group (Figure 2E). Importantly, the therapeutic effect of a bi-daily administration of SEVs was extensive to SEVs obtained from different donors (Figure S4A) and to different animal models, i.e., non-diabetic mice (Figure S4B) and type II diabetic mice (Figure S4C). In this last case (type II), the healing time of wounds treated with SEV (approx. 17 days) is 4 days earlier than the control treatment.

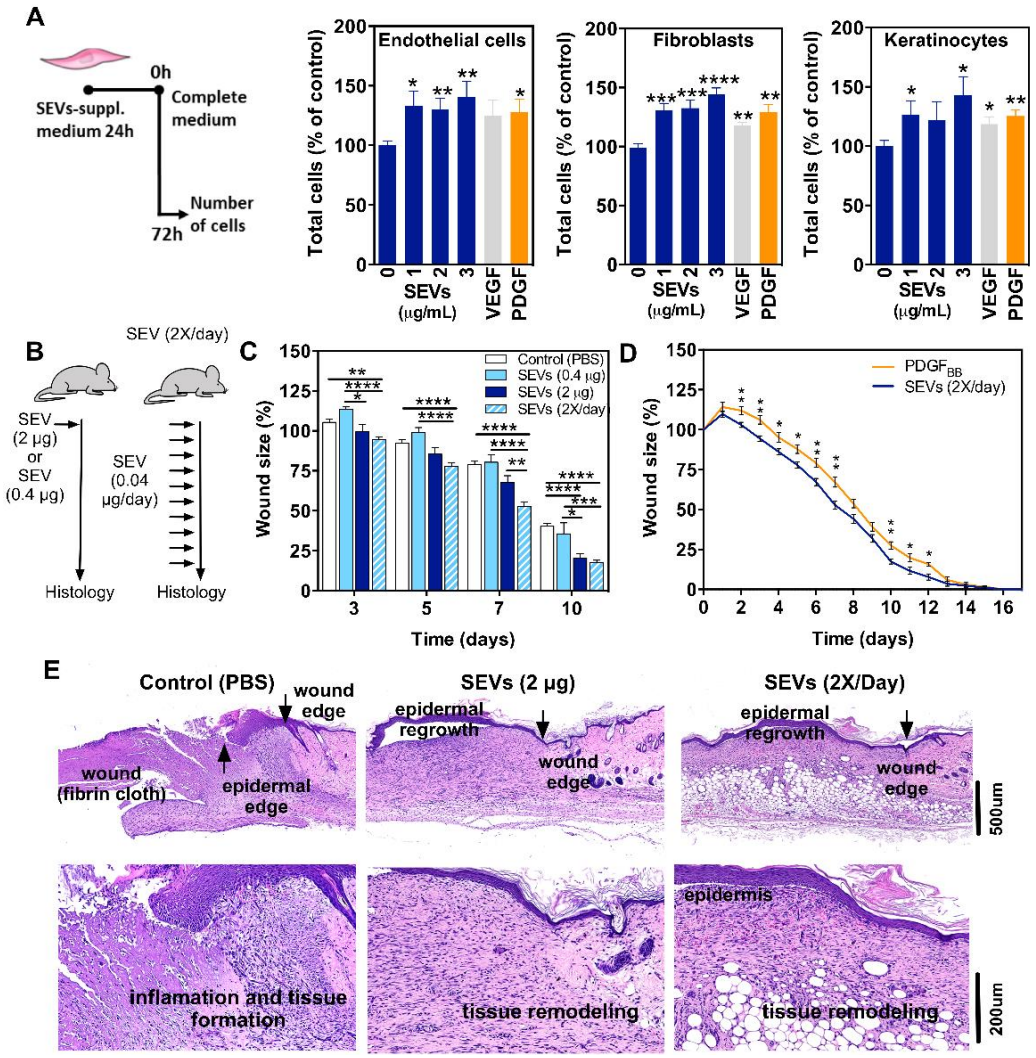

Figure 16. In vitro and in vivo bioactivity of SEVs.

(A) Proliferation of endothelial cells, fibroblasts and keratinocytes upon treatment with SEVs. Vascular endothelial growth factor (VEGF, 50 ng/mL) and platelet derived growth factor (PDGF-BB, 50 ng/mL) were used as controls. Results are average ± SEM, n= 3 SEVs from different donors, 3 replicates per condition. Statistical analyses were performed by a Mann-Whitney test. (B) Schematic representation of wound treatments in a type I diabetic mice model. Topical application of 0.4 µg or 2 µg (in both cases a single application at day 0) or twice a day of 0.02 µg (for 10 days). Control wounds received a saline solution (PBS) only. (C) Wound area as a function of time, normalized by the initial wound area. Results are average ± SEM, n=12. Statistical analyses were performed by a two-way ANOVA followed by a Bonferroni's multiple comparisons test. (D) Wound area in type I diabetic mice treated by topical application of PDGF-BB or bi-daily doses of SEVs. Results are average ± SEM, n=12. Statistical analyses with t-test. (E) Representative images of H&E-stained histological sections of control, SEV (2 µg) and SEV (2X/day) groups at day 10 post-treatment. In A, C and D, *p<0.05; **p<0.01; ***p<0.001; ****p<0.0001.

Overall, our *in vitro* results showed that SEVs modulated skin cell activity including cell proliferation, migration, survival and angiogenesis. Moreover, our *in vivo* results showed that SEVs enhanced wound healing activity, being the activity dependent on the dose and application frequency of SEVs while independent of the donor and the diabetic animal model.

Preparation and characterization of a light-triggerable hydrogel for the controlled release of SEVs. Previous studies have demonstrated the positive effect of HA hydrogels in maintaining a moist wound environment and thus in enhancing wound healing.[27] In addition, HA (non-crosslinked) has its own bioactivity since it promotes keratinocyte proliferation and migration.[35] Here, we have developed a light-triggerable HA hydrogel for the remote release control of SEVs. Our hypothesis was that a remotely triggerable hydrogel could be more efficient to orchestrate SEV release with the dynamics of skin tissue formation. To prepare the HA hydrogels we have initially conjugated the HA with cysteine to have HA with thiol groups (Figure 3A and Figure S5A). Low viscosity HA with a degree of substitution of 15-20% of L-cysteine ethyl ester (HA-SH, 50% of free thiols as evaluated by an Ellman test) was used for the preparation of the hydrogel. In a separate reaction, the thiol groups of SEVs (ca. 80%) were reacted with a PCL (Figure 3B). The PCL is composed by a photolabile ortho-nitrobenzyl ester moiety that is sensitive to UV/blue light. The light sensitivity of PCL-conjugated SEVs was confirmed after exposure to UV irradiation for 5 min (Figure 3C). Both HA-SH (5%, w/v) and PCL-conjugated SEVs containing a large excess of non-reacted PCL (1:10, thiol: acrylate) were reacted. The reaction between PCL-conjugated SEVs and HA-SH was confirmed by a reduction in the percentage of free thiols in HA-SH (Figure 3D) by the detection of acrylate groups on the surface of SEVs (Figure 3 E) and by an increase in the complex viscosity of the mixture (Figure 3F). The gel point occurred after 35 min (Figure 3G). The hydrogel incubated for 96 h in PBS had a G´/G´´ that is approximately 70% of the initial G´/G´´, and thus able to preserve a significant part of its mechanical properties in absence of light (Figure S5B). The hydrogel swelling ratio was 53±5 (average±SD, n=3) and showed the capacity of the hydrogel to retain high levels of water.

To demonstrate that the hydrogel was light-disassembled with the capacity to release SEVs, we exposed the hydrogel to sequential irradiations (405 nm, 80 mW or UV-Light 365 nm,). The release of SEVs was dependent on the number of irradiations (Figure 3H) and on the exposure time (Figure S5). Importantly, the SEVs released were bioactive as evaluated by a keratinocyte proliferation assay (Figure S5D). Moreover, irradiation of keratynocytes with a 405 nm laser up to 3 min does not induce significant toxicity (Figure S5F).Taken together, we have developed a light-triggerable hydrogel for the controlled release of SEVs. The formulation released cumulative levels of SEVs according to the number of irradiations.

Wound healing efficacy of SEVs released from a light-triggerable hydrogel. Next, we asked whether light-triggerable HA hydrogel containing SEVs could improve the closure of diabetic type I full-thickness wounds. Therefore, wounds were treated with: (i) HA hydrogel without SEVs but light activated each day for 1 min during the 10 days of the experiment (named as Gel + Light), (ii) HA hydrogel containing 2 μg of SEVs but not light-activated (Gel + SEV) and (iii) HA hydrogel containing 2 μg of SEVs and light-activated (Gel + SEV + Light) each day for 1 min during the 10 days of the experiment (Figure 4A1). The progress of wound healing was monitored daily by measuring the wound area. A significant acceleration of wound closure was observed in animals treated with Gel + SEV or Gel + SEV + Light during the first 5 days (Figure 4A2). At day 10, the group Gel + SEV + Light presented 30% improvement on the wound closure compared to control group (PBS) and 10% relative to Gel + Light and Gel + SEV (Figure 4A2). Importantly, the wound closure monitored in wounds treated with Gel + SEV + Light, was significantly faster relative to the bi-daily administration of SEVs (2X/day) (Figure 4B). To confirm that the controlled released of SEVs was indeed mediating the enhancement on wound closure, we compared the wound healing in animals treated with Gel + SEV + Light and animals treated with SEVs (2 μg) plus HA hydrogel on top (Gel over SEVs + Light**)** without

reaction. Significant differences were observed from early stages up to 10 days, demonstrating the importance of the controlled release system to enhance wound healing (Figure 4C).

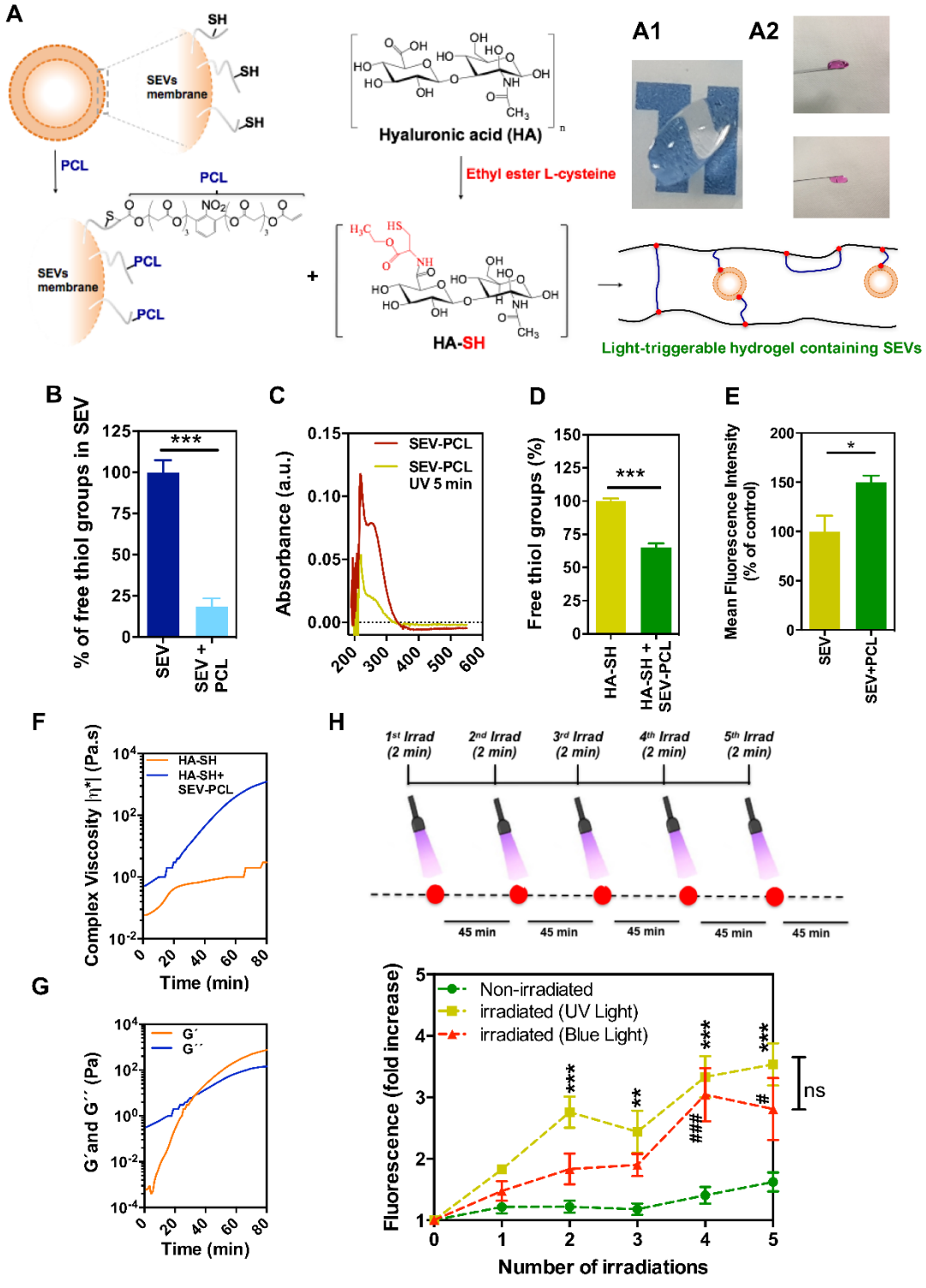

Figure 17. Characterization of a light-triggerable hydrogel for the controlled release of SEVs.
(A) HA was conjugated with cysteine to have terminal thiol groups while the SEV membrane thiol groups were reacted with a PCL containing terminal acrylate groups. The mixture of both components at 37ºC yielded a gel. Gel is translucid (A1, gel swollen in PBS; A2, gel swollen in DMEM media). (B) Conjugation yield of SEVs with PCL (1:10 mol of thiol:acrylate). Average ± SEM (n=4). (C) Absorption spectra of the soluble linker after irradiation (5 min) and separation from SEVs using a 7 kDa cut-off filter. (D) HA free thiol groups after 10 min reaction of HA-SH with PCL-modified SEVs. (E) Relative amount of acrylate groups on the surface of SEVs determined after reacting FAM-thiol with SEVs or SEVs-PCL. Average ± SEM (n=3). In B, D and E statistical analyses were performed by an unpaired t-

test. (F and G) Complex viscosity (F) as well as G´and G´´(G) as a function of time. (H) Time course photo-cleavage of HA hydrogel containing SEV-PCL (100 µg) stained with Syto RNASelect ™. The gel localized in the top part of the transwell was irradiated with a UV light (405 nm) for 2 min, followed by 45 min of equilibrium under agitation. In each experimental timepoint an aliquot was withdraw from the bottom of the transwell and used to read the fluorescence intensity at 530 nm. Results are Mean ± SEM (n=3-4). Statistical analyses by a two-way ANOVA test followed by a Bonferroni's multiple comparisons test. *p<0.05; **p<0.01; ***p<0.001; ****p<0.0001. * denotes comparison between UV-Light and non-irradiated, # denotes comparison between Blue-Light and non-irradiated.

To evaluate the wound healing process at the tissue and cellular levels, we performed histology and immunofluorescence analyses (Figures 4D and 4E). At day 5 post-wounding, low epidermal regrowth and relatively low/moderate vessel density was observed in wounds treated with PBS or Gel + Light. Wounds treated with Gel + SEV were partially covered by epidermis and showed moderate vessel density, while wounds treated with Gel + SEV + Light showed the highest epidermal regrowth, vessel density and wound score. The epidermal regrowth in animals treated with Gel + SEV + Light was characterized by a high number of cells expressing keratin 14 at the wound edges (Figure S6). This keratin is synthesized by epidermal keratinocytes in the basal proliferative layer.[36] At day 10 post-wounding, wounds treated with PBS or Gel + Light showed a granulation tissue with low levels of macrophages and incomplete epithelialization while wounds treated with Gel + SEV + Light showed late stages of remodeling, high vessel density and complete epithelialization (Figure S6A).

Overall, our results demonstrate the importance of SEV controlled release to enhance wound healing, characterized at a cellular level by increased skin re-epithelization and neovascularization. The formulation proposed in this work is applied topically in a single administration followed by their incorporation in the wound. This approach decreases significantly the number of applications for the treatment of chronic wounds and consequently the interference in the wound healing process. Besides the clinical impact, the strategy proposed here can reduce the cost of the treatment and reduce the pain and discomfort in patients. The incorporation of the gel in the wound is likely beneficial to support cell migration to the wound bed as has demonstrated in previous studies after topical administration of soluble hyaluronic acid in diabetic mice.[27] Specifically, the degradation of hyaluronic acid by hyaluronidases leads to the formation of low molecular weight hyaluronan fragments that are angiogenic and immunostimulatory.[27] This might explain in part the wound healing properties of HA gel + light (without SEVs). Although formulations for SEV delivery have been reported during the preparation of this manuscript, [22, 24, 26, 37] those studies did not demonstrate the effect of SEV delivery kinetics in tissue regeneration at tissue, cellular and molecular levels. Few studies have highlighted the effect of SEV retention in injured tissue but not the effect of SEV´s kinetics delivery.[8, 24] Our results show that the controlled delivery of SEVs during skin healing enhanced tissue regeneration. This was confirmed at two different levels: by the administration of a single or multiple doses of the same total concentration of SEVs and by the use of a hydrogel that allowed temporal controlled release. In the last case, our results showed that the non-activation of the hydrogel (and thus the release of SEVs depending in the degradation of the hydrogel) led to inferior wound healing results. This clearly showed that the kinetics of the sustained release had a significant impact in tissue regeneration. Further corroborating the advantages of our approach, a previous study has shown that the absence of temporal control in SEV release and scaffold degradation only increased healing up to 15% relative to wounds treated with scaffold without SEVs [22] while in our case we had an increase of more than 40%.

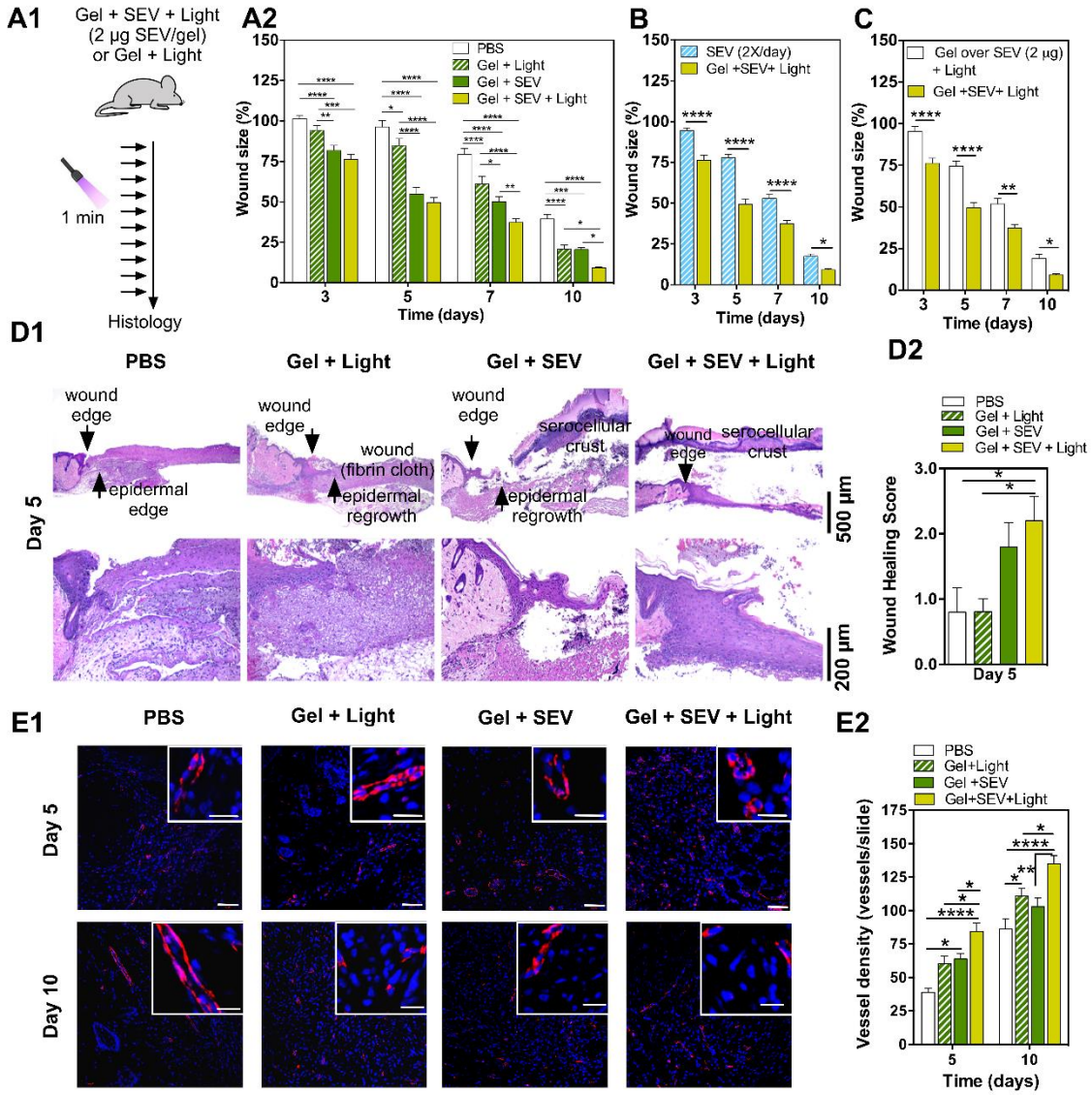

Figure 18. Healing effect of a light-triggerable hydrogel containing SEVs in type I diabetic chronic wounds.
(A) Schematic representation of the *in vivo* testing. Type I diabetic mice were treated topically with: (i) PBS, (ii) light-triggerable HA hydrogel irradiated everyday by a blue laser (405 nm) for 1 min, for 10 days, (iii and iv) light-triggerable HA hydrogel containing SEVs without (iii) or with (iv) blue laser (405 nm, 1 min) irradiation, once a day for 10 days. Results are average ± SEM, n=7-14. (B) Percentage of wound area after treatment with Gel + SEV + Light (2 μg of SEVs per wound) or bi-daily doses of SEVs (2×0.02 μg day/wound). Results are average ± SEM, n=14-34. (C) Percentage of wound area after topical treatment with Gel + SEV (2 μg of SEVs per gel; the SEVs were crosslinked within the gel) or with SEVs (2 μg) which were then covered by a Gel (in this case SEVs were not crosslinked). In both cases, the gels were irradiated (405 nm, 1 min), once a day for 10 days. Results are average ± SEM, n=6-14. (D1) Representative images of H&E-stained histological sections of explants at day 5. (D2) Wound healing score obtained after a graded qualitative analysis of H&E histological tissue samples of the different experimental groups at day 5. Results are average ± SEM, n=5. (E1) Representative images of CD31 staining after 5 and 10 days. (E2) Vessel density quantification based on vessel positive for CD31 marker. Results are average ± SEM, n=12-19. Two-way ANOVA and Newman-Keuls multiple comparisons test (A e D) or uncorrected Fisher's LSD (B, D and E) were used, statistical differences: *p<0.05; **p<0.01; ***p<0.001; ****p<0.0001.

***In vivo* biodistribution of SEVs.** To evaluate the biodistribution of SEVs after wound administration, SEVs were labeled with lipid-conjugated dyes and monitored by an IVIS imaging system. The two lipid-conjugated dyes were synthetized by reacting DPPE with Cy5.5 or Cy7 dyes (Figure 5A) and their absorbance and emission profiles successfully confirmed (Figure 5B). SEVs labeled with Cy7- DPPE, purified by ultracentrifugation (Figure S5B) and

applied topically in the wound bed were rapidly eliminated since 70% of their fluorescence was lost after two days (Figure 5C). In contrast, fluorescently-labeled SEVs chemically immobilized in the light-triggerable gel and administered in the wound bed maintained the same concentration for at least 3 days in the absence of light; however, the concentration decreased after light activation and consequent release in the wound bed (Figure 5D).

We then asked whether the hydrogel could preserve the *in vivo* integrity of SEVs. To address this issue, we have incorporated a FRET system in the membrane of SEVs. Cy5.5 and Cy7 present good overlap between the emission spectra of Cy5.5 and the absorbance spectra of Cy7 and a large separation between the emission bands, resulting in a good FRET pair (Figure 5E1). The topical administration of a SEV solution in the wound bed leads to a rapid loss in FRET efficiency (ca. 20% in the first 1 h) as opposed to the one monitored on SEVs chemically crosslinked in a light-triggerable hydrogel (Figure 5E2). After 24 h, the decrease in FRET efficiency was around 50%, 20% and 30% in the groups SEVs, Gel + SEV and Gel + SEV + Light, respectively. These results indicate that when SEVs were chemically conjugated to the light-triggerable hydrogel, their stability increased. Taken together, the hydrogel maintained SEV integrity and sustained the topic release at the wound bed.

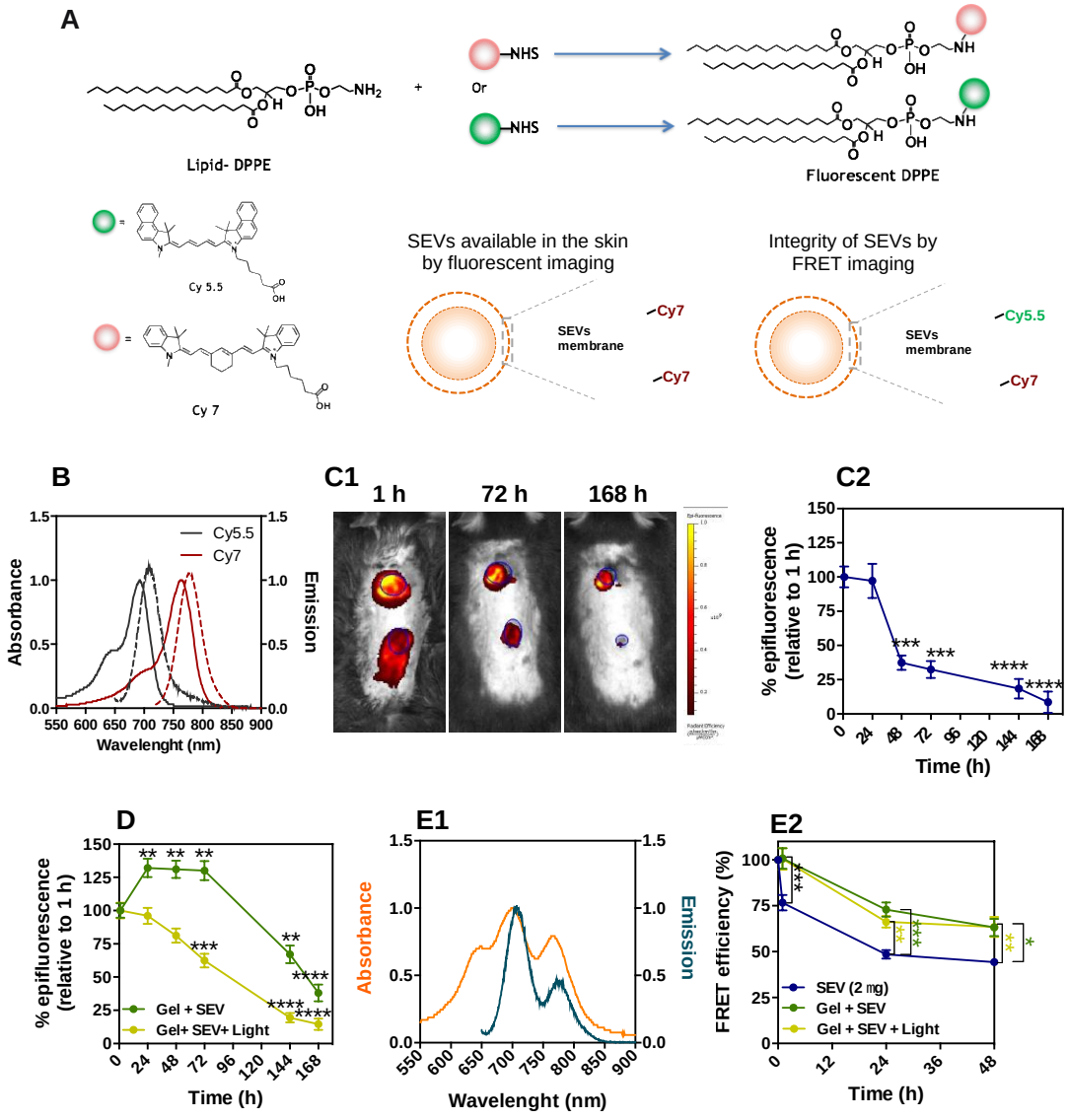

Figure 19. Biodistribution and integrity of SEVs administrated in the wound site.

(A) Schematic representation of the synthesis of lipid-conjugated dyes. DPPE was conjugated either with Cy5.5 or Cy7. The lipids (one dye or a pair of dyes in 1:1 molar ratio) were then incorporated in the SEVs followed by their purification with a column. (B) Normalized absorbance (solid line) and emission (dotted line) spectra for the DPPE-fluorophore conjugates. Cy5.5-DPPE (grey) and Cy7-DPPE (red). (C and D) SEVs biodistribution in the skin wound as evaluated by IVIS imaging. Two excisional wounds (two spots in each mice) were made in the backs of the mice. SEVs in solution or in a gel were topically applied to each wound. In (C) a single dose of SEVs labelled with DPPE-Cy7 in solution (2 μg) was administered while in (D) SEVs labelled with DPPE-Cy7 were administered in a gel (with and without light activation; 2 μg of SEVs per gel). (C1) Representative images by IVIS (λex: 745nm, λem: 810-875nm). (C2) Epifluorescence quantifications of IVIS. Results are average ± SEM, n=3-10. *p<0.05; **p<0.01; ***p<0.001; ****p<0.0001, denotes statistical difference relatively to 1 h post-delivery of SEVs. (E) Integrity of SEVs labelled with FRET pair (DPPE-Cy5.5 and DPPE-Cy7) in the skin wound as evaluated by FRET overtime. (E1) FRET effect in SEVs before administration (in case of emission spectra the λex was 640nm). (E2) FRET efficiency (%) evaluated overtime in skin wounds of animals administered with SEVs alone (2 μg) or 20 μL Gel + SEVs (2 μg) with or without light activation. Results are average ± SEM, n=3-10. *p<0.05; **p<0.01; ***p<0.001, between Gel + SEV (with or without light) and SEV group. A one or two-way ANOVA test followed by a Bonferroni's multiple comparisons test was used.

***In vivo* mechanism of SEV bioactivity.** To determine whether miRNAs were responsible for SEV wound healing activity, we performed an endothelial cell survival assay in the presence of aurintricarboxylic acid (ATA),[7, 38] an inhibitor of the miRNA processing machinery. Our results indicate that the pro-survival effect of SEVs was lost and thus demonstrating the involvement of miRNAs in the bioactivity of SEVs (Figure S7A).

To identify the miRNAs responsible for SEV bioactivity we performed RNASeq analyses of SEVs obtained from 4 different donors. SEVs were found to be rich in small RNAs, including miRNAs (Figures S7B and S7C). We selected the 15 most expressed miRNAs for further studies (Figure 6A). The expression of these 15 miRNAs was confirmed by qRT-PCR in SEVs collected from 10 individuals, with the hsa-miR-150-5p the most expressed (Figure 6A, Figure S7D). SEVs treated with RNase prior to RNA isolation had similar expression of miR-150-5p, thus showing that the miRNA was within the SEVs, protected from enzymatic degradation (Figure S7E).

Next, we asked whether the 15 miRNAs contained in SEVs were differentially expressed in wounds at day zero in diabetic (type I) and non-diabetic animals. No statistical differences were observed in miRNA expression between non-diabetic and diabetic mouse skin (data not shown). Additionally, the effect of Gel + SEV + Light treatment *versus* PBS in skin expression of these miRNAs was studied at day 5 and 10 post wound. Gel + SEV + Light treatment of diabetic mice significantly influenced the expression of 7 miRNAs in the wound skin, either by stabilizing and sustaining their expression (miR-150-5p, miR-181a-5p, let-7a-5p and miR-342-3p), or by increasing their expression at day 5 (miR-223-3p and miR-142-3p) or at day 10 (let-7f-5p; Figure 6B). The 8 other miRNAs studied did not present significant differences to the control (data not shown).

From the 7 miRNAs that were differentially expressed in wounds treated with PBS or SEVs released in the wound bed by the light-triggerable hydrogel, we focused our attention on miR-150-5p because (i) it was the miRNA with the highest expression in SEVs, (ii) it was differentially expressed at day 10 in skin wounds treated with PBS or Gel + SEV + Light and (iii) its effect in the setting of wound healing was relatively unknown. Our *in vitro* results showed that miR-150-5p alone increased keratinocyte proliferation and migration and enhanced fibroblasts survival under ischemic conditions (Figure 6C and Figures S8A-S8F). Moreover, our *in vivo* results show that the topical administration of miR-150-5p complexed with lipofectamine in acute wounds enhanced their healing kinetics (Figure 6D and Figure S8G).

The main function of a miRNA is to inhibit the translation of a series of mRNA targets (miRNA target “genes”). Four hundred and eighty gene targets have been validated for miR-

150-5p, mostly involved in cellular and metabolic processes (Figure S9A). Because re-epithelization is improved in the setting of wound healing by SEVs (Figure 2), we have identified 9 possible targets by literature mining that could be involved in keratinocyte proliferation, survival and migration (Figure S9B and S9C). A putative interaction between miR-150-5p and the 9 gene targets was evaluated using different bioinformatics platforms. From the 9 gene targets, we selected 3 genes for further analyses: *MYB*, *BAK1* and *SHMT2*. SEVs and miR-150-5p impact on the expression of the 3 gene targets was evaluated in the 3 skin cells by qRT-PCR. Significant down-regulation of the 3 gene targets was observed for skin cells transfected with miR-150-5p (the only exception was *SHMT2* gene in endothelial cells). A similar effect was observed in endothelial cells transfected with SEVs; however, a clear down-regulation profile of gene targets was not observed in keratinocytes or fibroblasts transfected with SEVs (Figure S10A). To evaluate the effect of the 3 target genes in skin cell activity, we knockdown each gene by a siRNA. Only the *MYB* gene knockdown (demonstrated at gene and protein levels; Figures S10B and 10C) lead to an increase in keratinocytes proliferation (Figure 6E). Therefore, the MYB gene is an important gene target of miR-150-5p in the setting of wound healing.

Overall, our results indicate that miRNAs mediate, at least in part, the bioactivity of SEVs. From the 15 miRNAs most expressed in SEVs, we found that 7 may mediate the bioactivity of SEVs, particularly miR-150-5p, having *MYB* as the genetic target (Figure 6F). This translated at cellular level in the proliferation of epidermal keratinocytes (keratin 14 positive cells) at the wound edges and endothelial cells (CD31 positive cells) forming new vessels and at tissue level, in the enhancement of re-epithelization, likely due to a sustained release of SEVs from day 3 to day 5 (Figure 6F). Importantly, wounds treated with light-activated hydrogel containing SEVs had altered expression profile of miRNAs relative to control wounds for at least 10 days. Therefore, our results show that the coordination between SEV release and tissue regeneration allows that specific miRNAs encapsulated in SEVs actuate at specific times during the regenerative program, maximizing the overall therapeutic effect of SEVs. It is known that several miRNAs have important roles at different stages of wound healing including cell proliferation, migration, immunomodulation, survival and angiogenesis.[18] Some miRNAs have been reported as being imbalanced in diabetic wounds such as miR-150, miR-342 and miR-142.[18] Wounds treated with light-activated hydrogel containing SEVs had higher levels of miR-223 and miR-142 at day 5 than non-treated wounds. The increase of both miRNAs likely increased the inflammatory activity in the wound bed which is very relevant at the early stages of wound healing.[39] On the other end, wounds treated with light-activated hydrogel containing SEVs had higher levels of miR-150 and miR-342 at day 10 than non-treated wounds. This increase likely contributes for re-epithelization and neovascularization processes, since both miRNAs are involved on cell proliferation, migration and survival processes. [40, 41] Indeed, the current study highlights for the first time the importance of miR-150 in the context of wound healing. More studies are necessary to identify *in vivo* which cells are mostly targeted by SEVs. It is possible that different cell populations are target at different times during the release of SEVs from hydrogel and thus single cell studies may be relevant to address this issue.

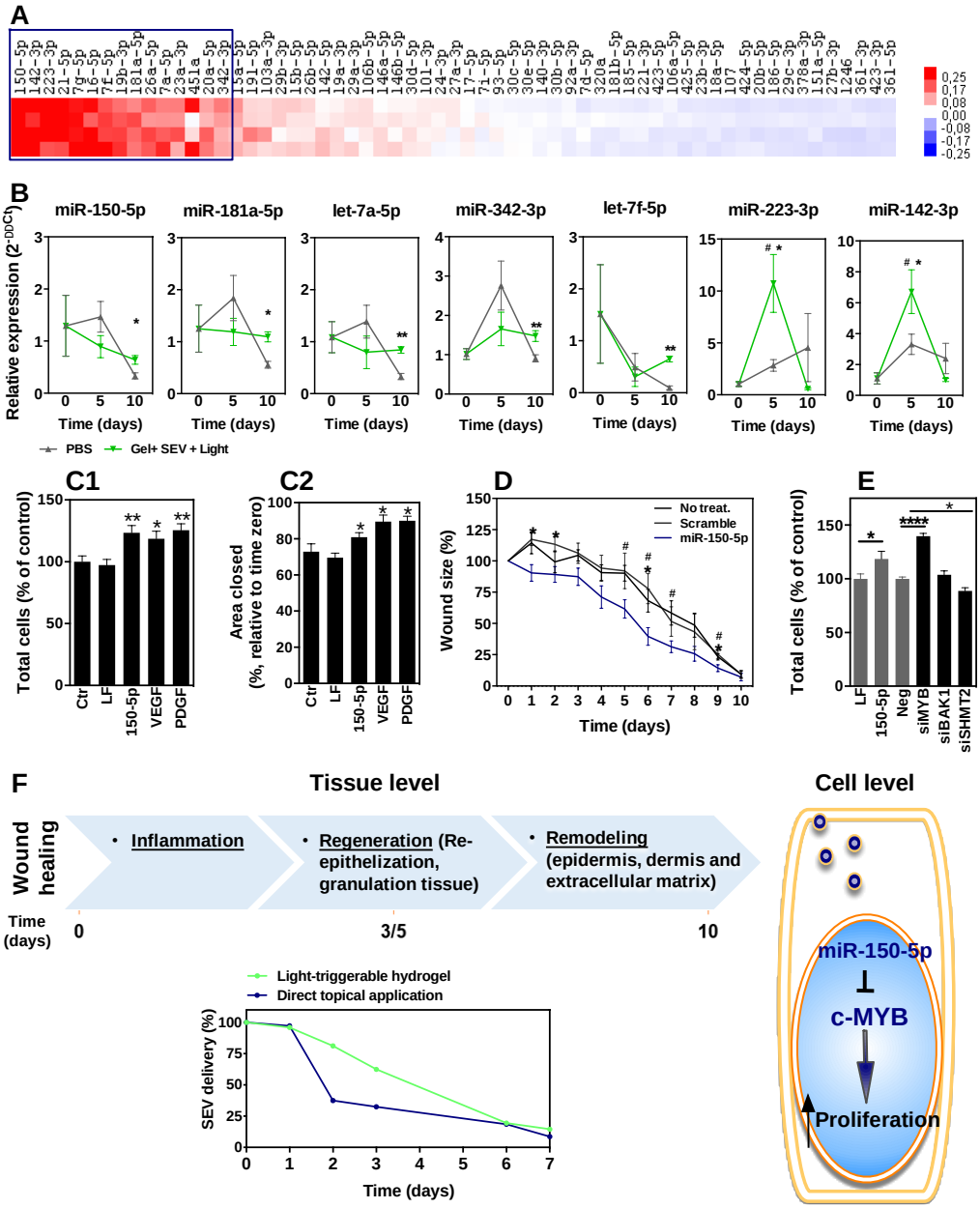

Figure 20. The healing effect of SEVs is mediated at least in part by miR-150-5p which targets *MYB* gene.
(A) Heatmap of 45 miRNAs identified in SEVs of four different donors, presenting over 20 counts/reads. Red designates increased expression, and blue designates decreased expression relative to the mean. (B) miRNAs (both human and mouse) differentially expressed in wounds treated with Gel + SEV + Light or PBS, as evaluated by qRT-PCR analyses. The expression of the different miRNAs was normalized by RNU6 expression. Results are average ± SEM, n=3-5 mice. Statistical analyses were performed by Mann-Whitney test. * denotes statistical difference to control (PBS) while # denotes statistical difference to day 0. (C1) Proliferation and (C2) migration of keratinocytes after transfection with miR-150-5p. Results are average ± SEM, n=9-19. Cells cultured in medium supplemented with VEGF or PDGF-BB were used as positive controls. Untreated cells (Ctr) and cells transfected with lipofectamine (LF) were used as negative controls. Statistical analyses by Mann-Whitney test. (D) Wound healing after topical administration of miR-150-5p, scramble miR or PBS. The results are average ± SEM, n=5-6. Statistical analyses by t-test relatively to scramble miR (*) or PBS (#). * or # denotes statistical significance ($p<0.05$). (E) Proliferation of keratinocytes. Cells were transfected with siRNAs against *MYB*, *BAK1* or *SHMT2* genes. Lipofectamine (LF) or scramble siRNA (Neg) were used as negative controls. miR-150-5p was used as positive control. Results are average ± SEM, n=7-20. Statistical analysis by Mann-Whitney test. (G) Schematic representation of the therapeutic mechanism (tissue and cell levels) of SEVs released by a light-triggerable hydrogel. In B, C, D and E, statistical analyses mean: *,#$p<0.05$; **,##$p<0.01$; ***,###$p<0.001$.

Conclusions

Here, we demonstrate that the kinetics in SEV delivery has impact in tissue regeneration at tissue, cellular and molecular levels. The light-activated hydrogel containing SEVs accelerated wound healing relative to a single or multiple administrations of SEVs or the same hydrogel without light activation, which releases SEVs by the enzymatic/chemical degradation of the polymeric network. This was due to a coordinated action between SEV delivery and hydrogel degradation with the skin regeneration process. It is important to note that SEVs remained stable in the hydrogel before *in vivo* release as confirmed by a FRET system developed in the setting of this work. The regenerative program was characterized at the cellular level by an enhanced re-epithelization process, due to the proliferation of epidermal keratinocytes expressing keratin 14, and by an increase in the neovascularization process, and at molecular level, by alteration in the expression of 7 miRNAs at the skin, being one (miR-150) validated at functional level.

Recent interventions for diabetes-impaired wound healing include the development of therapies based on extracellular components (acellular), biomaterials, stem cells as well as tissue engineering products.[17] Despite the difficulty to compare the healing activity of all these strategies due to differences in the animal models (genetic *versus* chemically induced; type I *versus* type II), wound types (splinted *versus* nonsplinted wounds), therapeutic doses and approaches to monitor skin healing, the results obtained for our formulation are superior than other studies. For example, dressings coated with angiopoietin-derived peptide closed ≈75% of nonsplinted diabetic mouse wounds in 14 days[42] while dressings coated with laminin-derived peptide closed ≈50% of splinted diabetic wounds in 10 days.[43] Moreover, injectable, interconnected microporous gel scaffolds induced 40% closure of splinted diabetic wounds in 7 days.[44]

The injectable triggerable hydrogel reported here allows SEV release with the dynamics of skin tissue regeneration. The injectable formulation can be easily applied in wound beds with different geometries. Because diabetic chronic wounds have recurrent infection and necrosis, one can incorporate autolytic enzymes such as collagenases and antimicrobial peptides[45] in the SEV-containing hydrogel to provide tissue management and antimicrobial activity, respectively. The hydrogel can be irradiated by a commercial available blue laser (a 50 mW blue laser with a 4 mm spot can be acquired by less than $50; this laser has a lower power than dental lasers at 420-480 nm, *i.e.*, 1500 mW/cm^2) and operated by the patient at home, reducing the need for professional assistance and patient dislocation to a health center, thus improving patient quality of life during the treatment. In addition, the release can be aligned with circadian rhythms, *i.e.*, the activation may be performed at the same time every day which may be beneficial in terms of biologic response.[46] With further optimization, it may be interested to consider applications where sun light could be used as a trigger for SEV release.

We have synthesized the hydrogel by the crosslinking of thiolated HA with both PCL and PCL-conjugated SEVs. The photolabile ortho-nitrobenzyl ester moiety in the PCL makes these hydrogels sensitive to blue light. Therefore, SEV release and a decrease in the network crosslink density, both controlled by the cleavage of PCL, occurs simultaneously after hydrogel exposure to a blue light. Although photodegradable HA hydrogels have been previously described,[47] the ability to couple network degradation and release of bioactive agents by the same photolabile linker has not been demonstrated. We have further demonstrated that the hydrogel maintained the stability and integrity of SEVs for several days *in vivo* and the bioactivity of SEVs maintained after light activation and release from the network. For proof of

concept, the programmable SEV delivery system reported here was used for a topical application. Light-triggerable release can be used as a tool to identify the ideal dosing regimen for a range of tissues targets including skin, ocular and gastrointestinal tissues. For gastrointestinal applications, endoscopic techniques can be used for light activation. In addition, the properties of the hydrogel such as mechanical properties, swelling ratio, gelling rate might be tuned according to the final application. In the setting of this work, we irradiated the hydrogel every day for 1 min; however, the irradiation protocol may be further optimized to coordinate SEV delivery with the regenerative process. The hydrogel proposed here offers advantages to specialized controlled release polymers/systems because the operator/user can coordinate hydrogel degradation and SEV release with the tissue regeneration process. Therefore, it offers an exquisite control in SEV delivery and ultimately in tissue regeneration.

The bioactivity mechanism of SEVs was mediated by at least 7 miRNAs (150-5p, 181a-5p, let-7a-5p, 342-3p, let-7f-5p, 223-3p and 142-3p). Some of these miRNAs have been reported to be imbalanced in diabetic chronic wounds including miR-150, 342 and 142.[18] In the current study, we demonstrate for the first time the importance and mechanism of miR-150-5p in the context of wound healing. The delivery of these miRNA´s enhanced the proliferation of epidermal keratinocytes and ECs which in turn promoted skin re-epithelization. Our results demonstrate that the coordination in the release of these miRNAs by SEVs and tissue regeneration maximized their regenerative programs. When SEVs or $PDGF_{BB}$ (FDA-approved wound regenerative therapy) were daily administered into diabetic chronic wounds the most significant effect of SEVs was observed at early stages of wound healing which was then preserved during the healing process.

The clinical relevance of our formulation was demonstrated against an FDA approved formulation based on $PDGF_{BB}$. This growth factor stimulates the proliferation of mesenchymal cells, including fibroblasts. Clinical results have shown that the healing of chronic wounds (*i.e.* wounds that did not heal after 20 weeks with standardized care) with the $PDGF_{BB}$-based formulation was more than 30% higher than the control.[34] Our results show that wounds treated with a daily dose of $PDGF_{BB}$ (*i.e.* ~8 μg of the growth factor per cm^2 of wound; concentration recommended for the application of Regranex)[28] had an average size that corresponds to 88%, at day 5, and 28 %, at day 10, of the initial wound size; while wounds treated with a single application of a light-triggerable hydrogel containing 2 μg of SEVs had an average size that corresponds to 49%, at day 5, and 9%, at day 10 (therefore more than 30% increase in wound healing as compared to $PDGF_{BB}$-treated wounds), of the initial wound size.

In summary, we have demonstrated the impact of SEV delivery kinetics in tissue regeneration at tissue, cellular and molecular levels. A class of injectable biomaterials for the temporal controlled delivery of potent SEVs was developed and the *in vivo* release of these vesicles demonstrated using a FRET imaging system. The hydrogel has the potential to prolong local SEV availability, reduce dosing frequency and maximize SEV therapeutic efficacy (more than 40% improvement beyond the scaffold alone without SEVs and single administration of SEVs). The efficacy is due to a coordination between SEV release, hydrogel degradation and skin regeneration. Our study also sheds light on the bioactivity mechanism of SEVs in the context of tissue regeneration.

Experimental Section

Extended protocols are available in the online supplementary file.

Isolation of hUCBMNCs. All hUCB samples were obtained upon signed informed consent, in compliance with Portuguese legislation. The collection was approved by the ethical committees of Centro Hospitalar e Universitário de Coimbra, Portugal. The samples were stored and transported to the laboratory in sterile bags with anticoagulant solution (citrate-phosphate-dextrose). Samples were processed within 48 h after collection as previously described by us [29]. Mononuclear cells (MNCs) were isolated by density gradient separation (Lymphoprep TM - StemCell Technologies SARL, Grenoble, France). For some experiments, $CD34^+$ cells were positively selected (2 times) after MNC isolation using the mini-MACS immunomagnetic separation system (Miltenyi Biotec, Bergisch Gladbach, Germany), according to the manufacturer's recommendations. MNCs, with and without $CD34^+$ cells, were cryopreserved (FBS:IMDM:DMSO 55%:40%:5%) until usage.

Isolation and labeling of SEVs. Human umbilical cord blood mononuclear cells (hUCBMNCs) (2×10^6 cells/mL) were cultured in X-VIVO 15 serum-free cell culture medium (Lonza) supplemented with Flt-3 (100 ng/mL, PeproTech) and stem-cell factor (100 ng/mL, PeproTech) under hypoxia (0.5% O_2) conditions for 18 h. SEVs were purified from the conditioned media of hUCBMNCs by differential centrifugation as described previously [32]. The pellet containing the SEVs was resuspended in PBS. The SEVs were quantified based in their protein content using the DC protein assay from BioRad™. Typically, 33.5 $\pm$ 16.7 μg (media $\pm$ SD, n= 57 donors) of total protein per 50×10^6 MNCs were obtained. This concentration is in agreement with other studies published elsewhere [48]. To estimate the purity of SEVs, we have quantified the number of particles (measured by NTA) and the protein. The number of particles per μg of protein has a 4-fold enrichment after combining differential centrifugation with size-exclusion chromatography (qEV columns, Izon). For some *in vitro* experiments, SEVs were labelled with NBD-DPPE, PKH67 or Syto® RNASelect™. For *in vivo* experiments, SEVs were labeled with near-infrared dyes, Cy5.5-DPPE and/or Cy7-DPPE.

***In vitro* SEV bioactivity assay.** Human umbilical vein endothelial cells (HUVECs, Lonza), normal dermal human fibroblasts (NDHF, Lonza) and human keratinocytes (HaCaT, CLS) were used as skin cell models. Endothelial cells were cultured in EGM-2 (Lonza) with 2% FBS, fibroblasts and keratinocytes were cultured in DMEM (Invitrogen) with 0.5% Pen Strep and 10% FBS. Whenever cells were treated with SEVs, the media used to dilute the SEVs for transfection was centrifuged overnight at 100.000 g and filtered (0.2 μm pore) in order to deplete the exosomes from FBS (exo-depleted media). For cell proliferation assay, cells were plated at very low density in 96 well plates, stained with Hoechst at time 20 h (1 μg/mL, Life Technologies) for 15 min, washed with PBS and incubated in exo-depleted medium with or without supplementation with SEVs. Vascular endothelial growth factor (VEGF, 50 ng/mL, PeproTech) and platelet derived growth factor (PDGF-BB, 50 ng/mL, PeproTech) were used as positive controls. Cells were photographed (IN Cell, GE Healthcare) and cell number was obtained by counting the nuclei. Proliferation was determined as percentage of control at 72 h after treatment ((Total cells $_{\text{treatment group}}$ / Total cells $_{\text{control group}}$) × 100%).

Preparation and characterization of a light-triggerable hydrogel. (A) *Purification of 2-carboxyethyl acrylate oligomers.* Anhydrous 2-carboxyethyl acrylate oligomers (6.5 g, n=0-3, Aldrich, Ref. 407585, average MW~170) were separated by gravity chromatography (silica, AcOEt/Hex: 0 → 30%). Right after purification, fractions were collected and analyzed by HPLC-MS (Agilent 1100, Zorbax 3.5μm 3×150mm column, H_2O/CH_3CN: 5 → 95%). Desired fraction, n=3, was dried under vacuum to get a transparent oil (0.7 g), confirmed by NMR as the desired product. ^{1}H NMR (400 MHz, $CDCl_3$): δ 6.39 (d, *J* = 17.3 Hz, 1H, −CH=*CH*$_2$), 6.12-6.06 (dd, 1H, −C*H*=CH_2), 5.83 (d, *J* = 10.4 Hz, 1H, −CH=C*H*$_2$), 4.41-4.35 (m, 6H, −OC*H*$_2$−CH_2−), 2.71-2.64 (m,

6H, –OCH_2–CH_2–). (B) *Synthesis of the photo-crosslinker linker (PCL)*. Purified 3-((3-((3-(acryloyloxy)propanoyl)oxy)propanoyl)oxy)propanoic acid (2-Carboxyethyl acrylate n=3, 0.5 mL, 1.0 equiv.) was solubilized in dichloromethane (10 mL, Fisher Chemical) under nitrogen atmosphere and dimethylformamide (0.15 mL). Then, thionyl chloride (0.50 mL, 2.0 equiv., Acros Organics) was added dropwise at 0 ºC, under vigorous stirring and by using a dropping funnel. After 1 h of reaction water-bath was removed and reaction was stirred overnight at room temperature (15 h reaction time). Solvent was then evaporated and compound was dried under vacuum. Then, the resulting crude was solubilized in (distilled) dichloromethane (3 mL) and added dropwise under nitrogen atmosphere to a previously prepared cooled (0 ºC) solution of (2-nitro-1,3-phenylene) dimethanol (0.25 g, 0.4 equiv., ARCH Bioscience) and *N,N*-diisopropylethylamine (0.12 mL, 0.2 equiv, Sigma-Aldrich) in (distilled) dichloromethane (5 mL) over 20 min. Reaction was then left to reach room temperature overnight. Finally, double distilled water (5 mL) was added to the reaction crude and the reaction product extracted with ethyl acetate (3 × 5 mL, Fisher Chemical). The corresponding organic fractions were dried with magnesium sulfate, filtered and solvent was evaporated under reduced pressure. Reaction crude was purified by gravity chromatography (silica, AcOEt/Hex: 0 → 60%), to obtain the photo-cleavable linker as brown oil (yield 54%). ^{1}H NMR (400 MHz, $CDCl_3$): δ 7.53 (m, 3H, ArH), 6.39 (d, *J* = 16.9 Hz, 2H, –CH=C*H*$_2$), 6.19-6.03 (dd, 2H, –C*H*=CH_2), 5.84 (d, *J* = 10.4 Hz, 2H, –CH=C*H*$_2$), 5.25 (s, 4H, ArC*H*$_2$O–), 4.45-4.31 (m, 12H, –OC*H*$_2$–CH_2–), 2.77-2.62 (m, 12H, –OCH_2–C*H*$_2$–). (C) *Thiolation of hyaluronic acid (HA)*. HA (0.2 g, 180 kDa, Bioiberica) was dissolved in ultra-pure deionized water (10 mL) to obtain a final 2% (w/v) polymer solution. The pH of the reaction mixture was adjusted to 5.5 by the addition of 0.1 M HCl. Afterwards, EDC and NHS (both from Sigma-Aldrich) were added to the polymer reaction mixture at a final concentration of 112 mM (2:1 molar ratio (EDC/NHS):cysteine). The pH was readjusted to 5.5 and the reaction mixture was stirred for 20 min at a room temperature. Then, L-cysteine ethyl ester hydrochloride (0.2 g, Sigma-Aldrich) was added and the pH was increased to 6.0. The reaction mixture proceeded for 4-6 h at room temperature, under nitrogen environment and protected from direct light exposure. The resulting conjugate was dialyzed in a dialysis membrane (molecular weight cutoff 12 kDa) at 4 ºC, three times against a pre-cooled 1% (w/v) NaCl (Applichem) solution and finally against demineralized water. After 48 h of dialysis, the thiol-conjugated hyaluronic acid was lyophilized for two days and stored at -20 ºC until further use. (D) *Conjugation of SEVs with PCL and formation of hydrogel*. The free thiol groups concentration in SEVs was 2.4±0.5 nM per 1 µg of vesicles, as determined by a Thiol Fluorescent Probe IV (20 µM, Calbiochem - Merck Millipore, calibration curve was against L-cysteine ethyl ester hydrochloride). Initially, the photo-cleavable linker (1% v/v) was allowed to react for ~10 min with free thiol groups present in the SEVs surface (free thiol 1:5 acrylate, molar ratio). Then, the thiolated-HA was dissolved in a solution containing the acrylate-surface modified SEVs to give a final 5% (w/v) polymer solution. The reaction between free acrylate groups present in the SEVs and the thiol of the HA was allowed to occur for at least 10 min, with vortex cycles, after which we added more free acrylate groups to give a final acrylate to thiol ratio of 1:1. The final reaction solution was allowed to crosslink for 1 h at 37 ºC.

***In vivo* testing.** *In vivo* experimental protocols were approved by the Portuguese National Authority for Animal Health (DGAV). Male C57BL/6 wild-type (WT) mice (8 to 10-week-old), purchased from Charles River (France) and weighing between 20 and 30 g were used for the experiments. Diabetes mellitus type I was induced in mice by intraperitoneal injections of streptozotocin for 5 consecutive days (STZ; citrate buffer, pH 4.5; 50 mg/kg, Sigma-Aldrich). Animals were anesthetized by an intramuscular injection of a /ketamine/xylazine solution (100/10 mg/kg). Analgesia (buprenorphine, 0.1 mg/kg) was given subcutaneously, 30 minutes before the wound induction and every 6-8h up to 48 h. After shaving and disinfecting the area

with a povidone-iodine solution (Betadine®), two 6 mm diameter full-thickness excision wounds were performed with a sterile biopsy punch in the dorsum of each animal. Topical treatments were applied immediately after wound induction and were repeated as indicated. Animals were divided into different groups according to the treatment applied. SEVs were applied topically to the wound bed. In all experiments, animals were kept in individual cages with food and water *ad libitum* and observed daily during the total period of the experiment. The progress of wound closure was monitored daily by measuring the wound area. The percentage of wound area was presented as percentage of the original wound (day 0) and calculated following the equation: (area of actual wound/area of original wound) × 100%. Wounds were considered completely closed when the area at a particular time point was zero.

Statistical analyses. All analyses were performed in at least biological triplicates. Statistical analyses were performed by a Mann-Whitney test or by a one or two-way ANOVA test followed by a Bonferroni's or a Newman-Keuls multiple comparisons test. Statistical analyses were performed by GraphPad Prism 6 software (GraphPad Software, Inc.). Significance levels were set at *P < 0.05, **P < 0.01, ***P < 0.001, and ****P < 0.0001. The values for *N*, *P*, and the specific statistical test performed for each experiment was included in the appropriate figure legend.

ASSOCIATED CONTENT

Supporting Information. Supporting Information Available: PDF file with extended experimental protocols and results regarding: characterization of hUCBMNCs and SEVs; cellular uptake and biological effect of SEVs; *in vivo* wound healing activity of SEVs; characterization of HA hydrogel and bioactivity of SEVs released from hydrogel; expression of keratin 5 and 14 in wounds; composition of miRNAs in SEVs; bioactivity of miR-150-5p; gene targets of miR-150-5p. This material is available free of charge *via* the Internet at http://pubs.acs.org

AUTHOR INFORMATION

Corresponding Author

* lino@uc-biotech.pt

Author Contributions

H.H.A, R.M.S.C., A. Z. and L.F. designed the research; H.H.A, R.M.S.C., A. Z., J.C., E.C.L., A.J.B., M.L., A.B., I.K., C.G. performed the research; H.H.A, R.M.S.C., A. Z., E.C.L., A.J.B., J.K., E.C. and L.F. analyzed the data; and H.H.A, R.M.S.C. and L.F. wrote the paper. ‡ These authors contributed equally.

ACKNOWLEDGMENTS

This work was supported by FCT (SFRH/BDE/103512/2014;SFRH/BPD/112883/2015; SFRH/BPD/97286/2013; MITP-TB/ECE/0013/2013; EXCL/DTP-PIC/0069/2012; UID/NEU/04539/2013); EFSD/JDRF/Novo Nordisk European Programme in Type 1 Diabetes Research; QREN-COMPETE funding (FCOMP-01-0202-FEDER-038631; Project "ExoCord" promoted by Stemlab, SA and Biocant), Portugal 2020-COMPETE funding (Project "Stem cell based platforms for Regenerative and Therapeutic Medicine", Centro-07-ST24-FEDER-002008; Project "StrokeTherapy" co-promoted by Stemlab, Rovisco Pais and Universidade de Coimbra, POCI-01-0247-FEDER-003386) and EC project ERAatUC (Ref:669088).

REFERENCES

1. Valadi, H.; Ekstrom, K.; Bossios, A.; Sjostrand, M.; Lee, J. J.; Lotvall, J. O., Exosome-Mediated Transfer of mRNAs and MicroRNAs is a Novel Mechanism of Genetic Exchange between Cells. *Nat Cell Biol* 2007, *9*, 654-659.

2. EL Andaloussi, S.; Mager, I.; Breakefield, X. O.; Wood, M. J., Extracellular Vesicles: Biology and Emerging Therapeutic Opportunities. *Nat Rev Drug Discov* 2013, *12*, 347-357.

3. Fang, S.; Xu, C.; Zhang, Y.; Xue, C.; Yang, C.; Bi, H.; Qian, X.; Wu, M.; Ji, K.; Zhao, Y.; Wang, Y.; Liu, H.; Xing, X., Umbilical Cord-Derived Mesenchymal Stem Cell-Derived Exosomal MicroRNAs Suppress Myofibroblast Differentiation by Inhibiting the Transforming Growth Factor-beta/SMAD2 Pathway During Wound Healing. *Stem Cells Transl Med* 2016, *5*, 1425-1439.

4. Zhang, B.; Wu, X.; Zhang, X.; Sun, Y.; Yan, Y.; Shi, H.; Zhu, Y.; Wu, L.; Pan, Z.; Zhu, W.; Qian, H.; Xu, W., Human Umbilical Cord Mesenchymal Stem Cell Exosomes Enhance Angiogenesis through the Wnt4/beta-Catenin Pathway. *Stem Cells Transl Med* 2015, *4*, 513-522.

5. Zhang, B.; Wang, M.; Gong, A.; Zhang, X.; Wu, X.; Zhu, Y.; Shi, H.; Wu, L.; Zhu, W.; Qian, H.; Xu, W., HucMSC-Exosome Mediated-Wnt4 Signaling Is Required for Cutaneous Wound Healing. *Stem Cells* 2015, *33*, 2158-2168.

6. Mathiyalagan, P.; Liang, Y.; Kim, D.; Misener, S.; Thorne, T.; Kamide, C. E.; Klyachko, E.; Losordo, D. W.; Hajjar, R. J.; Sahoo, S., Angiogenic Mechanisms of Human CD34+ Stem Cell Exosomes in the Repair of Ischemic Hindlimb. *Circ Res* 2017, *120*, 1466-1476.

7. Gray, W. D.; French, K. M.; Ghosh-Choudhary, S.; Maxwell, J. T.; Brown, M. E.; Platt, M. O.; Searles, C. D.; Davis, M. E., Identification of Therapeutic Covariant MicroRNA Clusters in Hypoxia-Treated Cardiac Progenitor Cell Exosomes Using Systems Biology. *Circ Res* 2015, *116*, 255-263.

8. Liu, B.; Lee, B. W.; Nakanishi, K.; Villasante, A.; Williamson, R.; Metz, J.; Kim, J.; Kanai, M.; Bi, L.; Brown, K.; Di Paolo, G.; Homma, S.; Sims, P. A.; Topkara, V. K.; Vunjak-Novakovic, G., Cardiac Recovery *via* Extended Cell-Free Delivery of Extracellular Vesicles Secreted by Cardiomyocytes Derived from Induced Pluripotent Stem Cells. *Nat Biomed Eng* 2018, *2*, 293-303.

9. Sun, Y. X.; Shi, H.; Yin, S. Q.; Ji, C.; Zhang, X.; Zhang, B.; Wu, P. P.; Shi, Y. H.; Mao, F.; Yan, Y. M.; Xu, W. R.; Qian, H., Human Mesenchymal Stem Cell Derived Exosomes Alleviate Type 2 Diabetes Mellitus by Reversing Peripheral Insulin Resistance and Relieving beta-Cell Destruction. *ACS Nano* 2018, *12*, 7613-7628.

10. Cabral, J.; Ryan, A. E.; Griffin, M. D.; Ritter, T., Extracellular Vesicles as Modulators of Wound Healing. *Adv Drug Deliver Rev* 2018, *129*, 394-406.

11. Lai, C. P.; Mardini, O.; Ericsson, M.; Prabhakar, S.; Maguire, C.; Chen, J. W.; Tannous, B. A.; Breakefield, X. O., Dynamic Biodistribution of Extracellular Vesicles *In Vivo* Using a Multimodal Imaging Reporter. *ACS Nano* 2014, *8*, 483-494.

12. Imai, T.; Takahashi, Y.; Nishikawa, M.; Kato, K.; Morishita, M.; Yamashita, T.; Matsumoto, A.; Charoenviriyakul, C.; Takakura, Y., Macrophage-Dependent Clearance of Systemically Administered B16BL6-Derived Exosomes from the Blood Circulation in Mice. *J Extracell Vesicles* 2015, *4*, 26238.

13. Heusermann, W.; Hean, J.; Trojer, D.; Steib, E.; von Bueren, S.; Graff-Meyer, A.; Genoud, C.; Martin, K.; Pizzato, N.; Voshol, J.; Morrissey, D. V.; Andaloussi, S. E.; Wood, M. J.; Meisner-Kober, N. C., Exosomes Surf on Filopodia to Enter Cells at Endocytic Hot Spots, Traffic within Endosomes, and Are Targeted to the ER. *J Cell Biol* 2016, *213*, 173-184.

14. Richardson, T. P.; Peters, M. C.; Ennett, A. B.; Mooney, D. J., Polymeric System for Dual Growth Factor Delivery. *Nat Biotechnol* 2001, *19*, 1029-1034.

15. Lu, H.; Xu, X.; Zhang, M.; Cao, R.; Brakenhielm, E.; Li, C.; Lin, H.; Yao, G.; Sun, H.; Qi, L.; Tang, M.; Dai, H.; Zhang, Y.; Su, R.; Bi, Y.; Zhang, Y.; Cao, Y., Combinatorial Protein Therapy of Angiogenic and Arteriogenic Factors Remarkably Improves Collaterogenesis and Cardiac Function in Pigs. *Proc Natl Acad Sci U S A* 2007, *104*, 12140-12145.

16. Borselli, C.; Storrie, H.; Benesch-Lee, F.; Shvartsman, D.; Cezar, C.; Lichtman, J. W.; Vandenburgh, H. H.; Mooney, D. J., Functional Muscle Regeneration with Combined Delivery of Angiogenesis and Myogenesis Factors. *Proc Natl Acad Sci U S A* 2010, *107*, 3287-3292.

17. Eming, S. A.; Martin, P.; Tomic-Canic, M., Wound Repair and Regeneration: Mechanisms, Signaling, and Translation. *Sci Transl Med* 2014, *6*, 265sr6.

18. Moura, J.; Børsheim, E.; Carvalho, E., The Role of MicroRNAs in Diabetic Complications - Special Emphasis on Wound Healing. *Genes* 2014, *5*, 926-956.

19. Frykberg, R. G.; Banks, J., Challenges in the Treatment of Chronic Wounds. *Adv Wound Care (New Rochelle)* 2015, *4*, 560-582.

20. Hu, L.; Wang, J.; Zhou, X.; Xiong, Z.; Zhao, J.; Yu, R.; Huang, F.; Zhang, H.; Chen, L., Exosomes Derived from Human Adipose Mensenchymal Stem Cells Accelerates Cutaneous Wound Healing *via* Optimizing the Characteristics of Fibroblasts. *Sci Rep* 2016, *6*, 32993.

21. Shabbir, A.; Cox, A.; Rodriguez-Menocal, L.; Salgado, M.; Van Badiavas, E., Mesenchymal Stem Cell Exosomes Induce Proliferation and Migration of Normal and Chronic Wound Fibroblasts, and Enhance Angiogenesis *In Vitro*. *Stem Cells Dev* 2015, *24*, 1635-1647.

22. Tao, S. C.; Guo, S. C.; Li, M.; Ke, Q. F.; Guo, Y. P.; Zhang, C. Q., Chitosan Wound Dressings Incorporating Exosomes Derived from MicroRNA-126-Overexpressing Synovium Mesenchymal Stem Cells Provide Sustained Release of Exosomes and Heal Full-Thickness Skin Defects in a Diabetic Rat Model. *Stem Cells Transl Med* 2017, *6*, 736-747.

23. Shi, Q.; Qian, Z.; Liu, D.; Sun, J.; Wang, X.; Liu, H.; Xu, J.; Guo, X., GMSC-Derived Exosomes Combined with a Chitosan/Silk Hydrogel Sponge Accelerates Wound Healing in a Diabetic Rat Skin Defect Model. *Front Physiol* 2017, *8*, 904.

24. Zhang, K.; Zhao, X.; Chen, X.; Wei, Y.; Du, W.; Wang, Y.; Liu, L.; Zhao, W.; Han, Z.; Kong, D.; Zhao, Q.; Guo, Z.; Han, Z.; Liu, N.; Ma, F.; Li, Z., Enhanced Therapeutic Effects of Mesenchymal Stem Cell-Derived Exosomes with an Injectable Hydrogel for Hindlimb Ischemia Treatment. *ACS Appl Mater Interfaces* 2018, *10*, 30081-30091.

25. Wang, C.; Wang, M.; Xu, T.; Zhang, X.; Lin, C.; Gao, W.; Xu, H.; Lei, B.; Mao, C., Engineering Bioactive Self-Healing Antibacterial Exosomes Hydrogel for Promoting Chronic Diabetic Wound Healing and Complete Skin Regeneration. *Theranostics* 2019, *9*, 65-76.

26. Chen, C. W.; Wang, L. L.; Zaman, S.; Gordon, J.; Arisi, M. F.; Venkataraman, C. M.; Chung, J. J.; Hung, G.; Gaffey, A. C.; Spruce, L. A.; Fazelinia, H.; Gorman, R. C.; Seeholzer, S. H.; Burdick, J. A.; Atluri, P., Sustained Release of Endothelial Progenitor Cell-Derived Extracellular Vesicles from Shear-Thinning Hydrogels Improves Angiogenesis and Promotes Function after Myocardial Infarction. *Cardiovasc Res* 2018, *114*, 1029-1040.

27. Aya, K. L.; Stern, R., Hyaluronan in Wound Healing: Rediscovering a Major Player. *Wound Repair Regen* 2014, *22*, 579-593.

28. REGRANEX Gel 0.01% https://www.fda.gov/media/76010/download. (accessed Nov. 2018).

29. Pedroso, D. C.; Tellechea, A.; Moura, L.; Fidalgo-Carvalho, I.; Duarte, J.; Carvalho, E.; Ferreira, L., Improved Survival, Vascular Differentiation and Wound Healing Potential of Stem Cells Co-Cultured with Endothelial Cells. *PLoS One* 2011, *6*, e16114.

30. Mildner, M.; Hacker, S.; Haider, T.; Gschwandtner, M.; Werba, G.; Barresi, C.; Zimmermann, M.; Golabi, B.; Tschachler, E.; Ankersmit, H. J., Secretome of Peripheral Blood Mononuclear Cells Enhances Wound Healing. *PLoS One* 2013, *8*, e60103.

31. Agarwal, U.; George, A.; Bhutani, S.; Ghosh-Choudhary, S.; Maxwell, J. T.; Brown, M. E.; Mehta, Y.; Platt, M. O.; Liang, Y.; Sahoo, S.; Davis, M. E., Experimental, Systems, and Computational Approaches to Understanding the MicroRNA-Mediated Reparative Potential of Cardiac Progenitor Cell-Derived Exosomes From Pediatric Patients. *Circ Res* 2017, *120*, 701-712.

32. Thery, C.; Amigorena, S.; Raposo, G.; Clayton, A., Isolation and Characterization of Exosomes from Cell Culture Supernatants and Biological Fluids. *Curr Protoc Cell Biol* 2006, *Chapter 3*, Unit 3 22.

33. Horibe, S.; Tanahashi, T.; Kawauchi, S.; Murakami, Y.; Rikitake, Y., Mechanism of Recipient Cell-Dependent Differences in Exosome Uptake. *Bmc Cancer* 2018, *18*.

34. Smiell, J. M.; Wieman, T. J.; Steed, D. L.; Perry, B. H.; Sampson, A. R.; Schwab, B. H., Efficacy and Safety of Becaplermin (Recombinant Human Platelet-Derived Growth Factor-BB) in Patients with Nonhealing, Lower Extremity Diabetic Ulcers: a Combined Analysis of Four Randomized Studies. *Wound Repair Regen* 1999, *7*, 335-46.

35. Voigt, J.; Driver, V. R., Hyaluronic Acid Derivatives and their Healing Effect on Burns, Epithelial Surgical Wounds, and Chronic Wounds: a Systematic Review and Meta-Analysis of Randomized Controlled Trials. *Wound Repair Regen* 2012, *20*, 317-331.

36. Fuchs, E., Keratins and the skin. *Annu Rev Cell Dev Biol* 1995, *11*, 123-153.

37. Fuhrmann, G.; Chandrawati, R.; Parmar, P. A.; Keane, T. J.; Maynard, S. A.; Bertazzo, S.; Stevens, M. M., Engineering Extracellular Vesicles with the Tools of Enzyme Prodrug Therapy. *Adv Mater* 2018, *30*, e1706616.

38. Tan, G. S.; Chiu, C.-H.; Garchow, B. G.; Metzler, D.; Diamond, S. L.; Kiriakidou, M., Small Molecule Inhibition of RISC Loading. *ACS Chem Biol* 2012, *7*, 403-410.

39. Naqvi, A. R.; Fordham, J. B.; Ganesh, B.; Nares, S., MiR-24, MiR-30b and MiR-142-3p Interfere with Antigen Processing and Presentation by Primary Macrophages and Dendritic Cells. *Scientific Reports* 2016, *6*, 32925.

40. Czimmerer, Z.; Varga, T.; Kiss, M.; Vázquez, C. O.; Doan-Xuan, Q. M.; Rückerl, D.; Tattikota, S. G.; Yan, X.; Nagy, Z. S.; Daniel, B.; Poliska, S.; Horvath, A.; Nagy, G.; Varallyay, E.; Poy, M. N.; Allen, J. E.; Bacso, Z.; Abreu-Goodger, C.; Nagy, L., The IL-4/STAT6 Signaling Axis Establishes a Conserved MicroRNA Signature in Human and Mouse Macrophages Regulating Cell Survival *via* MiR-342-3p. *Genome Medicine* 2016, *8*, 63.

41. Li, Y.; Su, J.; Li, F.; Chen, X.; Zhang, G., MiR-150 Regulates Human Keratinocyte Proliferation in Hypoxic Conditions through Targeting HIF-1Alpha and VEGFA: Implications for Psoriasis Treatment. *PLoS One* 2017, *12*, e0175459.

42. Xiao, Y.; Reis, L. A.; Feric, N.; Knee, E. J.; Gu, J.; Cao, S.; Laschinger, C.; Londono, C.; Antolovich, J.; McGuigan, A. P.; Radisic, M., Diabetic Wound Regeneration Using Peptide-Modified Hydrogels to Target Re-epithelialization. *Proc Natl Acad Sci U S A* 2016, *113*, E5792-E5801.

43. Zhu, Y.; Cankova, Z.; Iwanaszko, M.; Lichtor, S.; Mrksich, M.; Ameer, G. A., Potent Laminin-Inspired Antioxidant Regenerative Dressing Accelerates Wound Healing in Diabetes. *Proc Natl Acad Sci U S A* 2018, *115*, 6816-6821.

44. Griffin, D. R.; Weaver, W. M.; Scumpia, P. O.; Di Carlo, D.; Segura, T., Accelerated Wound Healing by Injectable Microporous Gel Scaffolds Assembled from Annealed Building Blocks. *Nat Mater* 2015, *14*, 737-744.

45. Comune, M.; Rai, A.; Chereddy, K. K.; Pinto, S.; Aday, S.; Ferreira, A. F.; Zonari, A.; Blersch, J.; Cunha, R.; Rodrigues, R.; Lerma, J.; Simoes, P. N.; Preat, V.; Ferreira, L., Antimicrobial Peptide-Gold Nanoscale Therapeutic Formulation with High Skin Regenerative Potential. *J Control Release* 2017, *262*, 58-71.

46. Hoyle, N. P.; Seinkmane, E.; Putker, M.; Feeney, K. A.; Krogager, T. P.; Chesham, J. E.; Bray, L. K.; Thomas, J. M.; Dunn, K.; Blaikley, J.; O'Neill, J. S., Circadian Actin Dynamics Drive Rhythmic Fibroblast Mobilization During Wound Healing. *Sci Transl Med* 2017, *9*, eaal2774

47. Rosales, A. M.; Vega, S. L.; DelRio, F. W.; Burdick, J. A.; Anseth, K. S., Hydrogels with Reversible Mechanics to Probe Dynamic Cell Microenvironments. *Angew Chem Int Ed Engl* 2017, *56*, 12132-12136.

48. Van Deun, J.; Mestdagh, P.; Sormunen, R.; Cocquyt, V.; Vermaelen, K.; Vandesompele, J.; Bracke, M.; De Wever, O.; Hendrix, A., The Impact of Disparate Isolation Methods for Extracellular Vesicles on Downstream RNA Profiling. *J Extracell Vesicles* 2014, *3*, 24858

Supplementary material

Material and methods

Secreting cells: human umbilical cord blood (hUCB) mononuclear cells isolation

All hUCB samples were obtained upon signed informed consent, in compliance with Portuguese legislation. The collection was approved by the ethical committees of Centro Hospitalar e Universitário de Coimbra, Portugal. The samples were stored and transported to the laboratory in sterile bags with anticoagulant solution (citrate-phosphate-dextrose). Samples were processed within 48 h after collection as previously described by us[1] . Mononuclear cells (MNCs) were isolated by density gradient separation (Lymphoprep TM - StemCell Technologies SARL, Grenoble, France). For some experiments, CD34+ cells were positively selected (2 times) after MNC isolation using the mini-MACS immunomagnetic separation system (Miltenyi Biotec, Bergisch Gladbach, Germany), according to the manufacturer's recommendations. MNCs, with and without CD34+ cells, were cryopreserved (FBS:IMDM:DMSO 55%:40%:5%) until usage.

Secreting cells: MNCs characterization by a hematologic analyzer

The hUCB cells were characterized before and after MNCs and CD34+ cells isolation and cryopreservation using an Automated Hematology System (Sysmex XE-2100 TM, Mundelein, IL, USA). The cells were characterized regarding their composition in white blood cells (neutrophils, lymphocytes, monocytes, eosinophils, basophils, immature granulocytes and other cells) and nucleated red blood cells, taking in account their size and complexity.

Secreting cells: MNCs characterization by flow cytometry

Cells were further characterized by flow cytometry for CD45 and CD34 expression, before and after CD34+ cells isolation. Total buffy coat cells (white blood cells) were incubated for 15 min at room temperature with CD45 and CD34 antibodies followed by incubation (for some minutes) with 7-amino-actinomycin D (7-AAD) for cell viability assessment (Supplementary Table I). Lysing solution (VersaLyse) was added and after 20 min samples were washed and resuspended in PBS (300 µL). Cells were then analyzed in a Cytomics FC500 flow cytometer (Beckman Coulter).

Isolation of SEVs

The total number of MNCs (lymphocytes and monocytes) was used for SEV secretion. Both MNCs CD34+ and MNCs CD34- (2×106 cells/mL) were cultured in X-VIVO 15 serum-free cell-culture medium (Lonza Group Ltd, Basel, Switzerland) supplemented with Flt-3 (100 ng/mL, PeproTech) and stem-cell factor (SCF, 100 ng/mL, PeproTech) under hypoxia (0.5% O2) conditions for 18 h. SEVs were purified from the conditioned media of MNCs by differential centrifugation. Briefly, the conditioned medium was subjected to sequential centrifugation steps of 300 ×g (10 min), 2000 ×g (20 min), and two times of 10.000 ×g (30 min), for removal of

cells, cell debris, and microvesicles, respectively. After a 2 h centrifugation at 100.000 ×g in a SW41Ti or SW32Ti swinging bucket rotor (Beckman) the pellet was washed with 7 mL of PBS and centrifuged at 100.000 ×g for another 2 h. The pellet containing the SEVs was resuspended in PBS (250 µL). The SEVs were quantified based in their protein content using the DC protein assay from BioRad™. In these conditions, we obtained 134.1 $\pm$ 66.9 µg/mL (media $\pm$ SD, n= 57) of total protein per 50 $\times$ 10^6 cells. To estimate the purity of SEVs, we have quantified the number of particles (measured by NTA, see below) and the protein (this time measured by a micro-BCA assay, that is more sensitive than the DC protein assay from Biorad mentioned above). The number of particles per µg of protein was 1.3 ×10^9 after differential centrifugation. The number increased to 5.3×10^9 combining differential centrifugation with size-exclusion chromatography (qEV columns, Izon; therefore a 4-fold enrichment).

SEV characterization: dynamic light scattering and zeta potential analyses

After thawing the SEVs at room temperature, particle size and zeta potential were determined using light scattering via Zeta PALS Zeta Potential Analyzer and ZetaPlus Particle Sizing Software, v. 2.27 (Brookhaven Instruments Corporation). For particle size, a suspension of SEVs (50 µL) was diluted in PBS (200 µL) and five measurements were performed at 25ºC. For the zeta potential, SEVs (50 µL) were diluted 25 times with biological molecular grade water filtered through a 0.2 µM pore (final PBS concentration of 5 mM). Each sample was measured 5 times and the results presented are the arithmetic means of different biological replicates.

SEV characterization: NTA analyses

A suspension of SEVs (15 µg) was diluted in MilliQ water (1 mL), to yield a final concentration of 5×10^8 to 1×10^9 particles /mL, 30 and 60 particles per frame. Samples were loaded into the sample chamber of an LM10 unit (Nanosight, Amesbury, UK) using a syringe pump speed of 10 µL per minute. Five videos (60 sec) of each sample were recorded. Temperature was monitored across all samples. Camera level was set at 11 or 12 and detection threshold at 4. Data analysis was performed using NTA 2.2 software.

SEV characterization: TEM analyses

The samples were mounted on 300 mesh formvar copper grids, stained with uranyl acetate 1%, and were examined using a Jeol JEM 1400 transmission electron microscope (Tokyo). Images were digitally recorded using a Gatan SC 1000 ORIUS CCD camera (Warrendale, PA, USA), and photomontages were performed using Adobe Photoshop CS software (Adobe Systems, San Jose, CA), at the HEMS / IBMC - Institute for Molecular and Cell Biology (IBMC) of the University of Porto, Portugal.

SEV characterization: SEV surface markers characterization by flow cytometry

Flow cytometry analyses were performed according to published protocols [2]. Briefly, a suspension of SEVs (10-50 µg) was incubated with aldehyde/sulfate latex beads (3.8 µm, 4% (m/v)) (Molecular probes®, A37304), in a proportion of 2 (SEV):1(beads) (w/v), for 15 min at room temperature. PBS was then added to reach a reactional volume of 1 mL and the solution

was kept overnight at 4 ºC under a constant stirring in a microtube rotator. After the addition of glycine (110 µL, 1 mM) during 30 min the beads coated with SEVs were washed two times with PBS/0.5% BSA (500 µL). The SEVs attached to the beads were incubated with fluorescent antibodies and their corresponding IgG, for 30 min on ice (Supplementary Table I). The labelled SEVs were washed twice with PBS/ 0.5% BSA, resuspended in PBS (200 µL) and finally characterized by flow cytometry (BD AccuriTM C6, BD Biosciences). SEV- secreting cells were also characterized by flow cytometry for SEV and MNC markers. In this case, cells were incubated for 30 min at 4ºC with specific antibodies, washed twice and resuspended in PBS/0.5% BSA (300 µL). Propidium iodide (PI, 1 µg/mL) was added for cell viability assessment immediately before analysis.

SEV characterization: western blot analyses

Protein was extracted from MNCs and respective SEVs by incubation on ice for 30 min (vortex every 10 min) with RIPA buffer (R 0278, Sigma-Aldrich) and a cocktail of phosphatase / protease inhibitors (PIC, #5872, Cell Signaling Technologies), followed by sonication for 5 min of SEVs isolates. Samples were centrifuged at 14.000 g for 15 min, 4º C and the supernatant was kept. Total protein was quantified by BCA (Thermo fisher). Samples were diluted in loading buffer (Laemmli sample buffer) and 50 µg were applied in a 10% polyacrylamide gel. Protein was transferred to a Westran (Whatman) membrane and analyzed for exosomal and cellular markers CD63 and GAPDH (Supplementary Table I) using the VWR Imager Transiluminator and VWR® Image Capture Software. Relative quantification of western blot bands was performed with ImageJ Software.

SEV characterization: RNA profile

Extraction of RNA. SEVs were collected from 50×10^6 MNCs, using the protocol described above. For some experiments, SEVs from 3 donors were treated with RNase (10 µg/mL, SigmaAldrich, R5125) at 37ºC for 10 min prior to RNA isolation. RNase was inactivated by adding RNase inhibitor at approximately 1000 U/mL (Sigma-Aldrich, R1158). Total RNA was extracted from SEVs with the miRCURY RNA Isolation Kit – Cell & Plant (EXIQON) using the lysate preparation from cultured animal cells protocol and the total RNA purification from all types of samples with small modifications. SEV lysis was performed with lysis buffer (700 µL lysis solution + 7 µL β-mercaptoethanol) by vortexing for 1 min. Then ethanol (600 µL) was added to the lysate and samples were transferred to columns (600 µL at a time). Samples were centrifuged at 14.000 g for 1 min and washed with 600 µL of washing solution 3 times. RNA was eluted on elution buffer (25 µL) by centrifuging 2 min at 200 g followed by a centrifugation at 14.000 g for 1 min. RNA was quantified in a NanoDrop ND-1000 spectrophotometer (NanoDrop Technologies, Inc., USA) at 260 nm.

Quality control of RNA. For RNASeq analysis the quantity and quality of total RNA (2 samples) and small RNA (4 samples) were assessed using the RNA 6000 Pico kit and the Small RNA kit in the Agilent 2100 Bioanalyzer (Agilent Technologies), respectively.

cDNA library preparation. Whole Transcriptome (WT) library was prepared for 2 samples and Small RNA libraries for the 4 samples, has described by Ion Total RNA-Seq Kit v2 User Guide (Life Technologies). All procedures were carried out according to manufacturer's instructions, except the RNA fragmentation step that was skipped in the preparation of the whole transcriptome libraries since the starting material was already of the required length. Briefly, 2.1-8.4 ng of small RNA were used to construct the small libraries and 20 ng of total

RNA for the WT libraries. RNA adaptors were ligated at 16ºC for 16 h to small and at 30ºC for 1 h to WT libraries. The first and second cDNA strands were synthesized, and purified cDNA was then amplified with specific barcoded primers by PCR and the resulting fragments selected for the correct size with magnetic beads. The cDNA libraries were quantified and their quality assessed with the Agilent High Sensitivity DNA Kit for WT RNA libraries and the Agilent DNA 1000 kit for small libraries in the 2100 Bioanalyzer (Agilent Technologies). Two pools of barcoded libraries (WT and small RNA) were prepared and clonally amplified by emulsion PCR using the Ion PI Template OT2 200 kit v2 and the Ion OneTouch 2 System (Life Technologies), and the positive Ion Sphere Particles enriched in the Ion OneTouch ES machine (Life Technologies). Finally, the positive spheres were loaded into a single Ion PI chip v2 and sequenced in the Ion Proton System (Life Technologies) at Genoinseq (Cantanhede, Portugal). All procedures were carried out according to manufacturer's instructions.

Analyses. Ion Proton adapter sequences and low-quality bases were trimmed using the Torrent Suite software (Life Technologies). Sequence reads were then filtered by length, where reads with less than 15 bp were removed from the small library and 18 bp for the large library. Next, rRNA (ribosomal RNA), tRNA (transfer RNA), miRNA (micro RNA), mRNA (messenger RNA) and ncRNA (non-coding RNA) were identified by aligning the reads from each sample to their specific libraries (rRNA: 5S - NR_023379.1, 5.8S - NR_003285.2, 18S - NR_003286.2, 28S - NR_003287.2; tRNA: library of tRNA extracted from UCSC; microRNA: mirbase; mRNA: CDS library from Ensembl; ncRNA library from Ensembl and ENCODE) using TMAP version 4.1 (Life Technologies). The eXpress software (Roberts and Pachter, 2013) was then used to count the number of total reads (reads that aligned in one or more transcripts) and unique reads (reads that aligned in only one transcript) per transcript in each library. In addition, the number of scaRNA (small cajal body-specific RNA), snRNA (small nuclear RNA) and snoRNA (small nucleolar RNA) comprised in the Ensembl ncRNA library was also calculated. The total number of reads for each microRNA (miR) identified was considered, in a total of approximately 400.000 reads per sample. The identified miRs presenting above 20 counts were considered valid. Clustering analysis of RNASeq data was performed with Cluster 3.0 software and the resulting heatmap and hierarchical clustering tree were obtained and visualized using the TreeView v1.1.6 program. All the miR with more than 20 reads in all samples were considered for clustering analysis.

Validation of miRNA expression by qRT-PCR. The expression of the 15 most expressed microRNAs, as determined by the RNASeq data was confirmed by qRT-PCR in RNA samples extracted from SEVs of 10 different donors. After isolation of total RNA of SEVs a cDNA library was constructed with the NCode™ miRNA First-Strand cDNA Synthesis and qRT-PCR Kit (Invitrogen™, Life Technologies, Carlsbad, California, USA). First, all the miRNAs in the samples (30 ng of total RNA) were polyadenylated using poly A polymerase and ATP. Following the polyadenylation, the tailed miRNA population was used to synthetize the cDNA library with SuperScriptR III RT and a Universal RT Primer. Specific primers for each microRNA were designed accordingly to NCode kit instructions and RNU6 was used as endogenous control (Supplementary Table II). PCR was performed using the Fluidigm Flex Six™ Gene Expression IFC in the BioMark™ System (Fluidigm Corporation, South San Francisco, CA, USA), following the manufacturer's instructions, using specific forward primers for microRNAs and RNU6 and the universal reverse primer of NCode cDNA kit. The data was analyzed with Real-Time PCR Analysis Software in the Biomark instrument (Fluidigm Corporation, CA) and relative expression of each microRNA was determined by the ΔCt method.

Cell culture

Human umbilical vein endothelial cells (HUVECs, Lonza, Switzerland; between passage 3 and 7), normal dermal human fibroblasts (NDHF, Lonza, Switzerland; between passage 5 and 11) and human spontaneously transformed keratinocytes (HaCaT, Cell lines services, Germany; between passage 37 and 42) were used to investigate the bioactive effects of SEVs. Endothelial cells were cultured in EGM-2 (Lonza) with all the factors and 2% FBS, fibroblasts and keratinocytes were cultured in DMEM (Invitrogen) with 0.5% Pen Strep and 10% FBS. Starvation media was EBM-2 with gentamicin and amphotericin for endothelial cells and DMEM with Pen Strep for fibroblasts and keratinocytes. When cells were treated with SEVs, the cell culture media used to dilute the SEVs for transfection was centrifuged overnight at 100.000 g and filtered (0.2 µm pore) in order to deplete SEVs from FBS (SEV-depleted media). In case of endothelial cells, SEV-depleted media was obtained by ultracentrifugation of EGM2 medium prepared without VEGF.

Cell transfection

For miR-150-5p in vitro bioactivity evaluation, cells were transfected with miR-150-5p (25 nM, miRIDIAN microRNA Human hsa-miR-150-5p mimic MIMAT0000082, Dharmacon) and lipofectamine® RNAiMAX transfection reagent (Invitrogen™) in 100 µL of complete medium without antibiotics. Cells transfected with lipofectamine were used as negative controls. In siRNA in vitro assays, cells were transfected with 100 nM of specific siRNAs for MYB, BAK1 and SHMT2 genes (hs.Ri.MYB.13.1, hs.Ri.BAK1.13.1, hs.Ri.SHMT2.13.1 - Custom DicerSubstrate siRNA, IDT - Integrated DNA Technologies) or a negative control siRNA (MISSION® siRNA Universal Negative Control #1, Sigma-Aldrich) in lipofectamine® RNAiMAX. Vascular endothelial growth factor (VEGF, 50 ng/mL, PeproTech) and platelet derived growth factor (PDGF-BB, 50 ng/mL, PeproTech) were used as positive controls for the in vitro bioactivity assays.

Cytotoxicity analyses

Endothelial cells (1×10^4), fibroblasts (5×10^3) and keratinocytes (2×10^4) were cultured in 96 well plates for 20 h, washed with PBS and incubated with exo-depleted medium either alone (100 µL) or supplemented with SEVs (2, 5 or 10 µg/mL). After 4 h, additional exo-depleted medium was added (100 µL) and cells were incubated for more 18-20 h. At the end, the media was changed and cells were incubated in control conditions (exo-depleted full media) for 72 h. Cells were photographed (IN Cell, GE Healthcare) and cell death was determined by Hoechst/ PI staining.

SEV internalization studies: labelling of SEVs

For skin cell internalization studies, SEVs were labelled with NBD-DPPE, PKH-67 or Syto® RNASelect™. PKH-67 labelling was performed to track SEVs by confocal microscopy. PKH67 (1 µL, 1 mM) was added to SEVs (65 µL, 50 µg/mL), incubated for 3 min at room temperature, followed by purification with an exosome spin column (Invitrogen). NBD-DPPE or Syto® RNASelect™ labelling was performed to track SEVs by high-content microscopy and flow cytometry. NBD-DPPE (1 µL) or Syto® RNASelect™ (1 µL) were added to SEVs (100 µL, at a

concentration of 60 to 70 µg/mL of protein) to a final concentration of 16 µM and 10 µM, respectively. The final mixture containing the dye and the SEVs was incubated during 30 min at 37ºC. After blocking the reaction with 1% of BSA the SEVs were washed with 6 mL of PBS and the free dye was removed by ultracentrifugation at 100.000 g for 1 h. The labelled SEVs were resuspended in PBS (100 µL). This procedure was always performed with freshly prepared SEVs which were used immediately after labelling.

SEV internalization studies: flow cytometry analyses

Endothelial cells ($8\times10_4$ per well), fibroblasts (5×10^4) and keratinocytes (16×10^4) were cultured in a 24 well-plate for 18-24 h, after which they were incubated with NBD-DPPE labeled SEVs for 4 h in starvation (0% FBS), at final concentrations of 1, 2 and 3 µg/mL. At the end, cells were washed with PBS, detached with trypsin (HUVEC and NDHF) or trypLE™ Express (HaCaT), washed twice in PBS and analyzed by flow cytometry. The percentage of skin cells with internalized SEVs was obtained by the ratio between positive cells versus total number of cells.

SEV internalization studies: confocal microscopy analyses

HUVECs (1×10^4 cells per well) were seeded in an IBIDI™ µ-slide angiogenesis plate and left to adhere for 24 h. Then, cells were incubated for 4 h or 24 h with PKH-67 labelled SEVs (5 µg/mL) in exo-depleted medium. After incubation, cells were washed and incubated with lysotracker® red DND-99 (100 nM) for 30 min. Afterwards, cells were washed with PBS and fixed in 4% PFA. In order to stain the cell membrane, samples were first blocked with 1% BSA for 1 h and then incubated with primary antibody mouse anti human CD31 (1:50, Dako) for 1 h, followed by incubation with secondary antibody Alexa fluor-633 anti-mouse (1:1000, Invitrogen). Finally, nuclei were stained with DAPI and cells were imaged using a Zeiss LSM 710 confocal scanning equipment, with the excitation wavelengths of, 405, 488 and 633 and a Plan-Apochromat 40×/1.4 oil immersion objective. Cell fluorescence and colocalization between SEVs and lysotracker red were quantified using ImageJ.

SEV internalization studies: high content microscopy analyses

Endothelial cells (1×10^4 per well), fibroblasts (5×10^3 per well) and keratinocytes (5×10^3 per well) were cultured for 24 h in an ibidi ™ µ-slide angiogenesis plate. The Syto® RNASelect™ labeled SEVs (1-20 µg/mL) were added to confluent cells in exo-depleted medium for the time of the experiment. Images were taken by a GE Healthcare™ InCell 2200 Analyzer imaging system, using a 40× objective, excitation wavelengths of 405 and 488 nm, at times 2, 4, 16, and 24 h. The analysis of the images was done using a In Cell Investigator package where we were able to define the cell and the nuclear mask and recovering the fluorescence of the cytoplasm using the equation $Cytoplasm_{Intensity} = (Cell_{Intensity} - Nucleus_{Intensity}) / (Cell_{Area} - Nucleus_{Area})$.

SEV bioactive assay: cell proliferation assay

Endothelial cells (2.5×10^3 per well), fibroblasts (1×10^3 per well) or keratinocytes (1×10^3 per well) were cultured in 96 well plates for 20 h and then stained with Hoechst (1 µg/mL, 33342, Sigma-Aldrich) for 15 min, washed with PBS, and finally incubated with exo-depleted

medium either alone (100 µL) or supplemented with SEVs (1, 2 or 3 µg/mL). After 4 h, additional exodepleted medium (100 µL) was added and cells were incubated for 18-20 h. Then, cell culture medium was changed and cells incubated (37ºC, 5% CO2, 0.1% O2) with exo-depleted medium (200 µL) for 72 h. At 48 h, Hoechst (0.25 µg/mL) was added to the cells to reinforce the 9 staining. Cells were photographed (IN Cell, GE Healthcare) and cell number was obtained by counting cell nuclei. Proliferation was calculated as percentage of control at 72 h after treatment ((Total cells $_{\text{treatment group}}$ / Total cells $_{\text{control group}}$) × 100%). For miR-150-5p (25 nM) and siRNA (100 nM) assays the protocol was similar; however, the complex was formed with lipofectamine in basal medium (without FBS or antibiotics) and cells were transfected in free-antibiotic cell culture medium.

SEV bioactive assay: cell survival assay

Endothelial cells (1×10^4 per well), fibroblasts (5×10^3 per well) and keratinocytes (2×10^4 per well) were cultured in 96 plates. After 20 h, cells were washed with PBS and incubated with exo-depleted medium (100 µL) either alone or supplemented with SEVs (1, 2, 3 or 5 µg/mL). To evaluate the contribution of miRNAs on vesicle bioactivity, ATA (6.25 µM) was added with SEVs to cells[3,4]. After 48 h, cells were incubated in ischemia conditions (starvation media, 0.1% O2, 5% CO2, 37ºC) for 48 h for endothelial cells and keratinocytes, or 72 h for fibroblasts. At the end, cell viability was quantified by Hoechst/ PI staining using a high-content microscope. Cell survival was calculated according to the following equation: ((Live cells $_{\text{treatment group}}$ – Live cells $_{\text{control group}}$) / Live cells $_{\text{control group}}$) × 100%. For miR-150-5p (25 nM) assay the protocol was similar; however, the complex was formed with lipofectamine in basal medium (without FBS or antibiotics) and cells were transfected in free-antibiotic cell culture medium.

SEV bioactive assay: cell scratch assay

Fibroblasts (1×10^3) and keratinocytes (2×10^4) were seeded in 96 plates until confluency. Then a vertical scratch was made in the middle of the well with a pipette tip. Cells were washed with PBS and cultured in exo-depleted medium (100 µL, DMEM with 0.5% FBS) either alone or supplemented with SEVs (1, 2 or 3 µg/mL). Additional exo-depleted medium (100 µL) was added after 4 h followed by cell culture for 18-20 h. At the end, cell media was changed to exodepleted medium alone and cells were incubated at 37ºC, 5% CO2, 0.1% O2 for 48 h. Pictures of the wells were taken immediately after scratch (time zero - T0) and 48 h (T48) later by a high content microscope. Wound area was measured by a AxioVision software 4.6.3 (Carl Zeiss Imaging Solutions GmbH) and the percentage of area closed calculated by the ratio between T48 and T0 scratch areas. For miR-150-5p (25 nM) assay the protocol was similar; however, the complex was formed with lipofectamine in basal medium (without FBS or antibiotics) and cells were transfected in free-antibiotic cell culture medium

SEV bioactive assay: impact in cell phenotype

Endothelial cells (50.000 cells/well, 24 well plate) were cultured in the presence or absence of SEVs (10 µg/mL) for 24 h, washed and then cultured for 72 h. Cells were then harvested with trypLE™ Express and resuspended in PBS/0.5% BSA (100 µL). They were then incubated for 30 min on ice with a specific antibody, washed twice, resuspended in PBS/0.5% BSA (300 µL) and cell labeling for specific epitopes (Supplementary Table I) monitored by a BD AccuriTM C6 (BD Biosciences). When needed, cells were fixated with 1% PFA and

permeabilized with TRITON X-100 (0.1%) before incubation with specific antibody. When a secondary antibody was used, cells were washed after primary antibody incubation and incubated on ice for 30 min with respective secondary antibody prior to flow cytometry analysis. The transcripts of endothelial gene markers were also analyzed upon SEVs treatment of endothelial cell phenotype (Supplementary Table II). Relative gene expression was calculated by the ΔCt method using GAPDH expression as control.

Hydrogel synthesis: purification of *2-carboxyethyl acrylate oligomers*

Anhydrous 2-carboxyethyl acrylate oligomers (6.5 g, n=0-3, Aldrich, Ref. 407585, average MW~170) were separated by gravity chromatography (silica, AcOEt/Hex: 0 → 30%). Right after purification, fractions were collected and analyzed by HPLC-MS (Agilent 1100, Zorbax 3.5μm 3×150mm column, H2O/CH3CN: 5 → 95%). Desired fraction, n=3, was dried under vacuum to get a transparent oil (0.7 g), confirmed by NMR as the desired product. 1H NMR 11 (400 MHz, CDCl3): δ 6.39 (d, J = 17.3 Hz, 1H, –CH=CH2), 6.12-6.06 (dd, 1H, –CH=CH2), 5.83 (d, J = 10.4 Hz, 1H, –CH=CH2), 4.41-4.35 (m, 6H, –OCH2–CH2–), 2.71-2.64 (m, 6H, –OCH2–CH2–).

Hydrogel synthesis: *synthesis of the photo-crosslinker linker (PCL)*

Purified 3-((3-((3-(acryloyloxy)propanoyl)oxy)propanoyl)oxy)propanoic acid (2-Carboxyethyl acrylate n=3, 0.5 mL, 1.0 equiv.) was solubilized in dichloromethane (10 mL, Fisher Chemical) under nitrogen atmosphere and dimethylformamide (0.15 mL). Then, thionyl chloride (0.50 mL, 2.0 equiv., Acros Organics) was added dropwise at 0 ºC, under vigorous stirring and by using a dropping funnel. After 1 h of reaction water-bath was removed and reaction was stirred overnight at room temperature (15 h reaction time). Solvent was then evaporated and compound was dried under vacuum. Then, the resulting crude was solubilized in (distilled) dichloromethane (3 mL) and added dropwise under nitrogen atmosphere to a previously prepared cooled (0 ºC) solution of (2-nitro-1,3-phenylene) dimethanol (0.25 g, 0.4 equiv., ARCH Bioscience) and N,N-diisopropylethylamine (0.12 mL, 0.2 equiv, Sigma-Aldrich) in (distilled) dichloromethane (5 mL) over 20 min. Reaction was then left to reach room temperature overnight. Finally, double distilled water (5 mL) was added to the reaction crude and the reaction product extracted with ethyl acetate (3 × 5 mL, Fisher Chemical). The corresponding organic fractions were dried with magnesium sulfate, filtered and solvent was evaporated under reduced pressure. Reaction crude was purified by gravity chromatography (silica, AcOEt/Hex: 0 → 60%), to obtain the photo-cleavable linker as brown oil (yield 54%). 1H NMR (400 MHz, CDCl3): δ 7.53 (m, 3H, ArH), 6.39 (d, J = 16.9 Hz, 2H, –CH=CH2), 6.19- 6.03 (dd, 2H, –CH=CH2), 5.84 (d, J = 10.4 Hz, 2H, –CH=CH2), 5.25 (s, 4H, ArCH2O–), 4.45- 4.31 (m, 12H, –OCH2–CH2–), 2.77-2.62 (m, 12H, –OCH2–CH2–).

Hydrogel synthesis: *thiolation of hyaluronic acid (HA)*

HA (0.2 g, 180 kDa, Bioiberica) was dissolved in ultra-pure deionized water (10 mL) to obtain a final 2% (w/v) polymer solution. The pH of the reaction mixture was adjusted to 5.5 by the addition of 0.1 M HCl. Afterwards, EDC and NHS (both from Sigma-Aldrich) were added to the polymer reaction mixture at a final concentration of 112 mM (2:1 molar ratio (EDC/NHS):cysteine). The pH was readjusted to 5.5 and the reaction mixture was stirred for 20 min at a room temperature. Then, L-cysteine ethyl ester hydrochloride (0.2 g, SigmaAldrich)

was added and the pH was increased to 6.0. The reaction mixture proceeded for 4-6 h at room temperature, under nitrogen environment and protected from direct light exposure. The resulting conjugate was dialyzed in a dialysis membrane (molecular weight cutoff 12 kDa) at 4 12 ºC, three times against a pre-cooled 1% (w/v) NaCl (Applichem) solution and finally against demineralized water. After 48 h of dialysis, the thiol-conjugated hyaluronic acid was lyophilized for two days and stored at -20 ºC until further use.

Hydrogel synthesis. *conjugation of SEVs with PCL*

The free thiol groups concentration in SEVs was 2.4±0.5 nM per 1 μg of vesicles, as determined by a Thiol Fluorescent Probe IV (20 μM, Calbiochem - Merck Millipore, calibration curve was against L-cysteine ethyl ester hydrochloride). Initially, the photo-cleavable linker (1% v/v) was allowed to react for ~10 min with free thiol groups present on the SEVs surface (free thiol 1:5 acrylate, molar ratio). To assess the presence of acrylate groups on the SEV surface, SEVs or SEVs-PCL (16 μg) were conjugated with Exosome-Human CD9 Flow Detection Beads (Invitrogen) and then reacted with FAM-thiol (molar ratio 1:20, PCL:FAM-thiol). Finally, the beads conjugated with SEVs were analyzed by flow cytometry.

H**ydrogel synthesis. *formation of hydrogel***

The thiolated-HA was dissolved in a solution containing the acrylate-surface modified SEVs to give a final 5% (w/v) polymer solution. The reaction between free acrylate groups present in the SEVs and the thiol of the HA was allowed to occur for at least 10 min, with vortex cycles, after which we added more free acrylate groups to give a final acrylate to thiol ratio of 1:1. The final reaction solution was allowed to crosslink for 1 h at 37 ºC.

Hydrogel characterization: NMR analyses

The 1H NMR spectra were acquired on a Bruker Avance III 400 MHz spectrometer. All solutions were prepared in D2O.

Hydrogel characterization: rheology analyses

The oscillatory shear measurements of the elastic (G’) and viscous (G’’) modulus were obtained at 37 ºC in a Haake Mars III Rheometer with a peltier thermostatic system, using a 35 mm titanium plate and a gap of 0.1 mm. The G’ and G’’ of several samples gel was determined with an oscillation frequency of 0.1 Hz and a stress of 10 Pa. The stability of the hydrogel was performed post its gelation point (45 min, 37 ºC) and after its immersion in water (swollen hydrogel) during 96 h. The G’ and G’’ of the swollen hydrogel post-crosslinking were measured at an oscillation frequency of 0.1 Hz and a stress of 10 Pa.

Hydrogel characterization: FTIR analyses

The vibrational analysis of the samples was performed by a Frontier spectrophotometer from Perkin Elmer (FT-NIR/MIR) equipped with a FR-DTGS detector. Lyophilized sample (5 mg) was mixed in a potassium bromide disk and the spectra were obtained at room temperature from 4000-400 cm^{-1}.

Hydrogel characterization: swelling analyses

The swelling ratio of the hydrogel was determined by immersion in phosphate buffer for 24h, after which the hydrogel was weighted obtaining the mass of the swollen gel (Ws). The hydrogel was then dried and its mass was determined by weighing (Wd). The swelling ratio was calculated from $SR= (W_s - W_d)/ W_d$.

Hydrogel characterization: in vitro release of SEVs from the hydrogel

SEVs (100 µg) where labeled with Syto® RNASelect™ before gel formation. The hydrogel was placed in the top compartment of a transwell system (Corning) and activated by a blue laser (405 nm, 80 mW) for 2 min followed by 45 min of agitation. This procedure was repeated 5 times. The fluorescence was measured from an aliquot withdraw from the bottom of the transwell, collected 45 min after each irradiation and measured using a fluorimeter (λ_{ex}: 490 nm, λ_{em}: 530 nm). Non-irradiated hydrogel was used as negative control. The experiment was performed in 4 hydrogels and the measurement performed in triplicate.

Bioactivity evaluation of SEVs released from the hydrogel

As before, SEVs (100 µg) were conjugated with a photo-cleavable linker and then reacted with thiolated hyaluronic acid to form a hydrogel. The hydrogel (50 µL) was prepared in the top of a transwell system and incubated for 45-60 min at 37ºC. The bottom (1 mL) and the top (200 µL) of the transwell was filled with exo-depleted DMEM containing 10% FBS. The hydrogel was irradiated (blue laser) 5 times for 2 min followed by 45 min of agitation and the supernatant of the bottom of the transwell collected and incubated for 24 h with keratinocytes (2.5×103 / well), that were seeded in a 96 well plate the day before. The media was then changed to full media and cell number quantified after 3 days by staining cell nuclei with Hoechst and monitoring the fluorescence by a high content microscope (In Cell analyzer 2200). The bottom of a transwell containing a hydrogel without SEVs and irradiated by a blue laser was used as a negative control. The experiment was performed with SEVs from 3 different donors.

Animal testing: animal model

Animal testing protocols were approved by the Portuguese National Authority for Animal Health (DGAV), and all the surgical and necropsy procedures were performed according to the applicable national regulations respecting international animal welfare rules. Male C57BL/6 wild-type mice (8-10 week-old), purchased from Charles River (France) and weighing between 20 and 30 g, were housed in a conventional animal facility on a 12 h light/12 h dark regimen and fed a regular chow ad libitum. Diabetes mellitus was induced in mice by consecutive intraperitoneal injection of streptozotocin (50 mg/kg; in citrate buffer, pH 4.5; STZ, SigmaAldrich).. An intraperitoneal injection was given once a day during 5 consecutive days. Glycemia was monitored weekly after STZ treatment with an Accu-Chek Aviva glucometer (Roche Diagnostics, Germany) with respective glucose test strips (Accu-Chek Aviva, Roche) and only animals with blood glucose levels greater than 300 mg/dL were used in this study (6- 8 weeks after induction). Insulin (16-32 U/Kg or 0.4-0.8 U/mouse, Sigma-Aldrich) was injected for weight maintenance, if necessary. To induce wounds animals were anesthetized with an

intramuscular injection of a xylazine /ketamine solution (ketamine hydrochloride, 10 mg/mL, (Imalgene®, Merial, Barcelona, Spain), 50 mg/kg of body weight, and xylazine hydrochloride, 2 mg/mL, (Rompun®, Bayer Healthcare, Germany), 10 mg/kg of body weight). Animals were then shaved, and the dorsum was disinfected with a povidone-iodine solution (Betadine®). Two 6 mm diameter full-thickness excision wounds were performed 5 cm apart with a sterile biopsy punch in the dorsum of each animal. The treatments were topically applied immediately after wound induction and were repeated as indicated. Animals were kept in individual cages with food and water ad libitum, and they were observed daily during the total period of the experiment.

Animal testing: wound treatment and healing monitoring

The animals were divided into different groups accordingly to the treatment applied (Supplementary Table III). SEVs were applied topically in the wound bead, as a single application after wound induction (day 0), twice a day until complete healing (closure) or in a single application conjugated with hyaluronic acid. For treatment with miR-150-5p, a single dose of miR-150-5p (5 μM), complexed with DharmaFECT 1 (120 μL) siRNA transfection reagent (Dharmacon, Lafayette, Colorado, EUA), was subcutaneously injected in the wound edge (2 × 40 μL) immediately after wound induction. A scramble miR (microRNA Mimic 15 Negative Control, Dharmacon, Lafayette, Colorado, EUA) and PBS were used as negative controls. Animals were kept in individual cages with food and water ad libitum. The progress of wound closure was monitored daily by measuring the size of the wound area. The wound area was measured by ImageJ software (NIH). The percentage of wound area was presented as percentage of original wound (day 0) and calculated following the equation: (area of actual wound / area of original wound) × 100%. Wounds were considered completely closed when the area at a particular time point was zero.

Animal testing: histological analyses of excised wounds

Animals were sacrificed five and ten days post-wounding and 10 mm-diameter skin biopsy specimens, centered on the wound bed and comprising the wound margins, were collected and processed for routine histology. Skin samples were fixed in 10% neutral buffered formalin, trimmed longitudinally in the direction of the hair flow and centered on the wound, embedded in paraffin, sectioned at 4 μm, and stained with hematoxylin and eosin. Qualitative histological analysis was performed by a pathologist blinded to experimental groups, according to a numerical score (Supplementary Table IV) and measurements were performed using NDP.view2 software coupled to a Nanozoomer SQ slide scanner (Hamamatsu).

Animal testing: quantification of vessel density

The number of vessels was quantified at days 5 and 10 post wound excision using CD31-stained skin samples. Briefly, after deparaffinization and rehydration procedure of skin tissue sections, heat mediated antigen retrieval was performed using citrate buffer at pH 6.0. Next, the sections were blocked with a solution containing BSA (1%) and serum (5%) for 30 min and incubated with primary antibody CD31 (1:100, Abcam, ab28364) overnight at 4ºC. Alexa fluor 647 goat anti-rabbit (1:800, Invitrogen) was used as secondary antibody and nuclei were stained with DAPI. Images were acquired using a Zeiss LSM 710 confocal scanning equipment. Quantification and measurement were performed in randomly selected five high-power fields

of four nonconsecutive tissue sections per time point and per animal within each group. Mean results of the number of vessels per slide are expressed as vessels density.

Animal testing: quantification of re-epithelization

The expression of keratin 5 and keratin 14 was quantified 5 days post-wounding by immunofluorescence. After deparaffinization and rehydration procedure, heat mediated antigen retrieval was performed using citrate buffer at pH 6.0. The samples were blocked for 1 h with BSA (5%) in PBS and then permeabilized with Triton X-100 (0.2%) for 10 min. After washing with PBS, the sections were incubated overnight at 4ºC with the primary antibodies diluted in 1% BSA (keratin 5 polyclonal chicken antibody 1:200; 905901, Biolegend; keratin 14 polyclonal rabbit antibody 1:1000; 905301, Biolegend). Alexa fluor-488 goat anti-chicken (1:500, Invitrogen) and Alexa fluor-633 goat anti-rabbit (1:500, Invitrogen) were used as secondary antibodies. Cell nuclei were stained with DAPI. Images were acquired using In Cell 2200 (GE Healthcare) microscope. Fluorescence intensity in the borders of the wound was quantified using Image J.

Animal testing: preparation of lipid-conjugated dyes for SEVs labeling

To perform the in vivo biodistribution and FRET assay, SEVs were labeled with 1,2-dipalmitoyl-sn-glycero-3-phosphoethanolamine (DPPE, Avanti Polar Lipids Inc.) conjugated with Cy5.5 or Cy7. The fluorescent lipid was synthesized by the reaction between the terminal amine of DPPE and the NHS of Cy5.5-NHS or Cy7-NHS (Lumiprobe). DPPE (43 µmoles) was dissolved in a solution of chloroform/ methanol (2:1), after which the dye (8.6 µmoles, 5 times less) was added and the reaction performed overnight at room temperature, under nitrogen environment and protected from direct light exposure. At the end, the solvent was evaporated and the reaction product dissolved in a mixture of chloroform/ methanol (9:1, 1 mL). The compound of interest was separated by column chromatography and confirmed by High Performance Liquid Chromatography (HPLC) in a Shimadzu SPD-20A with a UV/Vis photodiode array detector. The column used was a Zorbax ODS 4.6×250mm, 5 um and the solvent for elution was methanol/ chlorophorm (2/1) at 1 mL/min.

Animal testing: in vivo biodistribution of labeled SEVs

SEVs (100 µL, protein concentration between 180 and 250 µg/mL) were mixed with Cy7- DPPE (final concentration of 20 µM) and the mixture incubated at 37oC for 30 min. SEVs were then washed with PBS (6 mL), the free dye removed by ultracentrifugation at 100 000 xg for 1 h, and SEVs re-suspended in PBS to a final concentration of 200 µg/mL or 100 µg/mL, depending on the final application. Full-thickness wounds were created in the dorsum of C57BL/6 wild-type mice using the same protocol as described above. The wounds were treated with (i) SEVs in solution (10 µL, 2 µg of SEVs), (ii) hydrogel containing SEVs (2 µg) and (iii) hydrogel containing SEVs (2 µg) activated by light (2 min irradiation at day 0 + 1 min irradiation per day). The biodistribution was followed by acquisition of fluorescent images 17 (λex: 745nm, λem: 810-875nm) using the IVIS Imaging System (Xenogen Imaging Technologies, Alameda, CA). All quantification of fluorescence recovery from animal imaging is presented as radiant efficiency, which is the ratio of radiant flux to input electrical power. The data was analyzed by an IVIS software (Living Image Software for IVIS®, Caliper Life Sciences, Perkin Elmer).

Animal testing: in vivo SEV stability as measured by a FRET assay

SEVs were labeled with both CY5.5-DPPE and Cy7-DPPE. SEVs (100 µL, protein concentration between 180 and 250 µg/mL) were mixed with Cy7-DPPE (final concentration of 20 µM) and the mixture incubated at 37oC for 10 min. Next, Cy5.5-DPPE (final concentration of 10 µM) was added and incubated for additional 30 min at 37°C. At the end, SEVs were purified by exosome spin columns (MW3000, Invitrogen) and ressuspended to a final concentration of 200 µg/mL (for solution injection) or 100 µg/mL (for gel formulation). IVIS live-animal fluorescence imaging was employed for SEV tracking up to 48 h at the following fluorescent channels: donor (λex: 640 nm; λem: 695-770 nm); acceptor (λex: 745 nm; λem: 810-875nm); FRET (λex: 640 nm; λem: 810-875nm). FRET efficiency was calculated as the ratio of signal collected from the FRET channel (λex: 640 nm; λem: 810-875nm) to the one obtained at the donor channel (λex: 640 nm; λem: 695-770 nm). This value was obtained from the Living Image Software for IVIS following region of interest identification of the fluorescence desired for quantification. Images presented in panel format were normalized against a "pre" image from which the minimum and maximum values for radiant efficiency were set to visualize this change in fluorescence following the treatment with SEVs.

Animal testing: skin miRNA expression analyses

The expression of miRs was evaluated in animal skin samples (Supplementary Table II). MirX TM miRNA first-strand synthesis kit (Clontech Laboratories, Inc. Takara Bio, Montain View, California, USA) was used to synthetize cDNA library, accordingly to the manufacturer's instructions. Briefly, total RNA (3.75 µL, 125-250 ng) was mixed with mRQ enzyme (1.25 µL) in mRQ buffer (5 µL) and incubated for 1 h at 37ºC, followed by enzyme inactivation at 85ºC for 5 min. cDNA samples were diluted (10 fold when 250 ng of initial RNA was used) prior to PCR analysis. PCR was performed using the Fluidigm 48.48 Dynamic Array™ IFC for Gene Expression in the BioMark™ System (Fluidigm Corporation, South San Francisco, CA, USA), following the manufacturer's instructions, with specific forward primers for each microRNA and RNU6, and the universal reverse primer from Mir-X ™ kit (Supplementary Table II). The data was analyzed with Real-Time PCR Analysis Software in the Biomark instrument (Fluidigm Corporation, CA) and relative microRNA expression was determined by the ΔCt method.

Evaluation of miR-150-5p expression in skin cells by qRT-PCR analyses

The level of miR-150-5p in skin cells including endothelial cells, keratinocytes and fibroblasts, upon transfection and SEVs treatment was evaluated by qRT-PCR. Cells were lysed 24 h after transfection and total RNA (125 ng) was extracted followed of polyadenylation and cDNA library construction with Mir-X ™ kit, as described previously. Specific amplification of mature miR-150-5p and RNU6 was performed in diluted (5 fold) cDNA samples with fluorescent dye SYBR green (NZYTech, Lda. – Genes and Enzymes, Lisboa, Portugal) and specific forward primer (Supplementary Table II) and universal reverse primer (mRQ 3' primer from Mir-X TM kit) in the 7500 Fast Real Time PCR System (Applied Biosystems). Briefly, cDNA (2 µL) was mixed with NZYtech SYBR green (12.5 µL) and each primer (0.5 µL, 10 µM) and water to a final volume of 25 µL. Samples were denaturated at 95ºC for 2 min, followed by 40 cycles at 95ºC 5 sec and 60ºC for 30 sec and melting curve program. The data was analyzed with RealTime PCR Analysis Software in the 7500 Fast Real Time PCR System (Applied Biosystems).

The increase in miR-150-5p expression determined by the ΔΔCt method using RNU6 as housekeeping and non-treated cells as control.

Evaluation of miR-150-5p targets and putative interaction

Ten possible gene targets of miR-150-5p (Supplementary Table II), likely involved in cell survival, proliferation and migration, were evaluated. A putative direct interaction between miR-150-5p and these targets was evaluated using TargetScan, DIANA MicroT-CDS and DIANA MR-microT. RNA was extracted from plated skin cells as described before and cDNA synthetized from total RNA (250 ng, 19.25 µL) with random hexamers (2.5 µL) using TaqMan reverse transcription reagents kit (Invitrogen), Buffer Taqman (5 µL) MgCl2 (11 µL), dNTPs (10 µL), RNAse inhibitor (1 µL) and reverse transcriptase (1.25 µL), according to the manufacturer's instructions, by incubation at 25ºC for 10 min followed by 30 min at 48ºC and then 5 min at 95ºC. Real-time PCR was performed using the fluorescent dye NZYTech SYBR green in the 7500 Fast Real Time PCR System (Applied Biosystems), with specific sets of primers designed by Sigma-Aldrich (Table VIII and Table IX). PCR was performed accordingly to the manufactures instructions, 2 µL of cDNA was mixed with 10 µL of NZYtech SYBR green and 0.8 µL of each primer (10 µM) and water to a final volume of 20 µL. PCR conditions and analysis were performed as describe earlier. The expression of c-MYB, BAK1 and SHMT2 described to be regulated by miR-150-5p was also evaluated in all 3 types of skin cells studied upon treatment with SEVs (Supplementary Table II). Relative gene expression was calculated by the ΔΔCt method using GAPDH as housekeeping gene and non-treated cells as control.

Immunocytochemistry analysis of c-MYB

Keratinocytes ($2.5x10^3$) were seeded in a 96 well plate and transfected, 20h later, with SEVs, miR-150-5p and siRNA-MYB for 24h. The media was changed and the levels of c-MYB evaluated by immunocytochemistry at 72h. Briefly, cells were washed with PBS and fixed with 4% PFA (04336, Alfa Aesar) for 10 minutes at room temperature. Washed with PBS, permeabilized with 1% Triton X-100 (HFH-10, Life technologies) for 15 minutes and blocked with BSA 1% (A4503, Sigma-Aldrich) for 30 min, room temperature. Washed with PBS and incubated with a primary antibody anti-c-MYB (mouse origin, D-7, sc-74512, Santa Cruz Biotechnology, Inc.), diluted 1:50 in antibody diluent (S3022, Dako) and 0.1% Triton X-100, over-night at 4ºC. Cells were washed again with PBS and incubated with secondary antibody Alexa fluor™ 555 goat anti-mouse (A21422, Invitrogen), 1:500 in antibody diluent and 0.1% Triton X-100, for 1 hour at room temperature. Finally, cells were washed with PBS and the nuclei stained with Dapi (D9542, Sigma-Aldrich), 1 minute at room temperature. Pictures were taken in InCell 2200 Analyzer imaging system, 40x objective. The level of c-MYB expression was calculated based on the specific fluorescence intensity ratio between nuclei and cytoplasm (c-MYB levels = (Intensity $_{nuclei}$/Intensity $_{cytoplasm}$)-1) × 100%).

Statistical analyses

Statistical analyses were performed by GraphPad Prism 6 software (GraphPad Software, Inc.).

Supplementary tables

Table Supp. I. Antibodies used for cells and SEVs characterization.

Marker	Origin	Catalog number	Dilution	Application
CD45	Mouse IgG1 (clone: J33)	A07782, Beckman Coulter	1:10	hUCBMNCs cells characterization by flow cytometry
CD34	Mouse IgG1 (clone 581)	A07776, Beckman Coulter	1:10	
7-AAD	n. a.	A07704, Beckman Coulter	1:10	
CD45	Mouse IgG2a (clone: 5B1)	130-080-202, MACS - Miltenyi Biotec	1:10	hUCBMNCs cells versus SEVs characterization by flow cytometry
HLA-DR	Mouse IgG1 (clone: MEM-12)	1F-474-T025, EXBIO	1:10	
CD9	Mouse IgG2b (clone: 209306)	FAB1880F, RD Systems	1:10	
CD81	Mouse IgG2b (clone: 454720)	FAB4615F, RD Systems	1:10	
TSG101	Mouse IgG2aκ (clone: C-2)	sc-7964, Santa Cruz Biotech.	1:10	
Propidium Iodide	n.a.	P4170, Sigma-Aldrich	1:10	
GAPDH	Rabbit monoclonal	14C10, Cell signaling	1:5000	hUCBMNCs cells versus SEVs characterization by western blot
CD63	Rabbit monoclonal	ab134045, abcam	1:500	
PECAM-1 / CD31	Mouse IgG1κ (clone: WM59)	11-0319-42, Thermo Scient., eBioscience	1:10	Endothelial cells characterization by flow cytometry
VEcad	Mouse IgG1 monoclonal	Sc-9981, Sta Cruz Biotechnology	1:10	
vWF	Rabbit polyclonal	A0082, Dako	1:10	

Table Supp. II. Sequences of the primers used for qRT-PCR.

#	Name	Forward Primer	Reverse primer
1	**hsa-mir-150-5p**	TCTCCCAACCCTTGTACC	Universal qPCR Primer of NCode cDNA kit or of Mir-X cDNA kit
2	**hsa-mir-16-5p**	TAGCAGCACGTAAATATTG	
3	**hsa-mir-142-3p**	TGTAGTGTTTCCTACTTTATGGA	
4	**hsa-mir-223-3p**	TGTCAGTTTGTCAAATACCC	
5	**hsa-let-7g-5p**	TGAGGTAGTAGTTTGTACAGTT	
6	**hsa-mir-21-5p**	TAGCTTATCAGACTGATGTTGA	
7	**hsa-let-7f-5p**	TGAGGTAGTAGATTGTATAGTT	
8	**hsa-mir-19b-3p**	TGTGCAAATCCATGCAAAA	
9	**hsa-let-7a-5p**	TGAGGTAGTAGGTTGTATAGTT	
10	**hsa-mir-26a-1-5p**	TTCAAGTAATCCAGGATAGGCT	
11	**hsa-mir-20a-5p**	TAAAGTGCTTATAGTGCAGGTAG	
12	**hsa-miR-181a-5p**	AACATTCAACGCTGTCGGG	
13	**hsa-miR-451a**	AAACCGTTACCATTACTGAGTT	
14	**hsa-miR-23a-3p**	ATCACATTGCCAGGGATT	
15	**hsa-miR-342-3p**	TCTCACACAGAAATCGCAC	
16	**RNU6**	ACACGCAAATTCGTGAAG	
17	***GAPDH***	AGCCACATCGCTCAGACACC	GTACTCAGCGCCAGCATCG
18	***PECAM1 / CD31***	AGATACTCTAGAACGGAAGG	CAGAGGTCTTGAAATACAGG
19	***CD34***	TGAAGCCTAGCCTGTCACCT	CGCACAGCTGGAGGTCTTAT
20	***vWF***	TGTATCTAGAAACTGAGGCTG	CCTTCTTGGGTCATAAAGTC
21	***CDH5 / VEcad***	CGCAATAGACAAGGACATAAC	TATCGTGATTATCCGTGAGG
22	***ENG / CD105***	CAAGTCTTGCAGAAACAGTC	TAGTGGTATATGTCACCTCG
23	***MCAM / CD146***	TAAGAGCGAACTTGTAGTTG	TCAGATCGATGTATTTCTCTCC
24	***KDR***	GTACATAGTTGTCGTTGTAGG	TCAATCCCCACATTTAGTTC
25	***BAK1***	CTATGACTCAGAGTTCCAGAC	AATTGATGCCACTCTCAAAC
26	***MYB***	CCGAATATTCTTACAAGCTCC	GGACCTGTTTTTAGGTACTG
27	***CDKN3***	GAAGAACTAAAGAGCTGTGG	TTCCATTATTTCACAGCAGC
28	***FADS1***	ATGATTACCTTCTACGTCCG	TCAATGTGCATGGGAATATG
29	***SHMT2***	CATTTGAGGACCGAATCAAC	CACCTGATACCAGTGAGTAG
30	***TDO2***	AAGAAAAAGAGGAACAGGTG	CACCTTTACTAAGGAGATGTTC
31	***INSIG1***	ACCCCACAAATTTAAGAGAG	TTCTGGAACGATCAAATGTC
32	***CD38***	CAGACCTGACAAGTTTCTTC	GATGACATAAACCACAAGGAG

Table Supp. III. *In vivo* treatment groups.

#	Groups	Animal model	Treatment
1	**WT - PBS**	C57BL/6 wild-type	PBS
2	**STZ - PBS**	C57BL/6, diabetic I, STZ-induced	PBS
3	**STZ - SEVs (0.4 µg)**	C57BL/6, diabetic I, STZ-induced	Single dose of 10 µL SEVs (0.4 µg) after wound creation
4	**STZ – SEVs (2 µg)**	C57BL/6, diabetic I, STZ-induced	Single dose of 10 µL SEVs (2 µg) after wound creation
5	**WT - SEVs (2X/day)**	C57BL/6 wild-type	Bi-daily doses of 10 µL SEVs (total: 0.4 µg/wound)
6	**STZ - SEVs (2X/day)**	C57BL/6, diabetic I, STZ-induced	Bi-daily doses of 10 µL SEVs (total: 0.4 µg/wound)
7	**Db/db - SEVs (2X/day)**	Db/db mice, diabetic II, genetic model	Bi-daily doses of 10 µL SEVs (total: 0.4 µg/wound)
8	**STZ - PDGF**	C57BL/6, diabetic I, STZ-induced	PDGF-BB, 100 µg/mL (PeproTech); 4 µg/cm^2; twice a day
9	**STZ - Gel + Light**	C57BL/6, diabetic I, STZ-induced	HA Gel plus irradiation of 2 min at day 0 followed by 1 min irradiation per day (λ laser: 405 nm)
10	**STZ - Gel + SEVs**	C57BL/6, diabetic I, STZ-induced	HA Gel with SEVs (2 µg), single application
11	**STZ - Gel + SEVs + Light**	C57BL/6, diabetic I, STZ-induced	HA Gel with SEVs (2 µg) plus irradiation of 2 min at day 0 followed by 1 min irradiation per day (λ laser: 405 nm).
12	**STZ - SEVs & Gel + Light**	C57BL/6, diabetic I, STZ-induced	HA Gel on top of SEVs (2 µg), irradiated for 2 min at day 0 followed by 1 min irradiation per day (λ laser: 405 nm).
13	**WT - miR-150-5p**	C57BL/6 wild-type	Single dose of mimic miR-150-5p (5 µM, Dharmacon), two injections (40 µL each) in the wound edge immediately after wound creation.

Table Supp. IV. Wound healing histopathological evaluation criteria**.**

Score	Microscopic observation	Description
1	**Inflammation**	inflammatory cell infiltration, neutrophil and macrophage rich
2	**Inflammation and tissue formation**	fibroblast proliferation and inflammatory cell infiltration, macrophage-rich with few neutrophils
3	**Tissue formation**	epithelialization, fibroblast proliferation and extracellular matrix reorganization
4	**Tissue remodeling**	remodeling and wound contraction
5	**Wound resolved**	wound resolved with hair re-growth

References

1 Pedroso, D. C.; Tellechea, A.; Moura, L.; Fidalgo-Carvalho, I.; Duarte, J.; Carvalho, E.; Ferreira, L., Improved Survival, Vascular Differentiation and Wound Healing Potential of Stem Cells Co-Cultured with Endothelial Cells. PLoS One 2011, 6, e16114.

2 Thery, C.; Amigorena, S.; Raposo, G.; Clayton, A., Isolation and Characterization of Exosomes from Cell Culture Supernatants and Biological Fluids. Curr Protoc Cell Biol 2006, Chapter 3, Unit 3 22.

3 Gray, W. D.; French, K. M.; Ghosh-Choudhary, S.; Maxwell, J. T.; Brown, M. E.; Platt, M. O.; Searles, C. D.; Davis, M. E., Identification of Therapeutic Covariant MicroRNA Clusters in HypoxiaTreated Cardiac Progenitor Cell Exosomes Using Systems Biology. Circ Res 2015, 116, 255-263.

4 Tan, G. S.; Chiu, C.-H.; Garchow, B. G.; Metzler, D.; Diamond, S. L.; Kiriakidou, M., Small Molecule Inhibition of RISC Loading. ACS Chem Biol 2012, 7, 403-410.

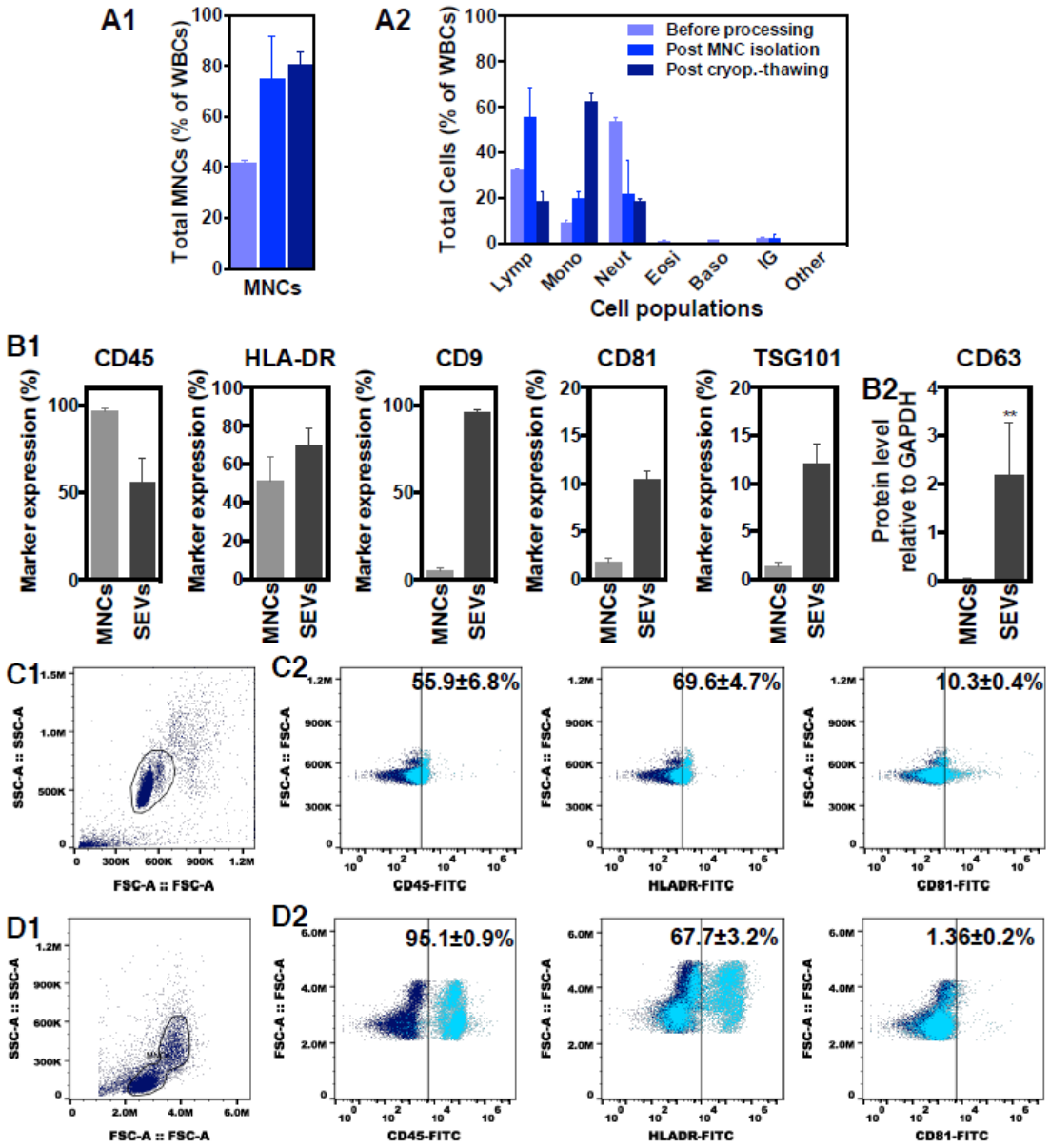

Figure S21- Characterisation of hUCBMNCs and SEVs secreted by these cells.

(A) hUBMNCs were isolated from umbilical cord by a density gradient. Isolated MNCs were cryopreserved until use. (A1) Percentage of MNCs before or after the density gradient separation (with or without cryopreservation), as analyzed by a haematological analyser. (A2) Impact of cell cryopreservation in the composition of MNCs (Lymp = Lymphocytes, Mono = Monocytes, Neut = Neutrophils, Eosi = Eosinophils, Baso = Basophils; IG = Imature Granulocytes and Other) relative to the total white blood cells (WBCs). In A1 and A2, results are average ± SEM, n=3. (B) Comparison of protein expression in SEVs and respective secreting cells (MNCs) as evaluated by flow cytometry (B1) and western blot (B2). Results are average ± SEM, n=4. Statistical analyses were performed by a Mann-Whitney test, $p<0.05$; **$p<0.01$; ***$p<0.001$. (C1) Scatter plot and gating of SEVs bounded to aldehyde-sulfate latex beads, as analysed by flow cytometry. (C2) Flow cytometry scatter plots for some of the proteins expressed in SEVs. Results are average ± SEM, n=4. (D1) Scatter plot and gating of hUCBMNCs, as analysed by flow cytometry. (D2) Flow cytometry scatter plots for some of the proteins expressed in hUCBMNCs. Results are average ± SEM, n=4.

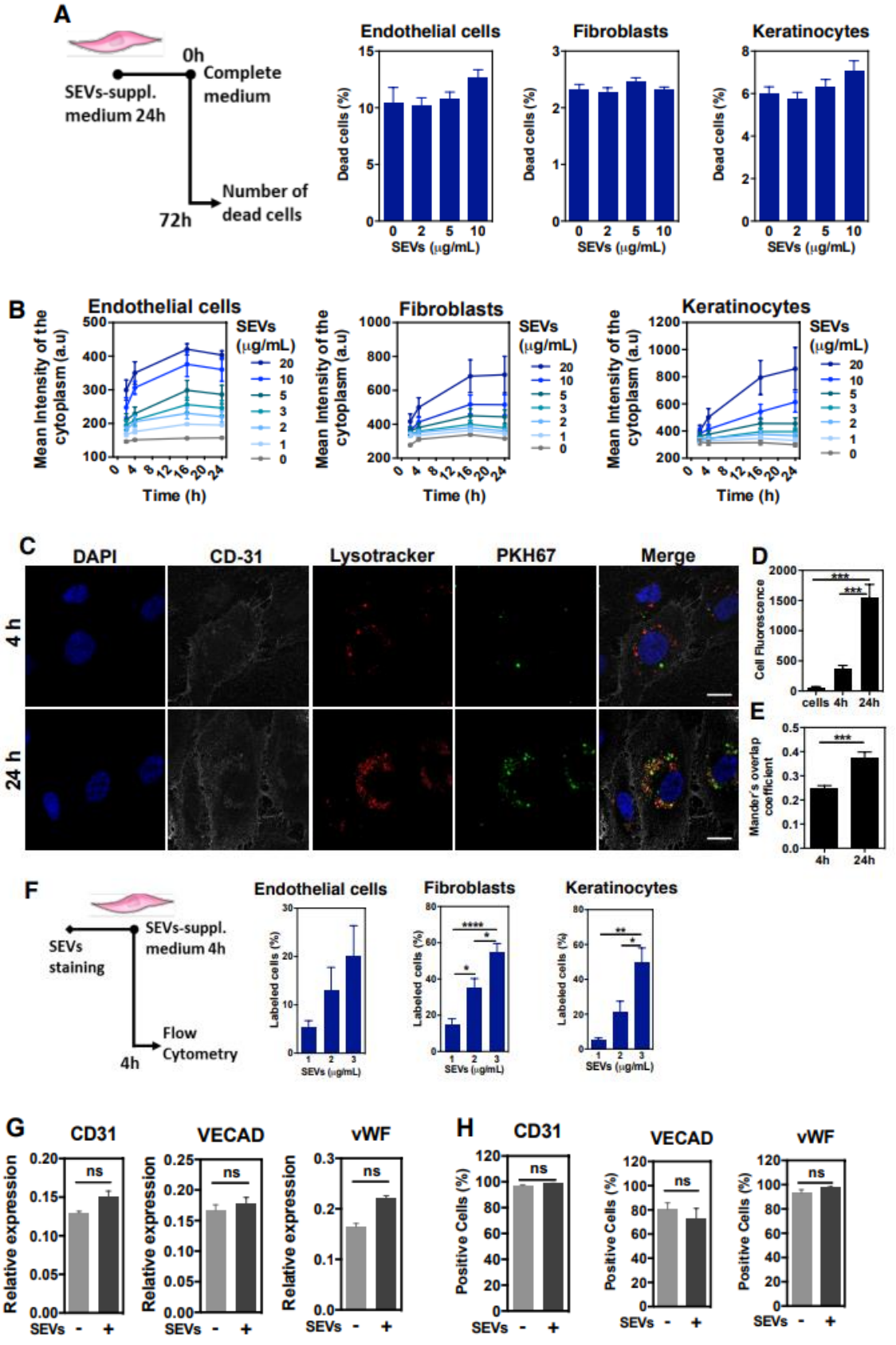

Figure S22- Cellular uptake and biological effect of SEVs.

(A) Cells were exposed to SEVs for 24 h and maintained in culture for 72 h. Cytotoxicity was evaluated by Hoechst/propidium iodide (PI) staining. Results are average ± SEM, n=3 different donors, 3 technical replicates per donor. Statistical analyses were performed by a Mann-Whitney test. (B) Cellular uptake of Syto® RNASelect™-labeled SEVs, as monitored by a high content microscope (mean intensity). Results

are average ± SEM, n=4. (C) Intracellular location of SEVs as confirmed by confocal microscopy. Endothelial cells were incubated with PKH67-labeled SEVs (5 µg/mL) for 4 or 24 h. Bar corresponds to 15 µm. (D) Quantification of PKH67 fluorescence within the cells (n=3, 5-6 images per replicate). (E) Colocalization between PKH67-labeled SEVs and lysotracker red, as expressed by the Mander´s overlap coefficient. A coefficient equal to 1 corresponds to 100% of colocalization. In D and E, results are average ± SEM, n=3. Statistical analyses were performed by a t-test or by a one-way ANOVA test followed by a Bonferroni's multiple comparisons test. (F) Cellular uptake of SEVs, as evaluated by flow cytometry. SEVs (3 µg/mL) were labeled with NBD-DPPE and incubated with cells for 4 h. Percentages of positive cells were calculated from gates defined from non-labeled cells. Results are average ± SEM, n=4-6. Statistical differences were evaluated by a Two Way Anova with a Tukey's post test. * p<0.05; **p<0.01; ***p<0.001. (G, H) Effect of SEVs in the gene and protein signature of endothelial cells. Endothelial cells were incubated with SEVs for 24 h and endothelial markers evaluated by qRT-PCR (G) and flow cytometry (H) at 72 h. Relative gene expression was calculated by the ΔCt method using GAPDH expression as control. The results are average ± SEM, n=3. Statistical analyses were performed by a MannWhitney test.

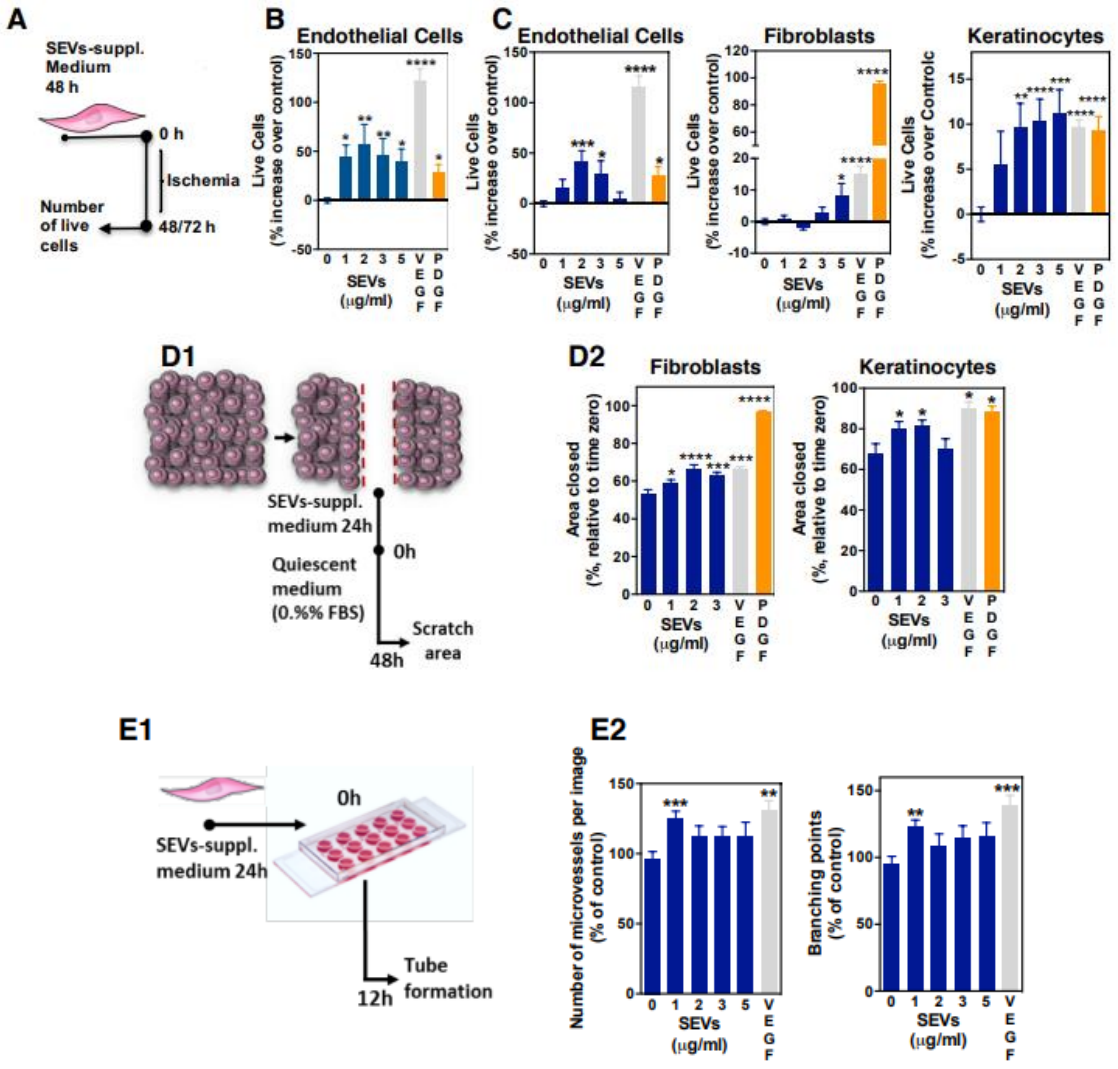

Figure S23- SEV bioactivity.

MNCs with or depleted from CD34+ cells were incubated for 18 h in hypoxic conditions, the conditioned medium collected and SEVs isolated by sequential centrifugation. (A) Schematic representation of survival assay. Skin cells were incubated with SEV-depleted medium alone or with SEVs for 48 h after which they were washed and cultured in ischemic conditions (0.1% O2), in starvation media for 48 h (endothelial and keratinocytes) or 72 h (fibroblasts). The viability of the cells was then monitored by a highcontent microscope using Hoescht/propidium iodide staining. (B) Survival of endothelial cells after

treatment with SEVs secreted by hUCBMNC containing CD34+ cells. (C) Survival of endothelial cells, fibroblasts and keratinocytes upon treatment with SEVs secreted by hUCBMNC without CD34+ cells. Vascular endothelial growth factor (VEGF, 50 ng/mL) and platelet derived growth factor (PDGF-BB, 50 ng/mL) were used as controls. The results are average ± SEM, n=3 different donors, 3 technical replicates per donor. (D1) Scratch assay. Keratinocytes or fibroblasts were cultured until confluence, after which a scratch was made. Cells were washed with PBS and SEV-depleted medium alone or with SEVs was added. Cells were cultured for 24 h. Afterwards, cell media was changed to SEV-depleted media alone and cells incubated for 48 h. Wound area was evaluated by a high-content microscope. (D2) Percentage of wound area closed. The results are average ± SEM, n=3. (E1) Tube formation assay. Endothelial cells were treated with SEVs for 24 h, trypsinized and plated on Matrigel for 12 h. (E2) Number of micro vessels and branching points. Control is cells without SEVs. The results are average ± SEM, n=3. In B, C D and E, statistical analyses were performed by Mann-Whitney test, * p<0.05; **p<0.01; ***p<0.001; ****p<0.0001.

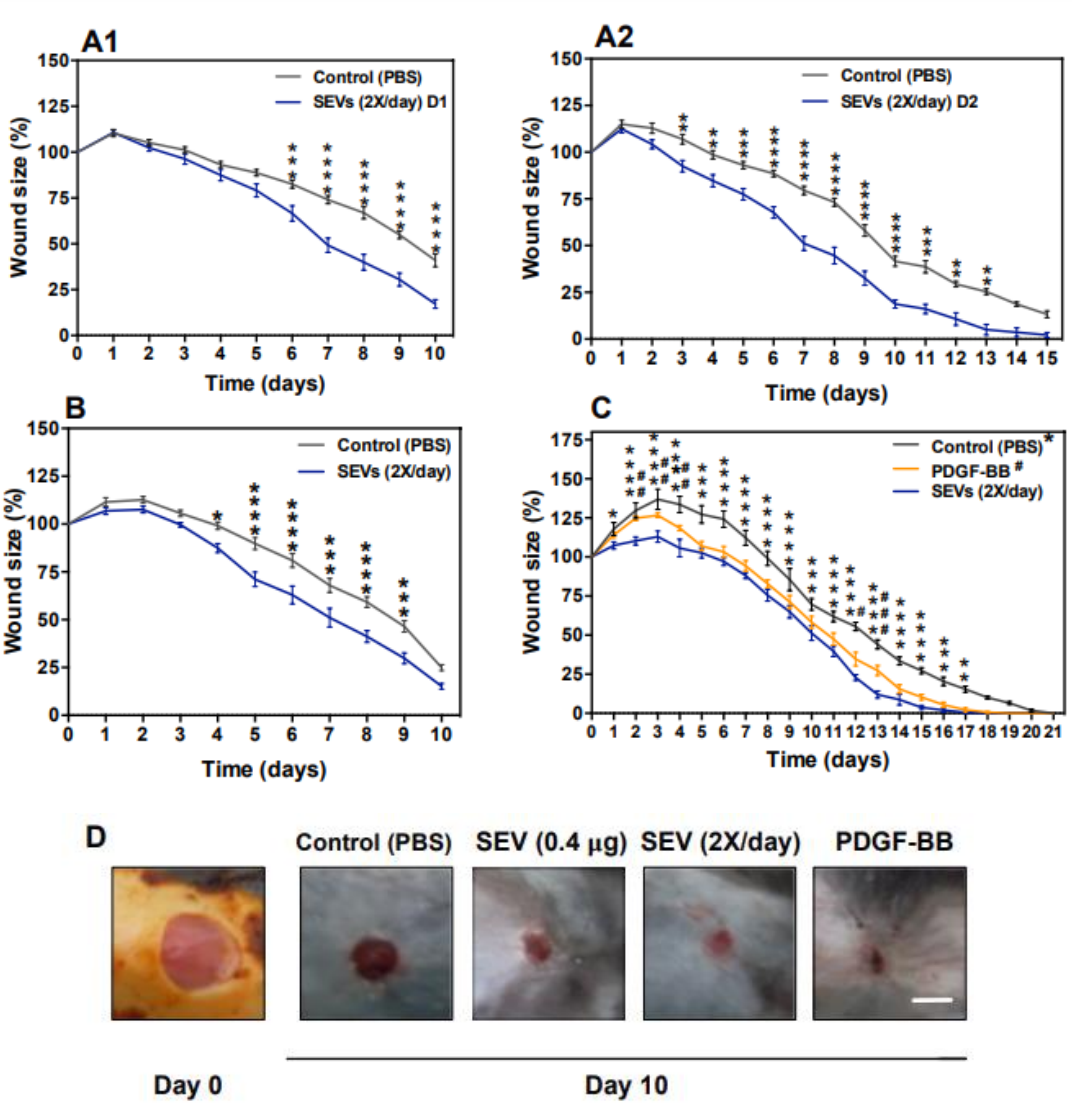

Figure S24- In vivo wound healing activity of SEVs.
Bi-daily treatment of wounds with SEVs isolated from different donors (A1 and A2) in type 1 diabetic mice (A, streptozotocin-induced animal model), wild type mice (B) and type 2 diabetic mice (db/db genetic model) (C). D1 and D2 are donor 1 and donor 2. Results are presented as mean ± SEM, n=10-11. Two-way ANOVA with Bonferroni's multiple comparisons test was applied, * p<0.05; **p<0.01; ***p<0.001; ****p<0.0001; * represents statistical difference to Control (PBS) and # represents

statistical difference to PDGF-BB (positive control). (D) Representative images of wounds in type 1 diabetic mice at days 0 and 10 after treatment. Scale bar corresponds to 3 mm.

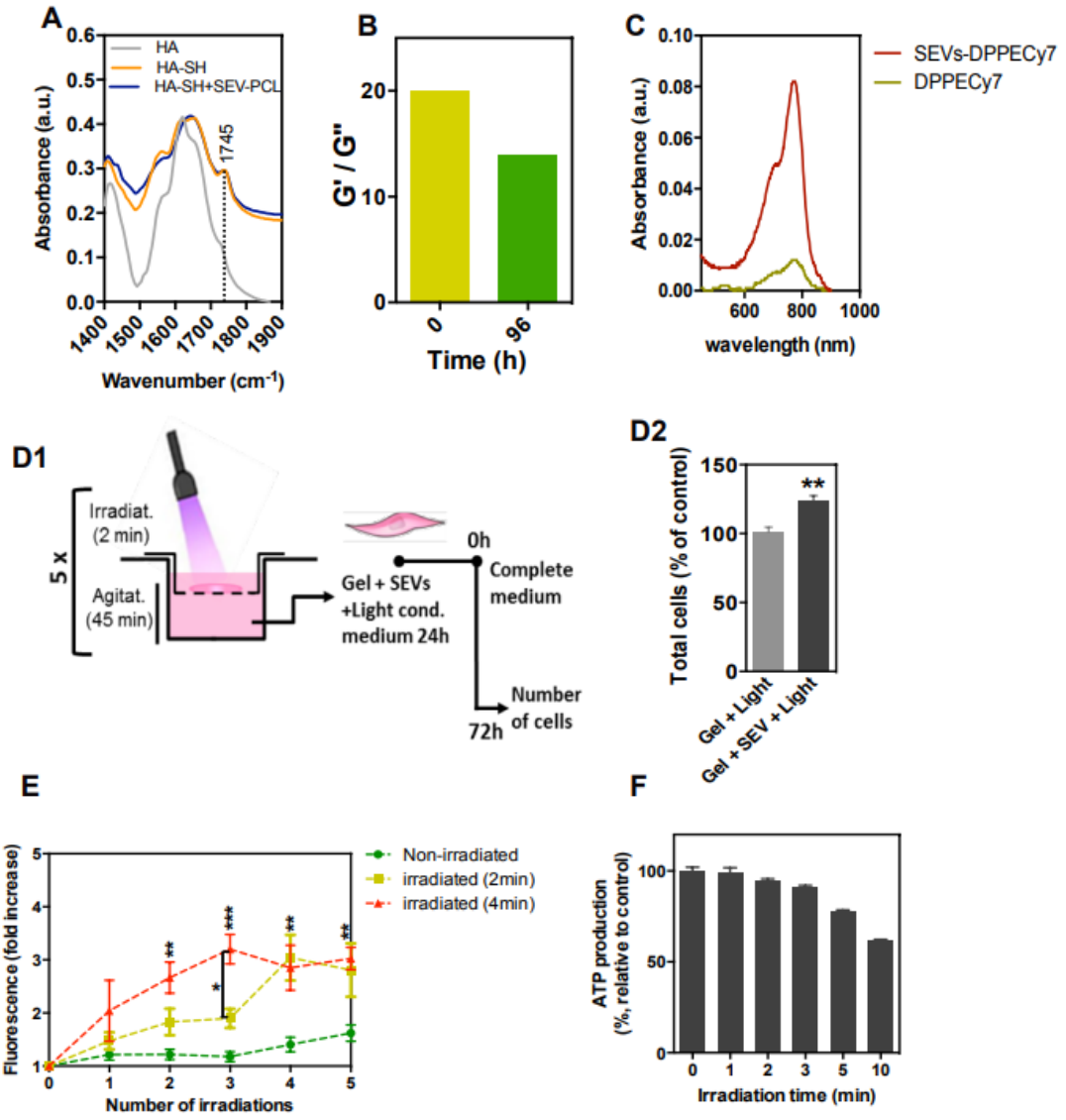

Figure S25- HA hydrogel characterization and in vitro release of SEVs from hydrogel.
(A) FTIR spectra of HA, HA-SH and HA-SH after reaction with SEV-PCL. The incorporation of L-cysteine ethyl ester in the HA polymer is confirmed by the stretching band of the ester group at 1745 cm-1. (B) G´/G´´ of hydrogel after preparation (time 0 h) and after 96 h in PBS, 25ºC. The mechanical properties of the hydrogel were obtained with the following conditions: frequency 0.1 Hz, stress 10 Pa and temperature 37 ºC. (C) Absorbance spectrum of SEVs after labelling with DPPECy7 and purification by ultracentrifugation. A control with DPPECy7 alone was made to monitor the formation of DPPECy7 precipitates (D1) Bioactivity of SEVs released from a light-triggerable HA hydrogel. Five irradiations of 2 min followed by 45 min of agitation were performed to release SEVs chemically conjugated to HA hydrogel. The media containing SEVs was exposed to keratinocytes for 24 h, washed, followed by cell culture in complete media for 72 h. (D2) Cell proliferation assay. The results are average ± SEM, n=3 different donors. Statistical analyses were performed by Mann-Whitney test, * p<0.05; **p<0.01; ***p<0.001; ****p<0.0001. (E) Time course photocleavage of HA hydrogel containing SEV-PCL. HA hydrogel containing 100 µg of SEV-PCL stained with Syto RNASelect was placed on the top part of a transwell and irradiated for 2 or 4 min with a 405 nm laser (80mW/cm2), followed by 45 min of equilibrium under agitation. In each time point an aliquot was collected from the bottom of the transwell and used to read the fluorescence intensity at 530 nm. Results are Mean SEM (n=3-4). Two-way ANOVA followed by Bonferroni's multiple comparison test was used. (* p<0.05; **p<0.01;

***p<0.001). (F) Cytotoxicity caused by laser irradiation. Keratinocytes were exposed to a 405 nm laser (80mW/cm2) for different times. After irradiation cells were kept at 37ºC for 24h and then cell viability was tested using a luminescent assay (Celltiter Glo, Promega).

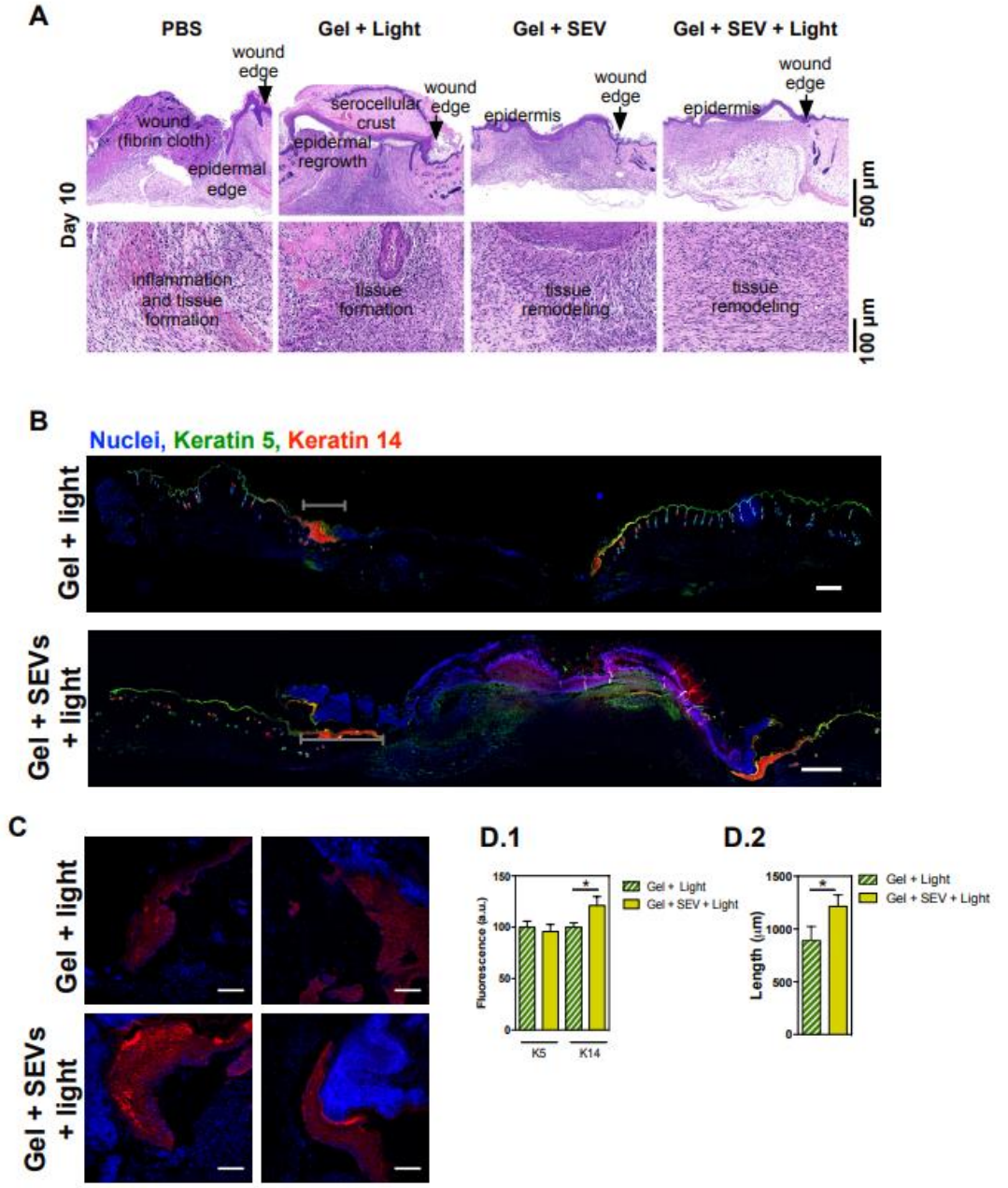

Figure S26- Histology and immunocytochemistry of wounds.
(A) Representative microphotographs of skin wounds in mice at day 10 post-wounding. Multifocal hemorrhages and highly vascularized granulation tissue with minimal macrophage component and incomplete epithelialization is seen in PBS and Gel+Light groups. More stabilized vasculature, with proliferation of fibrous tissue, often already organized in parallel bundles, with complete epithelialization and with evidence of hair re-growth, seen in Gel+SEV and Gel+SEV+Light groups. (B) Fluorescence microscopy images of wound sections, 5 days after treatment, stained for keratin 5 and keratin 14. Images from the entire tissue section were acquired with a 10x objective using InCell Analyzer 2200 and then stitched together using ImageJ. Gray bars denote proliferative/migratory edges. Epithelium with increased expression of keratin 14 was considered as proliferative edge. Scale bar corresponds to 500 µm. (C) Fluorescence microscopy images of the proliferative/migratory edge acquired with a 20x objective. Scale bar corresponds to 100 µm. (D.1) Quantification of the expression

of keratin 5 and keratin 14 in the proliferative edge. (D.2) Length of the proliferative edge. Statistical analyses were performed by Mann-Whitney test, *p<0.05.

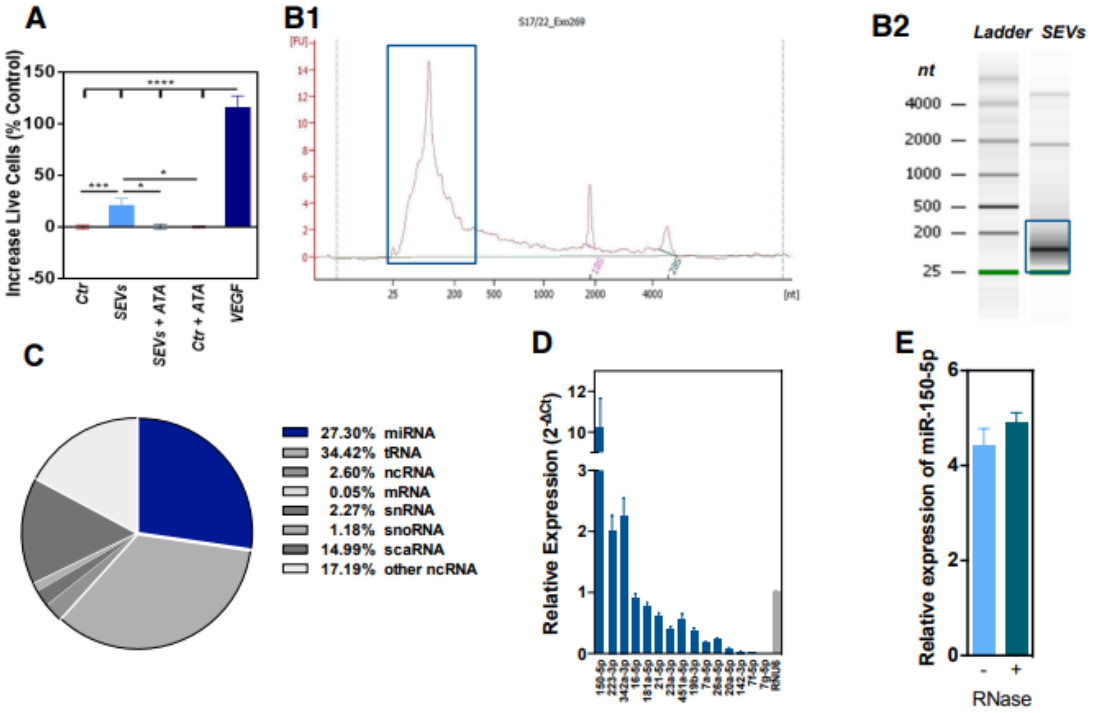

Figure S27- Importance and composition of miRNAs in SEVs.
(A) Survival assay on endothelial cells treated with media supplemented with SEVs alone or SEVs with ATA, a RISC complex inhibitor. Endothelial cells were incubated with SEV-depleted medium alone or with SEVs for 48 h after which they were washed and cultured in ischemic conditions (0.1% O2), in starvation media for 48 h. The viability of the cells was then monitored by a high-content microscope using Hoescht/propidium iodide staining. Results are average ± SEM, n=4 different donors. Statistical analyses were performed by Mann-Whitney test, * p<0.05; **p<0.01; ***p<0.001; ****p<0.0001. (B1) Bioanalyzer profile showing that SEVs are rich in small RNA molecules, n=7. (B2) Representative image of the Bioanalyzer gel profile of SEV (1 donor) comparing with the ladder (nt - nucleotides). (C) Composition of SEVs in terms of different small RNA molecules. (miRNA - microRNA; tRNA - transfer RNA; ncRNA - non-coding RNA; mRNA - messenger RNA; snRNA - small nuclear RNA; snoRNA - small nucleolar RNA; scaRNA - small canal body-specific RNA). The plot represents the average composition of SEVs from 4 different donors. (D) Relative expression of the 15 most expressed miRNAs detected by RNASeq as confirmed by qRT-PCR of SEVs from 10 different donors. Results are average ± SEM, n=10, 3-4 technical replicates per donor. RNU6 was used as endogenous control. (E) Evaluation of miR-150-5p expression of SEVs with and without RNase treatment. Results are average ± SEM, n=3 different donors.

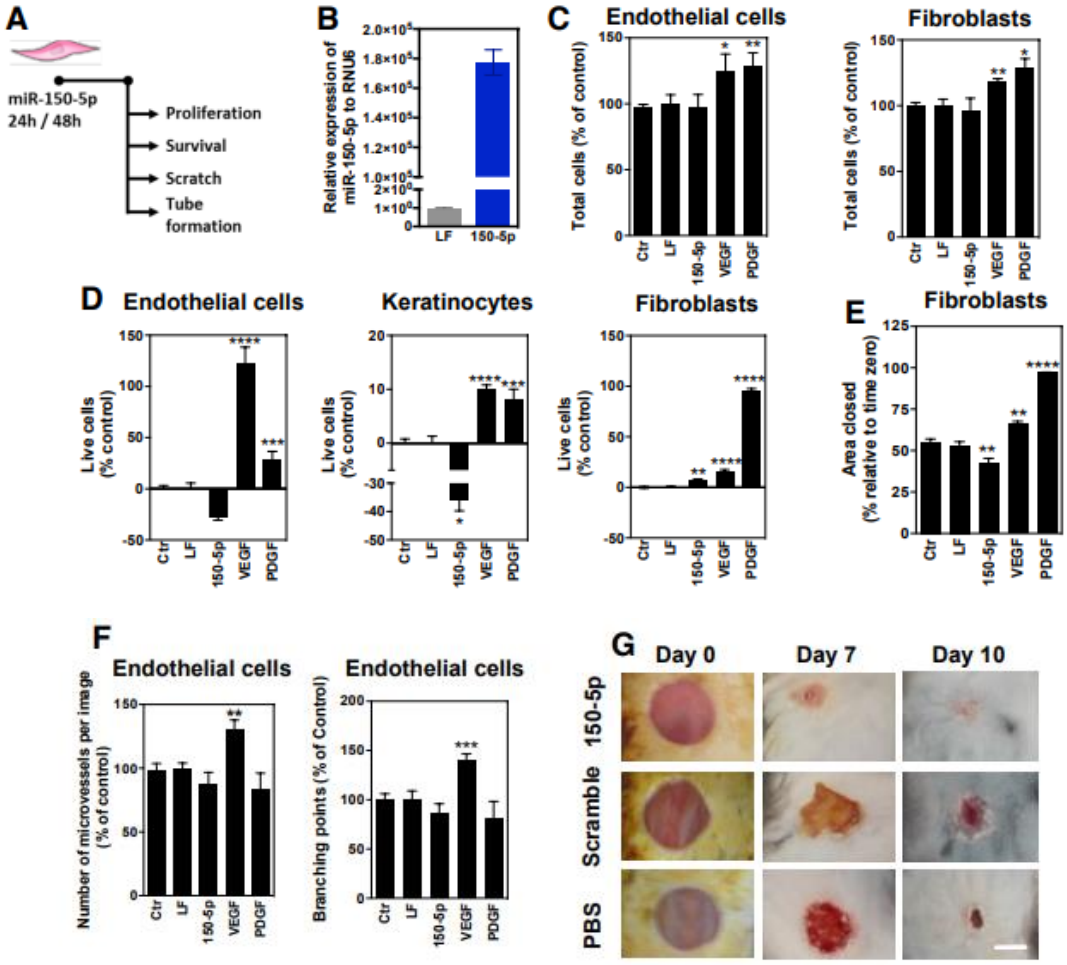

Figure S28- Bioactivity of miR-150-5p on skin cells.

(A) Schematic representation of the bioactivity assays. Cells were transfected miR-150-5p (25 nM) for 24 (proliferation and migration) or 48 h (survival and angiogenesis), after which they were used for the different bioactivity assays. Cells cultured in media supplemented with VEGF (50 ng/mL) or PDGF-BB (50 ng/mL) were used as positive controls. (B) Validation of miR-150-5p transfection of endothelial cells as evaluated by qRT-PCR. Results are average ± SEM, n=3 (C) Proliferation assay. Proliferation of endothelial cells and fibroblasts after 72 h. Results are average ± SEM, n=4-5. Cell number was quantified by a high-content microscope using Hoescht staining. (D) Survival assay. Skin cells were cultured in ischemic conditions (0.1% O2), in starvation media for 48 h (endothelial and keratinocytes) or 72 h (fibroblasts). The viability of the cells was then monitored by a high-content microscope using Hoescht/propidium iodide staining. The results are average ± SEM, n=3. (E) Scratch assay. A scratch in the middle of the well containing transfected fibroblasts was made. Cells were incubated for 48 h. Wound area was evaluated by a high-content microscope. Results are average ± SEM, n=9-10. (F) Endothelial tube assay in Matrigel. Cells were cultured in Matrigel for 12 h. The results are average ± SEM, n=3. In C, D, E and F, statistical analyses were performed by a Mann-Whitney test, * $p<0.05$; ** $p<0.01$; *** $p<0.001$. (G) Representative images of wounds treated with miR-150-5p, scramble miR or PBS at days 0, 7 and 10. Scale bar corresponds to 3 mm.

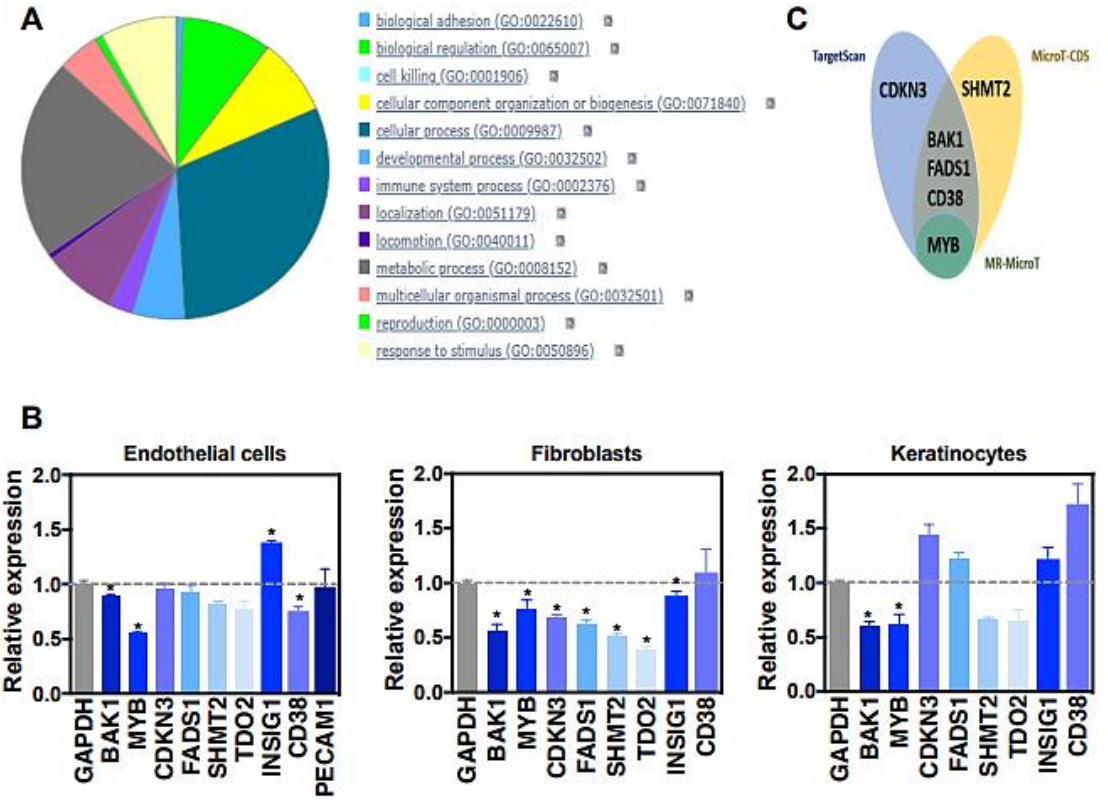

Figure S29 - Gene targets of miR-150-5p.

(A) Gene onthology (GO) analysis pie chart view of validated gene targets of miR-150 (480 gene targets as found through miRWalk 2.0 in 20180117), by biological process, obtained with the PANTHER classification system (pantherdb.org) in 20180117. (B) Expression of 9 putative gene targets of miR-150-5p, previously documented in the literature, after cell transfection with miR-150-5p. Expression was evaluated by qRT-PCR. Statistical analyses were performed by a MannWhitney test, * p<0.05; **p<0.01; ***p<0.001. The results are average ± SEM, n=3. GAPDH was used as housekeeping gene. (C) Venn diagram of the miR-150-5p interaction with the 9 target genes. Putative interaction was evaluated by 3 different tools available online: TargetScan, DIANA MicroT-CDS and DIANA MR-MicroTS. The target genes INSIG1, TDO2 and PECAM1 did not appear in any database, and thus were not presented.

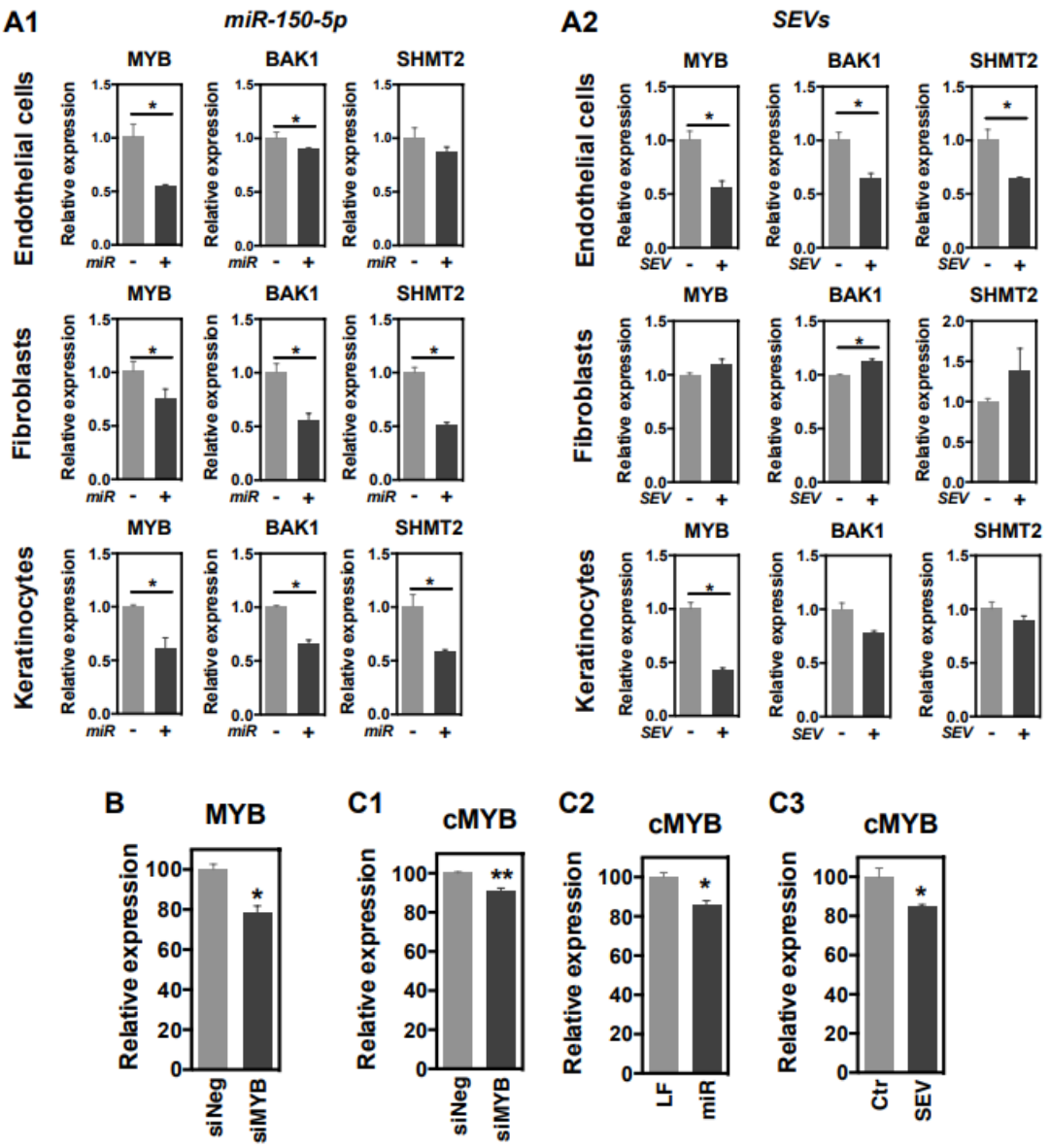

Figure S300 - miR-150-5p gene target validation.

(A) qRT-PCR quantification of MYB, BAK1 and SHMT2 mRNA transcripts on endothelial cells, fibroblasts and keratinocytes transfected with miR-150-5p (A1) or SEVs (A2). Relative gene expression was calculated by the ΔCt method using GAPDH expression as control. The results are average ± SEM, n=3. Statistical analyses were performed by a t-test. (B) MYB mRNA expression down regulation by specific siRNA as evaluated by qRT-PCR. GAPDH was used as endogenous control. (C) Immunocytochemistry evaluation of c-Myb demonstrates protein levels down regulation by specific siRNA and by treatment with miR-150-5p and SEVs in keratinocytes. The results are average ± SEM, n=3. Statistical analyses were performed by Mann-Whitney test, p<0.05; **p<0.01; ***p<0.001.

V. General Discussion and Conclusions

Exosomes (or EVs) from different sources have been shown to significantly enhance the healing of chronic wounds. Exosome-based treatments have revealed not only to reduce wound closure time on full-thickness wounds of diabetes type I mouse models, by reducing inflammation, increasing angiogenesis and tissue reepithelization, but also by promoting tissue maturation with less scarring [207, 216, 226, 229, 230, 232]. In the present study, we show that SEVs isolated from UCBMNCs were able to modulate the biology of 3 different skin cell types: endothelial cells (ECs), fibroblasts and keratinocytes. In vitro results show that SEVs enhanced skin cell proliferation and survival to ischemia, enhanced EC tube formation in Matrigel, and induced a faster closure of a scratch by fibroblast and keratinocytes. EVs from UCBMNCs are able to enhance the wound healing kinetics in more than 30% relatively to the topical administration of the growth factor PDGF-BB (this growth factor has been described to reduce diabetic wound size of STZ mice, by increasing neo-vascularization, trough augmentation of EPC recruitment, and enhancing granulation tissue formation [151]). In addition, our *in vivo* results (in 3 mouse models: type I and II diabetic mice and wild type mice) show that chronic wounds treated with SEVs from UCBMNCs had higher neovascularization and reepithelization than non-treated wounds [126].

In general, due to differences on animal models and experimental procedures between pre-clinical studies it is difficult to compare the therapeutic effect of exosomes relatively to other advanced approaches such as growth factor and cell-based therapies. Our study is one of the few studies that compare side by side the therapeutic effect of exosomes with another advanced therapy, in this case, a growth factor therapy (PDGF-BB). Despite the differences already noted between studies, it is possible to extrapolate the findings of our study relatively to other advanced therapies. For example, cell –based therapies (MNCs of PB) applied to the wounds of STZ-mice were found to increase wound revascularization from day 7, but not able to fully promote collagen reorganization by day 21. Essentially, vessel size was observed to be larger than the non-treated wound, mostly through the effect of paracrine factors rather than cell engraftment and differentiation [170]. On the other end, UC-MSCs application to wound of a type II diabetic mouse model (db/db) was found to accelerate wound closure by enhancing re-epithelization, granulation tissue formation and neovascularization, again mainly by paracrine action [167]. In fact, exosomes / SEVs have been recently applied in the field of wound healing, surpassing cell-therapies main concerns, such as cell survival and costs [10, 188-193, 197, 202-205]. For example, vesicles from platelet-rich plasma (PRP), UCB Endothelial progenitor cells (EPCs) and Synovial Mesenchymal Stem/stromal Cells (SMSCs) increased wound closure in type I diabetes rat model by enhancing reepithelization and angiogenesis [125, 207, 217]. Adipose Mesenchymal Stem/stromal Cells (ASCs) SEVs had a similar effect in wounds inflicted in a diabetic mice model [123]. Furthermore, SMSCs and ASCs derived SEVs were administrated to the wound in a hydrogel matrix with significant improvement of the healing kinetics, with wound closure rates at day 14 of approximately 25% and 50%, respectively [123, 217]. Our study showed that UCBMNCs SEVs enhanced wound healing *in vivo* promoting neovascularization and reepithelization, being the activity dependent on the dose and application frequency of SEVs while independent of the donor and the diabetic animal model [126]. Additionally the SEVs controlled release hydrogel system developed increased wound closure of diabetic wounds from 15% (SEVs alone or SEVs + HA) to 25% (SEVs + HA + light), at day 10 post wound. Approximated values of wound closure rates for these three studies, at day 7, data available in all studies, is presented on Table XVIII.

Table XVIII. Effect of Hydrogel-SEVs based therapies in diabetic wounds closure rates.

SEVs source	Hydrogel	*Wound closure (%) / Treatment*					Ref.
		Control	SEVs	Gel	SEVs+Gel	SEVs+Gel +light	
human SMSCs	**SAH**	**40%**	**_**	**50%**	**60%**	**_**	[217]
human ASCs	**FEH**	**10%**	**_**	**45%**	**65%**	**_**	[123]
hUCB MNCs	**Photolabille - HA**	**20%**	**30%** (1 dose) / **50%** (2x/day)	**40%** (+light)	**50%**	**70%**	[126]

The work presented in this thesis has four major innovations:

- First the use of UCBMNCs as a competitive source of bioactive SEVs with regenerative properties. The SEVs were obtained from cells cultured under hypoxic conditions. Our results also suggest that exosomes obtained from $CD34^-$ cell population of the MNCs have also regenerative potential.

- Second, the development of a controlled system for the *in vivo* delivery of SEVs, based on covalently binding of SEVs to a light-triggerable linker in a hyaluronic acid gel matrix, which offers a more hydrated environment stabilizing the vesicles in the wound bed, while the linker allows for an effective control on the release of the vesicles from the gel to the wound tissue, monitored by a new FRET system that allows *in vivo* evaluation of vesicle integrity and stability in the wound bed.

- Third, the demonstration that the controlled release of SEVs at a specific concentration during a time window enhances the regenerative potential of SEVs and SEVs exert their pro-healing activity at a tissue/cell level by enhancing wound reepithelization and angiogenesis, and at a molecular level by modulating skin miRNAs expression.

- Fourth, the demonstration that miR-150-5p mediates at least in part the wound healing properties of SEVs. It is the first evidence of the wound healing properties of miR-150-5p. Additionally, we were able to determine that the miR-150-5p bioactivity is due to the targeting of the MYB gene.

Umbilical cord blood as source of bioactive EVs with pro-regenerative properties

Over the past few years, stem cells have emerged as a promising therapy to enhance wound healing [86, 88, 89, 98-100, 163-176]. Human umbilical cord blood (UCB) is an attractive source of cells for wound repair. This source of cells does not imply risks to donors during collection, raises minimal ethical concerns and it is relatively easy to access [89, 465]. In addition, fetal stem/progenitor cells might offer higher regenerative potential than adult and aged counterparts which might have been exposed to diseases. For example, EPC cells were found to be present in less number in diabetic patients and to be dysfunctional, thus with less pro-angiogenic capability [163, 301]. Moreover, UCBMNCs induce angiogenesis in wounds and have already been applied in fibrin-platelet glue platform to human non-healing wounds with promising results [170, 172].

UCBMNCs fraction represent a heterogeneous cell source of exosomes which have variable molecular composition and biological properties [466, 467]. The exosomal cargo is dependent on the physiological condition of the cell of their origin [206]. The fetal origin of these exosomes may offer a higher therapeutic value than adult exosomes. This was demonstrated with fetal exosomes isolated from cardiac progenitor cell (CPC) and MSCs. CPC-derived exosomes isolated from neonatal patients were found to have higher regenerative potential for cardiac tissue repair compared to CPC exosomes from older children, demonstrating the high potential associated to young or perinatal cells [303, 304].

Exosomes derived from fetal cells may have promising applications in the setting of wound healing. A recent study has demonstrated that SEVs isolated from UCB plasma can effectively enhance cutaneous wound healing in mice, partially through miR-21-3p, that induces proliferation and migration of fibroblasts and endothelial cells and angiogenesis [226]. In the setting of this thesis we have used SEVs from hUCBMNCs cultured under ischemic conditions. Previous studies have shown that ischemic cell conditioning increases cellular regenerative potential in the setting of wound repair and angiogenesis [181, 188]. In addition, SEVs isolated from $CD34^{+}$ cells or CPCs cultured under ischemic conditions had higher regenerative potential than SEVs isolated from the same cells cultured under normoxic conditions [206, 337]. It was demonstrated that the miRNA composition in SEVs isolated from ischemic cells had an enrichment of miRNAs [206, 337]. For example, under hypoxia conditions cardiac progenitor cells secreted exosomes enriched in miR-292; miR-210, miR-103; miR-17; miR-199a; miR-20a; miR-15b [337]. Our results show that SEVs secretion is stimulated by hypoxia, but the miRs composition is only slightly different between hypoxic and normoxic secreted SEVs (Figure - 15.).

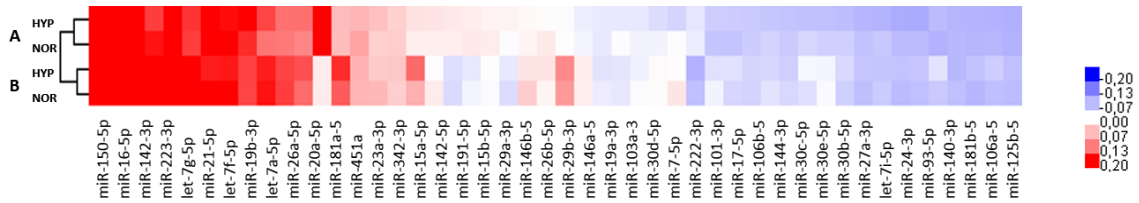

Figure - 31. Comparison of miRNA composition of SEVs obtained in Hypoxia and Normoxia.
Data obtained by RNASeq, 2 donors per condition.

Our results show that hUCBMNC-derived SEVs have a broad spectrum of activity, as they enhance several aspects of skin cells including cell survival, proliferation, migration and angiogenesis. In addition, the regenerative effect of this SEVs was also transversal to several animal models of chronic (diabetes type I, STZ-induced mice, and diabetes type II, db/db mice) and acute wounds (wild type C57BL/6 mice) [126].

Enhancing EV bioactivity through a novel light-activatable hydrogel system

A novelty of this PhD thesis was related to the development of a controlled delivery system of SEVs that was remotely activated by light. The system was designed to: (i) allow the release of SEVs under specific kinetics, to enhance their bioactivity, and (ii) to minimize the re-application of SEVs. Our *in vivo* data indicates that the way SEVs were administered in the wound was crucial for their bioactivity. For the same concentration of SEVs applied in the wound, the healing process was superior for SEVs applied in a low dose multiple time than a high dose in one time. This is likely due to the fact that SEVs have a cocktail of miRNAs that play an active role at a specific time during wound healing. Our miRNA expression results indicate that the controled release of SEVs seems to modulate skin miRNAs expression towards a more healthy profile when comparing to miRNA expression in wounds of wild-type mice, wile maintaining a sustained delivery of a cocktail of miRNAs.

Biomaterials have been used to increase EV bioavailability in the wound site [124, 125, 216, 217, 228]. Until now, the developed systems did not allow for an effective control of the delivery by the operator. The controlled delivery is by the passive diffusion of SEVs from the polymeric formulation either by the swelling of the formulation or by its degradation (by chemical or enzymatic means). Until now, no study has demonstrated the benefit of these controlled release systems in wound healing since a side-by-side study with an experimental control, i.e. without the controlled delivery system, was not performed [124, 125, 216, 217, 228]. Furthermore, these platforms do not provide de necessary control of EVs release, not fully exploiting this strategy in wound healing.

Here, we developed a hydrogel conjugated with SEVs by a photo-cleavable linker (PCL). This system allows the delivery of SEVs in the wound after UV/blue laser activation. HA is a polysaccharide that has been used on clinical applications, including wound healing, for many years [24, 108, 468, 469]. In this work, we covalently bounded a PCL to HA, followed by the conjugation of SEVs to the terminal acrylate groups of PCL. After blue laser activation, the effective SEV release and integrity from HA gel was monitored by an innovative FRET system developed by us. SEVs were released from the hydrogel for up to 6 days. When SEVs were directly applied to the wound, they were lost at day 2. Our results are aligned with a previous study showing that SEVs could be retained for 3 days in the wound [226]. Therefore, our light-activatable hydrogel allowed the sustained release of SEVs.

Control delivery of UCBMNCs vesicles modulates miRNA expression in the skin

Vesicles from UCBMNCs present a rich and diverse miRNA composition, harboring near 45 different miRNAs species. From the miRNAs found in SEVs derived of UCBMNCs we selected the 15 most expressed miRNA: hsa-miR-150-5p, hsa-miR-142-3p, hsa-miR-223-3p, hsa-miR-21-5p, hsa-let-7g-5p, hsa-miR-16-5p, hsa-let-7f-5p, hsa-miR-19b-3p, hsa-miR-181a-5p, hsa-miR-26a-5p, hsa-let-7a-5p, hsa-miR-23a-3p, hsa-miR-451a, hsa-miR-20a-5p and hsa-miR-342-3p, for further studies. Most of them have already been described as relevant for the wound healing process and / or as impaired in chronic wounds (Table XVIII).

Table XIX. Changes in miRNAs expression in diabetic vs acute wounds.

#	miRNAs	*Diabetic wounds*			Reported bioactivity
		D0	D3	D10	
1	**miR-150-5p**	Up [470]	Up [470]	Down [470]	Pro-angiogenic [471]. Enhances endothelial cell migration [472].Increases cell proliferation and decreases apoptosis [470]. VEGF mediates miR-150 action on tube formation, proliferation, and migration of BMVECs [473].
2	**miR-342-3p**	Up [470]	Down [470]	Down [470]	Inhibit macrophage activation; reduce macrophage viability and induces apoptosis [474]. Predictably targets TGF-β, a growth factor secreted by macrophages in the inflammatory phase, and that stimulates cell proliferation during the proliferative phase [475].
2	**miR-223-3p**	Down [470]	Up / Down [470]	Down [470]	Directly targets chemokine ligands (CXCL)2 and CCL3, important for neutrophil recruitment to the wound [154]. Anti-inflammatory via STAT3, induces M2 polarization [476]. Pro-apoptotic in endothelial cell [154, 477].
4	**miR-16-5p**	Up [470]	Down [470]	Down [470]	Anti-inflammatory by inhibiting Cox-2 expression in monocytes [154]. Related to delayed epithelialization and granulation tissue formation [158]. Antiangiogenic [156, 478]. Pro-apoptotic [479].
5	**miR-181a-5p**	_	_	_	Involved in stress and immune responses [480].
6	**miR-21-5p**	_	Up [481]	_	Induces keratinocyte and fibroblast proliferation and migration [154, 158, 160, 482]. Promotes wound contraction, enhances collagen production and deposition of mature collagen fibrils. May favor re-epithelialization due to cell proliferation and wound contraction [159, 160, 225, 483]. Activates TGF-β1 signaling, promoting the proliferation of fibroblasts [161]. Promotes M1/M2 polarization [476]. Anti-apoptotic [484].
7	**miR-451a**	_	_	_	Probably anti-inflammatory [485].
8	**miR-23a-3p**	_	_	_	Anti-apoptotic in HUVECs; possibly plays a general role in the regulation of TNF-α-mediated apoptotic signaling pathways [486]. Probably anti-angiogenic [487].
9	**miR-19b-3p**	Down [470]	Down [470]	Down [470]	Belongs to a pro-angiogenic miRNAs cluster (miR-17-92) [157]. Induces fibroblasts senescence [153].
10	**miR-26a-5p**	Up [162]	Up [162]	Up [162]	Anti-angiogenic, decreases endothelial cells proliferation, migration, sprouting, and tube formation [162, 488, 489]. Have cell-type specific effect: pro-angiogenic in glioma and anti-angiogenic in hepatocellular carcinoma [488]. Suppresses autoimmune diabetes [488]. Involved in stress and immune responses [480].
11	**let-7a-5p**	_	_	_	The let-7 family is referred as key regulators of the angiogenic responses of endothelial cells [490]. Present pro-apoptotic activity [479].
12	**miR-20a-5p**	_	_	_	Involved wound healing, reviewed in [154]. Belongs to a pro-angiogenic miRNAs cluster (miR-17-92) [157]. Delays epithelialization and granulation tissue formation [153]. Can suppress TGF signaling [158].
13	**miR-142-3p**	Down [482]	Down [482]	Down [482]	Modulator of Wnt signaling in a context dependent manner, controlling cell cycle [491].
14	**let-7f-5p**	_	_	_	The let-7 family is referred as a key regulator of the angiogenic responses of endothelial cells [490]. Pro-angiogenic [153].
15	**let-7g-5p**	_	_	_	The let-7 family is referred as a key regulator of the angiogenic responses of endothelial cells [490].

SEV miRNAs modulate inflammation, re-epithelization and angiogenesis during wound healing. It is interesting to note that some of the miRNAs induce wound closure (e.g. miR-21, miR-150-5p, let-7 family, etc…) while others seem to impair wound closure (e.g. miR-26a, miR-

20a, etc…). miR-21 promotes inflammation by M1 macrophage polarization [476], induces keratinocyte and fibroblast proliferation and migration, promoting wound contraction, and enhances collagen production and deposition of mature collagen fibrils [154, 158-160, 225, 482, 483]. miR-150-5p was demonstrated to enhance endothelial cell migration [472], to increase cell proliferation and reduce apoptosis [470]. The let-7 family is referred as key regulators of the angiogenic responses of endothelial cells [490]. By other hand, mir-26a delays wound closure and is anti-angiogenic, i.e., decreases endothelial cell proliferation, migration, sprouting and tube formation [162, 488, 489]. Nevertheless, this effect seems to be cell-type specific [488]. Interestingly miR-26a is able to suppress autoimmune diabetes [488]. miR-20a delays wound closure due to inhibition of epithelization and granulation tissue formation [153].

Several miRNAs on UCBMNCs-SEVs are reported to be imbalanced in diabetic skin and/or wounds: miR-150, miR-342, miR-223, miR-16, miR-21, miR-19b, and miR-142-3p [470, 481, 482]. Thus, the controlled release of SEVs from the light-activatable gel on STZ-mice wounds seems to stabilize skin miRNAs expression to levels similar to the expression in wild-type animals, thus inducing a more acute-wound profile and improving significantly the healing kinetics. The gel containing SEVs significantly influenced the expression of 7 miRNAs in skin, stabilizing and sustaining miR-150-5p, miR-342-3p, miR-181a-5p and let-7a-5p expression while increasing the expression of miR-223-3p and miR-142-3p at day 5, and of let-7f-5p at day 10 post wounding. The 8 other miRNAs studied did not present significant differences to the control. The increase in the expression of miR-223 and miR-142 at day 5, typically down-regulated in diabetic wounds at day 3, may lead to an increase in the anti-inflammatory activity on the wound [470, 476, 492]. In addition, the stabilization of miR-150 and miR-342 levels in the wound at day 5 and increase at day 10, may be responsible for the reepithelization and neo-vessels maturation, since these miRNAs are described to be related to cell proliferation, migration and survival [470, 474]. The let-7f-5p upregulation at day 10, may have an impact in the wound vascularization, since this miRNA belongs to a family described to regulate angiogenesis.

Our results indicate that we are not only delivering bioactive miRNAs to the wound and observing their direct action, but also modulating miRNA expression on skin cells. This effect have been already described for MSC-EVs modulated miR-205 expression [228]. Although miR-205 is present inside the EVs from stem cells, we could not assume at this point that the increased expression observed in qPCR experiments is strictly due to the transfer from EVs to cells with the experiments described here. The fact is that miRNA biology is very complex and can be modulated by several factors, including other miRNAs [493, 494].

We demonstrated that the controlled release of the SEVs significantly enhanced their healing properties as compared to a single or multiple applications of SEVs in a diabetic animal model. This effect can be explained by several factors, the synergistic effect of the gel, associated with a sustained and continued delivery of miRNAs, and other pro-healing factors, present in the SEVs and lower destabilization of the wound associated with the application of the treatments.

miR-150-5p mediates in part the wound healing activity of SEVs.

It is likely that the modulatory role of miR-150 depends on its concentration, the targeted cell, and the environment (e.g., presence of other regulating factors). miR-150 appears to be a master regulator of cell cycle and function. For example, miR-150 presents anti-apoptotic activity by targeting BAK1 protein in non small-cell lung cancer (NSCLC) [470, 495, 496]. miR-150-5p has been described as being secreted by monocytes and lymphocytes, the major cell types in UCBMNCs [497-500]. miR-150 targets c-Myb, a highly conserved and regulated transcription factor, regulating the production of hematopoietic progenitor cells and the development and differentiation of B cells [497, 501]. miR-150 enhances endothelial cell migration (by the inhibition of c-Myb) and induce endothelial cell tube formation in vitro and angiogenesis *in vivo* [471, 472]. In addition, miR-150 regulates the expression of VEGF [473, 502, 503] and VEGFR2. The gene encoding VEGFR2 has four c-Myb binding sites in its promoter region, suggesting that Vegfr2 expression is promoted by c-Myb [504]. Moreover, high levels of miR-150-5p in neutrophils down-regulate the expression of Protein Kinase C Alpha gene (PRKCA) [505].

miR-150 has been mostly studied in the context of vision impairment related to age, diabetes and ischemia [157, 502, 504, 506-511]. In diabetic retinopathy (DR), low levels of miR-150 were correlated with excess of neovascularization [504]. In age-related macular degeneration (AMD), miR-150 was verified to be upregulated in disease-promoting murine macrophages and in human peripheral blood mononuclear cells [511]. miR-150 deregulation seems to play an important role in ischemic diseases, since its expression or secretion is down-regulated in hypoxic conditions and up-regulated by oxidative stress [157, 472, 502].

In this thesis, we evaluated the bioactivity of mir-150-5p in the context of wound healing. Only one study has reported the expression of miR-150 in the setting of wound healing. The study indicated a deregulation of miR-150 on STZ-induce mouse full thickness wounds [470]. Our *in vitro* results show that keratinocytes transfected with mir-150-5p had increased proliferation and migration while transfected fibroblasts had enhanced survival under ischemic conditions. Our *in vivo* results show that wounds treated with miR-150-5p had enhanced healing.

Interestingly, the levels of miR-150-5p were found to be sensitive to our system, which was able to regulate this miRNA expression to similar levels of the ones described in acute wounds (mild-type mice). Initially, on day 3, miR-150-5p appears up-regulated by 226% in STZ-mice wounds, versus the expression profile of wild type wound. But, by day 10, a strong decrease on miR-150-5p levels can be observed, when comparing to day 0. MiR-150 is described to increase cell proliferation and decrease apoptosis, thus enhancing wound healing. Could it be that the high levels of miR-150-5p observed in the early days of diabetic wounds is a physiological response of the skin to promote wound healing. But the effect is worn off in between day 3 and day 10 in STZ mice, leading to a chronic non-healing wound phenotype [470]. Although this pro-healing activity described for miR-150-5, it is well known that in biological systems thigh regulation of molecules levels is of utmost importance to maintain the equilibrium. Could this be the case, and the high levels of miR-150 observed at day 3 activate a mechanism of negative feedback that reduces its expression, but to very low levels of expression, which could be pathological. For example, a study describes that up-regulation of miR-150 increased permeability of BBB, therefore, may facilitate SEVs bioavailability in the brain [512]. Despite of reported anti-angiogenic activity of miR-150 in stroke, it's downregulation by ischemia, and the probability that it could decrease vascular density of infarct border zone, by negatively regulate the expression of VEGF [513]. The effect is most probably related to the concentration of this miRNA, and has seen in our chronic wound

model, it may also have a positive effect in neo-angiogenesis and neuronal cells proliferation, survival.

The miR-150-5p is a widely conserved miRNA interacting with 480 different validated gene targets in miRWalk 2.0 (20180117) (see **Appendix I** [514, 515]). The targets identified are related to several biological processes, as evaluated by PANTHER 13.1 GO 1.2. From the genes identified in the literature as targets of miR-150-5p, we selected 10 genes for validation in this thesis [496, 497, 516, 517]. The expression of the 10 gene targets selected was evaluated in the 3 cell lines studied upon transfection with miR-150-5p (endothelial cells, fibroblasts and keratinocytes).

A putative interaction between miR-150-5p and these 10 targets was evaluated using TargetScan [518], DIANA MicroT-CDS [519, 520] and DIANA MR-MicroT [520, 521]. The interaction between miR-150-5p seed sequence and the 3'-UTR of the targets was probable for 6 of genes, as revealed by one or more databases and /or algorithms used (Figure VI.5). Based on these analysis we selected 3 targets that are related to cell survival and proliferation: MYB, BAK1 and SHMT2 [496, 497, 516, 517]. According to our results, both SEVs and miR-150-5p modulated the expression of mRNA of these targets in the 3 skin cells studied. Additionally, c-Myb protein levels were reduced by SEVs and miR-150-5p treatment. The protein c-Myb is a transcription factor highly conserved and regulated, known to be critical to several cellular processes, like cell migration, proliferation, survival, death and differentiation [522, 523]. The targeting of c-Myb by the miR-150-5p was found to be evolutionary conserved, and to play an important role in embryonic developmental processes, hematopoiesis and B cell differentiation [497, 516, 524]. Thus, c-Myb *per se*, acts like a master regulator of cell function and fate (Table VI.4), modulating the expression of many important genes [497, 516, 522-525]. We believe that inhibition of this transcription factor can trigger a cascade of events by down regulation of several proteins, like Set, Casp6 and Mad1/1, that would be reflected in the increase of keratinocyte proliferation at a cellular level, as observed by the treatment with specific siRNA, and the maturation of the wound at a tissue level [498].

Table XX. Target genes of Myb by cellular function. *In [525].*

Cellular function	Target gene
Cell cycle	Mad1l1
Cell death	Api5; Bcl2; Birc3; Casp6; Cd53; Set
Cell adhesion/cytoskeletal regulation	Actn1; Emi2; Iqgap1; Msn; Psd4
Golgi/ER and trafficking	Bet1l; Copa; Lca; Sec31l1
Solute transporters	Slc1a5; Slc20a1; Slc25a3
Molecular chaperones	Cct2; Hspa8; Stch
Mitochondrial	Tfb1m; Timm44
Signal transduction	Ppp3ca
Transcription	Cbx4; Set; Tcfec

In summary, miR-150-5p acts as a master regulator of several cellular processes, which are of great importance for wound resolution, namely proliferation, survival, migration and angiogenesis. This miRNA might have a great therapeutic potential in the setting of different pathological conditions, such as stroke, cardiac ischemia and cancer [157, 340, 512, 513].

VI. Future work

To identify and study other biomolecules entrapped on SEVs

It is possible that other biomolecules, besides miRNAs, may participate and influence the healing properties of SEVs. So, it would be interesting to further analyze the content of these SEVs in terms of mRNAs, proteins, lipids, among others and further explore their therapeutic potential. For example, although mRNAs represent a small percentage of the RNA composition of the UCBMNCs-SEVs, it would be interesting to evaluate the biological role of RNAs that encode growth factors or signaling molecules. Additionally, SEVs enclose other ncRNAs that might also be bioactive and play a role on the regenerative effect of these vesicles. Moreover, a proteomic analysis could be performed in order to identify proteins transported by UCBMNCs-SEVs including growth factors, cytokines and signaling molecules. Finally, few studies described the lipid composition of EVs and discussed their possible biological function. A lipidomic analysis would allow for a more complete characterization of UCBMNCs-SEVs.

To study deeply the molecular and cellular mechanisms involved in the wound healing effect of SEVs

The therapeutic mechanism of UCBMNCs-SEVs deserves further study. For example, it will be to study other gene targets for miR-150, like BAK-1, a pro-apoptotic protein [470, 495, 496], and to study other miRNAs that are reported to be imbalanced in diabetic skin and/or wounds (miR-342, miR-223, miR-16, miR-21, miR-19b, and miR-142-3p [470, 481, 482]), which would unravel more of the UCBMNCs SEV therapeutic potential.

In this thesis, we focused our attention on miR-150-5p bioactivity; however, it would be interesting to study the wound healing properties of other miRNAs. For example, miR-16 is reported to stimulate miR-150 expression and, accordingly to TargetScan, miR-16-5p also targets c-Myb [471]. It is possible that the single administration of miR-16-5p may reproduce or even surpass the effect observed by miR-150-5p treatment. In addition, it would be interesting to evaluate if the administration of miR-16 and miR-150 is able to enhance even further wound healing, versus the solo administration of miR-150.

The study of sequential administration of different miRNAs during wound healing is another issue that deserves further attention. For example, it would be interesting to analyze the sequential delivery of miR-223, a miRNA with anti-inflammatory properties, followed by the delivery of miR-150, a miRNA with proliferative properties. This would allow to tackle non-healing wounds in to different stages, first by reducing chronic inflammation followed by the promotion of granulation tissue formation. Recently, a system has been developed in our lab that would allow us to evaluate the bioactivity and sequential release of different miRNA molecules [526].

A recent work, postulates over the importance of migration versus proliferation in wound healing: '*epithelial regeneration contributes approximately to two-thirds of the healing process, and wound contraction (…) is responsible for the remainder*.'[527]. From this interesting work emerged the question of what are we actually observing in our case. Our *in vitro* assays, particularly with miR-150-5p, the enhancement of proliferation, particularly of keratinocytes, was the most prominent effect of miR-150-5p. Which correlates with the *in vivo* results,

maturation of skin tissue upon treatment with Gel+SEV+Light. Studies involving specific markers of migration and proliferation would permit to conclude about the effect of SEVs and miR-150-5p that we are actually potentiating with this treatment platform, and at which extent.

To improve the controlled release system

We have used light as a trigger in our formulation because light may induce skin regeneration. In fact, phototherapy is known to promote fibroblast proliferation, collagen synthesis and growth factor expression [101]. The light exposure of our gel formulation (the gel was irradiated every day for 1 min) promoted the sustained release of SEVs into the wound. Yet, the protocol of irradiation can be further optimized for SEV delivery at specific times during wound healing. For example, the system might be activated only in the first days (0-3 days after wounding) to promote the release of higher amounts of SEVs in this stage, and the remaining SEVs might be progressively released upon natural gel degradation in the wound.

In theory, it is possible that the gel would degrade after exposure to sun light and thus would not require a blue laser activation. This would eliminate the need of the patient for medical assistance during the treatment. However, further studies are needed to study in detail the sensitivity of the gel to sun light and the release kinetics of SEVs. The use of sun light as a trigger for SEV release, presents another advantage, the circadian cycle advantage. Skin cells, namely fibroblasts, exhibit a circadian behavior, and daytime wounds present 60% faster healing than nighttime wounds [528]. Thus, the wound exposure to the sun is expected to increase even more SEV effect.

Further tests should be performed with our gel formulation for SEVs isolated from different donors and SEVs from other cell types and / or engineered vesicles [529]. In addition, the delivery properties of the gel formulation may be further tuned by the incorporation of different linkers, namely hydrocarbon chain molecules presenting different light-activation properties to allow the controlled release of vesicles / molecules at different times. Furthermore, SEVs of different sources, could be integrated in the same platform, and associated with linkers with different photo-sensitive profile, diferentiated delivery of these vesicles could be obtained. Per example, SEVs of MSCs, described for their anti-inflammatory profiles could be release primarly to control excessive inflamation in the wound bed, followed by the release of SECs from MNCs or HSCs, enhancing the regenerative profile of SEVs delivered to the wound.

References

1. Mostow, E.N., *Diagnosis and classification of chronic wounds.* Clinics in Dermatology, 1994. **12**: p. 3-9.
2. Lazarus, G.S., et al., *Definitions and guidelines for assessment of wounds and evaluation of healing.* Archives of Dhermatology, 1994. **2**: p. 165-70.
3. Rahman, G.A., I.A. Adigun, and A. Fadeyi, *Epidemiology, etiology, and treatment of chronic leg ulcer: expirience with sixty patients.* Annals of African Medicine, 2010. **9**(1): p. 1-4.
4. Sen, C.K., et al., *Human skin wounds: a major and snowballing threat to public health and the economy.* Wound Repair Regen, 2009. **17**(6): p. 763-71.
5. Kirketerp-Møller, K., K. Zulkowski, and G. James, *Chapter 2 - Chronic wound colonization, infection and biofilms.* Biofilm Infections. T. Bjarnsholt at al (eds.), 2011: p. 11-24.
6. Davies, C.E., et al., *A prospective study of the microbiology of chronic venous leg ulcers to reevaluate the clinical predictive value of tissue biopsies and swabs.* Wound Repair and Regeneration, 2007. **15**(1): p. 17-22.
7. Klein TM, A.V., Kirsten N, Protz K, Augustin M and Blome C., *Social participation of people with chronic wounds: A systematic review.* Int Wound J., 2021(18): p. 287–311.
8. Olsson M, J.K., Divakar U, Bajpai R, Upton Z, Schmidtchen A, and Car J., *The humanistic and economic burden of chronic wounds: A systematic review* Wound Repair Regen, 2019. **Jan 27**((1)): p. 114-125.
9. Arya, A.K., et al., *Recent advances on the association of apoptosis in chronic non healing diabetic wound.* World Jounal of Diabetes, 2014. **5**(6): p. 756-62.
10. Rani, S. and T. Ritter, *The Exosome - A Naturally Secreted Nanoparticle and its Application to Wound Healing.* Advanced Materials, 2016. **28**(27): p. 5542-52.
11. Singh, N., D.G. Armstrong, and B.A. Lipsky, *Preventing foot ulcers in patients with diabetes.* . JAMA, 2005. **293**(2): p. 217-228.
12. Boulton, A.J., et al., *The global burden of diabetic foot disease.* Lancet, 2005. **366**(9498): p. 1719-24.
13. Scully, T., *Diabetes in Numbers.* Nature, 2012. **485**(7398): p. S2-3.
14. Singer, A.J. and R.A. Clark, *Cutaneous wound healing.* N Engl J Med, 1999. **341**(10): p. 738-46.
15. Gurtner, G.C., et al., *Wound repair and regeneration.* Nature, 2008. **453**(7193): p. 314-21.
16. Demidova-Rice, T.N., M.R. Hamblin, and I.M. Herman, *Acute and impaired wound healing: pathophysiology and current methods for drug delivery, part 2: role of growth factors in normal and pathological wound healing: therapeutic potential and methods of delivery.* Advances in Skin & Wound Care., 2012. **25**(8): p. 349-70.
17. Eming, S.A., P. Martin, and M. Tomic-Canic, *Wound repair and regeneration: mechanisms, signaling, and translation.* Sci Transl Med, 2014. **6**(265): p. 265sr6.
18. Falanga, V., *Wound healing and its impairment in the diabetic foot.* Lancet, 2005. **366**(9498): p. 1736-43.
19. Bielefeld, K.A., S. Amini-Nik, and B.A. Alman, *Cutaneous wound healing: recruiting developmental pathways for regeneration.* Cell Mol Life Sci, 2013. **70**(12): p. 2059-81.
20. Demidova-Rice, T.N., M.R. Hamblin, and I.M. Herman, *Acute and impaired wound healing: pathophysiology and current methods for drug delivery, part 1: normal and chronic wounds: biology, causes, and approaches to care.* Adv Skin Wound Care, 2012. **25**(7): p. 304-14.
21. Wilkinson HN, H.M., *Wound healing: cellular mechanisms and pathological outcomes.* Open Biol., 2020. **10**: p. 200223.
22. Lavery, L.A., et al., *WHS guidelines update: Diabetic foot ulcer treatment guidelines.* Wound Repair and Regeneration, 2016. **24**(1): p. 112-26.
23. Frykberg, R.G. and J. Banks, *Challenges in the Treatment of Chronic Wounds.* Advances in Wound Care., 2015. **4**(9): p. 560-582.
24. Moura, L.I., et al., *Recent advances on the development of wound dressings for diabetic foot ulcer treatment--a review.* Acta Biomaterialia, 2013. **9**(7): p. 7093-114.
25. Boateng, J.S., et al., *Wound Healing Dressings and Drug Delivery Systems: A Review.* Journal of Pharmaceutical Sciences, 2008. **97**(8): p. 2892-923.
26. Das, S. and A.B. Baker, *Biomaterials and Nanotherapeutics for Enhancing Skin Wound Healing.* Frontiers in Bioengineering and Biotechnology, 2016. **4**(82): p. 1-20.
27. Mir, M., Ali, MN, Barakullah, A, Gulzar, A, Arshad, A, Fatima, S, and Asad, M., *Synthetic polymeric biomaterials for wound healing: a review.* Progress in Biomaterials, 2018(7): p. 1-21.

28. Smiell, J.M., et al., *Efficacy and safety of becaplermin (recombinant human platelet-derived growth factor-BB) in patients with nonhealing, lower extremity diabetic ulcers: a combined analysis of four randomized studies.* Wound Repair and Regeneration, 1999. **7**(5): p. 335-46.
29. Han, G., and Ceilly, R., *Chronic Wound Healing: A Review of Current Management and Treatments.* Adv Ther, 2017. **34**: p. 599-610.
30. Armstrong, D.G., A.J. Boulton, and P. Banwell, *Negative pressure wound therapy in treatment of diabetic foot wounds: a marriage of modalities.* Ostomy Wound Management, 2004. **50**: p. 9-12.
31. Banwell, P.E., *Topical negative pressure therapy in wound care.* Journal of Wound Care, 1999. **8**: p. 79-84.
32. Petrie, N., M. Potter, and P. Banwell, *The management of lower extremity wounds using topical negative pressure. .* The International Journal Low Extremity Wounds, 2003. **2**: p. 198-206.
33. Saxena, V., et al., *Vacuum-assisted closure: microdeformations of wounds and cell proliferation.* Plastic and Reconstructive Surgery, 2004. **114**(5): p. 1086-96; discussion 1097-8.
34. Scherer, S.S., et al., *The mechanism of action of the vacuum-assisted closure device.* Plastic and Reconstructive Surgery, 2008. **122**(3): p. 786-97.
35. Zamboni, W.A., L.K. Browder, and J. Martinez, *Hyperbaric oxygen and wound healing.* Clinics in Plastic Surgery, 2003. **30**(1): p. 67-75.
36. Wunderlich, R.P., E.J. Peters, and L.A. Lavery, *Systemic hyperbaric oxygen therapy: lower-extremity wound healing and the diabetic foot.* Diabetes Care, 2000. **23**(10): p. 1551-5.
37. Roeckl-Wiedmann, I., M. Bennett, and P. Kranke, *Systematic review of hyperbaric oxygen in the management of chronic wounds.* The British Journal of Surgery, 2005. **92**(1): p. 24-32.
38. Stoekenbroek, R.M., et al., *Hyperbaric oxygen for the treatment of diabetic foot ulcers: a systematic review.* European Journal of Vascular and Endovascular Surgery., 2014. **47**(6): p. 647-55.
39. Margolis, D.J., et al., *Lack of effectiveness of hyperbaric oxygen therapy for the treatment of diabetic foot ulcer and the prevention of amputation: a cohort study. .* Diabetes Care, 2013. **36**(7): p. 1961-6.
40. Fedorko, L., Bowen, JM, Jones, W, Oreopoulos, G, Goeree, R, Hopkins, RB, and O'Reilly, DJ, *Hyperbaric Oxygen Therapy Does Not Reduce Indications for Amputation in Patients With Diabetes With Nonhealing Ulcers of the Lower Limb: A Prospective, Double-Blind, Randomized Controlled Clinical Trial.* Diabetes Care, 2016. **39**((3)): p. 392-399.
41. Ennis, W.J., et al., *Current status of the use of modalities in wound care: electrical stimulation and ultrasound therapy.* Plastic and Reconstructive Surgery, 2011. **127**(Suppl 1): p. 93S-102S.
42. Graebert, J.K., et al., *Systemic evaluation of electrical stimulation for ischemic wound therapy in a preclinical model.* Advances in Wound Care., 2014. **3**(6): p. 428-37.
43. Kloth, L., *Electrical stimulation technologies for wound healing.* Advances in Wound Care., 2014. **3**(2): p. 81-90.
44. Baker, L.L., et al., *Effects of electrical stimulation on wound healing in patients with diabetic ulcers. .* Diabetes Care, 1997. **20**(3): p. 405-12.
45. Kloth, L., *Electrical stimulation for wound healing: a review of evidence from in vitro studies, animal experiments, and clinical trials.* International Journal of Low Extremity Wounds, 2005. **4**(1): p. 23-44.
46. McCulloch, J., *Electrical stimulation in wound repair.* Yee BY, ed. The Wound Management Manual. New York, NY: McGraw Hill., 2005: p. 80-9.
47. Frykberg, R., et al., *Cell proliferation induction: healing chronic wounds through low-energy pulsed radiofrequency. .* International Journal of Low Extremity Wounds, 2009. **8**(1): p. 45-51.
48. Frykberg, R.G., et al., *The use of pulsed radio frequency energy therapy in treating lower extremity wounds: results of a retrospective study of a wound registry.* Ostomy Wound Management, 2011. **57**(3): p. 22-9.
49. Wendelken, M.E., L. Markowitz, and O.M. Alvarez, *A closer look at ultrasonic debridement.* Podiatry Today, 2010. **23**(8): p. 23-8.
50. Chang, Y.R., J. Perry, and K. Cross, *Low-Frequency Ultrasound Debridement in Chronic Wound Healing: A Systematic Review of Current Evidence.* Plastic Surgery, 2017. **25**(1): p. 21-6.
51. Amini, S., et al., *Low-frequency ultrasound debridement in patients with diabetic foot ulcers and osteomyelitis.* Wounds, 2013. **25**(7): p. 193-8.
52. Stanisic, M.M., et al., *Wound debridement with 25 kHz ultrasound.* Advances in Skin & Wound Care., 2005. **18**(9): p. 484-90.

53. Dymarek, R., et al., *Extracorporeal shock wave therapy as an adjunct wound treatment: a systematic review of the literature.* Ostomy Wound Management, 2014. **60**(7): p. 26-39.
54. Mittermayr, R., et al., *Extracorporeal shock wave therapy (ESWT) for wound healing: technology, mechanisms, and clinical efficacy.* Wound Repair and Regeneration, 2012. **20**(4): p. 456-65.
55. Wang, C.J., R.W. Wu, and Y.J. Yang, *Treatment of diabetic foot ulcers: a comparative study of extracorporeal shockwave therapy and hyperbaric oxygen therapy.* Diabetes Research and Clinical Practice, 2011. **92**(2): p. 187-93.
56. Khan, M.N. and C.G. Davies, *Advances in the management of leg ulcers-the potential role of growth factors.* International Wound Journal, 2006. **3**(2): p. 113-20.
57. Li, V.W., E. Kung, and W. Li, *Molecular therapy for wounds: modalities for stimulating angiogenesis and granulation.* Yee BY, ed. The Wound Management Manual. New York, NY: McGraw Hill., 2005: p. 17-43.
58. Knighton, D.R., et al., *Stimulation of repair in chronic, nonhealing, cutaneous ulcers using plateletderived wound healing formula.* Surgery Gynecology & Obstetrics., 1990. **170**(1): p. 56-60.
59. Frykberg, R.G., et al., *Chronic wounds treated with a physiologically relevant concentration of platelet-rich plasma gel: a prospective case series. .* Ostomy Wound Management, 2010. **56**(6): p. 36-44.
60. Driver, V.R., et al., *A prospective, randomized, controlled trial of autologous platelet-rich plasma gel for the treatment of diabetic foot ulcers.* Ostomy Wound Management, 2006. **52**(6): p. 68-70, 72, 74 passim.
61. Ramos-Torrecillas, J., et al., *Clinical utility of growth factors and platelet-rich plasma in tissue regeneration: a review. .* Wounds, 2014. **26**(7): p. 207-13.
62. Steed, D.L., *Clinical evaluation of recombinant human platelet-derived growth factor for the treatment of lower extremity ulcers.* Plastic and Reconstructive Surgery, 2006. **117**(7 Suppl): p. 143S-9S; discussion 150S-1S.
63. Franklin, J.D. and J.B. Lynch, *Effects of topical applications of epidermal growth factor on wound healing. Experimental study on rabbit ears.* Plastic and Reconstructive Surgery, 1979. **64**(6): p. 766-70.
64. Falanga, V., et al., *Topical use of human recombinant epidermal growth factor (h-EGF) in venous ulcers.* The Journal of Dermatologic Surgery and Oncology, 1992. **18**(7): p. 604-6.
65. Fernandez-Montequin, J.I., et al., *Intra-lesional injections of recombinant human epidermal growth factor promote granulation and healing in advanced diabetic foot ulcers: multicenter, randomised, placebo-controlled, double-blind study.* International Wound Journal, 2009. **6**(6): p. 432-43.
66. Singla, S., et al., *Efficacy of topical application of beta urogastrone (recombinant human epidermal growth factor) in Wagner's Grade 1 and 2 diabetic foot ulcers: Comparative analysis of 50 patients.* Journal of Natural Science, Biology and Medicine., 2014. **5**(2): p. 273-7.
67. Ohura, T., et al., *Clinical efficacy of basic fibroblast growth factor on pressure ulcers: case-control pairing study using a new evaluation method.* Wound Repair and Regeneration, 2011. **19**(5): p. 542-51.
68. Robson, M.C., et al., *Randomized trial of topically applied repifermin (recombinant human keratinocyte growth factor-2) to accelerate wound healing in venous ulcers.* Wound Repair and Regeneration, 2001. **9**(5): p. 347-52.
69. Tagashir, S., et al., *Cloning of mouse FGF10 and up-regulation of its gene expression during wound healing.* Gene, 1997. **197**(1-2): p. 399-404.
70. Mulder, G., M. Tenenhaus, and G.F. D'Souza, *Reduction of diabetic foot ulcer healing times through use of advanced treatment modalities.* The International Journal of Lower Extremity Wounds, 2014. **13**(4): p. 335-46.
71. Schultz, G.S., et al., *Dynamic reciprocity in the wound microenvironment. .* Wound Repair and Regeneration, 2011. **19**(2): p. 134-48.
72. Greaves, N.S., et al., *The role of skin substitutes in the management of chronic cutaneous wounds.* Wound Repair and Regeneration, 2013. **21**(2): p. 194-210.
73. Badylak, S.F., D.O. Freytes, and T.W. Gilbert, *Extracellular matrix as a biological scaffold material: Structure and function.* Acta Biomaterialia, 2009. **5**(1): p. 1-13.
74. Reyzelman, A., et al., *Clinical effectiveness of an acellular dermal regenerative tissue matrix compared to standard wound management in healing diabetic foot ulcers: a prospective, randomised, multicentre study.* International Wound Journal, 2009. **6**(3): p. 196-208.

75. Landsman, A.S., et al., *A retrospective clinical study of 188 consecutive patients to examine the effectiveness of a biologically active cryopreserved human skin allograft (TheraSkin®) on the treatment of diabetic foot ulcers and venous leg ulcers.* Foot & Anckle Specialist., 2011. **4**(1): p. 29-41.
76. Sanders, L., et al., *A prospective, multicenter, randomized, controlled clinical trial comparing a bioengineered skin substitute to a human skin allograft.* Ostomy Wound Management, 2014. **60**(9): p. 26-38.
77. Yonehiro, L., G. Burleson, and V. Sauer, *Use of a new acellular dermal matrix for treatment of nonhealing wounds in the lower extremities of patients with diabetes.* Wounds, 2013. **25**(12): p. 340-4.
78. Koob, T.J., et al., *Biological properties of dehydrated human amnion/chorion composite graft: implications for chronic wound healing.* International Wound Journal, 2013. **10**(5): p. 493-500.
79. Maan, Z.N., et al., *Cell recruitment by amnion chorion grafts promotes neovascularization.* The Journal of Surgical Research., 2015. **193**(2): p. 953-62.
80. Eaglstein, W.H., ., V. Falanga, and A.W.C. 1998;11:1-8., *Tissue engineering and the development of Apligraf a human skin equivalent.* Advances in Wound Care, 1998. **11**(4 Suppl): p. 1-8.
81. Falanga, V., et al., *Rapid healing of venous ulcers and lack of clinical rejection with an allogeneic cultured human skin equivalent. Human Skin Equivalent Investigators Group.* Archives of Dermatology., 1998. **134**(3): p. 293-300.
82. Eaglstein, W.H., I. M., and K. Laszlo, *A composite skin substitute (graftskin) for surgical wounds. A clinical experience.* Dermatologic Surgery, 1995. **21**(10): p. 839-43.
83. Mansbridge, J., et al., *Three-dimensional fibroblast culture implant for the treatment of diabetic foot ulcers: metabolic activity and therapeutic range.* Tissue Engineering, 1998. **4**(4): p. 403-14.
84. Hart, C.E., A. Loewen-Rodriguez, and J. Lessem, *Dermagraft: Use in the Treatment of Chronic Wounds.* Advances in Wound Care, 2012. **1**(3): p. 123-41.
85. Naughton, G., J. Mansbridge, and G. Gentzkow, *A metabolically active human dermal replacement for the treatment of diabetic foot ulcers.* Artificial Organs, 1997. **21**(11): p. 1203-10.
86. Shin, L. and D.A. Peterson, *Human mesenchymal stem cell grafts enhance normal and impaired wound healing by recruiting existing endogenous tissue stem/progenitor cells.* Stem Cells Translational Medicine, 2013. **2**(1): p. 33-42.
87. Caplan, A.I., *Adult mesenchymal stem cells for tissue engineering versus regenerative medicine.* Journal Cell Phisiology, 2007. **213**(2): p. 341-7.
88. Maxson, S., et al., *Concise review: role of mesenchymal stem cells in wound repair.* Stem Cells Translational Medicine, 2012. **1**(2): p. 142-9.
89. Doi, H., et al., *Potency of umbilical cord blood- and Wharton's jelly-derived mesenchymal stem cells for scarless wound healing.* Scientific Reports, 2016. **6**: p. 18844.
90. Peng, Y., et al., *Mesenchymal stem cells: a revolution in therapeutic strategies of age-related diseases.* Ageing Research Reviews, 2013. **12**(1): p. 103-15.
91. Darwin, E., and Tomic-Canic, M., *Healing Chronic Wounds: Current Challenges and Potential Solutions.* Curr Dermatol Rep, 2018. **7**(4): p. 296-302.
92. Mahmoudi, M., and Gould, JL., *Opportunities and Challenges of the Management of Chronic Wounds: A Multidisciplinary Viewpoint.* Chronic Wound Care Management and Research, 2020. **7**: p. 27-36.
93. Papanas, N. and E. Maltezos, *Becaplermin gel in the treatment of diabetic neuropathic foot ulcers.* Clinical Intervations in aging., 2008. **3**(2): p. 233-40.
94. Laiva, A., O´Brien, FJ, and Keogh, MB, *Innovations in gene and growth factor delivery systems for diabetic wound healing.* J Tissue Eng Regen Med., 2018. **12**: p. e296-e312.
95. Amariglio, N., et al., *Donor-derived brain tumor following neural stem cell transplantation in an ataxia telangiectasia patient.* PLoS Med, 2009. **6**(2): p. e1000029.
96. Kansu, E., *Thrombosis in stem cell transplantation.* Hematology, 2012. **17 Suppl 1**: p. S159-62.
97. Herberts, C.A., M.S. Kwa, and H.P. Hermsen, *Risk factors in the development of stem cell therapy.* J Transl Med, 2011. **9**: p. 29.
98. O'Loughlin, A. and T. O'Brien, *Topical Stem and Progenitor Cell Therapy for Diabetic Foot Ulcers.* Stem Cells in Clinic and Research. Dr. Ali Gholamrezanezhad (Ed.), ISBN: 978-953-307-797-0, InTech., 2011.
99. Blumberg, S.N., et al., *The role of stem cells in treatment of diabetic foot ulcers.* Diabetes Research and Clinical Practice, 2012. **96**: p. 1-9.

100. Ojeh, N., et al., *Stem Cells in Skin Regeneration, Wound Healing, and Their Clinical Applications.* International Jounal of Molecular Sciences, 2015. **16**: p. 25476-25501.
101. Korrapati, P.S., et al., *Recent advancements in nanotechnological strategies in selection, design and delivery of biomolecules for skin regeneration.* Materials Science and Engineering C, 2016. **67**: p. 747-765.
102. Riha, S., Marrof, M, and Fauzi, MhB, *Synergistic Effect of Biomaterial and Stem Cell for Skin Tissue Engineering in Cutaneous Wound Healing: A Concise Review.* Polymers, 2021. **13**(1546): p. (2-28).
103. Pop, M., and Almquist, BD., *Biomaterials: A potential pathway to healing chronic wounds?* Exp Dermatol, 2017. **26**(9): p. 760-763.
104. Naskar, A., and Kim, K., *Recent Advances in Nanomaterial-Based Wound-Healing Therapeutics.* Pharmaceutics, 2020. **12**: p. 499 (1-20).
105. Annabi, N., Tamayol, A, Uquillas, JA, Akbari, M, Bertassoni, LE, Cha, C, Camci-Unal, G, Dokmeci, MR, Peppas, NA, and Khademhosseini, A., *25th Anniversary Article: Rational Design and Applications of Hydrogels in Regenerative Medicine.* Adv Mater, 2014. **26**(1): p. 85-124.
106. Gainza, G., et al., *Advances in drug delivery systems (DDSs) to release growth factors for wound healing and skin regeneration.* Nanomedicine, 2015. **11**(6): p. 1551-73.
107. Griffin, D., Weaver, WM, Scumpia, PO, Di-Carlo, D, Segura,T, *Accelerated wound healing by injectable microporous gel scaffolds assembled from annealed building blocks.* Nat. Mater., 2015. **14**(7): p. 737-744.
108. Neuman, M.G., et al., *Hyaluronic acid and wound healing.* J Pharm Pharm Sci, 2015. **18**(1): p. 53-60.
109. Burdick, J.A. and G.D. Prestwich, *Hyaluronic acid hydrogels for biomedical applications.* Adv Mater, 2011. **23**(12): p. H41-56.
110. Sun, G., et al., *Dextran hydrogel scaffolds enhance angiogenic responses and promote complete skin regeneration during burn wound healing.* Proc Natl Acad Sci U S A, 2011. **108**(52): p. 20976-81.
111. Lohmann, N., et al., *Glycosaminoglycan-based hydrogels capture inflammatory chemokines and rescue defective wound healing in mice.* Science Translacional Medicine, 2017. **9**(386): p. eaai9044.
112. Tavakoli, S., Kharaziha, M, Nemati, S, and Kalateh, A., *Nanocomposite hydrogel based on carrageenan-coated starch/cellulose nanofibers as a hemorrhage control material.* Carbohydrate Polymers, 2021. **251**: p. 117013.
113. Park, K., and Gerecht, S., *Hypoxia-Inducible Hydrogels.* Nat Commun, 2014. **5**: p. 4075 (1-26).
114. Song, A., Raine, AA, and Christman, KL., *Antibacterial and cell-adhesive polypeptide and poly(ethylene glycol) hydrogel as a potential scaffold for wound healing.* Acta Biomaterialia, 2012. **8**: p. 41-50.
115. Shi, Y., Truong, VX, Kulkarni, K, Qu, Y, Simon, GP, Boyd, RL, Perlmutter, P, Lithgow, T, and Forsythe, JS. , *Light-triggered release of ciprofloxacin from an in situ forming click hydrogel for antibacterial wound dressings.* J. Mater. Chem. B, 2015. **3**: p. 8771-8774.
116. Obara, K., Ishihara, M, Fujita, M, Kanatani, Y, Hattori, H, Matsui, T, Takase, B, Ozeki, Y, Nakamura, S, Ishizuka, T, Tominaga, S, Hiroi, S, Kawai, T, Maehara, T, *Acceleration of wound healing in healing-impaired db/db mice with a photocrosslinkable chitosan hydrogel containing fibroblast growth factor-2.* Wound Repair Regen, 2005. **13**(4): p. 390-397.
117. Jee, J.-P., Pangeni, R, Jha, SK, Byun, Y, and Parl, JW., *Preparation and in vivo evaluation of a topical hydrogel system incorporating highly skin-permeable growth factors, quercetin, and oxygen carriers for enhanced diabetic wound-healing therapy.* Int J Nanomedicine 2019. **14**: p. 5449-5475.
118. Ribeiro, M., et al., *Dextran-based hydrogel containing chitosan microparticles loaded with growth factors to be used in wound healing.* Mater Sci Eng C 2013. **33**: p. 2958-2966.
119. Ziv-Polat, O., et al., *Novel magnetic fibrin hydrogel scaffolds containing thrombin and growth factors conjugated iron oxide nanoparticles for tissue engineering.* International Jounal of Nanomedicine, 2012. **7**: p. 1259-74.
120. Tokatlian, T., Cam, C, Segura,T, *Porous hyaluronic acid hydrogels for localized nonviral DNA delivery in a diabetic wound healing model.* Adv Healthc Mater, 2015. **4**(7): p. 1084-1091.
121. Chen, S., Shi, J, Zhang, M, Chen, Y, Wang, X, Zhang, L, Tian, Z, Yan, Y, Li, Q, Zhong, W, Xing, M, Zhang, L, Zhang, L., *Mesenchymal stem cell-laden antiinflammatory hydrogel enhances diabetic wound healing.* Sci Rep, 2015. **5**: p. 18104 (1-12).

122. Zheng, X., Ding, Z, Cheng, W, Lu, Q, Kong, X, Zhou, X, Lu, X, and Kaplan, DL, *Microskin-Inspired Injectable MSC-Laden Hydrogels for Scarless Wound Healing with Hair Follicles.* Adv. Healthcare Mater., 2020: p. 2000041 (1-14).
123. Wang, C., Wang, M, Xu, T, Zhang, X, Lin, C, Gao, W, Xu, H, Lei, B, Mao,C, *Engineering Bioactive Self-Healing Antibacterial Exosomes Hydrogel for Promoting Chronic Diabetic Wound Healing and Complete Skin Regeneration.* Theranostics, 2019. **9**(1): p. 65-76.
124. Shi, Q., et al., *GMSC-Derived Exosomes Combined with a Chitosan/Silk Hydrogel Sponge Accelerates Wound Healing in a Diabetic Rat Skin Defect Model.* Frontiers in Physiology, 2017. **8**: p. 904.
125. Guo, S.C., et al., *Exosomes derived from platelet-rich plasma promote the re-epithelization of chronic cutaneous wounds via activation of YAP in a diabetic rat model.* Theranostics, 2017. **7**(1): p. 81-96.
126. Henriques-Antunes, H., et al., *The Kinetics of Small Extracellular Vesicle Delivery Impacts Skin Tissue Regeneration.* ACS Nano, 2019. **13**(8): p. 8694-8707.
127. Ziv-Polat, O., Topaz, M, Brosh, T, Margel, S., *Enhancement of incisional wound healing by thrombin conjugated iron oxide nanoparticles.* Biomaterials, 2010. **31**(4): p. 741-747.
128. Comune, M., et al., *Antimicrobial peptide-gold nanoscale therapeutic formulation with high skin regenerative potential.* Journal of Controlled Release, 2017. **262**: p. 58-71.
129. Han, G., Nguyen, L. N., Macherla, C., Chi, Y., Friedman, J. M., Nosanchuk, J. D., *Nitric oxide-releasing nanoparticles accelerate wound healing by promoting fibroblast migration and collagen deposition.* Am J Pathol, 2012. **April**(180): p. 1465-1473.
130. Hetrick EM, S.J., Paul HS, Schoenfisch MH, *Anti-biofilm efficacy of nitric oxide-releasing silica nanoparticles.* Biomaterials, 2009(30): p. 2782–2789.
131. Martinez, L., Han, G, Chacko, M, Mihu, MR, Jacobson, M, Gialanella, P, Friedman, AJ, Nosanchuk, JD, Friedman, JM, *Antimicrobial and healing efficacy of sustained release nitric oxide nanoparticles against Staphylococcus aureus skin infection.* J Invest Dermatol, 2009. **129**(10): p. 2463-2469.
132. Ferreira, A.M., et al., *Bioinspired porous membranes containing polymer nanoparticles for wound healing.* Journal of Biomedical Materials Research - Part A, 2014. **102**(12): p. 4394-405.
133. Shoba, E., Lakra, R, Kiran, MS, Korrapati,PS, *Design and development of papain–urea loaded PVA nanofibers for wound debridement.* RSC Adv., 2014. **4**(104): p. 60209-60215.
134. Tyrone, J., Mogford, JE, Chandler,LA, Ma, C, Xia, Y, Pierce, GF, Mustoe,TA, *Collagen-embedded platelet-derived growth factor DNA plasmid promotes wound healing in a dermal ulcer model.* J Surg Res, 2000. **93**(2): p. 230-236.
135. Sun, L., et al., *Transfection with aFGF cDNA improves wound healing.* The Journal of Investigatuve Dermatology, 1997. **108**(3): p. 313-8.
136. Li, N., Luo, H-C, Yang, C, Deng, J-J, Ren, M, Xie, X-Y, Lin, D_Z, Yan, Li, Zhang, L-M, *Cationic star-shaped polymer as an siRNA carrier for reducing MMP-9 expression in skin fibroblast cells and promoting wound healing in diabetic rats.* Int J Nanomedicine, 2014. **9**: p. 3377-3387.
137. Lucas, T., et al., *Light-inducible antimiR-92a as a therapeutic strategy to promote skin repair in healing-impaired diabetic mice.* Nature Communications, 2017. **8**: p. 15162.
138. Werner, S. and R. Grose, *Regulation of wound healing by growth factors and cytokines.* Physiological Reviews, 2003. **83**: p. 835-70.
139. Barrientos, S., et al., *Growth factors and cytokines in wound healing.* Wound Repair and Regeneration, 2008. **16**(5): p. 585-601.
140. Brown, G.L., et al., *Enhancement of wound healing by topical treatment with epidermal growth factor.* The New England Journal of Medicine, 1989. **321**(2): p. 76-9.
141. McGee, G.S., et al., *Recombinant basic fibroblast growth factor accelerates wound healing.* The Journal of Surgical Research., 1988. **45**(1): p. 145-53.
142. Phillips, L.G., et al., *Application of basic fibroblast growth factor may reverse diabetic wound healing impairment.* Annals of Plastic Surgery, 1993. **31**(4): p. 331-4.
143. Pierce, G.F., et al., *Detection of platelet-derived growth factor (PDGF)-AA in actively healing human wounds treated with recombinant PDGF-BB and absence of PDGF in chronic nonhealing wounds.* The Journal of Clinical Investigation., 1995. **96**(3): p. 1336-50.
144. Da Costa, R.M., et al., *Randomized, double-blind, placebo-controlled, dose- ranging study of granulocyte-macrophage colony stimulating factor in patients with chronic venous leg ulcers.* Wound Repair and Regeneration, 1999. **7**(1): p. 17-25.

145. Jaschke, E., A. Zabernigg, and C. Gattringer, *Recombinant human granulocyte-macrophage colony-stimulating factor applied locally in low doses enhances healing and prevents recurrence of chronic venous ulcers.* International Journal of Dermatology, 1999. **38**(5): p. 380-6.
146. Yildirimer, L., N.T. Thanh, and A.M. Seifalian, *Skin regeneration scaffolds: a multimodal bottom-up approach.* Trends in Biotechnology, 2012. **30**(12): p. 638-18.
147. Robson, M.C., et al., *Platelet-derived growth factor BB for the treatment of chronic pressure ulcers.* Lancet, 1992. **339**(8784): p. 23-5.
148. Robson, M.C., et al., *Recombinant human platelet-derived growth factor-BB for the treatment of chronic pressure ulcers.* Ann Plast Surg, 1992. **29**(3): p. 193-201.
149. Deonarine, K., et al., *Gene expression profiling of cutaneous wound healing.* Journal of Translational Medicine, 2007. **5**(11): p. 1-11.
150. Eming, S.A., T. Krieg, and J.M. Davidson, *Gene therapy and wound healing.* Clinics in Dermatology, 2007. **25**(1): p. 79-92.
151. Keswani, S.G., et al., *Adenoviral mediated gene transfer of PDGF-B enhances wound healing in type I and type II diabetic wounds.* Wound Repair and Regeneration, 2004. **12**(5): p. 497-504.
152. Marti, G., et al., *Electroporative transfection with KGF-1 DNA improves wound healing in a diabetic mouse model.* Gene Therapy, 2004. **11**(24): p. 1780-5.
153. Pastar, I., et al., *Micro-RNAs: New regulators of wound healing.* SURGICAL TECHNOLOGY INTERNATIONAL XXI, 2011. **December**(1): p. 51-60.
154. Moura, J., E. Børsheim, and E. Carvalho, *The role of microRNAs in diabetic complications - special emphasis on wound healing.* Genes, 2014. **5**: p. 926-956.
155. Li, P., et al., *Differentially expressed miRNAs in acute wound healing skin.* Medicine, 2015. **94**(7): p. e458.
156. Banerjee, J., Y.C. Chan, and C.K. Sen, *MicroRNAs in skin and wound healing.* Physiological Genomics, 2011. **43**: p. 543-556.
157. Fasanaro, P., et al., *microRNA: emerging therapeutic targets in acute ischemic diseases.* Pharmacol Ther, 2010. **125**(1): p. 92-104.
158. Pastar, I., et al., *Induction of specific microRNAs inhibits cutaneous wound healing.* The Journal of Bilogical Chemistry, 2012. **287**(35): p. 29324-35.
159. Wang, T., et al., *miR-21 regulates skin wound healing by targeting multiple aspects of the healing process.* The American Journal of Pathology, 2012. **181**(6): p. 1911-20.
160. Yang, X., et al., *miR-21 promotes keratinocyte migration and re-epithelialization during wound healing.* International Journal of Biological Sciences, 2011. **7**(5): p. 685-90.
161. Li, G., et al., *Fibroproliferative effect of microRNA-21 in hypertrophic scar derived fibroblasts.* Experimental Cell Research, 2016. **345**(1): p. 93-9.
162. Icli, B., et al., *Regulation of impaired angiogenesis in diabetic dermal wound healing by microRNA-26a.* Journal of Molecullar and Cellular Cardiology, 2016. **91**: p. 151-9.
163. Jarajapu, Y. and M. Grant, *The promise of cell-based therapies for diabetic complications: challenges and solutions.* Circ Res, 2010. **106**(5): p. 854-69.
164. Cha, J. and V. Falanga, *Stem cells in cutaneous wound healing.* Clin Dermatol, 2007. **25**(1): p. 73-8.
165. Mishra, P.J., P.J. Mishra, and D. Banerjee, *Cell-free derivatives from mesenchymal stem cells are effective in wound therapy.* World Journal of Stem Cells, 2012. **4**(5): p. 35-43.
166. Wu, Y., et al., *Mesenchymal stem cells enhance wound healing through differentiation and angiogenesis.* Stem Cells, 2007. **25**(10): p. 2648-59.
167. Shrestha, C., et al., *Enhanced healing of diabetic wounds by subcutaneous administration of human umbilical cord derived stem cells and their conditioned media.* International Journal of Endocrinology, 2013. **2013**: p. 592454.
168. Huang, S., et al., *Promotion of wound healing using adipose-derived stem cells in radiation ulcer of a rat model.* Journal of Biomedical Science., 2013. **20**: p. 51.
169. Rodriguez, J., et al., *Intradermal injection of human adipose-derived stem cells accelerates skin wound healing in nude mice.* Stem Cell Research and Therapy, 2015. **6**: p. 241 (1-11).
170. Sivan-Loukianova, E., et al., *CD34+ blood cells accelerate vascularization and healing of diabetic mouse skin wounds.* J Vasc Res, 2003. **40**(4): p. 368-77.
171. El-Mesallamy, H., et al., *Cell-based regenerative strategies for treatment of diabetic skin wounds, a comparative study between human umbilical cord blood-mononuclear cells and calves' blood haemodialysate.* PLoS One, 2014. **9**(3): p. e89853.
172. Valbonesi, M., et al., *Cord blood (CB) stem cells for wound repair. Preliminary report of 2 cases.* Transfus Apher Sci, 2004. **30**(2): p. 153-156.

173. Çil, N., et al., *Effects of umbilical cord blood stem cells on healing factors for diabetic foot injuries.* Biotechnic & Histochemistry, 2017. **92**(1): p. 15-28.
174. Pedroso, D.C., et al., *Improved survival, vascular differentiation and wound healing potential of stem cells co-cultured with endothelial cells.* PLoS One, 2011. **6**(1): p. e16114.
175. Suh, W., et al., *Transplantation of endothelial progenitor cells accelerates dermal wound healing with increased recruitment of monocytes/macrophages and neovascularization.* Stem Cells, 2005. **23**(10): p. 1571-8.
176. Mulder, G., D.K. Lee, and N. Faghihnia, *Autologous bone marrow-derived stem cells for chronic wounds of the lower extremity: a retrospective study.* Wounds, 2010. **22**(9): p. 219-25.
177. Falanga, V., et al., *Autologous bone marrow-derived cultured mesenchymal stem cells delivered in a fibrin spray accelerate healing in murine and human cutaneous wounds.* Tissue Eng, 2007. **13**(6): p. 1299-312.
178. Sîrbulescu, R.F., et al., *Mature B cells accelerate wound healing after acute and chronic diabetic skin lesions.* Wound Repair and Regeneration, 2017. **25**(5): p. 774-91.
179. Lee, S., J. Lee, and K. Cho, *Effects of Human Adipose-derived Stem Cells on Cutaneous Wound Healing in Nude Mice.* Annals of Dermatology, 2011. **23**(2): p. 150-5.
180. Kanji, S., et al., *Nanofiber-expanded human umbilical cord blood-derived CD34+ cell therapy accelerates murine cutaneous wound closure by attenuating pro-inflammatory factors and secreting IL-10.* Stem Cell Research, 2014. **12**(1): p. 275-88.
181. Tong, C., et al., *Hypoxia pretreatment of bone marrow-derived mesenchymal stem cells seeded in a collagen-chitosan sponge scaffold promotes skin wound healing in diabetic rats with hindlimb ischemia.* Wound Repair and Regeneration, 2016. **24**(1): p. 45-56.
182. Clinicaltrials.gov, *Cell therapies clinical trials for chronic ulcers (https://clinicaltrials.gov/ct2/results?term=cell+therapy&cond=Chronic+Ulcer).* 2018.
183. Clinicaltrials.gov, *Map of cell therapies clinical trials for chronic ulcers (https://clinicaltrials.gov/ct2/results/map?term=cell+therapy&cond=Chronic+Ulcer&map=).* 2018.
184. Beer, L., et al., *Peripheral blood mononuclear cell secretome for tissue repair.* Apoptosis, 2016. **21**(12): p. 1336-53.
185. Mildner, M., et al., *Secretome of peripheral blood mononuclear cells enhances wound healing.* PLoS One, 2013. **8**(3): p. e60103.
186. Hacker, S., et al., *Paracrine Factors from Irradiated Peripheral Blood Mononuclear Cells Improve Skin Regeneration and Angiogenesis in a Porcine Burn Model.* Scientific Reports, 2016. **6**: p. 25168.
187. Simader, E., et al., *Safety and tolerability of topically administered autologous, apoptotic PBMC secretome (APOSEC) in dermal wounds: a randomized Phase 1 trial (MARSYAS I).* Scientific Reports, 2017. **7**(1): p. 6216.
188. Himal, I., U. Goyal, and M. Ta, *Evaluating Wharton's Jelly-Derived Mesenchymal Stem Cell's Survival, Migration, and Expression of Wound Repair Markers under Conditions of Ischemia-Like Stress.* Stem Cells International, 2017. **20017**: p. 5259849.
189. Ratajczak, M.Z., et al., *Pivotal role of paracrine effects in stem cell therapies in regenerative medicine: can we translate stem cell-secreted paracrine factors and microvesicles into better therapeutic strategies?* Leukemia, 2012. **26**(6): p. 1166-73.
190. Yu, B., X. Zhang, and X. Li, *Exosomes derived from mesenchymal stem cells.* Int J Mol Sci, 2014. **15**(3): p. 4142-57.
191. Than, U.T.T., et al., *Association of Extracellular Membrane Vesicles with Cutaneous Wound Healing.* International Journal of Molecular Sciences, 2017. **18**(5): p. pii: E956.
192. Kalra, H., et al., *Vesiclepedia: a compendium for extracellular vesicles with continuous community annotation.* PLoS Biology, 2012. **10**(12): p. e1001450.
193. Kim, D.-K., et al., *EVpedia: a community web portal for extracellular vesicles research.* Bioinformatics, 2015. **31**(6): p. 933-9.
194. Quezada, C., et al., *Role of extracellular vesicles in glioma progression.* Molecular Aspects of Medicine, 2017. **S0098-2997**(17): p. 30094-8.
195. Alcayaga-Miranda, F., M. Varas-Godoy, and M. Khoury, *Harnessing the Angiogenic Potential of Stem Cell-Derived Exosomes for Vascular Regeneration.* Stem Cells International, 2016. **2016**: p. 3409169.
196. Gyorgy, B., et al., *Membrane vesicles, current state-of-the-art: emerging role of extracellular vesicles.* Cell Mol Life Sci, 2011. **68**(16): p. 2667-88.

197. EL Andaloussi, S., et al., *Extracellular vesicles: biology and emerging therapeutic opportunities.* Nat Rev Drug Discov, 2013. **12**(5): p. 347-57.
198. Elmore, S., *Apoptosis: a review of programmed cell death.* Toxicologic Pathology, 2007. **35**(4): p. 495-516.
199. Simpson, R.J. and S. Mathivanan, *Extracellular microvesicles: The need for internationally tecognised nomenclature and stringent purification criteria.* Journal of Proteomics and Bioinformatics, 2012. **5**: p. 2.
200. Théry, C., M. Ostrowski, and E. Segura, *Membrane vesicles as conveyors of immune responses.* Nature Reviews. Immunology., 2009. **9**(8): p. 581-93.
201. Stoorvogel, W., et al., *The biogenesis and functions of exosomes.* Traffic, 2002. **3**(5): p. 321-30.
202. Valadi, H., et al., *Exosome-mediated transfer of mRNAs and microRNAs is a novel mechanism of genetic exchange between cells.* Nat Cell Biol, 2007. **9**(6): p. 654-9.
203. Thery, C., L. Zitvogel, and S. Amigorena, *Exosomes: composition, biogenesis and function.* Nat Rev Immunol, 2002. **2**(8): p. 569-79.
204. Keerthikumar, S., et al., *ExoCarta: A Web-Based Compendium of Exosomal Cargo.* Journal of Molecular Biology, 2016. **428**(4): p. 688-92.
205. Mathivanan, S., et al., *ExoCarta 2012: database of exosomal proteins, RNA and lipids.* Nucleic Acids Res, 2012. **40**(Database issue): p. D1241-4.
206. Mathiyalagan, P., et al., *Angiogenic Mechanisms of Human CD34+ Stem Cell Exosomes in the Repair of Ischemic Hindlimb.* Circulation research, 2017. **120**(9): p. 1466-1476.
207. Zhang, J., et al., *Exosomes Derived from Human Endothelial Progenitor Cells Accelerate Cutaneous Wound Healing by Promoting Angiogenesis Through Erk1/2 Signaling.* International Journal Biological Sciences, 2016. **12**(12): p. 1472-1487.
208. Phinney, D.G. and M.F. Pittenger, *Concise Review: MSC-Derived Exosomes for Cell-Free Therapy.* Stem Cells, 2017. **35**(4): p. 851-8.
209. Akyurekli, C., et al., *A systematic review of preclinical studies on the therapeutic potential of mesenchymal stromal cell-derived microvesicles.* Stem Cell Reviews, 2015. **11**(1): p. 150-60.
210. Laberge, A., S. Arif, and V.J. Moulin, *Microvesicles: intercellular messegers in cutaneous wound healing.* Journal of Cellular Physiology, 2018. **[Epub ahead of print]**.
211. Bjørge, I.M., et al., *Extracellular vesicles, exosomes and shedding vesicles in regenerative medicine - a new paradigm for tissue repair.* Biomaterials Science, 2018. **6**(1): p. 60-78.
212. Golchin, A., S. Hosseinzadeh, and A. Ardeshirylajimi, *The Exosomes Released from Different Cell types and Their Effects in Wound Healing.* Journal of Cellular Biochemistry, 2018. **[Epub ahead of print]**.
213. Chen, B., et al., *Stem Cell-Derived Extracellular Vesicles as a Novel Potential Therapeutic Tool for Tissue Repair.* Stem Cells Translational Medicine, 2017. **6**(9): p. 1753-8.
214. Basu, J. and J.W. Ludlow, *Exosomes for repair, regeneration and rejuvenation.* Expert Opinion on Biological Therapy, 2016. **16**(4): p. 489-506.
215. Hettich, B., Greenwald, MB-Y, Werner, S, Leroux, J-C, *Exosomes for Wound Healing: Purification Optimization and Identification of Bioactive Components.* Adv Sci (Weinh), 2020. **7**(23): p. 2002596.
216. Fang, S., et al., *Umbilical Cord-Derived Mesenchymal Stem Cell-Derived Exosomal MicroRNAs Suppress Myofibroblast Differentiation by Inhibiting the Transforming Growth Factor-β/SMAD2 Pathway During Wound Healing.* Stem Cells Translational Medicine, 2016. **5**(10): p. 1425-39.
217. Tao, S., et al., *Chitosan Wound Dressings Incorporating Exosomes Derived from MicroRNA-126-Overexpressing Synovium Mesenchymal Stem Cells Provide Sustained Release of Exosomes and Heal Full-Thickness Skin Defects in a Diabetic Rat Model.* Stem Cells Transl Med, 2017. **6**(3): p. 736-747.
218. Xiong, Y., Chen, L, Yan, C, Hu, Y, Zhou, W, Cao, F, Xue, H, Hu, L, Lin, Z, Xie, X, Mi, B, Liu, G, *All-in-One: Multifunctional Hydrogel Accelerates Oxidative Diabetic Wound Healing through Timed-Release of Exosome and Fibroblast Growth Factor.* Small, 2021. **e2104229**: p. 1-14.
219. Zhang, Y., Zhang, P, Gao, X, Chang, L, Chen, Z, Mei, X, *Preparation of exosomes encapsulated nanohydrogel for accelerating wound healing of diabetic rats by promoting angiogenesis.* Mater Sci Eng C Mater Biol Appl, 2021. **120**: p. 111671.
220. Wu, K., He, C, Wu, Y, Zhou, X, Liy, P, Tang, W, Yu, M, Tian, W, *Preservation of Small Extracellular Vesicle in Gelatin Methacryloyl Hydrogel Through Reduced Particles Aggregation for Therapeutic Applications.* Int J Nanomedicine, 2021. **16**: p. 7831–7846.

221. Oh, E., Gangadaran, P, Rajendran, RL, Kim, HM, Oh, JM, Choi, KY, Chung, HY, Ahn,B-C, *Extracellular vesicles derived from fibroblasts promote wound healing by optimizing fibroblast and endothelial cellular functions.* Stem Cells, 2021. **39**(3): p. 266-279.
222. Li, X., C. Jiang, and J. Zhao, *Human endothelial progenitor cells-derived exosomes accelerate cutaneous wound healing in diabetic rats by promoting endothelial function.* Journal of Diabetes and its Complications, 2016. **30**(6): p. 986-92.
223. Ti, D., et al., *LPS-preconditioned mesenchymal stromal cells modify macrophage polarization for resolution of chronic inflammation via exosome-shuttled let-7b.* J Transl Med, 2015. **13**: p. 308.
224. Wang, C., Wang, M, Xu, T, Zhang, X, Lin, C, Gao, W, Xu, H, Lei, B, Mao,C, *Engineering Bioactive Self-Healing Antibacterial Exosomes Hydrogel for Promoting Chronic Diabetic Wound Healing and Complete Skin Regeneration: Erratum.* Theranostics, 2021. **11**(20): p. 10174–10175.
225. Geiger, A., A. Walker, and E. Nissen, *Human fibrocyte-derived exosomes accelerate wound healing in genetically diabetic mice.* Biochem Biophys Res Commun, 2015. **467**(2): p. 303-9.
226. Hu, Y., et al., *Exosomes from human umbilical cord blood accelerate cutaneous wound healing through miR-21-3p-mediated promotion of angiogenesis and fibroblast function.* Theranostics, 2018. **8**(1): p. 169-84.
227. El-Tookhy, O.S., et al., *Histological Evaluation of Experimentally Induced Critical Size Defect Skin Wounds Using Exosomal Solution of Mesenchymal Stem Cells Derived Microvesicles.* International Journal of Stem Cells, 2017. **10**(2): p. 144-53.
228. Ferreira, A.D.F., et al., *Extracellular Vesicles from Adipose-Derived Mesenchymal Stem/Stromal Cells Accelerate Migration and Activate AKT Pathway in Human Keratinocytes and Fibroblasts Independently of miR-205 Activity.* Stem Cells International, 2017. **2017**: p. 9841035.
229. Hu, L., et al., *Exosomes derived from human adipose mensenchymal stem cells accelerates cutaneous wound healing via optimizing the characteristics of fibroblasts.* Sci Rep, 2016. **6**: p. 32993.
230. Wang, L., et al., *Exosomes secreted by human adipose mesenchymal stem cells promote scarless cutaneous repair by regulating extracellular matrix remodelling.* Sci Rep, 2017. **7**(1): p. 13321.
231. Zhang, J., et al., *Exosomes released from human induced pluripotent stem cells-derived MSCs facilitate cutaneous wound healing by promoting collagen synthesis and angiogenesis.* Journal of Translational Medicine, 2015. **13**: p. 49.
232. Zhao, B., et al., *Exosomes derived from human amniotic epithelial cells accelerate wound healing and inhibit scar formation.* Journal of Molecular Histology, 2017. **48**(2): p. 121-32.
233. Ranghino, A., et al., *Endothelial progenitor cell-derived microvesicles improve neovascularization in a murine model of hindlimb ischemia.* International Journal of Immunopathology and Pharmacology, 2012. **25**(1): p. 75-85.
234. Zhang, B., et al., *HucMSC-Exosome Mediated-Wnt4 Signaling Is Required for Cutaneous Wound Healing.* Stem Cells, 2015. **33**(7): p. 2158-68.
235. Zhang, B., et al., *Human umbilical cord mesenchymal stem cell exosomes enhance angiogenesis through the Wnt4/beta-catenin pathway.* Stem Cells Transl Med, 2015. **4**(5): p. 513-22.
236. Li, X., et al., *Exosome Derived From Human Umbilical Cord Mesenchymal Stem Cell Mediates MiR-181c Attenuating Burn-induced Excessive Inflammation.* EBioMedicine, 2016. **8**: p. 72-82.
237. Shabbir, A., et al., *Mesenchymal Stem Cell Exosomes Induce Proliferation and Migration of Normal and Chronic Wound Fibroblasts, and Enhance Angiogenesis In Vitro.* Stem Cells Dev, 2015. **24**(14): p. 1635-47.
238. Clinicaltrials.gov, *Effect of Plasma Derived Exosomes on Cutaneous Wound Healing (https://ClinicalTrials.gov/show/NCT02565264).* 2018.
239. Raposo, G. and W. Stoorvogel, *Extracellular vesicles: exosomes, microvesicles, and friends.* The Journal of Cell Biology, 2013. **200**(4): p. 373-83.
240. Stoorvogel, W., et al., *Late endosomes derive from early endosomes by maturation.* Cell, 1991. **65**(3): p. 417-27.
241. Novikoff, A.B., E. Essner, and N. Quintana, *Golgi Apparatus and Lysosomes.* Fed Proc, 1964. **23**: p. 1010-22.
242. Keller, S., et al., *Exosomes: from biogenesis and secretion to biological function.* Immunol Lett, 2006. **107**(2): p. 102-8.
243. Kowal, J., M. Tkach, and C. Thery, *Biogenesis and secretion of exosomes.* Curr Opin Cell Biol, 2014. **29**: p. 116-25.
244. Colombo, M., G. Raposo, and C. Thery, *Biogenesis, secretion, and intercellular interactions of exosomes and other extracellular vesicles.* Annu Rev Cell Dev Biol, 2014. **30**: p. 255-89.

245. Trams, E.G., et al., *Exfoliation of membrane ecto-enzymes in the form of micro-vesicles.* Biochimica et Biophysica Acta, 1981. **645**(1): p. 63-70.
246. Harding, C., J. Heuser, and P. Stahl, *Endocytosis and intracellular processing of transferrin and colloidal gold-transferrin in rat reticulocytes: demonstration of a pathway for receptor shedding.* European Journal of Cell Biology, 1984. **35**(2): p. 256-63.
247. Pan, B.T., et al., *Electron microscopic evidence for externalization of the transferrin receptor in vesicular form in sheep reticulocytes.* Journal Cell Biology, 1985. **101**(3): p. 942-8.
248. Johnstone, R.M., et al., *Vesicle formation during reticulocyte maturation. Association of plasma membrane activities with released vesicles (exosomes).* J Biol Chem, 1987. **262**(19): p. 9412-20.
249. Raposo, G., et al., *B lymphocytes secrete antigen-presenting vesicles.* The Journal of Experimental Medicine., 1996. **183**(3): p. 1161-72.
250. Zitvogel, L., et al., *Eradication of established murine tumors using a novel cell-free vaccine: dendritic cell-derived exosomes.* Nature Medicine, 1998. **4**(5): p. 594-600.
251. Möbius, W., et al., *Immunoelectron microscopic localization of cholesterol using biotinylated and non-cytolytic perfringolysin O.* The Journal of Histchemistry and Cytochemistry, 2002. **50**(1): p. 43-55.
252. Johnstone, R.M., *Exosomes biological significance: A concise review.* Blood Cells, Molecules, and Diseases, 2006. **36**(2): p. 315-21.
253. Wubbolts, R., et al., *Proteomic and biochemical analyses of human B cell-derived exosomes. Potential implications for their function and multivesicular body formation.* The Journal of Biological Chemistry, 2003. **278**(13): p. 10963-72.
254. White, I.J., et al., *EGF stimulates annexin 1-dependent inward vesiculation in a multivesicular endosome subpopulation.* The EMBO Journal, 2006. **25**(1): p. 1-12.
255. Raiborg, C. and H. Stenmark, *The ESCRT machinery in endosomal sorting of ubiquitylated membrane proteins.* Nature, 2009. **458**(7237): p. 445-52.
256. Hurley, J.H., *The ESCRT complexes.* Crit Rev Biochem Mol Biol, 2010. **45**(6): p. 463-87.
257. Fader, C.M. and M.I. Colombo, *Autophagy and multivesicular bodies: two closely related partners.* Cell Death Differ, 2009. **16**(1): p. 70-8.
258. Lo Cicero, A., P.D. Stahl, and G. Raposo, *Extracellular vesicles shuffling intercellular messages: for good or for bad.* Curr Opin Cell Biol, 2015. **35**: p. 69-77.
259. Ludwig, A.K. and B. Giebel, *Exosomes: small vesicles participating in intercellular communication.* Int J Biochem Cell Biol, 2012. **44**(1): p. 11-5.
260. Geminard, C., et al., *Degradation of AP2 during reticulocyte maturation enhances binding of hsc70 and Alix to a common site on TFR for sorting into exosomes.* Traffic, 2004. **5**(3): p. 181-93.
261. Baietti, M.F., et al., *Syndecan-syntenin-ALIX regulates the biogenesis of exosomes.* Nat Cell Biol, 2012. **14**(7): p. 677-85.
262. Tamai, K., et al., *Exosome secretion of dendritic cells is regulated by Hrs, an ESCRT-0 protein.* Biochem Biophys Res Commun, 2010. **399**(3): p. 384-90.
263. Thery, C., et al., *Proteomic analysis of dendritic cell-derived exosomes: a secreted subcellular compartment distinct from apoptotic vesicles.* J Immunol, 2001. **166**(12): p. 7309-18.
264. Manohar, S., et al., *Chromatin modifying protein 1A (Chmp1A) of the endosomal sorting complex required for transport (ESCRT)-III family activates ataxia telangiectasia mutated (ATM) for PanC-1 cell growth inhibition.* Cell Cycle, 2011. **10**(15): p. 2529-39.
265. Yu, X., S.L. Harris, and A.J. Levine, *The regulation of exosome secretion: a novel function of the p53 protein.* Cancer Res, 2006. **66**(9): p. 4795-801.
266. Colombo, M., et al., *Analysis of ESCRT functions in exosome biogenesis, composition and secretion highlights the heterogeneity of extracellular vesicles.* J Cell Sci, 2013. **126**(Pt 24): p. 5553-65.
267. Beer, K.B. and A.M. Wehman, *Mechanisms and functions of extracellular vesicle release in vivo – What we can learn from flies and worms.* Cell Adhesion and Migration, 2017. **11**(2): p. 135-50.
268. van Niel, G., et al., *The tetraspanin CD63 regulates ESCRT-independent and -dependent endosomal sorting during melanogenesis.* Dev Cell, 2011. **21**(4): p. 708-21.
269. Wolfers, J., et al., *Tumor-derived exosomes are a source of shared tumor rejection antigens for CTL cross-priming.* Nat Med, 2001. **7**(3): p. 297-303.
270. Trajkovic, K., et al., *Ceramide triggers budding of exosome vesicles into multivesicular endosomes.* Science, 2008. **319**(5867): p. 1244-7.
271. Simons, M. and G. Raposo, *Exosomes--vesicular carriers for intercellular communication.* Curr Opin Cell Biol, 2009. **21**(4): p. 575-81.

272. Buschow, S.I., et al., *MHC II in dendritic cells is targeted to lysosomes or T cell-induced exosomes via distinct multivesicular body pathways.* Traffic, 2009. **10**(10): p. 1528-42.
273. Faure, J., et al., *Exosomes are released by cultured cortical neurones.* Mol Cell Neurosci, 2006. **31**(4): p. 642-8.
274. Lachenal, G., et al., *Release of exosomes from differentiated neurons and its regulation by synaptic glutamatergic activity.* Mol Cell Neurosci, 2011. **46**(2): p. 409-18.
275. Savina, A., et al., *Rab11 promotes docking and fusion of multivesicular bodies in a calcium-dependent manner.* Traffic, 2005. **6**(2): p. 131-43.
276. Raposo, G., et al., *Accumulation of major histocompatibility complex class II molecules in mast cell secretory granules and their release upon degranulation.* Mol Biol Cell, 1997. **8**(12): p. 2631-45.
277. Cai, H., K. Reinisch, and S. Ferro-Novick, *Coats, tethers, Rabs, and SNAREs work together to mediate the intracellular destination of a transport vesicle.* Dev Cell, 2007. **12**(5): p. 671-82.
278. Rashed, M.H., et al., *Exosomes: From Garbage Bins to Promising Therapeutic Targets.* Int J Mol Sci, 2017. **18**(3).
279. Rao, S.K., et al., *Identification of SNAREs involved in synaptotagmin VII-regulated lysosomal exocytosis.* J Biol Chem, 2004. **279**(19): p. 20471-9.
280. Proux-Gillardeaux, V., et al., *Expression of the Longin domain of TI-VAMP impairs lysosomal secretion and epithelial cell migration.* Biol Cell, 2007. **99**(5): p. 261-71.
281. Gross, J.C., et al., *Active Wnt proteins are secreted on exosomes.* Nat Cell Biol, 2012. **14**(10): p. 1036-45.
282. Savina, A., M. Vidal, and M.I. Colombo, *The exosome pathway in K562 cells is regulated by Rab11.* J Cell Sci, 2002. **115**(Pt 12): p. 2505-15.
283. Raposo, G., M.S. Marks, and D.F. Cutler, *Lysosome-related organelles: driving post-Golgi compartments into specialisation.* Curr Opin Cell Biol, 2007. **19**(4): p. 394-401.
284. Ostrowski, M., et al., *Rab27a and Rab27b control different steps of the exosome secretion pathway.* Nat Cell Biol, 2010. **12**(1): p. 19-30; sup pp 1-13.
285. Hsu, C., et al., *Regulation of exosome secretion by Rab35 and its GTPase-activating proteins TBC1D10A-C.* J Cell Biol, 2010. **189**(2): p. 223-32.
286. Belting, M. and H.C. Christianson, *Role of exosomes and microvesicles in hypoxia-associated tumour development and cardiovascular disease.* Journal of Internal Medicine., 2015. **278**(3): p. 251-63.
287. Caby, M.P., et al., *Exosomal-like vesicles are present in human blood plasma.* Int Immunol, 2005. **17**(7): p. 879-87.
288. Cheng, L., et al., *Exosomes provide a protective and enriched source of miRNA for biomarker profiling compared to intracellular and cell-free blood.* J Extracell Vesicles, 2014. **3**.
289. Gallo, A., et al., *The majority of microRNAs detectable in serum and saliva is concentrated in exosomes.* PLoS One, 2012. **7**(3): p. e30679.
290. Ogawa, Y., et al., *Proteomic analysis of two types of exosomes in human whole saliva.* Biol Pharm Bull, 2011. **34**(1): p. 13-23.
291. Pisitkun, T., R.F. Shen, and M.A. Knepper, *Identification and proteomic profiling of exosomes in human urine.* Proc Natl Acad Sci U S A, 2004. **101**(36): p. 13368-73.
292. Keller, S., et al., *CD24 is a marker of exosomes secreted into urine and amniotic fluid.* Kidney Int, 2007. **72**(9): p. 1095-102.
293. Asea, A., et al., *Heat shock protein-containing exosomes in mid-trimester amniotic fluids.* J Reprod Immunol, 2008. **79**(1): p. 12-7.
294. Ronquist, G. and I. Brody, *The prostasome: its secretion and function in man.* Biochim Biophys Acta, 1985. **822**(2): p. 203-18.
295. Aalberts, M., et al., *Identification of distinct populations of prostasomes that differentially express prostate stem cell antigen, annexin A1, and GLIPR2 in humans.* Biol Reprod, 2012. **86**(3): p. 82.
296. Admyre, C., et al., *Exosomes with immune modulatory features are present in human breast milk.* J Immunol, 2007. **179**(3): p. 1969-78.
297. Vella, L.J., et al., *Packaging of prions into exosomes is associated with a novel pathway of PrP processing.* J Pathol, 2007. **211**(5): p. 582-90.
298. Chiasserini, D., et al., *Proteomic analysis of cerebrospinal fluid extracellular vesicles: a comprehensive dataset.* J Proteomics, 2014. **106**: p. 191-204.
299. Hade, M.D.S., C.N.; Suo, Z. , *Mesenchymal Stem Cell-Derived Exosomes: Applications in Regenerative Medicine.* Cells, 2021. **10**: p. 1959.

300. Hoang, D., Nguyen, TD, Nguyen, H-P, Nguyen, X-H, Do, PTX, Dang, VD, Dam, PTM, Bui, HTH, Trinh, MQ, Vu, DM, Hoang, NTM, Thanh, LN, Than, UTT, *Differential Wound Healing Capacity of Mesenchymal Stem Cell-Derived Exosomes Originated From Bone Marrow, Adipose Tissue and Umbilical Cord Under Serum- and Xeno-Free Condition.* Front. Mol. Biosci., 2020. **7**: p. 119.
301. Caballero, S., et al., *Ischemic vascular damage can be repaired by healthy, but not diabetic, endothelial progenitor cells.* Diabetes, 2007. **56**(4): p. 960-7.
302. Schatteman, G.C. and N. Ma, *Old bone marrow cells inhibit skin wound vascularization.* Stem Cells, 2006. **24**(3): p. 717-21.
303. Agarwal, U., et al., *Experimental, Systems, and Computational Approaches to Understanding the MicroRNA-Mediated Reparative Potential of Cardiac Progenitor Cell-Derived Exosomes From Pediatric Patients.* Circ Res, 2017. **120**(4): p. 701-712.
304. Sun, J.M. and J. Kurtzberg, *Regenerative Potential of Cord Blood.* Umbilical Cord Blood Banking and Transplantation, Ballen, K. (ed.), 2014. **XIII**(286).
305. Eitan, E., et al., *Age-Related Changes in Plasma Extracellular Vesicle Characteristics and Internalization by Leukocytes.* Sci Rep, 2017. **7**(1): p. 1342.
306. Fafián-Labora, J., et al., *Effect of age on pro-inflammatory miRNAs contained in mesenchymal stem cell-derived extracellular vesicles.* Sci Rep, 2016. **7**: p. 43923.
307. Beer, L., et al., *Analysis of the Secretome of Apoptotic Peripheral Blood Mononuclear Cells: Impact of Released Proteins and Exosomes for Tissue Regeneration.* Sci Rep, 2015. **5**: p. 16662.
308. Dozio, V. and J.C. Sanchez, *Characterisation of extracellular vesicle-subsets derived from brain endothelial cells and analysis of their protein cargo modulation after TNF exposure.* J Extracell Vesicles, 2017. **6**(1): p. 1302705.
309. Feng, Y., et al., *Ischemic preconditioning potentiates the protective effect of stem cells through secretion of exosomes by targeting Mecp2 via miR-22.* PLoS One, 2014. **9**(2): p. e88685.
310. Kucharzewska, P., et al., *Exosomes reflect the hypoxic status of glioma cells and mediate hypoxia-dependent activation of vascular cells during tumor development.* Proc Natl Acad Sci U S A, 2013. **110**(18): p. 7312-7.
311. Ohyashiki, J.H., T. Umezu, and K. Ohyashiki, *Exosomes promote bone marrow angiogenesis in hematologic neoplasia: the role of hypoxia.* Curr Opin Hematol, 2016. **23**(3): p. 268-73.
312. Kastelowitz, N. and H. Yin, *Exosomes and microvesicles: identification and targeting by particle size and lipid chemical probes.* Chembiochem, 2014. **15**(7): p. 923-8.
313. Skotland, T., K. Sandvig, and A. Llorente, *Lipids in exosomes: Current knowledge and the way forward.* Prog Lipid Res, 2017. **66**: p. 30-41.
314. Record, M., et al., *Exosomes as new vesicular lipid transporters involved in cell-cell communication and various pathophysiologies.* Biochim Biophys Acta, 2014. **1841**(1): p. 108-20.
315. Ferguson, S.W. and J. Nguyen, *Exosomes as therapeutics: The implications of molecular composition and exosomal heterogeneity.* J Control Release, 2016. **228**: p. 179-190.
316. Laulagnier, K., et al., *Mast cell- and dendritic cell-derived exosomes display a specific lipid composition and an unusual membrane organization.* Biochem J, 2004. **380**(Pt 1): p. 161-71.
317. Subra, C., et al., *Exosome lipidomics unravels lipid sorting at the level of multivesicular bodies.* Biochimie, 2007. **89**(2): p. 205-12.
318. Llorente, A., et al., *Molecular lipidomics of exosomes released by PC-3 prostate cancer cells.* Biochim Biophys Acta, 2013. **1831**(7): p. 1302-9.
319. Mulcahy, L.A., R.C. Pink, and D.R. Carter, *Routes and mechanisms of extracellular vesicle uptake.* J Extracell Vesicles, 2014. **3**.
320. Kobayashi, T., F. Gu, and J. Gruenberg, *Lipids, lipid domains and lipid-protein interactions in endocytic membrane traffic.* Semin Cell Dev Biol, 1998. **9**(5): p. 517-26.
321. Urbanelli, L., et al., *Signaling pathways in exosomes biogenesis, secretion and fate.* Genes (Basel), 2013. **4**(2): p. 152-70.
322. Chu, Z., D.P. Witte, and X. Qi, *Saposin C-LBPA interaction in late-endosomes/lysosomes.* Experimental Cell Research, 2005. **303**(2): p. 300-7.
323. Matsuo, H., et al., *Role of LBPA and Alix in multivesicular liposome formation and endosome organization.* Science, 2004. **303**(5657): p. 531-4.
324. van Niel, G., et al., *Exosomes: a common pathway for a specialized function.* J Biochem, 2006. **140**(1): p. 13-21.
325. Hemler, M.E., *Tetraspanin proteins mediate cellular penetration, invasion, and fusion events and define a novel type of membrane microdomain.* Annu Rev Cell Dev Biol, 2003. **19**: p. 397-422.

326. Escola, J.M., et al., *Selective enrichment of tetraspan proteins on the internal vesicles of multivesicular endosomes and on exosomes secreted by human B-lymphocytes.* J Biol Chem, 1998. **273**(32): p. 20121-7.
327. Thery, C., et al., *Molecular characterization of dendritic cell-derived exosomes. Selective accumulation of the heat shock protein hsc73.* J Cell Biol, 1999. **147**(3): p. 599-610.
328. Thery, C., *Exosomes: secreted vesicles and intercellular communications.* F1000 Biol Rep, 2011. **3**: p. 15.
329. Buschow, S.I., et al., *MHC class II-associated proteins in B-cell exosomes and potential functional implications for exosome biogenesis.* Immunol Cell Biol, 2010. **88**(8): p. 851-6.
330. Simpson, R.J., et al., *Exosomes: proteomic insights and diagnostic potential.* Expert Rev Proteomics, 2009. **6**(3): p. 267-83.
331. Ratajczak, J., et al., *Membrane-derived microvesicles: important and underappreciated mediators of cell-to-cell communication.* Leukemia, 2006. **20**(9): p. 1487-95.
332. Skog, J., et al., *Glioblastoma microvesicles transport RNA and proteins that promote tumour growth and provide diagnostic biomarkers.* Nat Cell Biol, 2008. **10**(12): p. 1470-6.
333. Akbar, N., Digby, JE, Cahill, TJ, Tavare, AN, Corbin, AL, Saluja, S, Dawkins, S, Edgar, L, Rawlings ,N, Ziberna ,K, McNeill ,E, Oxford Acute Myocardial Infarction (OxAMI) Study, Johnson, E, Aljabali, AA, Dragovic, RA, Rohling, M, Belgard, TG, Udalova, IA, Greaves, DR, Channon, KM, Riley PR, Anthony,DC, Choudhury, RP, *Endothelium-derived extracellular vesicles promote splenic monocyte mobilization in myocardial infarction.* JCI Insight, 2017. **2**(17): p. e93344.
334. Ibrahim, A.-E., Cheng, K, Marbán, E, *Exosomes as Critical Agents of Cardiac Regeneration Triggered by Cell Therapy.* Stem Cell Reports, 2014. **2**: p. 606-619.
335. Xiao, D., et al., *Identifying mRNA, microRNA and protein profiles of melanoma exosomes.* PLoS One, 2012. **7**(10): p. e46874.
336. Eirin, A., et al., *MicroRNA and mRNA cargo of extracellular vesicles from porcine adipose tissue-derived mesenchymal stem cells.* Gene, 2014. **551**(1): p. 55-64.
337. Gray, W.D., et al., *Identification of therapeutic covariant microRNA clusters in hypoxia-treated cardiac progenitor cell exosomes using systems biology.* Circ Res, 2015. **116**(2): p. 255-63.
338. Zhang, J., et al., *Exosome and exosomal microRNA: trafficking, sorting, and function.* Genomics Proteomics Bioinformatics, 2015. **13**(1): p. 17-24.
339. Mateescu, B., et al., *Obstacles and opportunities in the functional analysis of extracellular vesicle RNA - an ISEV position paper.* J Extracell Vesicles, 2017. **6**(1): p. 1286095.
340. Caporali, A., et al., *MicroRNA transport in cardiovascular complication of diabetes.* Biochim Biophys Acta, 2016. **1861**(12 Pt B): p. 2111-2120.
341. Gibbings, D.J., et al., *Multivesicular bodies associate with components of miRNA effector complexes and modulate miRNA activity.* Nature Cell Biology, 2009. **11**(10): p. 1143-9.
342. Squadrito, M.L., et al., *Endogenous RNAs modulate microRNA sorting to exosomes and transfer to acceptor cells.* Cell Rep, 2014. **8**(5): p. 1432-46.
343. Kosaka, N., et al., *Secretory mechanisms and intercellular transfer of microRNAs in living cells.* J Biol Chem, 2010. **285**(23): p. 17442-52.
344. Villarroya-Beltri, C., et al., *Analysis of microRNA and protein transfer by exosomes during an immune synapse.* Methods Mol Biol, 2013. **1024**: p. 41-51.
345. Koppers-Lalic, D., et al., *Nontemplated nucleotide additions distinguish the small RNA composition in cells from exosomes.* Cell Rep, 2014. **8**(6): p. 1649-1658.
346. Cha, D.J., et al., *KRAS-dependent sorting of miRNA to exosomes.* Elife, 2015. **4**: p. e07197.
347. Janas, T., et al., *Mechanisms of RNA loading into exosomes.* FEBS Lett, 2015. **589**(13): p. 1391-8.
348. Batagov, A.O., V.A. Kuznetsov, and I.V. Kurochkin, *Identification of nucleotide patterns enriched in secreted RNAs as putative cis-acting elements targeting them to exosome nano-vesicles.* BMC Genomics, 2011. **12 Suppl 3**: p. S18.
349. Irion, U. and D. St Johnston, *bicoid RNA localization requires specific binding of an endosomal sorting complex.* Nature, 2007. **445**(7127): p. 554-8.
350. Mittelbrunn, M., et al., *Unidirectional transfer of microRNA-loaded exosomes from T cells to antigen-presenting cells.* Nat Commun, 2011. **2**: p. 282.
351. Montecalvo, A., et al., *Mechanism of transfer of functional microRNAs between mouse dendritic cells via exosomes.* Blood, 2012. **119**(3): p. 756-66.
352. Pegtel, D.M., et al., *Functional delivery of viral miRNAs via exosomes.* Proc Natl Acad Sci U S A, 2010. **107**(14): p. 6328-33.
353. Guay, C., et al., *Horizontal transfer of exosomal microRNAs transduce apoptotic signals between pancreatic beta-cells.* Cell Commun Signal, 2015. **13**: p. 17.

354. Nolte-'t Hoen, E.N., et al., *Deep sequencing of RNA from immune cell-derived vesicles uncovers the selective incorporation of small non-coding RNA biotypes with potential regulatory functions.* Nucleic Acids Res, 2012. **40**(18): p. 9272-85.
355. Bellingham, S.A., B.M. Coleman, and A.F. Hill, *Small RNA deep sequencing reveals a distinct miRNA signature released in exosomes from prion-infected neuronal cells.* Nucleic Acids Res, 2012. **40**(21): p. 10937-49.
356. van Balkom, B.W., et al., *Quantitative and qualitative analysis of small RNAs in human endothelial cells and exosomes provides insights into localized RNA processing, degradation and sorting.* J Extracell Vesicles, 2015. **4**: p. 26760.
357. Arroyo, J.D., et al., *Argonaute2 complexes carry a population of circulating microRNAs independent of vesicles in human plasma.* Proc Natl Acad Sci U S A, 2011. **108**(12): p. 5003-8.
358. Eldh, M., et al., *Importance of RNA isolation methods for analysis of exosomal RNA: evaluation of different methods.* Mol Immunol, 2012. **50**(4): p. 278-86.
359. Thery, C., et al., *Isolation and characterization of exosomes from cell culture supernatants and biological fluids.* Curr Protoc Cell Biol, 2006. **Chapter 3**: p. Unit 3 22.
360. Baranyai, T., et al., *Isolation of Exosomes from Blood Plasma: Qualitative and Quantitative Comparison of Ultracentrifugation and Size Exclusion Chromatography Methods.* PLoS One, 2015. **10**(12): p. e0145686.
361. Soo, C.Y., et al., *Nanoparticle tracking analysis monitors microvesicle and exosome secretion from immune cells.* Immunology, 2012. **136**(2): p. 192-7.
362. Nolte-'t Hoen, E.N., et al., *Quantitative and qualitative flow cytometric analysis of nanosized cell-derived membrane vesicles.* Nanomedicine, 2012. **8**(5): p. 712-20.
363. van der Vlist, E.J., et al., *Fluorescent labeling of nano-sized vesicles released by cells and subsequent quantitative and qualitative analysis by high-resolution flow cytometry.* Nat Protoc, 2012. **7**(7): p. 1311-26.
364. Booth, A.M., et al., *Exosomes and HIV Gag bud from endosome-like domains of the T cell plasma membrane.* Journal Cell Biology, 2006. **172**(6): p. 923-35.
365. Bobrie, A., et al., *Exosome secretion: molecular mechanisms and roles in immune responses.* Traffic, 2011. **12**(12): p. 1659-68.
366. Lotvall, J., et al., *The launch of Journal of Extracellular Vesicles (JEV), the official journal of the International Society for Extracellular Vesicles - about microvesicles, exosomes, ectosomes and other extracellular vesicles.* J Extracell Vesicles, 2012. **1**.
367. Lotvall, J., et al., *Minimal experimental requirements for definition of extracellular vesicles and their functions: a position statement from the International Society for Extracellular Vesicles.* J Extracell Vesicles, 2014. **3**: p. 26913.
368. Hill, A.F., et al., *ISEV position paper: extracellular vesicle RNA analysis and bioinformatics.* J Extracell Vesicles, 2013. **2**.
369. Lener, T., et al., *Applying extracellular vesicles based therapeutics in clinical trials - an ISEV position paper.* J Extracell Vesicles, 2015. **4**: p. 30087.
370. Witwer, K.W., et al., *Standardization of sample collection, isolation and analysis methods in extracellular vesicle research.* J Extracell Vesicles, 2013. **2**.
371. Théry C, W.K., Aikawa E, et al., *Minimal information for studies of extracellular vesicles 2018 (MISEV2018): a position statement of the International Society for Extracellular Vesicles and update of the MISEV2014 guidelines.* J. Extracell. Vesicles, 2018. **7**(1): p. 1535750.
372. Consortium, E.-T., et al., *EV-TRACK: transparent reporting and centralizing knowledge in extracellular vesicle research.* Nat Methods, 2017. **14**(3): p. 228-232.
373. Record, M., M. Poirot, and S. Silvente-Poirot, *Emerging concepts on the role of exosomes in lipid metabolic diseases.* Biochimie, 2014. **96**: p. 67-74.
374. Dai, S., et al., *More efficient induction of HLA-A*0201-restricted and carcinoembryonic antigen (CEA)-specific CTL response by immunization with exosomes prepared from heat-stressed CEA-positive tumor cells.* Clin Cancer Res, 2005. **11**(20): p. 7554-63.
375. Kim, J.W., et al., *Fas ligand-positive membranous vesicles isolated from sera of patients with oral cancer induce apoptosis of activated T lymphocytes.* Clin Cancer Res, 2005. **11**(3): p. 1010-20.
376. Taylor, D.D., S. Akyol, and C. Gercel-Taylor, *Pregnancy-associated exosomes and their modulation of T cell signaling.* J Immunol, 2006. **176**(3): p. 1534-42.
377. Lee, R.H., et al., *Intravenous hMSCs improve myocardial infarction in mice because cells embolized in lung are activated to secrete the anti-inflammatory protein TSG-6.* Cell Stem Cell, 2009. **5**(1): p. 54-63.

378. Potolicchio, I., et al., *Proteomic analysis of microglia-derived exosomes: metabolic role of the aminopeptidase CD13 in neuropeptide catabolism.* J Immunol, 2005. **175**(4): p. 2237-43.
379. Kramer-Albers, E.M., et al., *Oligodendrocytes secrete exosomes containing major myelin and stress-protective proteins: Trophic support for axons?* Proteomics Clin Appl, 2007. **1**(11): p. 1446-61.
380. Lopez-Verrilli, M.A., F. Picou, and F.A. Court, *Schwann cell-derived exosomes enhance axonal regeneration in the peripheral nervous system.* Glia, 2013. **61**(11): p. 1795-806.
381. Rajendran, L., et al., *Alzheimer's disease beta-amyloid peptides are released in association with exosomes.* Proc Natl Acad Sci U S A, 2006. **103**(30): p. 11172-7.
382. Schneider, A. and M. Simons, *Exosomes: vesicular carriers for intercellular communication in neurodegenerative disorders.* Cell Tissue Res, 2013. **352**(1): p. 33-47.
383. Lotvall, J. and H. Valadi, *Cell to cell signalling via exosomes through esRNA.* Cell Adh Migr, 2007. **1**(3): p. 156-8.
384. van Balkom, B.W., et al., *Endothelial cells require miR-214 to secrete exosomes that suppress senescence and induce angiogenesis in human and mouse endothelial cells.* Blood, 2013. **121**(19): p. 3997-4006.
385. Umezu, T., et al., *Leukemia cell to endothelial cell communication via exosomal miRNAs.* Oncogene, 2013. **32**: p. 2747-55.
386. Lo Cicero, A., et al., *Exosomes released by keratinocytes modulate melanocyte pigmentation.* Nature Communications, 2015. **6**: p. 7506.
387. Wiklander, O.P., et al., *Extracellular vesicle in vivo biodistribution is determined by cell source, route of administration and targeting.* J Extracell Vesicles, 2015. **4**: p. 26316.
388. Morishita, M., et al., *Pharmacokinetics of Exosomes-An Important Factor for Elucidating the Biological Roles of Exosomes and for the Development of Exosome-Based Therapeutics.* J Pharm Sci, 2017. **106**(9): p. 2265-2269.
389. Takakura, Y., Matsumoto, A, and Takahashi, Y, *Therapeutic Application of Small Extracellular Vesicles (sEVs): Pharmaceutical and Pharmacokinetic Challenges.* Biol. Pharm. Bull., 2020. **43**(4): p. 576-583.
390. Hoshino A, C.-S.B., Shen TL, Rodrigues G, Hashimoto A, Mark MT, Molina H, Kohsaka S, Di Giannatale A, Ceder S, Singh S, Williams C, Soplop N, Uryu K, Pharmer L,King T, Bojmar L, Davies AE, Ararso Y, Zhang T, Zhang H, Hernandez J, Weiss JM, Dumont-Cole VD, Kramer K, Wexler LH, Narendran A, Schwartz GK, Healey JH, Sandstrom P, Labori KJ, Kure EH, Grandgenett PM, Hollingsworth MA, de Sousa M, Kaur S, Jain M, Mallya K, Batra SK, Jarnagin WR, Brady MS, Fodstad O, Muller V, Pantel K, and B.M. Minn AJ, Garcia BA, Kang Y, Rajasekhar VK, Ghajar CM, Matei I, Peinado H, Bromberg J, Lyden D, *Tumour exosome integrins determine organotropic metastasis. .* Nature, 2015. **527**(329-335): p. 329.
391. Imai T, T.Y., Nishikawa M, Kato K, Morishita M, Yamashita T, Matsumoto A, Charoenviriyakul C, Takakura Y. , *Macrophage-dependent clearance of systemically administered B16BL6-derived exosomes from the blood circulation in mice.* J. Extracell. Vesicles, 2015. **4**: p. 26238.
392. Zhang H, F.D., Kim HS, Fabijanic K, Li Z, Chen H, Mark MT, Molina H, Martin AB, Bojmar L, Fang J, Rampersaud S, Hoshino A, Matei I, Kenific CM, Nakajima M, Mutvei AP, Sansone P, Buehring W, Wang H, Jimenez JP, and P.N. Cohen-Gould L, Brendel M, Manova-Todorova K, Magalhães A, Ferreira JA, Osório H, Silva AM, Massey A, Cubillos-Ruiz JR, Galletti G, Giannakakou P, Cuervo AM, Blenis J, Schwartz R, Brady MS, Peinado H, Bromberg J, Matsui H, Reis CA, Lyden D, *Identification of distinct nanoparticles and subsets of extracellular vesicles by asymmetric flow field-flow fractionation.* Nat. Cell Biol, 2018. **20**: p. 332-343.
393. Smyth T, K.M., Malik N, Smith-Jones P, Graner MW, Anchordoquy TJ., *Biodistribution and delivery efficiency of unmodified tumor-derived exosomes.* J. Control. Release, 2015. **199**: p. 145-155.
394. JB, S., *Pitfalls associated with lipophilic fluorophore staining of extracellular vesicles for uptake studies.* J. Extracell. Vesicles, 2019. **8**(1582237).
395. Takahashi, Y., et al., *Visualization and in vivo tracking of the exosomes of murine melanoma B16-BL6 cells in mice after intravenous injection*. J Biotechnol, 2013. **165**(2): p. 77-84.
396. Delcayre A, E.A., Sperinde J, Roulon T, Paz P, Aguilar B, Villanueva J, Khine S, Le Pecq JB, *Exosome display technology: applications to the development of new diagnostics and therapeutics.* Blood Cells Mol. Dis., 2005. **35**: p. 158-168.
397. Sedlik C, V.J., Torrieri-Dramard L, Pitoiset F, Denizeau J, Chesneau C, de la Rochere P, Lantz O, Thery C, Bellier B. , *Different immunogenicity but similar antitumor efficacy of two DNA vaccines*

coding for an antigen secreted in different membrane vesicle associated forms. . J. Extracell. Vesicles, 2014. **3**: p. 24646.

398. Charoenviriyakul C, T.Y., Morishita M, Nishikawa M, Takakura Y. , *Role of extracellular vesicle surface proteins in the pharmacokinetics of extracellular vesicles.* . Mol. Pharm., 2018. **15**: p. 1073-1080.
399. Suomalainen M, H.K., Garoff H. J., *Targeting of moloney murine leukemia virus gag precursor to the site of virus budding.* Cell Biol., 1996. **135**: p. 1841-1852.
400. Hamard-Peron E, J.F., Saad JS, Roy C, Roingeard P, Summers MF, Darlix JL, Picart C, Muriaux D., *Targeting of murine leukemia virus gag to the plasma membrane is mediated by PI(4,5)P2/PS and a polybasic region in the matrix.* J. Virol., 2010. **84**: p. 503-515.
401. Morishita M, T.Y., Nishikawa M, Sano K, Kato K, Yamashita T, Imai T, Saji H, Takakura Y., *Quantitative analysis of tissue distribution of the B16BL6-derived exosomes using a streptavidinelactadherin fusion protein and Iodine-125-labeled biotin derivative after intravenous injection in mice.* . J Pharm Sci. , 2015. **104**: p. 705-713.
402. Hwang DW, C.H., Jang SC, Yoo MY, Park JY, Choi NE, Oh HJ, and L.Y. Ha S, Jeong JM, Gho YS, Lee DS. , *Noninvasive imaging of radiolabeled exosome-mimetic nanovesicle using (99 m)Tc-HMPAO.* Sci. Rep., 2015. **5**: p. 15636.
403. Khan AA, R., RTM, *Radiolabelling of Extracellular Vesicles for PET and SPECT imaging.* Nanotheranostics, 2021. **5**(3): p. 256-274.
404. Hu L, W.S., Hood JL., *Magnetic resonance imaging of melanoma exosomes in lymph nodes.* . Magn Reson Med, 2015. **74**: p. 266-271.
405. Tada Y, Y., PC, *Iron Oxide Labeling and Tracking of Extracellular Vesicles.* Magnetochemistry, 2019. **5**: p. 60 (4-12).
406. Charoenviriyakul, C., et al., *Cell type-specific and common characteristics of exosomes derived from mouse cell lines: Yield, physicochemical properties, and pharmacokinetics.* Eur J Pharm Sci, 2017. **96**: p. 316-322.
407. Rand, M.L., et al., *Rapid clearance of procoagulant platelet-derived microparticles from the circulation of rabbits.* J Thromb Haemost, 2006. **4**(7): p. 1621-3.
408. Willekens, F.L., et al., *Liver Kupffer cells rapidly remove red blood cell-derived vesicles from the circulation by scavenger receptors.* Blood, 2005. **105**(5): p. 2141-5.
409. Saunderson, S.C., et al., *CD169 mediates the capture of exosomes in spleen and lymph node.* Blood, 2014. **123**(2): p. 208-16.
410. Driedonks T, J.L., Carlson B, Han Z, Liu G, Queen SE, Shirk EN, Gololobova O, Nyberg L, Lima G, Schonvisky K, Castell N, Stover M, Guerrero-Martin S, Richardson R, Smith B, Lai CP, Izzi JM, Hutchinson EK, Pate KAM, Witwer KW., *Pharmacokinetics and biodistribution of extracellular vesicles administered intravenously and intranasally to Macaca nemestrina.* bioRxiv, 2021. **preprint**.
411. Rank, A., et al., *Clearance of platelet microparticles in vivo.* Platelets, 2011. **22**(2): p. 111-6.
412. Matsumoto A, T.Y., Chang H-Y, Wub Y-W, Yamamoto A, Ishihama Y, Takakura Y., *Blood concentrations of small extracellular vesicles are determined by a balance between abundant secretion and rapid clearance.* JOURNAL OF EXTRACELLULAR VESICLES, 2019. **9**(1696517 (1-16)): p. 1696517.
413. Yanez-Mo, M., et al., *Biological properties of extracellular vesicles and their physiological functions.* J Extracell Vesicles, 2015. **4**: p. 27066.
414. PrabhuDas MR, B.C., Bollyky PL, Bowdish DME, Drickamer K, Febbraio M, et al. , *A consensus definitive classification of scavenger receptors and their roles in health and disease.* J. Immunol., 2017. **198**: p. 3775-3789.
415. Matsumoto A, T.Y., Nishikawa M, Sano K, Morishita M, Charoenviriyakul C, Saji H, Takakura Y. , *Role of phosphatidylserine-derived negative surface charges in the recognition and uptake of intravenously injected B16BL6-derived exosomes by macrophages.* J. Pharm. Sci., 2017. **106**: p. 168-175.
416. Kooijmans SAA, F.L., van der Meel R, Fens MHAM, Heijnen HFG, van Bergen En Henegouwen PMP, Vader P, Schiffelers RM. , *PEGylated and targeted extracellular vesicles display enhanced cell specificity and circulation time.* . J. Control. Release, 2016. **224**: p. 77-85.
417. Oussoren C, S.G., *Liposomes to target the lymphatics by subcutaneous administration.* . Adv. Drug Deliv. Rev., 2001. **50**: p. 143–156.
418. Srinivasan S, V.F., Dixon JB., *Lymphatic transport of exosomes as a rapid route of information dissemination to the lymph node.* Sci. Rep., 2016. **6**: p. 24436.

419. Munagala, R., et al., *Bovine milk-derived exosomes for drug delivery.* Cancer Lett, 2016. **371**(1): p. 48-61.
420. Smyth T, K.M., Malik N, Smith-Jones P, Graner MW, Anchordoquy TJ., *Biodistribution and delivery efficiency of unmodified tumor-derived exosomes.* J Control Release., 2015. **199**: p. 145-155.
421. Matsumoto A, T.Y., Nishikawa M, Sano K, Morishita M, Charoenviriyakul C, Saji H, Takakura Y. , *Accelerated growth of B16BL6 tumor in mice through efficient uptake of their own exosomes by B16BL6 cells. .* Cancer Sci. , 2017. **108**: p. 1803-1810.
422. Murphy DE, d.J.O., Brouwer M, Wood MJ, Lavieu G, Schiffelers RM, Vader, P., *Extracellular vesicle-based therapeutics: natural versus engineered targeting and trafficking.* Exp Mol Med., 2019. **51**(3): p. 1-12.
423. Haney MJ, K.N., Zhao Y, Gupta R, Plotnikova EG, He Z, et al., *Exosomes as drug delivery vehicles for Parkinson's disease therapy. .* J Control Release., 2015. **207**: p. 18-30.
424. Zhuang X, X.X., Grizzle W, Sun D, Zhang S, Axtell RC, Ju S, Mu J, Zhang L, Steinman L, Miller D, Zhang H-G., *Treatment of brain inflammatory diseases by delivering exosome encapsulated anti-inflammatory drugs from the nasal region to the brain.* Mol Ther., 2011. **19**(10): p. 1769-1779.
425. Shimoda A, T.Y., Sawada SI, Sasaki Y, Akiyoshi K. , *Glycan profiling analysis using evanescent-field fluorescence-assisted lectin array: Importance of sugar recognition for cellular uptake of exosomes from mesenchymal stem cells. .* Biochem. Biophys. Res. Commun., 2017. **491**: p. 701-707.
426. Yu G, J.H., Kang YY, Mok H., *Comparative evaluation of cell- and serum-derived exosomes to deliver immune stimulators to lymph nodes.* Biomaterials, 2018. **162**(71-81): p. 71.
427. Tian, T., et al., *Exosome uptake through clathrin-mediated endocytosis and macropinocytosis and mediating miR-21 delivery.* J Biol Chem, 2014. **289**(32): p. 22258-67.
428. Heusermann W, H.J., Trojer D, Steib E, von Bueren S, Graff-Meyer A, et al. , *Exosomes surf on filopodia to enter cells at endocytic hotspots, traffic within endosomes, and are targeted to the ER.* J Cell Biol., 2016. **213**(2): p. 173-184.
429. Hao S, B.O., Li F, Yuan J, Laferte S, Xiang J, *Mature dendritic cells pulsed with exosomes stimulate efficient cytotoxic T-lymphocyte responses and antitumour immunity. .* Immunology., 2007. **120**: p. 90-102.
430. Zhang Y, B.J., Huang J, Tang Y, Du S, Li P, *Exosome: A Review of Its Classification, Isolation Techniques, Storage, Diagnostic and Targeted Therapy Applications.* International Journal of Nanomedicine, 2020. **15**: p. 6917-6934.
431. Alvarez-Erviti, L., et al., *Delivery of siRNA to the mouse brain by systemic injection of targeted exosomes.* Nat Biotechnol, 2011. **29**(4): p. 341-5.
432. Zhu Q, L.X., Yang Y, et al, *Embryonic stem cells-derived exosomes endowed with targeting properties as chemotherapeutics delivery vehicles for glioblastoma therapy.* Adv Sci (Weinh), 2019. **6**(6): p. 1801899.
433. Ohno S, T.M., Sudo K, et al., *Systemically injected exo somes targeted to EGFR deliver antitumor microRNA to breast cancer cells.* Mol Ther. , 2013. **21**(1): p. 185-191.
434. Tian Y, L.S., Song J, et al. , *A doxorubicin delivery platform using engineered natural membrane vesicle exosomes for targeted tumor therapy. .* Biomaterials, 2014. **35**(7): p. 2383-2390.
435. Lee J, L.H., Goh U, et al., *Cellular engineering with membrane fusogenic liposomes to produce functionalized extracellular vesicles. .* ACS Appl Mater Interfaces, 2016. **8**(11): p. 6790-6795.
436. Nakase I, F.S., *Combined treatment with a pH-sensitive fusogenic peptide and cationic lipids achieves enhanced cytosolic delivery of exosomes. .* Sci Rep., 2015. **5**(1): p. 10112.
437. Qi H, L.C., Long L, et al., *Blood exosomes endowed with magnetic and targeting properties for cancer therapy.* ACS Nano, 2016. **10**(3): p. 3323-3333.
438. Ohno, S., G.P. Drummen, and M. Kuroda, *Focus on Extracellular Vesicles: Development of Extracellular Vesicle-Based Therapeutic Systems.* Int J Mol Sci, 2016. **17**(2): p. 172.
439. Batrakova, E.V. and M.S. Kim, *Development and regulation of exosome-based therapy products.* Wiley Interdiscip Rev Nanomed Nanobiotechnol, 2016. **8**(5): p. 744-57.
440. Clinicaltrials.gov, *Clinical trials with exosomes (https://clinicaltrials.gov/ct2/results?cond=&term=Exosome&cntry=&state=&city=&dist=)*. 2018.
441. Clinicaltrials.gov, *Clinical trials with extracellular vesicles (https://clinicaltrials.gov/ct2/results?cond=&term=extracellular+vesicles&cntry=&state=&city=&dist=)*. 2018.

442. Clinicaltrials.gov, *Map of clinical trials with exosomes (https://clinicaltrials.gov/ct2/results/map?term=Exosome&map=).* 2018.
443. Gimona, M., et al., *Manufacturing of Human Extracellular Vesicle-Based Therapeutics for Clinical Use.* Int J Mol Sci, 2017. **18**(6).
444. Lauer, G., et al., *Expression and proteolysis of vascular endothelial growth factor is increased in chronic wounds.* J Invest Dermatol, 2000. **115**(1): p. 12-8.
445. Wu, L., et al., *Transforming growth factor-beta1 fails to stimulate wound healing and impairs its signal transduction in an aged ischemic ulcer model: importance of oxygen and age.* Am J Pathol, 1999. **154**(1): p. 301-9.
446. Squarize, C.H., et al., *Accelerated wound healing by mTOR activation in genetically defined mouse models.* PLoS One, 2010. **5**(5): p. e10643.
447. Castilho, R.M., C.H. Squarize, and J.S. Gutkind, *Exploiting PI3K/mTOR signaling to accelerate epithelial wound healing.* Oral Dis, 2013. **19**(6): p. 551-8.
448. Huang, H., et al., *Impaired wound healing results from the dysfunction of the Akt/mTOR pathway in diabetic rats.* J Dermatol Sci, 2015. **79**(3): p. 241-51.
449. Li, G., et al., *ILK-PI3K/AKT pathway participates in cutaneous wound contraction by regulating fibroblast migration and differentiation to myofibroblast.* Lab Invest, 2016. **96**(7): p. 741-51.
450. Raffetto, J.D., et al., *Mitogen-activated protein kinase pathway regulates cell proliferation in venous ulcer fibroblasts.* Vasc Endovascular Surg, 2006. **40**(1): p. 59-66.
451. Mebratu, Y. and Y. Tesfaigzi, *How ERK1/2 activation controls cell proliferation and cell death: Is subcellular localization the answer?* Cell Cycle, 2009. **8**(8): p. 1168-75.
452. Shibata, S., et al., *Adiponectin regulates cutaneous wound healing by promoting keratinocyte proliferation and migration via the ERK signaling pathway.* J Immunol, 2012. **189**(6): p. 3231-41.
453. Sharma, G.D., J. He, and H.E. Bazan, *p38 and ERK1/2 coordinate cellular migration and proliferation in epithelial wound healing: evidence of cross-talk activation between MAP kinase cascades.* J Biol Chem, 2003. **278**(24): p. 21989-97.
454. Sano, S., K.S. Chan, and J. DiGiovanni, *Impact of Stat3 activation upon skin biology: a dichotomy of its role between homeostasis and diseases.* J Dermatol Sci, 2008. **50**(1): p. 1-14.
455. Song, Q., et al., *JAK/STAT3 and Smad3 activities are required for the wound healing properties of Periplaneta americana extracts.* Int J Mol Med, 2017. **40**(2): p. 465-473.
456. Yu, F.X., et al., *Regulation of the Hippo-YAP pathway by G-protein-coupled receptor signaling.* Cell, 2012. **150**(4): p. 780-91.
457. Lee, M.J., et al., *YAP and TAZ regulate skin wound healing.* J Invest Dermatol, 2014. **134**(2): p. 518-525.
458. Wang, J., et al., *An updated review of mechanotransduction in skin disorders: transcriptional regulators, ion channels, and microRNAs.* Cell Mol Life Sci, 2015. **72**(11): p. 2091-106.
459. Shi, Y., et al., *Wnt and Notch signaling pathway involved in wound healing by targeting c-Myc and Hes1 separately.* Stem Cell Res Ther, 2015. **6**: p. 120.
460. Bastakoty, D. and P.P. Young, *Wnt/beta-catenin pathway in tissue injury: roles in pathology and therapeutic opportunities for regeneration.* FASEB J, 2016. **30**(10): p. 3271-3284.
461. Chen, L., et al., *Toll-like receptor 4 has an essential role in early skin wound healing.* J Invest Dermatol, 2013. **133**(1): p. 258-67.
462. Carvalho, L., A. Jacinto, and N. Matova, *The Toll/NF-kappaB signaling pathway is required for epidermal wound repair in Drosophila.* Proc Natl Acad Sci U S A, 2014. **111**(50): p. E5373-82.
463. Chen, L. and L.A. DiPietro, *Toll-Like Receptor Function in Acute Wounds.* Adv Wound Care (New Rochelle), 2017. **6**(10): p. 344-355.
464. Sun, Q., et al., *Cross-talk between TGF-beta/Smad pathway and Wnt/beta-catenin pathway in pathological scar formation.* Int J Clin Exp Pathol, 2015. **8**(6): p. 7631-9.
465. He, B., et al., *Therapeutic potential of umbilical cord blood cells for type 1 diabetes mellitus.* J Diabetes, 2015. **7**(6): p. 762-73.
466. Willms, E., et al., *Cells release subpopulations of exosomes with distinct molecular and biological properties.* Sci Rep, 2016. **6**: p. 22519.
467. Broxmeyer, H.E., et al., *Hematopoietic stem/progenitor cells, generation of induced pluripotent stem cells, and isolation of endothelial progenitors from 21- to 23.5-year cryopreserved cord blood.* Blood, 2011. **117**(18): p. 4773-7.
468. Voinchet, V., P. Vasseur, and J. Kern, *Efficacy and safety of hyaluronic acid in the management of acute wounds.* Am J Clin Dermatol, 2006. **7**(6): p. 353-7.
469. Longaker, M.T., et al., *Studies in fetal wound healing. V. A prolonged presence of hyaluronic acid characterizes fetal wound fluid.* Ann Surg, 1991. **213**(4): p. 292-6.

470. Irakunda, G., et al., *Diabetes and wound healing* Bachelor in Science Thesis - Roskilde University, 2014.
471. Li, J., et al., *Microvesicle-mediated transfer of microRNA-150 from monocytes to endothelial cells promotes angiogenesis.* The Journal of Biological Chemistry, 2013. **288**(32): p. 23586-96.
472. Zhang, Y., et al., *Secreted monocytic miR-150 enhances targeted endothelial cell migration.* Molecullar Cell, 2010. **39**(1): p. 133-44.
473. He, Q.W., et al., *MiR-150 Regulates Poststroke Cerebral Angiogenesis via Vascular Endothelial Growth Factor in Rats.* CNS Neuroscience & Therapeutics, 2016. **22**(6): p. 507-17.
474. Czimmerer, Z., et al., *The IL-4/STAT6 signaling axis establishes a conserved microRNA signature in human and mouse macrophages regulating cell survival via miR-342-3p.* Genome Medicine, 2016. **8**(1): p. 63.
475. Zhao, L., et al., *MiRNA expression analysis of cancer-associated fibroblasts and normal fibroblasts in breast cancer.* Int J Biochem Cell Biol, 2012. **44**(11): p. 2051-9.
476. Essandoh, K., et al., *MiRNA-Mediated Macrophage Polarization and its Potential Role in the Regulation of Inflammatory Response.* Shock, 2016. **46**(2): p. 122-31.
477. Pan, Y., et al., *Platelet-secreted microRNA-223 promotes endothelial cell apoptosis induced by advanced glycation end products via targeting the insulin-like growth factor 1 receptor.* J Immunol, 2014. **192**(1): p. 437-46.
478. Goretti, E., et al., *MicroRNA-16 affects key functions of human endothelial progenitor cells.* J Leukoc Biol, 2013. **93**(5): p. 645-55.
479. Liu, G., et al., *Cycling exercise affects the expression of apoptosis-associated microRNAs after spinal cord injury in rats.* Exp Neurol, 2010. **226**(1): p. 200-6.
480. Zheng, Y., et al., *Identification and bioinformatics analysis of microRNAs associated with stress and immune response in serum of heat-stressed and normal Holstein cows.* Cell Stress Chaperones, 2014. **19**(6): p. 973-81.
481. Lai, W.F. and P.M. Siu, *MicroRNAs as regulators of cutaneous wound healing.* J Biosci, 2014. **39**(3): p. 519-24.
482. Madhyastha, R., et al., *MicroRNA signature in diabetic wound healing: promotive role of miR-21 in fibroblast migration.* Int Wound J, 2012. **9**(4): p. 355-61.
483. Chen, Z., et al., *Activation and regulation of the granulation tissue derived cells with stemness-related properties.* Stem Cell Res Ther, 2015. **6**: p. 85.
484. Yang, J., et al., *Identification of a miRNA signature in neutrophils after traumatic injury.* Acta Biochim Biophys Sin (Shanghai), 2013. **45**(11): p. 938-45.
485. Chen, L.J., et al., *MicroRNA mediation of endothelial inflammatory response to smooth muscle cells and its inhibition by atheroprotective shear stress.* Circ Res, 2015. **116**(7): p. 1157-69.
486. Ruan, W., et al., *Effects of down-regulation of microRNA-23a on TNF-alpha-induced endothelial cell apoptosis through caspase-dependent pathways.* Cardiovasc Res, 2012. **93**(4): p. 623-32.
487. Kwok, H.H., et al., *Ginsenoside-Rg1 induces angiogenesis by the inverse regulation of MET tyrosine kinase receptor expression through miR-23a.* Toxicol Appl Pharmacol, 2015. **287**(3): p. 276-83.
488. Zgheib, C. and K.W. Liechty, *Shedding light on miR-26a: Another key regulator of angiogenesis in diabetic wound healing.* J Mol Cell Cardiol, 2016. **92**: p. 203-5.
489. Icli, B., et al., *MicroRNA-26a regulates pathological and physiological angiogenesis by targeting BMP/SMAD1 signaling.* Circ Res, 2013. **113**(11): p. 1231-41.
490. Sen, C.K. and S. Roy, *microRNA in Cutaneous Wound Healing.* © Springer Science + Business Media B.V., 2008. **S.-Y. Ying (ed.) Current Perspectives in microRNAs (miRNA)**(Chapter 19): p. 349-366.
491. Selvamani, A., et al., *An antagomir to microRNA Let7f promotes neuroprotection in an ischemic stroke model.* PLoS One, 2012. **7**(2): p. e32662.
492. Naqvi, A.R., et al., *miR-24, miR-30b and miR-142-3p interfere with antigen processing and presentation by primary macrophages and dendritic cells.* Scientific Reports, 2016. **6**: p. 32925.
493. Wang, D., et al., *MicroRNA-205 controls neonatal expansion of skin stem cells by modulating the PI(3)K pathway.* Nat Cell Biol, 2013. **15**(10): p. 1153-63.
494. Yu, J., et al., *MicroRNA-205 promotes keratinocyte migration via the lipid phosphatase SHIP2.* FASEB J, 2010. **24**(10): p. 3950-9.
495. Shi, X.B., et al., *An androgen-regulated miRNA suppresses Bak1 expression and induces androgen-independent growth of prostate cancer cells.* Proc Natl Acad Sci U S A, 2007. **104**(50): p. 19983-8.

496. Gu, X.Y., et al., *Down-regulation of miR-150 induces cell proliferation inhibition and apoptosis in non-small-cell lung cancer by targeting BAK1 in vitro.* Tumour Biology, 2014. **35**(6): p. 5287-93.
497. Xiao, C., et al., *MiR-150 controls B cell differentiation by targeting the transcription factor c-Myb.* Cell, 2007. **131**(1): p. 146-59.
498. Creemers, E.E., A.J. Tijsen, and Y.M. Pinto, *Circulating microRNAs: novel biomarkers and extracellular communicators in cardiovascular disease?* Circ Res, 2012. **110**(3): p. 483-95.
499. Allantaz, F., et al., *Expression profiling of human immune cell subsets identifies miRNA-mRNA regulatory relationships correlated with cell type specific expression.* PLoS One, 2012. **7**(1): p. e29979.
500. Almanza, G., et al., *Synthesis and delivery of short, noncoding RNA by B lymphocytes.* Proc Natl Acad Sci U S A, 2013. **110**(50): p. 20182-7.
501. Zhou, B., et al., *miR-150, a microRNA expressed in mature B and T cells, blocks early B cell development when expressed prematurely.* Proc Natl Acad Sci U S A, 2007. **104**(17): p. 7080-5.
502. Shen, J., et al., *MicroRNAs regulate ocular neovascularization.* Molecullar Therapy, 2008. **16**(7): p. 1208-16.
503. Wang, W., et al., *MiR-150 enhances the motility of EPCs in vitro and promotes EPCs homing and thrombus resolving in vivo.* Thrombosis Research, 2014. **133**(4): p. 590-8.
504. Shi, L., et al., *Deletion of miR-150 Exacerbates Retinal Vascular Overgrowth in High-Fat-Diet Induced Diabetic Mice.* PLoS One, 2016. **11**(6): p. e0157543.
505. Parker, P.J. and J. Murray-Rust, *PKC at a glance.* J Cell Sci, 2004. **117**(Pt 2): p. 131-2.
506. Zhang, Y., et al., *Decoding Noncoding RNAs: Role of MicroRNAs and Long Noncoding RNAs in Ocular Neovascularization.* Theranostics, 2017. **7**(12): p. 3155-3167.
507. Liu, C.H., et al., *Endothelial microRNA-150 is an intrinsic suppressor of pathologic ocular neovascularization.* Proc Natl Acad Sci U S A, 2015. **112**(39): p. 12163-8.
508. Kovacs, B., et al., *MicroRNAs in early diabetic retinopathy in streptozotocin-induced diabetic rats.* Invest Ophthalmol Vis Sci, 2011. **52**(7): p. 4402-9.
509. Ertekin, S., et al., *Evaluation of circulating miRNAs in wet age-related macular degeneration.* Mol Vis, 2014. **20**: p. 1057-66.
510. Wang, S., et al., *miRNAs as potential therapeutic targets for age-related macular degeneration.* Future Med Chem, 2012. **4**(3): p. 277-87.
511. Lin, J.B., et al., *Macrophage microRNA-150 promotes pathological angiogenesis as seen in age-related macular degeneration.* JCI Insight, 2018. **3**(7).
512. Fang, Z., et al., *MicroRNA-150 regulates blood-brain barrier permeability via Tie-2 after permanent middle cerebral artery occlusion in rats.* FASEB J, 2016. **30**(6): p. 2097-107.
513. He, Q.W., et al., *MiR-150 Regulates Poststroke Cerebral Angiogenesis via Vascular Endothelial Growth Factor in Rats.* CNS Neurosci Ther, 2016. **22**(6): p. 507-17.
514. Dweep, H. and N. Gretz, *miRWalk2.0: a comprehensive atlas of microRNA-target interactions.* Nature Methods, 2015. **12**(8): p. 697.
515. Dweep, H., et al., *miRWalk--database: prediction of possible miRNA binding sites by "walking" the genes of three genomes.* Journal of Biomedical Informatics, 2011. **44**(5): p. 839-47.
516. Lin, Y.C., et al., *c-Myb is an evolutionary conserved miR-150 target and miR-150/c-Myb interaction is important for embryonic development.* Molecular Biology and Evolution, 2008. **25**(10): p. 2189-98.
517. Palagani, A., et al., *Ectopic microRNA-150-5p transcription sensitizes glucocorticoid therapy response in MM1S multiple myeloma cells but fails to overcome hormone therapy resistance in MM1R cells.* PLoS One, 2014. **9**(12): p. e113842.
518. Agarwal, V., et al., *Predicting effective microRNA target sites in mammalian mRNAs.* eLife, 2015. **4**: p. e05005.
519. Paraskevopoulou, M.D., et al., *DIANA-microT web server v5.0: service integration into miRNA functional analysis workflows.* Nucleic Acids Research, 2013. **41**((Web Server issue)): p. W169-73.
520. Reczko, M., et al., *Functional microRNA targets in protein coding sequences.* Bioinformatics, 2012. **28**(6): p. 771-6.
521. Kanellos, I., et al., *MR-microT: a MapReduce-based MicroRNA target prediction method.* SSDBM '14: Proceedings of the 26th International Conference on Scientific and Statistical Database Management, 2014. **47**.
522. Weston, K., *Myb proteins in life, death and differentiation.* Current opinion in genetics & development, 1998. **8**: p. 76-81.

523. Oh, I.H. and E.P. Reddy, *The myb gene family in cell growth, differentiation and apoptosis.* Oncogene, 1999. **18**(19): p. 3017-33.
524. Soza-Ried, C., et al., *Essential role of c-myb in definitive hematopoiesis is evolutionary conserved.* PNAS, 2010. **107**(40): p. 17304-17308.
525. Lang, G., et al., *Myb proteins regulate the expression of diverse target genes.* Oncogene, 2005. **24**(8): p. 1375-84.
526. Lino MM, S.S., Vilaça A, Antunes H, Zonari A, Ferreira L, *Modulation of Angiogenic Activity by Light-Activatable miRNA-Loaded Nanocarriers.* ACS Nano, 2018. **12**(6): p. 5207-5220.
527. Aragona, M., et al., *Defining stem cell dynamics and migration during wound healing in mouse skin epidermis.* Nat Commun, 2017. **8**: p. 14684.
528. Hoyle, N.P., et al., *Circadian actin dynamics drive rhythmic fibroblast mobilization during wound healing.* Sci Transl Med, 2017. **9**(415).
529. Shahabipour, F., et al., *Exosomes: Nanoparticulate tools for RNA interference and drug delivery.* Journal Cell Phtsiology, 2017. **232**(7): p. 1660-8.

Appendix I -Table of studies and validated targets of miR-150-5p

#	Gene	EntrezID	PMID
1	A1CF	29974	23446348
2	ABCB7	22	22291592
3	ABCG8	64241	23313552
4	ABHD15	116236	22012620
5	ABHD2	11057	23824327
6	ACOT9	23597	23313552
7	ACOX1	51	19536157
8	ACSL6	23305	23446348
9	ADIPOR2	79602	22815788
10	AGA	175	20218812
11	AGMAT	79814	23313552
12	Ago/03	192669	23824327
13	ago/03	192669	23446348
14	AGTPBP1	23287	23708386
15	AHI1	54806	23446348
16	AIFM2	84883	22815788
17	AIFM2	84883	23824327
18	AKIRIN1	79647	23824327
19	ALDOA	226	23824327
20	AMD1	262	23824327
21	AMOTL2	51421	19536157
22	ANKFY1	51479	23824327
23	ANKRD65	441869	22012620
24	ANKS4B	257629	23313552
25	ANO7	50636	23824327
26	APEX2	27301	23313552
27	APOH	350	23824327
28	APOPT1	84334	23824327
29	ARHGAP29	9411	23824327
30	ARSE	415	23824327
31	AS3MT	57412	23824327
32	ASB16	92591	21572407
33	ASB8	140461	23824327
34	ATAD2B	54454	19536157
35	ATCAY	85300	19536157
36	ATCAY	85300	23824327
37	ATP13A3	79572	23622248
38	ATP1B3	483	23313552
39	ATP2B1	490	19536157
40	ATP9A	10079	19536157
41	BBS5	129880	21572407
42	BCAS4	55653	23446348
43	BCL11B	64919	23824327
44	BDP1	55814	19536157
45	BHMT2	23743	23313552
46	BIRC5	332	24613688
47	BMP8B	656	21572407
48	BMP8B	656	23446348
49	BMP8B	656	20371350
50	BTN3A2	11118	24906430
51	C11orf1	64776	23313552
52	C12orf49	79794	23313552
53	C12orf65	91574	23313552
54	C14orf105	55195	23313552
55	C14orf119	55017	23313552
56	C15orf40	123207	23824327
57	C16orf58	64755	23824327
58	C18orf32	497661	22012620
59	C19orf40	91442	23313552
60	C21orf33	8209	23824327
61	C2CD4B	388125	23708386
62	C3orf36	80111	22012620
63	C3orf36	80111	20371350
64	C4orf29	80167	23446348
65	C4orf29	80167	22012620
66	C8orf37	157657	23824327
67	C8orf46	254778	23824327
68	CACYBP	27101	23446348
69	CALCOCO2	10241	23824327
70	CAMK1D	57118	23824327
71	CAMK4	814	19536157
72	CAPZA2	830	23313552
73	CARHSP1	23589	19536157
74	CAST	831	22815788
75	CBL	867	23604034
76	CBX5	23468	23824327
77	CCDC30	728621	23824327
78	CCDC30	728621	23446348
79	CCR6	1235	24385540
80	CCS	9973	23824327
81	CD96	10225	23824327
82	CDIPT	10423	19536157
83	CDK2	1017	23824327
84	CDKN2AIPNL	91368	23313552
85	CDS2	8760	19536157
86	CEP104	9731	23313552
87	CEP135	9662	23824327
88	CEP72	55722	20371350
89	CISH	1154	23723424
90	CNKSR3	154043	23446348
91	CNNM2	54805	23824327
92	CNPPD1	27013	23824327
93	CNST	163882	22815788
94	COL4A4	1286	23604143
95	COL9A2	1298	23824327
96	CORO2A	7464	19536157
97	CORO2A	7464	23824327
98	COX19	90639	23446348
99	COX19	90639	23313552
100	CPT1A	1374	23313552
101	CRCP	27297	19536157
102	CRISPLD2	83716	23313552
103	CSNK1E	1454	23824327
104	CTNS	1497	23824327
105	CWC25	54883	23824327
106	CXCR4	7852	22039399
107	CXorf21	80231	23824327
108	CXorf38	159013	23313552
109	CXorf38	159013	23824327
110	CXorf38	159013	22927820
111	CYB5A	1528	23824327
112	CYCS	54205	23824327
113	CYCS	54205	23446348
114	CYTIP	9595	23824327
115	DCTN5	84516	23313552
116	DDI2	84301	23313552
117	DEGS1	8560	23824327
118	DGCR6L	85359	22291592
119	DHTKD1	55526	23824327
120	DIS3	22894	23824327
121	DIS3L	115752	21572407
122	DNAAF3	352909	23824327
123	DNAJB13	374407	23313552
124	DNAJB13	374407	23824327
125	DNAJB4	11080	23313552
126	DNAL1	83544	23313552
127	DNASE2	1777	23824327
128	DPYSL5	56896	19536157
129	DRAXIN	374946	23313552
130	DSN1	79980	22012620
131	DSTYK	25778	23824327
132	EFCAB11	90141	21572407
133	EFCAB11	90141	23446348
134	EGR2	1959	20067763
135	EGR2	1959	23604034
136	EIF2B2	8892	23313552
137	ELK1	2002	23824327
138	EMC3	55831	23824327
139	EMC7	56851	23824327
140	EMP2	2013	23824327
141	ENTPD4	9583	22927820
142	EP300	2033	23211718
143	EPHB2	2048	23824327
144	EREG	2069	22815788
145	EREG	2069	23446348
146	ESR2	2100	23313552
147	ETV3	2117	23313552
148	EXO5	64789	19536157
149	EZH2	2146	23824327
150	F2R	2149	22927820
151	F2RL1	2150	23313552
152	FAHD1	81889	19536157
153	FAM13B	51306	23824327
154	FAM153B	202134	23313552
155	FAM185A	222234	23824327
156	FAM213A	84293	23313552
157	FAM89A	375061	21572407
158	FAXC	84553	23824327
159	FBXO47	494188	23824327
160	FFAR4	338557	23824327
161	FGD6	55785	23446348
162	FHDC1	85462	22012620
163	FKBP9	11328	23824327
164	FLT3	2322	23079661
165	FOPNL	123811	22815788
166	FOXK1	221937	23824327
167	FOXRED2	80020	23313552
168	FRAT2	23401	21572407
169	FXYD5	53827	21572407
170	FXYD5	53827	23446348
171	GAN	8139	22012620
172	GAN	8139	23592263
173	GAN	8139	20371350
174	GATAD2B	57459	19536157
175	GGA2	23062	23446348
176	GJD3	125111	23824327
177	GK5	256356	23313552
178	GK5	256356	23824327
179	GNB5	10681	23313552
180	GNE	10020	23824327
181	GOLGA2	2801	19536157
182	GOSR1	9527	21572407
183	GPN2	54707	23313552
184	GPR137B	7107	23313552
185	GPR182	11318	22012620
186	GPRIN3	285513	23313552
187	GRM6	2916	23824327
188	GTF2H2	2966	23824327
189	GTF2H2C	728340	23824327
190	GTF2H3	2967	23313552
191	HAS2	3037	22927820
192	HAS2	3037	23313552
193	HAUS2	55142	19536157
194	HIF1AN	55662	23824327
195	HILPDA	29923	23824327
196	HIP1	3092	23313552
197	HIP1	3092	23824327
198	HIST1H2BG	8339	23824327
199	HIST1H2BJ	8970	23313552
200	HMGB1	3146	21572407
201	HMGB1	3146	23313552
202	HOOK3	84376	23313552
203	HS3ST1	9957	23313552
204	HSPA4L	22824	23824327
205	HYPK	25764	23446348
206	ICA1L	130026	23824327
207	ICA1L	130026	23313552
208	IGF2	3481	21200031
209	INTS7	25896	23313552
210	INTU	27152	23446348
211	IP6K2	51447	19536157
212	IP6K2	51447	23824327
213	IPP	3652	23446348
214	IRAK4	51135	23313552
215	ISCA2	122961	23313552
216	ISG20L2	81875	23313552
217	JDP2	122953	23824327
218	KANSL3	55683	19536157
219	KCNK3	3777	23824327
220	KCNK5	8645	23824327
221	KIAA0930	23313	23313552
222	KIAA1549	57670	23313552
223	KIAA1551	55196	23446348
224	KIAA1715	80856	23824327
225	KIAA1841	84542	23313552
226	KLHL21	9903	23824327
227	KLHL7	55975	23824327
228	KRBOX4	55634	21572407
229	LAIR1	3903	23824327
230	LAT2	7462	23824327
231	LCTL	197021	23824327
232	LDHD	197257	23313552
233	LEAP2	116842	23824327
234	LGSN	51557	23313552
235	LIPG	9388	23824327
236	LMTK2	22853	19536157
237	LRIF1	55791	23313552
238	LRRC15	131578	19536157
239	LRRC27	80313	23824327
240	LRRD1	401387	23313552
241	LTBP2	4053	23824327
242	LY6G5B	58496	23313552
243	LYRM7	90624	19536157
244	MAN2B2	23324	23313552
245	MANEAL	149175	23824327
246	MAPK13	5603	23446348
247	MASTL	84930	21572407
248	MBD1	4152	23313552
249	MBD6	114785	20371350
250	MCTS1	28985	23824327
251	MED16	10025	21572407
252	METTL21A	151194	23313552
253	METTL8	79828	23313552
254	MFSD11	79157	22927820
255	MFSD11	79157	23824327
256	MFSD2A	84879	23824327
257	MICA	100507436	23313552
258	MIPOL1	145282	23824327
259	MIS18A	54069	23824327
260	MIS18A	54069	21572407
261	MIXL1	83881	23446348
262	MLN	4295	23824327
263	MMAB	326625	23824327
264	MON1B	22879	23824327
265	MRPL37	51253	23313552
266	MRPS27	23107	23592263
267	MS4A3	932	20218812
268	MSANTD3	91283	23824327
269	MSH3	4437	23313552
270	MTMR9	66036	22927820
271	MTRNR2L5	100463289	23824327
272	MTSS1L	92154	23824327

Appendix I -Table of studies and validated targets of miR-150-5p (continuation).

#	Gene	EntrezID	PMID
273	MUC4	4585	21983127
274	MUT	4594	23824327
275	MYB	4602	18667440
276	MYB	4602	18814950
277	MYB	4602	20603081
278	MYB	4602	23521217
279	MYB	4602	23604034
280	MYB	4602	22025269
281	MYB	4602	24086639
282	MYB	4602	24438945
283	MYB	4602	24613688
284	MYB	4602	21590770
285	MYB	4602	17923094
286	MYB	4602	18539114
287	MYH9	4627	24906430
288	MYLK3	91807	19536157
289	MYLK3	91807	23313552
290	MYO1F	4542	23824327
291	MYO1F	4542	23313552
292	N4BP2L2	10443	23706177
293	NDUFV3	4731	19536157
294	NEK8	284086	19536157
295	NFYA	4800	23824327
296	NIPAL1	152519	23824327
297	NKD1	85407	23446348
298	NKX2-1	7080	23824327
299	NME6	10201	22012620
300	NMNAT1	64802	23824327
301	NOL9	79707	23313552
302	NOTCH3	4854	21551231
303	NPHP1	4867	23824327
304	NPHS1	4868	23824327
305	NR2F2	7026	23824327
306	NSUN4	387338	23313552
307	NUDT3	11165	23313552
308	NUGGC	389643	23313552
309	OCIAD1	54940	23313552
310	ORAI2	80228	23313552
311	P2RX7	5027	18682393
312	P2RX7	5027	23824327
313	P2RX7	5027	24312495
314	PAIP2B	400961	23824327
315	PAK3	5063	23824327
316	PARD3	56288	23313552
317	PARD6G	84552	23824327
318	PCP4L1	654790	23313552
319	PCYT1A	5130	19536157
320	PDCD4	27250	23824327
321	PDE6A	5145	23824327
322	PDHB	5162	23313552
323	PDIA6	10130	22815788
324	PDZD8	118987	21572407
325	PGBD4	161779	23824327
326	PGM2L1	283209	23313552
327	PHF12	57649	22012620
328	PIAS2	9063	19536157
329	PIGM	93183	23824327
330	PIGR	5284	19536157
331	PIK3C2A	5286	23824327
332	PLA2G16	11145	23824327
333	PLAA	9373	23313552
334	PLEKHA2	59339	23824327
335	PLEKHM3	389072	23824327
336	PLXDC1	57125	22012620
337	PNPLA3	80339	23824327
338	PNRC1	10957	19536157
339	PNRC1	10957	23824327
340	POFUT1	23509	23824327
341	POLQ	10721	23824327
342	POLR3A	11128	21572407
343	PPAP2B	8613	23824327
344	PPIE	10450	23824327
345	PPM1A	5494	23446348
346	PPP2CB	5516	21572407
347	PPP2R3A	5523	23824327
348	PRIM1	5557	23313552
349	PRKAB1	5564	19536157
350	PROSC	11212	23446348
351	PRPF38A	84950	23824327
352	PSMC1	5700	23824327
353	PTCHD1	139411	24906430
354	PTCHD3	374308	23313552
355	PTGIS	5740	23313552
356	PTPN4	5775	23313552
357	PTPRR	5801	20218812
358	PTRF	284119	21572407
359	PURB	5814	21572407
360	PURB	5814	23824327
361	PURB	5814	20371350
362	PWWP2A	114825	23824327
363	PXMP4	11264	19536157
364	QRFPR	84109	23313552
365	QSOX1	5768	23446348
366	QSOX1	5768	23313552
367	RAB13	5872	23824327
368	RAB21	23011	19536157
369	RABAC1	10567	23824327
370	RABGAP1L	9910	23313552
371	RABIF	5877	23824327
372	RAI1	10743	21572407
373	RANGAP1	5905	23824327
374	RAPGEF6	51735	19536157
375	RBL1	5933	23824327
376	RBM3	5935	23824327
377	RBM3	5935	19536157
378	RBM41	55285	23313552
379	REL	5966	23824327
380	RFK	55312	23313552
381	RHOH	399	19536157
382	RNF115	27246	23313552
383	RNF157	114804	23824327
384	RNF165	494470	23824327
385	RNF19B	127544	23313552
386	RNF34	80196	23313552
387	RPL14	9045	23313552
388	RPL24	6152	23824327
389	RRP1B	23076	23824327
390	RRP36	88745	22012620
391	RRP36	88745	23446348
392	RRP36	88745	23824327
393	RTN2	6253	23313552
394	RUNDC1	146923	23824327
395	RUNDC3B	154661	20371350
396	S1PR1	1901	23824327
397	S1PR3	1903	23824327
398	SAR1A	56681	23824327
399	SCN2B	6327	23313552
400	SCO1	6341	23824327
401	SEC14L4	284904	23824327
402	SENP8	123228	23824327
403	SEPT14	346288	23446348
404	SEPT14	346288	23824327
405	SERF2	10169	23446348
406	SERINC1	57515	23313552
407	SGTB	54557	23313552
408	SH3BP5	9467	23313552
409	SHE	126669	23824327
410	SIGLEC11	114132	23446348
411	SIGLEC9	27180	23824327
412	SIGLEC9	27180	23313552
413	SKIDA1	387640	22012620
414	SLC1A5	6510	23824327
415	SLC25A37	51312	23824327
416	SLC25A44	9673	23824327
417	SLC33A1	9197	23824327
418	SLC35F5	80255	23313552
419	SLC35F5	80255	22927820
420	SLC35F6	54978	22927820
421	SLC35F6	54978	23824327
422	SLC35G1	159371	23824327
423	SLC6A4	6532	23313552
424	SLC7A11	23657	23313552
425	SLFN13	146857	23824327
426	SMIM7	79086	23824327
427	SMUG1	23583	23446348
428	SNX2	6643	23824327
429	SOCS5	9655	23446348
430	SP1	6667	23604143
431	SPAG16	79582	23824327
432	SPEM1	374768	23313552
433	SPIB	6689	23824327
434	SPIC	121599	23824327
435	SPPL3	121665	23824327
436	SRCAP	10847	23824327
437	SRCIN1	80725	19536157
438	SRCIN1	80725	24456795
439	STAC2	342667	22927820
440	STX4	6810	23313552
441	SUGT1	10910	23824327
442	SYAP1	94056	23824327
443	SYNJ2BP	55333	23824327
444	SYNPO2	171024	22815788
445	SYNPO2L	79933	23313552
446	TBC1D16	125058	23824327
447	TBL3	10607	19536157
448	TCEB2	6923	23824327
449	TCN2	6948	23824327
450	TEAD1	7003	19536157
451	TEP1	7011	22012620
452	TEP1	7011	23446348
453	THAP1	55145	23824327
454	TIAL1	7073	23824327
455	TIMM10	26519	23313552
456	TIMM50	92609	23824327
457	TLDC1	57707	23824327
458	TLR7	51284	23313552
459	TM4SF5	9032	23824327
460	TMEM127	55654	23313552
461	TMEM134	80194	23824327
462	TMEM174	134288	19536157
463	TMEM33	55161	23824327
464	TMEM50A	23585	23824327
465	TMEM92	162461	23824327
466	TMOD2	29767	23824327
467	TMOD2	29767	19536157
468	TMOD3	29766	23824327
469	TMOD3	29766	23313552
470	TNFAIP8L1	126282	22012620
471	TNFSF15	9966	23824327
472	TNIP3	79931	23313552
473	TNS4	84951	23824327
474	TOM1	10043	22815788
475	TP53	7157	23747308
476	TP53	7157	23670238
477	TRAF3IP2	10758	22012620
478	TRAF3IP2	10758	20371350
479	TRAPPC10	7109	23824327
480	TRIM35	23087	23824327
481	TRIM72	493829	23824327
482	TRIOBP	11078	23313552
483	TRIP11	9321	23824327
484	TRPS1	7227	22815788
485	TRPV2	51393	23824327
486	TRUB2	26995	19536157
487	TSPAN11	441631	19536157
488	TTC31	64427	23824327
489	TTC4	7268	23824327
490	TTLL12	23170	23446348
491	TTPAL	79183	23824327
492	TTYH3	80727	23824327
493	TUBB4A	10382	23446348
494	TXK	7294	22012620
495	UBE2V2	7336	23313552
496	UBOX5	22888	23313552
497	ULK2	9706	23824327
498	USP15	9958	23313552
499	VEGFA	7422	18320040
500	VPS53	55275	23313552
501	WDFY2	115825	23824327
502	WDR12	55759	23824327
503	WDR53	348793	23824327
504	WDR53	348793	23313552
505	WDR77	79084	22100165
506	WDR92	116143	23824327
507	WFDC6	140870	23824327
508	WNT7B	7477	23824327
509	WWC1	23286	23313552
510	WWC2	80014	23824327
511	XIAP	331	23824327
512	XPNPEP3	63929	19536157
513	XPOT	11260	23824327
514	XPR1	9213	22291592
515	YPEL1	29799	23824327
516	ZBED1	9189	19536157
517	ZBTB25	7597	23313552
518	ZBTB7A	51341	20371350
519	ZCCHC24	219654	19536157
520	ZEB1	6935	23013135
521	ZEB1	6935	23765923
522	ZHX3	23051	19536157
523	ZMAT3	64393	23313552
524	ZNF207	7756	23824327
525	ZNF347	84671	23313552
526	ZNF347	84671	23824327
527	ZNF426	79088	23313552
528	ZNF454	285676	19536157
529	ZNF460	10794	19536157
530	ZNF514	84874	21572407
531	ZNF551	90233	23824327
532	ZNF573	126231	23824327
533	ZNF578	147660	23313552
534	ZNF582	147948	23824327
535	ZNF626	199777	23824327
536	ZNF665	79788	23313552
537	ZNF682	91120	23824327
538	ZNF699	374879	23824327
539	ZNF7	7553	23313552
540	ZNF708	7562	23446348
541	ZNF708	7562	23824327
542	ZNF878	729747	23313552
543	ZSCAN2	54993	22927820
544	ZYG11A	440590	23313552

"Life is a
constant
journey
to find
the truth."

Nicholas Lea